The
University of Michigan

College of Engineering
Department of Aerospace Engineering

AE 483 -- Space System Design

ATHENA

Advanced Air Launched Space Booster

June 1994

USRA / NASA

Table of Contents

Foreword....................i
Chapter 1 -- INTRODUCTION....................1
1.0 INTRODUCTION....................3
2.0 HISTORY OF LAUNCHED VEHICLES....................3
2.1 First U.S. Space Launch Vehicle....................4
2.2 Minuteman Launch....................4
2.3 Pegasus....................4
3.0 PURPOSE OF ATHENA....................4
4.0 CLASS ORGANIZATION....................5
4.1 Group Objectives....................5
5.0 THE DESIGN PROCESS....................6
5.1 Summary of Design Process....................6
5.2 Discussion of Design Process....................6
5.3 Original Goals....................6
5.4 Limiting Factors....................6
5.4.1 Mass....................6
5.4.2 Cost....................7
5.4.3 Using Tested Technology....................7
5.4.4 Airplane Constraints....................7
5.4.5 Safety Concerns....................7
5.4.6 Mission Analysis....................8
5.5 Events....................8
5.5.1 Choosing the C-5 as the Carrier Plane....................8
5.5.2 Mission Analysis....................8
5.5.3 System Integration....................8
5.5.4 Mid-Term Report to NASA Lewis....................8
5.5.5 Preliminary Configuration....................9
5.5.6 Sled Consideration and Roll Out Masses....................9
5.5.7 Selection of Final Configuration....................9
5.5.8 Design Freeze Date....................9
5.5.9 Another Iteration....................9
5.6 Group Decision Process....................10
5.7 Ideas Not Seen in Final Design....................10
5.7.1 Solid Rocket Motors....................10
5.7.2 Top Launch....................10
5.7.3 Composite Structure....................11
5.7.4 Circular earth model for trajectory....................11
5.7.5 Larger Payload Shroud....................11
5.7.6 Side By Side Fuel Tanks....................11
6.0 CONCLUSION....................11
Chapter 2 -- SYSTEM INTEGRATION....................15
1.0 GROUP OVERVIEW....................17
2.0 BOOSTER CONFIGURATION....................17

- 2.1 Propulsion 17
- 2.2 Avionics 18
- 2.3 Structures 19
- 2.4 Configuration Analysis 20

3.0 INTEGRATION TIMELINE 28
- 3.1 Task List Assignments 28
  - 3.1.1 Receive Engines, Structures, etc 28
  - 3.1.2 Computer Programming 29
  - 3.1.3 Build Stage One, Build and Integrate Stages Two and Three 29
  - 3.1.4 Stage Testing and Final Stage Testing 29
  - 3.1.5 Receive Payload and Payload Integration 29
  - 3.1.6 Final Athena Testing 29
  - 3.1.7 Receive Fuel for Athena/Aircraft 29
  - 3.1.8 Aircraft Check-over 29
  - 3.1.9 Launch Readiness Review 30
  - 3.1.10 Launch Briefing and Mission Debriefing 30
  - 3.1.11 Post Flight Analysis/Receive Parts for Next Mission 30
- 3.2 Deviations 30
  - 3.2.1 Safety Concerns 30
  - 3.2.2 Construction Delays 30
  - 3.2.3 Aircraft Limitations 30

4.0 CARRIER AIRCRAFT - THE CHIMAERA 31
- 4.1 Lockheed C-5B Galaxy Capabilities 31
  - 4.1.1 C-5B Description 31
  - 4.1.2 C-5B Dimensions 32
  - 4.1.3 C-5B Weights and Loading 32
  - 4.1.4 C-5B Performance 32
- 4.2 Alternative Aircraft 33
  - 4.2.1 An-124 33
  - 4.2.2 An-225 Mriya (Dream) 34
- 4.3 Air Drop Testing Procedure 34
  - 4.3.1 Test Drop Number 1 34
  - 4.3.2 Test Drop Number 2 34
  - 4.3.3 Test Drop Number 3 34
  - 4.3.4 Test Drop Number 4 35
- 4.4 Chimaera Range Capabilities 35
- 4.5 Wing Bending Modes 36

5.0 PRE-FLIGHT OPERATIONS 38
- 5.1 Athena Stage Assembly 38
- 5.2 Payload Integration 39

Table of Contents

5.3 Athena Booster Transport....39
5.3.1 Athena - Truck Integration....39
5.3.2 Athena Transport....39
5.4 Aircraft Mating....41
5.4.1 Trailer to Aircraft Transfer....41
5.4.2 Primary and Secondary Locking Mechanisms....41
5.4.3 Payload Cooling Unit....42
5.5 Athena Fuel Safety and Storage....42
5.5.1 Fuel Safety....42
5.5.3 Fuel Transfer....45
5.5.4 Fueling Procedure....45
6.0 FINANCIAL ANALYSIS....45
6.1 Comparison with Competition....46
6.2 Detailed Launch Cost Analysis....47
6.2.1 Launch Operations....48
6.2.2 Mission Control....49
6.2.3 Power/Thermal/Control....49
6.2.4 Propulsion....49
6.2.5 Structures....49
6.3 Budget Determination....49
6.3.1 Project Lifetime....50
6.3.2 Start-up Time....50
6.3.3 Yearly limits....51
6.3.4 Contracts with Satellite Manufacturers....51
6.3.5 Pre-purchasing of Materials....51
6.3.6 Interest to Investors....51
6.3.7 Taxes....51
6.3.8 Minimum Cash Balance....52
Chapter 3 -- MISSION CONTROL....53
1.0 GROUP OVERVIEW....55
2.0 AIRPORT SELECTION....55
2.1 Mission Control Location....56
3.0 GUIDANCE, NAVIGATION, AND CONTROL (GNC)....57
3.1 Global Positioning System....60
4.0 ON-BOARD COMPUTER SYSTEM....60
4.1 On-board Computer Hardware....61
4.2 On-board Computer Software....64
5.0 MISSION TRACKING....64
5.1 C-5B Flight Path....64
5.2 External Tracking....65
5.3 Internal Tracking....66
6.0 AIRCRAFT SUPPORT....66
7.0 SAFETY FACTORS AND CONSIDERATIONS....68

7.1 Abort Scenarios 69
8.0 FLIGHT TERMINATION SYSTEM(FTS) 71
9.0 LAUNCH TIME SEQUENCE 72
10.0 CONCLUSION 73
Chapter 4 -- MISSION ANALYSIS 75
1.0 GROUP OVERVIEW 78
2.0 SATELLITE SELECTION 78
3.0 DESIGN CONSTRAINTS 79
4.0 ASCENT TRAJECTORY 80
4.1 Forces and Equations of Motion 80
4.2 Iteration Technique 82
4.3 Multi-stage Rocket 82
4.4 Fuel Mass Distribution 83
4.5 Ascent Trajectory Program 84
5.0 ORBIT TRANSFERS 85
5.1 Hohmann Transfer Orbits 85
5.2 Orbit Inclination Change 87
5.3 Mass Fraction Computation for Transfer 88
5.4 Phase Changes 89
6.0 SUMMARY 90
Chapter 5 -- PAYLOAD 91
1.0 GROUP OVERVIEW 93
2.0 ATHENA PAYLOAD CONFIGURATION 93
2.1 Initial Design and Adjustments 93
2.2 Final Configuration 94
3.0 PAYLOAD MARKET 94
3.1 Payloads Available 94
3.1.1 Communications Satellites 94
3.1.2 Other Satellites 95
3.2 Orbits 96
3.2.1 Low Earth Orbit (LEO) 96
3.2.2 Geosynchronous Earth Orbit (GEO) 97
3.3 Athena Payload Market 98
4.0 PAYLOAD BAY DESIGN 99
5.0 PAYLOAD STRUCTURAL INTERFACE 100
5.1 Fairing and Fairing Separation 100
5.2 Payload Separation and Interface 102
6.0 PAYLOAD CONCERNS 104
6.1 Cleanliness During Integration 104
6.2 Pressure in Payload Bay 104
6.2.1 Higher Pressure Inside Payload Bay 104
6.2.2 Higher Pressure Outside Payload Bay 104

Table of Contents

6.3 Electrical and Power Requirements....105
6.4 Launch Environment....105
6.4.1 Loading....106
6.4.2 Temperature....106
6.4.3 Other Environmental Concerns....106
6.5 Tracking and Communication....107
7.0 CONCLUSION....107
Chapter 6 -- PROPULSION....109
1.0 GROUP OVERVIEW....111
2.0 SELECTION OF ATHENA BOOSTER SYSTEM....111
2.1 Selection of Type of Propellant....112
2.1.1 General Propellant Requirements....112
2.1.2 Special Requirements for Liquid Propellants....112
2.1.3 Final Selection of the Propellant Type....113
2.2 Selection of Athena Booster Configuration....114
2.3 Selection of Engine Systems....114
2.3.1 Final Engine Configuration Choices....115
3.0 CALCULATIONS FOR CONFIGURATION CHOICES....116
3.1 Explanation of Calculations....117
3.2 Assumptions and Limitations....119
3.3 Results....120
4.0 ENGINES....120
4.1 Stage One Engine: LR87-AJ-11....120
4.2 Second Stage: LR91-AJ-11....121
4.3 Stage 3: The Transtage....121
5.0 OPERATIONS OF THE ENGINES....122
5.1 Stage One Engine: LR87-AJ-11....122
5.2 Second Stage: LR91-AJ-11....123
5.3 Stage Three: Transtage....124
6.0 PROPELLANTS....124
6.1 Nitrogen Tetroxide, The Oxidizer....124
6.2 Aerozine 50, The Fuel....125
6.3 Propellant Additives....126
7.0 Propellant Storage Tanks....127
7.1 Calculations....127
7.2 Tank Configurations....129
7.3 Overall Volume and Mass Calculations....129
7.4 Fireball Radius....132
8.0 COSTS....132
8.1 The Final Costs....132
9.0 CONCLUSION AND FUTURE PLANS....134
Chapter 7 -- STRUCTURE....135
1.0 GROUP OVERVIEW....137

2.0 STRUCTURAL DESIGN OF BOOSTER EXTERIOR 137
  2.1 Materials Selection and Properties 138
  2.2 Exterior Skin Design 138
  2.3 Longitudinal Stringer Design 139
  2.4 Internal Compression Rings 141
3.0 PAYLOAD SHROUD MATERIAL SELECTION AND DESIGN 142
  3.1 Initial Material Options 142
    3.1.1 Structural Materials 142
    3.1.2 Thermal Materials 145
  3.2 Final Materials Selected 145
    3.2.1 Structural Materials 145
    3.2.2 Thermal Materials 147
4.0 FREQUENCY RESPONSE OF BOOSTER STRUCTURE 149
  4.1 MODELING 149
  4.2 Results 150
5.0 ENGINE MOUNT DESIGN 151
  5.1 Material Selection 151
  5.2 Modeling 152
    5.2.1 Physical Model 152
    5.2.2 Finite Element Model 152
    5.2.3 Testing 153
    5.2.4 Conclusion 155
6.0 BOOSTER TRANSPORT STRUCTURE (BTS) 155
  6.1 Modeling of Cradle 156
  6.2 Testing Procedure 158
  6.3 Results 158
  6.4 Conclusion 159
Chapter 8 -- POWER/THERMAL/CONTROL 161
1.0 GROUP OVERVIEW 163
2.0 SELECTION OF DEPLOYMENT SYSTEM 163
  2.1 Criteria For Selection 164
  2.2 Answers to Criteria 164
  2.3 Alternatives to Parachutes 165
  2.4 Reasons for Rejection 165
  2.5 Analysis of Extraction System 165
3.0 SELECTION OF POWER SYSTEM 168
4.0 CONTROL AND STABILITY 168
  4.1 Introduction 168
  4.2 Longitudinal Dynamics And Stability 169
  4.3 Longitudinal Dynamics Of Stage I 169
  4.4 Longitudinal Dynamics of Stage III: 170
  4.5 Design Configuration And Performance of System 171

Table of Contents

4.6 Design For Stage I....171
4.7 Performance of Stage I....172
4.8 Control of Stage III....172
4.9 Performance of Stage III....173
5.0 THERMAL CONTROL SYSTEMS....174
5.1 Temperatures at the Stagnation Point....174
5.2 The Payload Bay....176
5.3 The Exterior of Athena....176
6.0 NOSE CONE ANALYSIS....177

Index of Figure and Tables

CHAPTER 1
INTRODUCTION

Tables:

1.1 Mass Breakdown....13
1.2 Stage Breakdown....14

CHAPTER 2
SYSTEM INTEGRATION

Figures:

2.1 Avionics Placement Diagram....18
2.2 Third Stage Layout....19
2.3 Center of Gravity Locations....20
2.4 Booster Configuration....27
2.5 Integration Timeline....28
2.6 Lockheed C-5B Galaxy....31
2.7 Aircraft range vs. Payload....36
2.8 Aircraft Wing Lift Distribution....37
2.9 Vandenberg Air Force Base....40
2.10 Payload Capability Comparison....46
2.11 Vehicle Cost Comparison....47
2.12 Launch Cost Breakdown....48
2.13 Graph of Financial Position....50

Tables:

2.1 Center of Gravity....21
2.2 Center of Gravity....22
2.3 Center of Gravity....23
2.4 Center of Gravity....24
2.5 Center of Gravity....25
2.6 Center of Gravity....26
2.7 Aircraft Data for Range Analysis....35

Appendices:

A.1 Configuration Chart....181
A.2 Overall Mass Allocation....185
A.3 Raw Data for Figure 2.7....189
A.4 Comparison with Competition....193
A.5 Overall Dollar Allocation....197
A.6 Drop Test Allocation....201
A.7 Budget Analysis Spreadsheet....205

Index of Figures and Tables

CHAPTER 3
MISSION CONTROL

Figures:

3.1 Athena IMU Block Diagram 59
3.2 C130 68030 - Based Computer 62
3.3 C401 Communication Controller 63
3.4 C-5B Flight Path 65
3.5 Abort Scenarios Prior to Launch 70
3.6 Abort Scenarios Prior to Extraction 70
3.7 Abort Scenarios After Extraction 71

Tables:

3.1 IMU Comparison 58
3.2 Features of LN-200 IMU 58
3.3 Characteristics of GPS Sensor 60
3.4 Athena Computer System Overview 63

Appendices:

CHAPTER 4
MISSION ANALYSIS

Figures:

4.1 Athena Free Body Diagram 81
4.2 Three Stage Rocket Nomenclature 83
4.3 Hohmann Transfer 86
4.4 Orbit Inclination 88

Tables:

4.1 Definition of Earth Orbits 78
4.2 Athena Engines 80
4.3 Athena Mass and Engine Data 84
4.4 Burn Times and Fuel Consumed 85
4.5 Key Trajectory Results 85
4.6 Transfer Orbit Insertion Mass Ratios 89
4.7 Recircularization Burn Mass Ratios 89

Appendices:

C.1 Matlab Trajectory Analysis Program 209
C.2 Trajectory Analysis Graphic Results 219

CHAPTER 5
PAYLOADS

Figures:

5.1 Typical Communications Sattelite....95
5.2 Tethered Sattelite System....96
5.3 Inclinde GEO Tracing....98
5.4 Athena's Payload Capabilities....99
5.5 Payload Static Envelope....100
5.6 Payload Fairing Separation....101
5.7 Payload Separation....102
5.8 Payload Interface/Deployment Mech....103
5.9 Double Payload Deployment....103

Appendices:

D.1 Preliminary Payload Bay Designs....223
D.2 Future Satellites....227
D.3 Recent Satellites....231

CHAPTER 6
PROPULSION

Figures:

6.1 Propellant Tank Shapes....129
6.2 Mass Allocation by Stage....131
6.3 Cost Allocation by Stage....133

Tables:

6.1 Initial Engine Configurations....115
6.2 Properties of Nitrogen Tetroxide....125
6.3 Properties of Aerozine 50....126
6.4 Fuel Volume and Mass by Stage....130
6.5 Tank Lengths and Geometry....130
6.6 Baffle and Tank Masses....131
6.7 Cost Estimates by Stage....133

Appendices:

E.1 Engines....235
E.2 Tank Design....239
E.3 Configurations....245

Index of Figures and Tables

CHAPTER 7
STRUCTURES

Figures:

7.1 First Stage Design Cut-Away....138
7.2 Stringer Configuration....140
7.3 Cross Section of C-Rings....142
7.4 (FIGURE 1) Booster Skin Configurations....144
7.5 Comparison of Thermal Conductivity of Ceramics....148
7.6 Problem Schematic....151
7.7 Sectional Areas of Engine Mount Members....152
7.8 Engine Mount Configuration....153
7.9 Finite Element Model of Engine Mount....153
7.10 Linear-Static Displacement of Engine Mount Model....154
7.11 Linear-Static Displacement of Engine Mount....155
7.12 Schematic of BTS....156
7.13 BTS Cross-Section with Contact Points....156
7.14 BTS Beam Cross-Sections....157
7.15 Placement of Contact Points....157
7.16 Finite Element Model of BTS....158
7.17 Deformed BTS for 2g Loading....159

Tables:

7.1 Material Properties of 7075-T6 Aluminum....138
7.2 Number of Stringers per Stage and Stringer Spacing....141
7.3 Number of C-Rings per Stage and C-Ring Spacing....142
7.4 Properties of Hexagonal 5056 Aluminum Honeycomb....146
7.5 Properties of PMR-15....146
7.6 Properties of Haveflex T.A.-117....147
7.7 Properties of Alumina Insulating Board, AL 30....148
7.8 Model Data....150
7.9 Material Properties....152
7.10 BTS Specifications....159

Appendices:
NOT INCLUDED

CHAPTER 8
POWER/THERMAL/CONTROL

Figures:

8.1 Booster Egress....164
8.2 Extraction Chute Packaging....165
8.3 Chute Size Comparison with Athena....166
8.4 Axial G Forces During Extraction....166
8.5 Pitch Angle During Extraction....167
8.6 Control System Config.: Stage 1....171
8.7 Control System Config.: Stage 3....172
8.8 Stagnation Temperature vs. Altitude....175
8.9 Athena Nose Cone....177
8.10 Drag Force vs. Altitude....178

Tables:

8.1 Power Requirements 168
8.2 Pitch Sensor Locations: Stage 1 172
8.3 Summary of MR-104 Characteristics 173
8.4 Stagnation Temperature vs. Altitude 175*
8.5 Nose Cone Characteristics 178
8.6 Drag Force vs. Altitude 178

Appendices:

G.1 Extraction Spreadsheet 251
G.2 Post-extraction Spreadsheet 255
G.3 Control and Stability 259

Preface -- **The Idea Behind Athena**

Foreword

The infrastructure for routine, reliable, and inexpensive access of space is a goal that has been actively pursued over the past 50 years, but has yet not been realized. Current launch systems utilize ground launching facilities which require the booster vehicle to plow up through the dense lower atmosphere before reaching space. An air launched system on the other hand has the advantage of being launched from a carrier aircraft above this densest portion of the atmosphere and hence can be smaller and lighter compared to its ground based counterpart. The goal of last years Aerospace Engineering Course 483 (AE 483) was to design a 227,272 Kg (500,000 lb.) air launched space booster which would beat the customer's launch cost on existing launch vehicles by at least 50%. While the cost analysis conducted by the class showed that this goal could be met, the cost and size of the carrier aircraft make it appear dubious that any private company would be willing to invest is such a project. To avoid this potential pitfall, this years AE 483 class was to design as large an air launched space booster as possible which can be launched from an existing or modification to an existing aircraft. An initial estimate of the weight of the booster is 136,363 Kg (300,000 lb.) to 159,091 Kg (350,000 lb.).

All costs will be strictly contained so the customer's launch costs is kept to less than 50% of what is currently charged by existing or near term launch system to insure a 15% return to investors. Also this launching system should be able to start launching payloads no later than 1997, which means the booster must use existing technology and off the shelf hardware. Candidate carrier aircraft are the C-5 A Galaxy, the Antonov An-124, and the Antonov An-225. The maximum payload capability of the C-5 A is 118,636 Kg (261,000 lb.), the An-124 is 159,091 Kg (350,000 lb.), and the An-225 is 250,000 Kg (550,000 lb.). Air launch trials of Minuteman I ICBM (34,091 Kg) were conducted in 1974 as the first step in determining the suitability of using the C-5 A for deployment of the MX missile (68,182 Kg). The former Soviet Union as of 1991 has considered using the An-124 for air launching of their SS-224 ICBM's converted for satellite mission. Both of these aircraft have or would deploy their booster out through their aft cargo doors. This produces a very dynamic environment both in terms of loads on the aircraft and booster, and also on the flight control system of the aircraft. A possible alternative would be to modify these aircraft so the booster could be dropped down through the aircraft's belly. All seven groups of the class will be key in producing a design which is well integrated with the carrier aircraft, meets the launch cost and payload requirements, and is operationally viable. This project was coined by the class of the Winter Term 94 AE 483 Class as ATHENA!

Athena was designed by a class of 25 students with aid and guidance of Professor Joe G. Eisley and Teaching Assistant (TA) Jim Akers. The class choose the Project Manager and the Assistant Project Manage, who happen to be Corey G. Brooker and John Ziemer respectively. The class members then picked their number one choice of the eight subsystems (Spacecraft Integration, Aircraft Interface, Mission Control, Mission Analysis, Payload, Propulsion, Structure, and Power/Thermal/Control), and for the most part people received those areas to specialize in. However due to low numbers in the class it was decided that Spacecraft Integration and Aircraft Interface merge to become System Integration. Team leaders were picked two weeks into the class by the individual groups (except Mission Analysis -- choose not to pick a team leader). Meetings were held outside the classroom between the Project Managers and the Professor/TA; between Project Managers and Team Leaders; and occasionally between groups.

This report is the culmination of a semester--PLUS--of hard work put in by all class members.

Thank you to everyone in the class for enjoyable semester. -- Project Leaders

Special thanks to all those who helped on finalizing this paper and the USRA Presentation. Jim Akers, Corey G. Brooker, Nikki Bellmore, Aaron T. Drielick, Professor Joe G. Eisley, Mary Ann Guariento, Scott Henderson, John Plonka, Jeff White, and John Ziemer.

Preface - **Class Organization Structure**

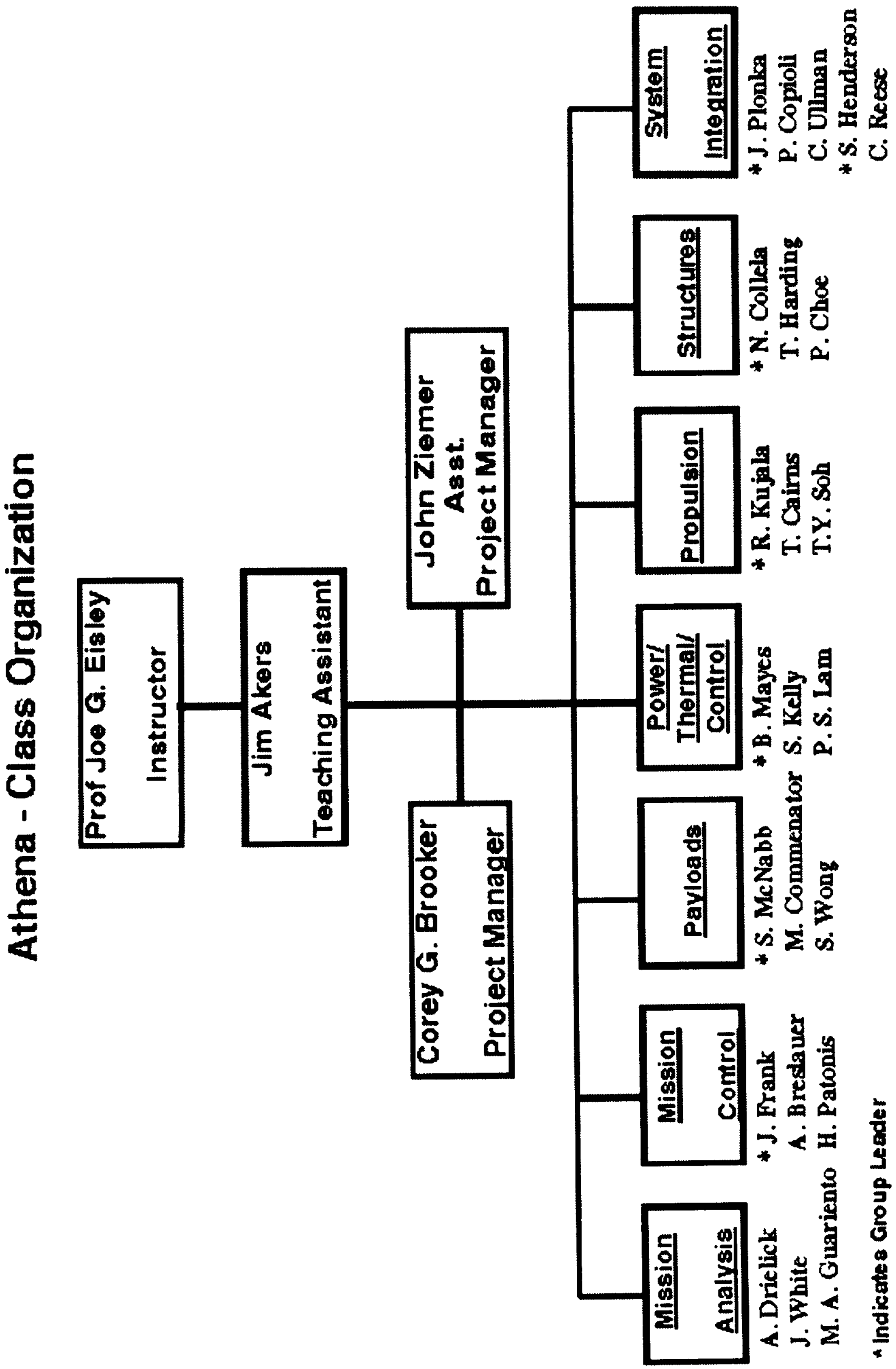
Athena - Class Organization
Prof Joe G. Eisley
Instructor
Jim Akers
Teaching Assistant
John Ziemer
Asst.
Project Manager
Corey G. Brooker
Project Manager
Mission Analysis
A. Drielick
J. White
M. A. Guariento
Mission Control
* J. Frank
A. Breslauer
H. Patonis
Payloads
* S. McNabb
M. Commentator
S. Wong
Power/ Thermal/ Control
* B. Mayes
S. Kelly
P. S. Lam
Propulsion
* R. Kujala
T. Cairns
T.Y. Soh
Structures
* N. Collela
T. Harding
P. Choe
System Integration
* J. Plonka
P. Copioli
C. Ullman
* S. Henderson
C. Reese
* Indicates Group Leader

ORIGINAL PAGE
BLACK AND WHITE PHOTOGRAPH

3rd Row (left to right): Jeff White, Nicholas Colella, Trevor Harding, John Ziemer (Assistant Project Manager), Mark Commenator, Scott McNabb, Bill Mayes, Christopher Ullman, Jim Akers (Teaching Assistant), Rodney Kujala, Tze-Yun Soh, Tim Cairns

2nd Row (left to Right): Hristos Patonis, Mary Ann Guariento, Charles Reese, Aaron Drielick, Scott Henderson, John Plonka, Alan Breslauer

1st Row (left to right): Jeremy Frank, Peter Choe, Shyun Wang, Corey Brooker (Project Manager) - kneeling, Paul Copioli, Professor Joe G. Eisley (Instructor), Shad Kelly, Ping Shun (Joseph) Lam

Preface - **Class Specialties**

The following is a list of each member's area of specialty within the Athena project.

Project Manager	Corey G. Brooker
Assistant Project Manager	John Ziemer
System Integration	*John Plonka *Scott Henderson Paul Copioli Charles Reese Christopher Ullman
Mission Control	*Jeremy Frank Alan Breslauer Hristos Patonis
Mission Analysis	Aaron Drielick Mary Ann Guariento Jeff White
Payload	*Scott McNabb Mark Commenator Shyun Wong
Propulsion	*Rodney Kujala Tim Cairns Tze-Yun Soh
Structure	*Nicholas Colella Peter Choe Trevor Harding
Power/Thermal/Control	*Shad Kelly Ping Shun (Joseph) Lam Bill Mayes

Note -- * Denotes Team Leader

ATHENA: THE AIR LAUNCHED SPACE BOOSTER

University of Michigan
Department of Aerospace Engineering
Ann, Arbor, Michigan

Professor Joe G. Eisley

Launching a space vehicle from the air instead of the ground reduces size, fuel, structure weight, and facility costs while improving performance. As long as the design including the plane remains practical and uses tested hardware, a competitive booster can be designed and implemented within three years.

Based on realistic considerations, the design for the system had to take into account: using a currently available carrier plane, implementing only developed and tested technology, and setting costs to be competitive to similar systems guaranteeing a 15% return for investors.

The Athena Air Launched Space Booster accomplishes these goals. The Athena design consists of three stages with storable liquid propulsion systems and an overall cylindrical shape (2.7 m in diameter). The booster, with a total mass of 83,235 kg (183,117 lb.), is capable of putting 1,715 kg (3773 lb.) into Low Earth Orbit (LEO) and 888 kg (1953.6 lb.) into Geosynchronous Transfer Orbit (GTO). Athena is designed to handle both lateral and axial loads up to six times gravity. It can be integrated and launched horizontally and also withstand vertical thrust forces. During the mission, Athena can survive heat and vibration problems normally associated with high velocity vehicles. Athena is controlled by engine gimbals and on board computers that are monitored through ground and air based tracking facilities. All integration, launch preparation and tracking are handled through Vandenberg Air Force Base (VAFB) and the California Commercial Space Industry (CCIS). The carrier aircraft, a C5-B Galaxy, flies south out of Vandenberg to an altitude of 10,000 meters before releasing and launching the booster into its 300 second ascent trajectory. The total cost of one launch is 18 million dollars. This is below the competitors based on a dollar per kilogram payload amount. In ten years the Athena project repays the investors' initial funds plus 15% per year.

Preface -- **REFERENCES**

1. Titan III Propulsion Systems. Aerojet Corp. October 1988.
2. NASA Technical Memorandum 104456, "Launch Vehicle Performance Using Metallized Propellants". Brian Palaszewski and Robert Powell. NASA. 1991.
3. See references 26 & 27 in above
4. Bryan Palaszewski, NASA Lewis Engine Research Center
5. Bill Sprow, Aerojet Corp.
6. Metals Handbook, Tenth Ed. Volume 1: Properties Selection; Irons, Steels, and High Performance Alloys. ASM International, 1990
7. Department of the Air Force, "Standard Prices for Missile Fuels Management Category Items"
8. Design of Liquid Propulsion Rocket Engines Huzeli Huang. 2nd Ed. 1971 332-341.
9. Handbook of Pyrotechnics.
10. Fundamental of Fire and Explosion. Daniel R. Stull. Americsn Institute of Chemical Engineering Vol 73. 1977.
11. Rocket Propellant Handbook. Boris Kit and Douglas S. Evered. Macmillian 1960.
12. Rocket Propulsion Elements. Sutton.
13. Space Directory 1992-93. Andrew Wilson. Interavia 1993.
14. Jane's Space Directory 1993-1994. Andrew Wilson. Jane's 1994.
15. Space Mission Analysis and Design. Janes R. Wertz and Wiley J. Larson. Kluwer Academic Publishers.
16. Rocket Propellant and Pressurization Systems. Elliot Ring. Prentice Hall.
17. Propeties of Liquid Propellants. Aerojet Corp.
18. Cornelisse, J. W., Rocket Propulsion and Spaceflight Mechanics Fearon-Pitman Publishers Inc., Belmont, CA; 1979
19. Bate, R., Mueller, D., White, J., Fundamentals of Astrodynamics Dover Publications Inc., New York, NY; 1971
20. Hill, P., Peterson, C., Mechanics and Thermodynamics of Propulsion, 2nd Ed.
21. Pegasus Program Review, Orbital Sciences Corporation and Hercules Aerospace Co.

22. Crouch, D. S., VanPelt, J. M., Flanders, H. A. 42 Congress of the International Astronautical Federation. " A Titan II Based Tethered Satellite System", Martin Marietta Astronautics Group. Denver, CO. October 5-11, 1991 in Montreal, Canada.

23. Recommended Tethered Satellite Follow-on Missions. Martin Marietta, June 1992.

24. DeBrock, Steve. Earth Observing System (EOS). Lockheed Missles and Space Company. Presentation at the University of Michigan. Sept. 24, 1993.

25. Cassini Mission Fact Sheet. NASA Jet Propulsion Labs.

26. Chetty, P. R. K. Satellite Technology and Its Applications. TAB Books. 1988.

27. Martin, Donald H. Communications Satellites.

28. Evans, B. G. editor. Satellite Communication Systems. 2nd Ed. Peter Pereginus Ltd., London 1991.

29. Agrawal, Brij N. Design of Geosynchronous Spacecraft. Prentice Hall Inc. Englewood Cliffs, NJ. 1986.

30. Gordon, Gary D. and Morgan, Walter L. Principles of Communications Satellites. John Wiley and Sons Inc. New York, NY. 1993.

31. Poncha, J. J. Introduction to Mission Design for Geastationary Satellites. D. Reidel Publishing Co. 1987.

32. Williamson, Mark. The Communications Satellite. IOP Publishing Ltd. 1990.

33. Fleet Satellite Communications Spacecraft, TRW, October 1980

34. Ariane: The European Launcher, Ariane Space, July 1989

35. Pattan, Bruno and Reinhold,Van Nostrand Satellite Systems: Principles and Technologies, 1993.

36. Carasa, F.Quest for Space, etc. Crescent Books, 1987 ed.

37. Pegasus Launch System Payload User's Guide, 1991-1992 Orbital Sciences Corporation

38. Interavia Space Directory, 1992/3

39. Berlin, Peter. The Geostationary Applications Satellite, Cambridge University Press, 1988

40. Caprara, Giovanni . The Complete Encyclopedia of Space Satellites, Portland House. 1986.

41. Aviation Week and Space Technology vol. 139 Number 7, Aug 16 1993, page 21.

42. Aviation Week and Space Technology vol. 139 Number 6, Aug 9 1993, page 56.

43. Small Satellite Technologies and Applications, editor Brian Horais, SPIE (The Society of Photo-Optical Instrumentation Engineers) vol 1691.

44. Greenberg, Joel S. and Hertzfeld, Henry R., Space Economics, Progress in Astronautics and Aeronautics, Volume 144, AIAA Inc., 1991. Washington D.C. pp. 3-319.

45. Jane's Information Group Limited, Jane's All the World's Aircraft 1989-1990. Sentinel House, Surrey, UK. pp. 240-244, 443-444.

46. Office of the Director of Defense Research and Engineering. Handling and Storage of Liquid Propellants. U.S. Washington D.C., 1963. pp. 111-121, 217-229, 299-309.

47. Shahrokhi, Greenberg, Al-Saud/Editors, Space Commercialization: Launch Vehicles and Programs. Progress in Astronautics and Aeronautics, Volume 126, AIAA Inc., 1990. Washington D.C.

48. Wilson, Andrew, Jane's Space Directory 1993-94, Ninth Edition, Jane's Information Group, Inc., 1993. Alexandria, VA. pp. 209-327.

AITech Defense Systems Inc.
Charles Ma
(408) 980-6200

Peter Sazhur
(408) 980-6200

California Commercial Spaceport, Inc.
Dominick Barry
(805) 733-7370

Delco Systems Operations
Ben Bay
(805) 961-5408

Wayne Sarnecki
(805) 961-7452

General Dynamics
John Niesley
(619) 974-3840

Honeywell
Bob Siebert
(813) 539-4097

Intraspace
Robert D'Ausilio
(801) 292-0440

Kearfott
Alexis Efremidis
(201) 785-6544

Litton
Joe Radocchio
(818) 715-3654

Genchi
(818) 715-4160

Lockheed Launch Vehicles
Larry Stuntz
(###) ###-####

Dominick R. Barry
Director, Business Operations
California Commercial Spaceport, Inc.
3865 Constellation Road, Suite A
Vandenberg Village, California 93436
(805) 733-7370

Loral Corporation
Glenn Norman
(713) 282-8922

Orbital Sciences Corporation
Brian Clark (student co-op)
(703) 802-8242

Kathy Derricks
(703) 406-5014

Tim Osowski
(703) 406-3412

Dan Rovner
(703) 406-5217

Jim Stowers
(703) 406-5255

Gary Vyhnalek
(703) 406-5253

Trimble
Jeff Tonnemacher
(408) 481-2933

Mike Leary
(408) 481- ????

Vandenberg AFB
Bob Smith
(805) 734-8232 ext. 61304

Captain Keith Tophan
(805) 734-8232 ext. 50255

Lockheed Contact for C-5B Information
Peter Norris
C-5B Project Engineer
Lockheed, GA.
(404) 494-4489

Preface -- **ACRONYMS**

ADS: Air Delivery System
AFB: Air Force Base

BIBO: Bounded Input, Bounded Output
BTS: Booster Transport System

CCSI: California Commercial Spaceport, Inc.
CPU: Central Processing Unit

DoD: Department of Defense

EPROM: Erasable Programmable Read-Only-Memory

FE: Finite Element
FEM: Finite Element Modeling
FTLU: Flight Termination Logic Unit
FTS: Flight Termination System

GEO: Geosynchronous Earth Orbit
GNC: Guidance, Navigation, and Control
GPS: Global Positioning System
GTO: Geosynchronous Transfer Orbit

IMU: Inertial Measurement Unit
IPF: Integrated Processing Facility
I/O: Input/Output

LEO: Low Earth Orbit
LPO: Launch Panel Operator
LSC: Linear Shaped Charge

KB: Kilobyte
KSC: Kennedy Space Center

MB: Megabyte
MEO: Middle Earth Orbit
MHz: Megahertz
MIL-E: Military Electronic
MIL-SPEC: Military Specifications

NASA: National Association for Space and Astronautics

OSC: Orbital Sciences Corporation

PC: Personal Computer
PCB: Printed Circuit Card
PID: Proportional Integral Differential
PPS: Precise Positioning Service

RCS: Reaction Control System
RPU: Receiver Processing Unit

SBC:	Single Board Computer
SLC:	Shuttle Launch Complex
SPS:	Standard Positioning Service
SRAM:	Static Random Access Memory
TANS:	Trimble (Quadrex) Advanced Navigation Sensor
TTC:	Trajectory Tracking and Control
UDMH:	Unsymetrical Dimethylhydrazine
US:	United States of America
VIC:	Variable Interface Controller
VAC:	Variable Address Controller
VAFB:	Vandenberg Air Force Base

***NOTE* ALL Numbers are in Metric Units**

Chapter 1

Introduction

CHAPTER 1 -- INTRODUCTION

1.0 INTRODUCTION

In 1994 the objective for the Aerospace 483 Space System Design Course was to design an advanced air launched space booster for routine, reliable, and inexpensive access of space! During the previous year, students in the same class designed an ideal conception of an air launched booster, the Gryphon. This year's design, Athena, is drastically different and more realistic due to the goals set by the Instructor, Dr. Joe G. Eisley, and the Teaching Assistant, Jim Akers. They proposed using existing technology and a carrier vehicle that already existed while staying cost competitive. The design of Athena follows in the footsteps of Orbital Sciences Corporation's current Pegasus project. Robert Lovell from Orbital Sciences also helped determine the cost effectiveness of such a booster with the goal of carrying a larger payload than Pegasus. This semester's class consisted of twenty-six senior aerospace students. These 26 students worked together as a team to overcome difficulties. Therefor, the purpose of this report is to present the Athena Design Project in as much detail as possible.

Along with this introduction, the history of space exploration, and a general description of Athena that follows, this report separates the important subdivisions of the project and presents each group's findings. The subtopics are: Spacecraft Integration, Aircraft Integration, Mission Control, Mission Analysis, Payloads, Propulsion, Structures, and Power/Thermal/Control. Each group played an important role in the final design of Athena. Their work is represented here to show Athena and all it's subsystems in a formal report.

2.0 HISTORY OF LAUNCHED VEHICLES

Human's domination of space has come in many different ways over past three decades. Starting with a very simple satellite, Sputnik 1 launched in 1957, the space race between the U.S. and what was then the U.S.S.R. began. Then came manned missions into orbits around Earth and then actually touching down on another world, the Moon. Today we launch the Shuttle, a reusable manned spacecraft that orbits the Earth in a Low Earth Orbit (LEO) regularly.

These manned missions do attract a lot of the world's attention, but it is also important

PRECEDING PAGE BLANK NOT FILMED

to keep in mind that probes and satellites have made our lives easier with new discoveries. Satellites also play an important working role in our every day lives, especially monitoring the Earth. Satellites do around the clock observations of the Earth giving weather updates, bouncing signals back and forth for our communications, seeing trends in rainfall and crop outputs, and providing many other services. Unmanned probes have also examined other Planets giving us new answers to what is happening to the Universe, as well as, learning about Earth from these other planets. With continuing scientific research and new discoveries there will most likely always be a need for satellite launch vehicles.

2.1 First U.S. Space Launch Vehicle

The United States Army Ballistic Missile Agency launched the first space vehicle, the Explorer 1 satellite aboard a Jupiter C launch vehicle. Jupiter C, a four stage rocket, launched the U.S. into the satellite business. Since the Jupiter C, the U.S. has developed its technology be leaps and bounds--sending man to the moon, and developing a reusable space vehicle (the Space Shuttle). Along with those changes, the launch vehicles used for commercial satellites have become larger, with an ever increasing payload capacity. However, Orbital Sciences Corporation would change the way in which we put satellites into space by launching a booster from the air instead of the ground eliminating fuel and mass. But in actuality, the whole ideal of launching a rocket from the air came from the United States Armed Forces during the Cold War Era and a Minuteman launching test..

2.2 Minuteman Launch

Air launched boosters were introduced by the United States Armed Forces during the 70's to prove to what was once the U.S.S.R. that we had the capability of launching an I.C.B.M. from a moving platform in the air. This project fell under the Lockheed Corporation, since they were the designers of the C-5B Galaxy, our nations largest lifting aircraft. Lockheed tested the responses of the C-5 when dropping a 79,000 kg missile out the back-end through its cargo door. This ideal launch method proved successful and would surface again in the commercialized industry. Orbital Sciences Corporation (OSC) began the Pegasus project.

2.3 Pegasus

In 1988 the Pegasus project was underway. The goal was to develop an air launched orbital transportation system capable of launching small satellites. The first Pegasus launch was on April 16, 1990, and was carried under the wing of a B-52. OSC's reasoning for Pegasus was to cut cost by minimizing the effects of gravity and the lower atmosphere (dense air) to allow larger payloads to be inserted into a particular orbit. This ideal of air launching also gives more options to the customer by allowing variable launch windows with capability of launching from the customer's choice in launch inclinations.

3.0 PURPOSE OF ATHENA

Mr. Robert Lovell, the President of Orbital Sciences Corporation, challenged the University of Michigan to design a large air launched booster. The goals were set by the Instructor and the Teaching assistant of the Aerospace 483 Space Systems Design Class. These goals for the Winter 1994 Aero 483 class were:

- To keep the booster's estimated initial mass between 136,000 and 159,000 kg.
- Having the booster be carried by an existing aircraft.
- Keeping the launch cost under the current competitor's costs by 50 percent.
- Using current technology--the booster must be ready to fly within three years

As mentioned previously, our purpose was to design a large air launched booster using the above criteria as strict guidelines. The outcome of the class' long and hard work was Athena. The name Athena comes from Greek Mythology, where it is said that Athena tamed Pegasus to fly. Although Athena does not match all the goals set by the instructors, it is a feasible booster that could exist in the real world. Athena is the combination of many ideas and used everyone's abilities to the highest.

4.0 CLASS ORGANIZATION

With these four goals in mind, the Winter 1994 Aero 483 class set out to accomplish the task of designing a large air launched booster. The class was led by Project Manager Corey G. Brooker and Assistant Project Manager John Ziemer. Twenty six students were split into seven groups. Each group had an objective to meet in order for this design to come together as one cohesive unit.

4.1 Group Objectives

Systems Integration was responsible for overall design and configuration of the booster. System Integration was actually made up of **Aircraft Interface** and **Spacecraft Integration**. These two teams combined their efforts, but did work on their individual specialization--aircraft or spacecraft. Aircraft Integration had to pick a suitable carrier aircraft for Athena, choose possible airports for the carrier aircraft, determine the egress method of the booster from the selected aircraft, and design the aircraft connection with the booster. Spacecraft Integration was responsible for monitoring the mass, dimensions, calculating the mass properties of the booster, and performing the cost analysis of Athena.

Mission Control took on the task of selecting facilities for Athena to be assembled, launched, and control centers for the launch and trajectory monitoring. The group also was in charge of identifying hardware for communication, tracking, and telemetry systems.

Mission Analysis was assigned the task of determining Athena's flight trajectory for different orbits, determining proper orbits and orbit transfers.

Payloads identified those satellites (by mass, dimensions, and orbits) that Athena would be in the market for launching. This group also designed the interface of the payload to the booster.

Propulsion's duties included selecting engines for each stage of the booster, the tank design for those engines, and the optimal staging of engines to increase Athena's performance.

Structures was responsible for coming up with material for the booster, the structural design for durability, and the sled design used to roll the booster out of the cargo bay. Along with these duties they shared the responsibility of the payload interface design and the shroud design with other groups.

Power/Thermal/Control set the power requirement of the booster with input from other groups. From this they chose suitable batteries and other components to meet these requirements. This group, along with Structures, designed the heat shielding for the payload (the shroud). They were also responsible for finding the response of the aircraft and booster during egress and separation. Finally they selected the Reaction Control Systems for Athena to keep the booster stable.

5.0 THE DESIGN PROCESS

The design process is a lengthy and detailed operation that includes many steps. Learning, trying out new ideas, and working together as a team are crucial parts of obtaining a valuable end result. The purpose of this section is to outline and discuss the design process during Athena.

5.1 Summary of Design Process

This year's design, Athena, has gone through some major revisions over the term. Starting with some basic goals, the final design used many compromises. Because of certain limiting factors, the design had to be modified many times. As the term continued, problems and events came up that also drove the design in certain directions. There were many ideas that came up that did not make it to the final design. Athena as it is presented in this section, represents the culmination of twenty-six students' work producing a viable product. Although this particular design may not be the most ideal, it does demonstrate the possibility for air launching a large booster.

5.2 Discussion of Design Process

There are many things that contributed to Athena's final state. The original goals set by Professor Eisley and Jim Akers began the project with a certain direction. Eventually other limiting factors came about and the goals changed. Events that outline Athena's change over the term point out decisions and why they were made. The process that the groups used to design the booster also impacted decisions. Finally, it is also important to note those ideas that did not get into the final design and why they were excluded.

5.3 Original Goals

Athena was set to have a mass between 136,000 kg and 159,000 kg and carry a payload of around 5,000 kg for larger geosynchronous satellites. The cost needed to be below competitors by 50% and guarantee repayment and a 15% return to investors. It had to use off the shelf technology with no advanced product development or research so the vehicle could be built and launched in three years.

5.4 Limiting Factors

In addition to mass, cost, and technology constraints, the booster had to use an existing aircraft, be safe, and deliver payloads to certain altitudes depending on the mission.

5.4.1 Mass

From the original goal of approximately 140,000 kg, the booster mass dropped to its final value of 83,000 kg. Along with a 4,000 kg sled, the C-5 would only roll out 87,000 kg, a new record for air-dropping. From some discussion with Lockheed on the C-5, the maximum roll out weight was 90,000 kg. This significantly reduced the target mass of the booster, the mass of the payload, and the efficiency of the engines.

5.4.2 Cost

The cost of the booster did not drive the design as much as expected. Since the design uses older technology, the prices are usually not that great. Early on, considering a 5,000 kg payload, the cost needed to be below $21 million. Eventually cost constraints helped to eliminate extra strap on solid boosters as their performance was not worth the cost to add them. Otherwise, cost can only be used to talk about feasibility and comparison with other systems. Simply put, Athena could work only one way, and cost did not set the design.

5.4.3 Using Tested Technology

Athena had to use only technology that was available at the time of the design. That eliminated designing solids especially for our use which could have been the most favorable propulsion configuration. Also, because composite technology is not yet fully understood, the structure implemented aluminum skin and stringers instead of advanced composites. The use of gels for fuels was also discussed for safety concerns but discarded for lack of development. Athena does use all "off the shelf" hardware and can be launched in three years.

5.4.4 Airplane Constraints

Three planes, the C-5 Galaxy, the An 124, and the An 225 are the largest lifting planes available in the world today. The An 225 and An 124 are Russian planes that can lift more cargo than the C-5. The C-5, however, is a familiar and easily accessible plane which proved to be the deciding factor.

The C-5 was chosen for its usability, availability, and refueling capability. Although choosing the C-5 made things easy, it cost the design mass and size, two crucial points. Limited to a total rolling mass of 90,000 kg and a diameter of 2.7 m, the booster had to be smaller than what was laid out in the original goals.

Finally, because the C-5 is a statically stable craft, the booster had to be designed to fit with the engines towards the front of the cargo bay so Athena's center of mass could be close to that of the C-5's.

5.4.5 Safety Concerns

There are many safety concerns when transporting a combustible rocket to 10,000 m above the ocean in the back of a carrier plane. The main concern is how volatile the fuels are during the carrier and pre-launch segment of the mission.

For that reason, cryogenics were eliminated for having to much potential for dangerous explosions. Solids were also eliminated based on their low performance and the size constraints of the C-5. Storable fuel was the only alternative left. Athena is completely fueled by storable liquids. These liquids, with further research, have the possibility of being "gelled" so that leaks do not present as much of a problem. In the current frame, however, gels are not available, and the Athena design does not rely on them for safety.

Using existing storable rocket engines also limited the options for the propulsion systems. Since only one set of storable engines for this size of booster exist, the Titan rocket engines made by Aerojet were the best and only choice.

5.4.6 Mission Analysis

Over the term, the Mission Analysis Group developed and tested over ten different programs to determine the trajectory. With changes in structural design and aircraft constraints, the programs evolved to contain drag, centripetal force, and a decreasing gravity field. Mission analysis was primarily responsible for deciding the final configuration.

5.5 Events

During the term many groups had an influence on the design. As time progressed, different events affected the design. Although most events came at expected and planned times, the most difficult problems to deal with came at unpredictable moments. A chronologically ordered summary of the important events and their repercussions follows.

5.5.1 Choosing the C-5 as the Carrier Plane

Originally the C-5 was chosen for ease and familiarity. Although it was not the largest plane, actually getting information about the aircraft was the most important factor. Using the C-5 originally limited the booster mass to 120,000 kg with a diameter of 3m.

5.5.2 Mission Analysis

Using a spread sheet based program, Mission Analysis determined that a booster that size would have a difficult time with any sizable payload. Facts on trajectories were unclear, and the program development was slow. From that information, the An-225 went back for consideration as a heavier lifting carrier vehicle.

With a second version of the trajectory program including a circular earth model, the mass of the booster could decrease and drop below the C-5's carrying capacity. Once again, the C-5 was then chosen as the carrier plane with an internal, roll out launch system. This turned out to be the final decision on the carrier aircraft.

5.5.3 System Integration

Using the information from the latest Mission Analysis program, the group created seven configurations using a variety of propulsion systems. Because of structural and performance constraints, most of these were eliminated shortly there after.

5.5.4 Mid-Term Report to NASA Lewis

As a class and project funded by the USRA and NASA, we decided to visit the NASA Lewis center and present a report about half way through the design process. The NASA Lewis trip allowed the group to see what things were expected for the final presentation. Only using three of the seven configurations, all storable liquid fueled, the trip solidified ideas about the project serving as a large deadline.

Vandenberg was chosen as the best launch site for its location away from populated areas, its abundance of appropriate facilities, and the new space industry company (CCSI) nearby. Although the C-5 has the capability, in air refueling for equator launching was excluded as a possibility for this mission based on logistical and tracking constraints.

The possibility of using gels also helped safety concerns if this technology would be available for our use in the future.

5.5.5 Preliminary Configuration

A booster with a mass of 110,000 kg capable of carrying 5,000 kg to LEO used configuration A, a single cylinder. Although length was a concern for the C-5, structurally, the booster's long thin shape generated concerns about the conditions during egress. Structures began work on designing an Aluminum structure for Athena. Power/Thermal/Controls continued work on the aircraft response.

5.5.6 Sled Consideration and Roll Out Masses

After some analysis on the structure, a sled would be required for Athena to survive the egress. This limited the diameter of the booster to 2.7 m to make room for a .3 m thick sled. It also increased the overall rolling mass to 120,000 kg (110, 000 kg booster and a 10,000 kg sled).

After more analysis of the plane's response to the egress of such a large and heavy vehicle, however, the mass was reduced. The total rolling mass was dropped to 90,000 kg for safety and response considerations. This made everyone change their idea of the design.

Each group scaled back. The overall booster mass was set at a maximum of 85,000 kg with a sled of 5,000 kg making the engines more inefficient for this lighter application. No engines could be added or changed, however, as that would affect the safety and monetary issues of the project. The payload was brought below the 5,000 kg goal for competitor cost constraining each groups material selection even more.

5.5.7 Selection of Final Configuration

The final configuration used a single cylinder design with a propulsion system similar to that of Titan rockets. Its total mass was 80,000 kg because of a heavier than expected sled of 10,000 kg. From the data available at that time, it was the most efficient design carrying 2,000 kg of payload into LEO.

5.5.8 Design Freeze Date

During the week between the configuration choice and the freeze date, new systems that added unexpected mass had to be included in the booster. Reaction control thrusters, extra fuel, larger fuel tanks, fuel tank baffles, avionics systems, and an unknown shroud mass assumed to be large all drove up the mass of the systems in the booster. Unfortunately to keep the total mass under 80,000 kg, keeping the same configuration, and not changing amounts of fuel, that extra mass needed for those systems came from the payload section to insure proper insertion into LEO.

As of the freeze date, the booster's mass was 80,600 kg having a length of 31.7 m carrying only 1300 kg of payload to LEO. This significantly reduced the share of market for Athena to launch. Also because the payload was lower than expected, the cost per kilogram of payload was higher than some competitors.

5.5.9 Another Iteration

Finally, after the project was presented and the term was over, the team went through a final iteration for the presentation in Pasadena. Knowing the extra masses allowed the team to bring up Athena's carrying capability to 1700 kg into LEO. Since the mass of the structures, fuel, and subsystems were kept fairly close to the original design, Athena's final mass was only 83,000 kg with a 4,000 kg sled that put the total rolling mass to 87,000 kg.

5.6 Group Decision Process

During the class, every group had to interact and work with every other group. Propulsion, Structures, and Mission Analysis were the groups primarily responsible for the iterative process. Other groups such as Mission Control, Aircraft Integration, and Power/Thermal/Control sent the constraints the booster had to conform to. Spacecraft Integration kept track of vital statistics and kept the cost in check. Payloads relayed how much each cut in payload mass reduced our market share as well as finding new potential customers for our capabilities.

The iterative step would follow a certain pattern. When a new constraint would come up, an estimate from the entire group of mass distributions would start the process going. Mission Analysis would find out how much fuel and how much payload the booster could carry with the new constraints. The new fuel masses would go to Propulsion for tank sizing and length determination. Structures would then calculate the actual mass of the structure for each stage necessary to carry the g-forces and bending constraints. These structure and tank masses would go back to Mission Analysis to make sure the numbers on burn times for each stage were still valid with earlier estimations. After that, depending on how close initial estimates were, there would or would not be another time through the loop. Each iteration took approximately a week.

5.7 Ideas Not Seen in Final Design

Throughout the course there were many ideas that came up to solve the problems we encountered. Many of them were adopted, but some were not accepted. The following section discusses those ideas that could have played a major impact in the design.

5.7.1 Solid Rocket Motors

Solid rockets could have provided a cheap, safe, and easy alternative to storable liquids. Unfortunately, due to initial thoughts on the C-5, the solids large enough to be useful were thought not to fit out the back cargo doors of the C-5. Smaller solid motors proved to be too expensive for the performance they added, especially with such a small booster to begin with. Because the design was limited to modern technology, no new solid motor designs were allowed.

5.7.2 Top Launch

We looked into launching Athena from the top of the An-225. We looked at wings and other lifting bodies and found that their mass, if added to Athena, would put the booster mass more than the total carrying capacity of any plane for a reasonably sized rocket. We also looked at rolling the booster off the top of the An-225 on rails that we would add. Unfortunately, not enough information was available for the An-225 to make the necessary calculations for airplane response. We decided to stay with the C-5 extraction method because it is proven, and information on the C-5 is more readily available.

5.7.3 Composite Structure

Composites are expensive, and not all the composites we found that we liked are in the fully developed stage. Because of that, the technology was not considered modern and off the shelf, and therefore, unusable by the goals set out earlier. The structures group found that they could design a structure using aluminum that was light and strong while remaining under cost using current technology.

5.7.4 Circular earth model for trajectory

The Mission Analysis program has gone from coordinate system to coordinate system trying to find something that seems reasonable. In order to get an intuitive feel for what was going on along with simplifying the model, a flat earth coordinate system provides the base of the current program. The circular earth model used difficult coordinate transformations and proved difficult to determine its veracity. The final model is based on a ballistic, single second time step, physical solution to the dynamic equations including drag, a variable gravity field and centripetal force.

5.7.5 Larger Payload Shroud

Our ability to use a payload bay built for two large packages decreased throughout the mass reductions. At one point, length was also a concern that helped to bring down the size of the payload bay and shroud. Currently, our payload bay is large for the mass of satellites we can carry. The fuel tanks have already been designed for the extra fuel needed to get to Geosynchronous Transfer Orbit (GTO) so no other engine or fuel tank volume shroud be required in the third stage. For our design, our payload bay provides ample room for any package in our mass capabilities.

5.7.6 Side By Side Fuel Tanks

When length was an important concern for the larger mass booster configuration, side by side fuel tanks were proposed as an answer. The C-5's cargo bay is a maximum 36 m long and 6 m wide. With tanks side by side in two tangential cylinders, the length could almost be cut in half. However, according to structure's analysis, the modeling for that would be difficult as well as the extra mass for more braces. After the goals were scaled down, however, length was not such an important consideration. It should also be noted that unless the rear doors of the C-5 are modified they only allow a 3 m clearance side to side. With those two facts in mind, choosing a single cylindrical design for our booster has the best integration with the C-5.

6.0 CONCLUSION

The final Athena project presented here is the result of long dedicated team work, research, and design techniques. Although it may not be the most efficient for its propulsion configuration and ascent trajectory, the Athena booster is a viable alternative to ground launching. Launch position, quick integration and payload preparation time, along with a lower cost still can lure customers away from ground based systems.

As part of a feasibility study, we found that if Athena were launched from the ground, however, with only eight extra seconds of burn time on the first stage, it would make it into a similar orbit. The energy savings for Athena do not directly out weigh the ground based boosters by that much.

When that is put with the other factors such as launching capabilities, however, Athena shows up as a beneficial means to place a satellite in orbit.

This design and the detail that follows show how a medium sized space booster can work. Athena could be put together and launched in three years providing a platform for many space and satellite missions to come.

STAGE 1	Total Mass:	55,153 kilograms
	Mass of Engine(s):	2,285 kilograms
	Mass of Fuel:	50,323 kilograms
	Mass of Fuel Tank:	1830 kilograms
	Mass of Structure:	715 kilograms
STAGE 2	Total Mass:	19,290 kilograms
	Mass of Engine(s):	584 kilograms
	Mass of Fuel:	17577 kilograms
	Mass of Fuel Tank:	803 kilograms
	Mass of Structure:	326 kilograms
STAGE 3 (LEO)	Total Mass:	5802 kilograms
	Mass of Engine(s):	220 kilograms
	Mass of Fuel:	5042 kilograms
	Mass of Fuel Tank:	310 kilograms
	Mass of Structure:	230 kilograms
PAYLOAD BAY	Total Mass:	2990 kilograms
(LEO)	Mass of Payload:	1715 kilograms
	Mass of Shroud:	885 kilograms
	Avionics:	390 kilograms
STAGE 3 (GTO)	Total Mass:	6629 kilograms
	Mass of Engine(s):	220 kilograms
	Mass of Fuel:	5869 kilograms
	Mass of Fuel Tank:	310 kilograms
	Mass of Structure:	230 kilograms
PAYLOAD BAY	Total Mass:	2163 kilograms
(GTO)	Mass of Payload:	888 kilograms
	Mass of Shroud:	885 kilograms
	Avionics:	390 kilograms

Overall Mass of the Athena Booster is 83,235 kilograms

Table 1.1 Mass Breakdown

STAGE 1	Outside Diameter:	2.7 meters
	Overall Length:	12.25 meters
	Engine(s):	1 x LR87-AJ11 Storable Liquid Rocket Motor
	Length of Engine(s):	3.84 meters
	Fuel:	Aerozine 50
	Length of Tanks:	8.41 meters
STAGE 2	Outside Diameter:	2.7 meters
	Overall Length:	7.65 meters
	Engine(s):	1 x LR91-AJ11 Storable Liquid Rocket Motor
	Length of Engine(s):	2.81 meters
	Fuel:	Aerozine 50
	Length of Tanks:	4.84 meters
STAGE 3	Outside Diameter:	2.7 meters
	Overall Length:	5.82 meters
	Engine(s):	2 x AJ10-138 Restartable-Storable Liquid Rocket Motor
	Length of Engine(s):	2.07 meters
	Fuel:	Aerozine 50
	Length of Tanks:	3.75 meters
PAYLOAD BAY	Outside Diameter:	2.7 meters at the base
	Overall Length:	6.0 meters

Table 1.2 Stage Breakdown

Chapter 2

System Integration

CHAPTER 2 -- SYSTEMS INTEGRATION

System Integration's Symbols

AL: Aluminum
d: displacement
E: elastic modulus
F: Force
I: moment of inertia
L: length

1.0 GROUP OVERVIEW

Our group used to be two separate groups, but due to a limited number of students participating in this project, the Aircraft Interface and Spacecraft Integration groups were merged into one group; Systems Integration. The purpose of Systems Integration was to:

- Keep track of the booster configuration (mass, lengths, size)
- Do a cost analysis to build our booster and compare with the competition
- Choose carrier aircraft
- Pre-flight procedures
- Fuel safety
- Integration timeline

2.0 BOOSTER CONFIGURATION

The Athena is designed to deliver 1715 kg to low earth orbit, and 888 kg to geosyncronous orbit. The total booster weight is 83,235 kg. The final detailed configuration is shown in Figure 2.4.

2.1 Propulsion

The Athena is a three stage booster. The first stage engine is an LR87-AJ11 mounted to the first stage stringer/compression ring structural configuration using a triad type mount. There are two cylindrical fuel tanks, the Aerosine-50 and the Oxidizer shown in Fig.2.0.1. They are mounted to the inside stringer/compression rings configuration. The LR87 provides the initial stage with 2,437,504 N of thrust to deliver the booster into the upper atmosphere. At this point the first stage drops off along with the first interstage ring. After a certain coast time the second stage fires.

The second stage uses LR91-AJ11 with 467040 N of thrust to deliver the booster to the second pre-orbit altitude. The LR91 also uses two cylindrical fuel tanks, the Aerosine-50 and the Oxidizer shown in Figure 2.4. The engine is mounted directly to the second stage Aerosine fuel tank. The tanks are mounted to the second stage stringer/compression ring configuration. At burnout, second stage drops off along with the second interstage ring and the payload faring which is extracted using small explosive chambers in the tip of the nose cone. The third stage and payload are set into a second coast.

PRECEDING PAGE BLANK NOT FILMED

The third stage engines are two AJ10-138's with 35584 N of thrust each and are mounted to the third stage stringer/compression ring configuration. After the second coast time the third engines fire delivering the booster into its target orbit. The AJ10 uses two spherical tanks, the first Aerosine, the second Oxidizer. The tanks are sized to accommodate the extra 952 kg of fuel for GTO delivery. The tanks are mounted to the third stage stringer/compression ring configuration. The third tank is the Hydrazine fuel for the Reaction/Control thrusters. These thrusters are used to adjust the axial spin stability (if applicable) of the satellite before it is released. Finally, the third stage releases the orbital satellite and descends to the atmosphere.

2.2 Avionics

The avionics equipment are mounted directly above the Oxidizer sphere of the third stage on a .06m disk of stringer material which extends into the payload area, see Figure 2.1. The satellite attachment is on the reverse side of the disk. The avionics equipment used are:

- Trimble Quadrex GPS Receiver (GPS)
- Litten LN-200 Inertial Measurement Unit (IMU)
- AITech Series 500 Flight Computer
    E101 - Board Enclosure
    C103 - Single Board Computer
    C401 - Communications Control Board
- Antennae
- Transmitters
- 2 14.52V Batteries (Four 3.63V Lithium Cells/battery)

The placement of these systems on the disk are shown in Figure 2.1. The position of the disk relative to the third stage Oxidizer tank is shown in Figure 2.2.

The guidance and power systems have an operating range of -40°C->+70°C (159.8°F). Research into the actual temperature in the guidance systems area was not conducted. Because of the large range in its operating temperature the problem of system failure due to temperature is not considered. A thermal protectant foam would be applied if further research proved necessary. A cooling system for the payload also was not researched. From further research a radiator system would have been designed to mount on the avionics disk. Guidance systems and power cabling are not shown in the figure.

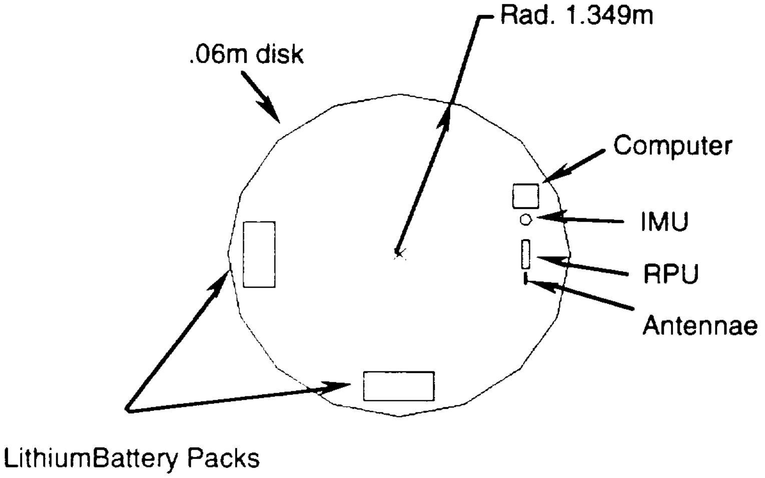

Figure 2.1: Avionics Placement Diagram

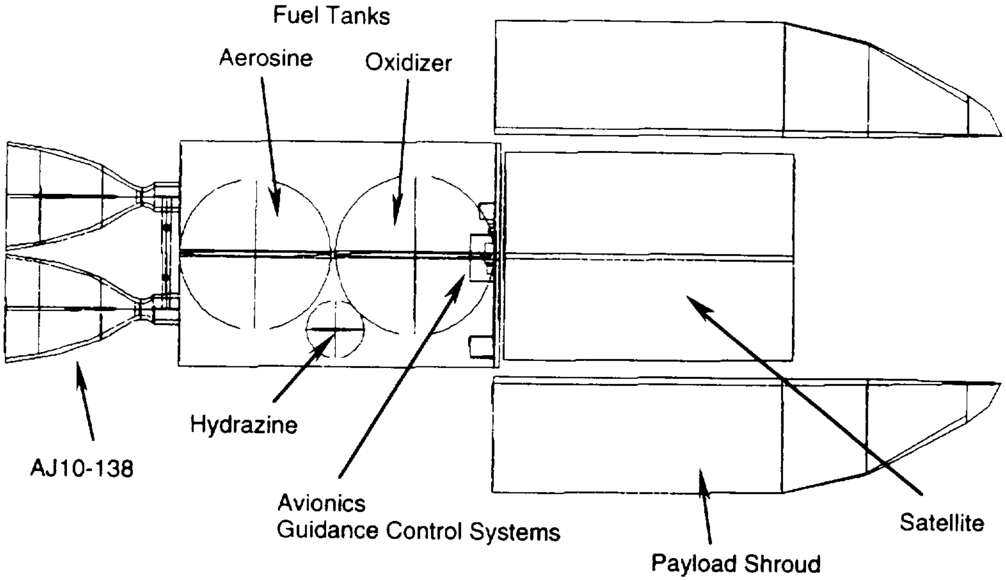
Fuel Tanks
Aerosine
Oxidizer
AJ10-138
Hydrazine
Avionics
Guidance Control Systems
Payload Shroud
Satellite

Figure 2.2: Third Stage Layout

2.3 Structures

The structural configuration used is a longitudinal z-stringer along the .001m skin with compression rings located laterally across the stringers. This structure supports the engine mounts, fuel tanks, guidance control system disk, payload and reaction/control thrusters mounted on the outside skin of the third stage.

Support Structure Configuration:

	Z-Stringers	Compression Rings
Stage	156	8
1st Interstage	56	2
Stage 2	36	4
2nd Interstage	36	2
Stage 3	24	6

The inside diameter of the compression rings is 2.5, the diameter of the first and second stage fuel tanks. The third stage tanks are spheres with diameters of 1.93m and 1.82m. Additional support structure mounted from stringer/compression ring configuration is used to support the two tanks.

2.4 Configuration Analysis

The moments of inertia and center of gravity where calculated and compiled for both full and empty tanks for each stage. The third stage calculations do not include the payload shroud. The center of gravity positions are shown in Figure 2.3. The Ideas program output of booster configuration analysis is attached to the report for further reference.

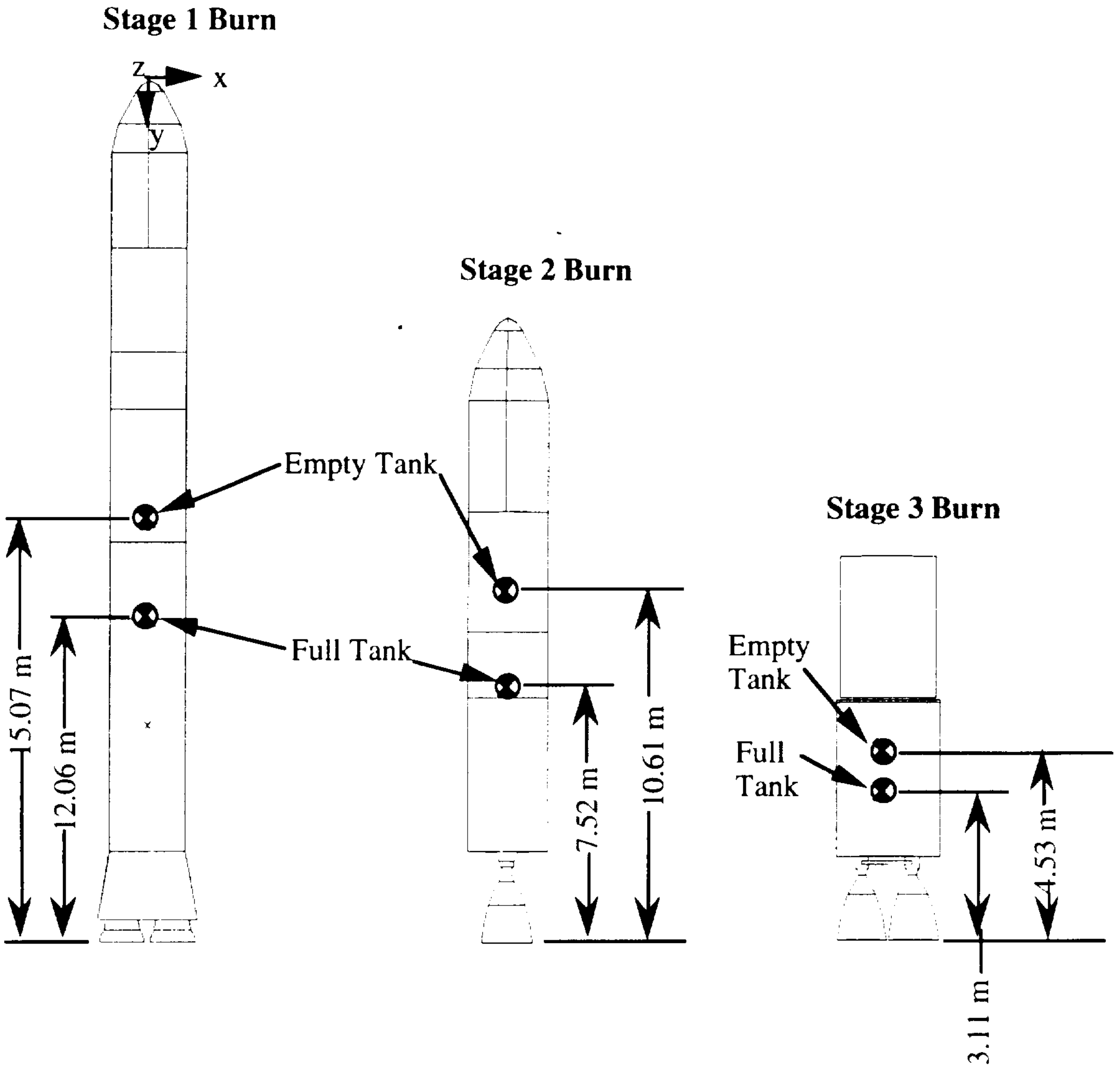

Stage 1 Burn

Stage 2 Burn

Stage 3 Burn

z
x
y
Empty Tank
Full Tank
15.07 m
12.06 m
7.52 m
10.61 m
Empty Tank
Full Tank
4.53 m
3.11 m

Figure 2.3: Center of Gravity Locations

STAGE 1 BURN, FULL TANKS

Surface Area	368.6073 m^2		
Volume	177.5405 m^2		
Average Density	497.2655 kg/m^3		
Mass	88284.73 kg		
Center of Gravity	12.06 m		
Moments of Inertia w.r.t. system axes	I_{xx} = 4.461041E+06 I_{xy} = 0.0	I_{yy} = 78,408.19 I_{yz} = 0.0	I_{zz} = 4.461041E+06 I_{xz} = 0.0
Rotation Matrix from System axes to principal axes			
row #1	0.0	1.0	0.0
row #2	1.0	0.0	0.0
row #3	0.0	0.0	-1.0
Rotation angles from System to Principal axes			
	angle about x	180.0 °	
	angle about y	0.0 °	
	angle about z	90.0 °	
Principal moments of Inertia	I_{11} = 78,408.19	I_{22} = 4.461041E+06	I_{33} = 4.461041E+06

Table 2.1 Center of Gravity (Stage 1 -- Full)

STAGE 1 BURN, EMPTY TANKS

Surface Area	368.6073 m^2		
Volume	177.5405 m^2		
Average Density	269.7673 kg/m^3		
Mass	47,894.60 kg		
Center of Gravity	15.07 m		
Moments of Inertia w.r.t. system axes	I_{xx} = 3.252826E+06 I_{xy} = 0.0	I_{yy} = 42,536.56 I_{yz} = 0.0	I_{xx} = 3.252826E+06 I_{xz} = 0.0
Rotation Matrix from System axes to principal axes			
row #1	0.0	1.0	0.0
row #2	1.0	0.0	0.0
row #3	0.0	0.0	-1.0
Rotation angles from System to Principal axes			
	angle about x	180.0 °	
	angle about y	0.0 °	
	angle about z	90.0 °	
Principal moments of Inertia	I_{11} = 42,536.56	I_{22} = 3.252826E+06	I_{33} = 3.252826E+06

Table 2.2 Center of Gravity (Stage 1 -- Empty)

STAGE 2 BURN, FULL TANKS

Surface Area	243.0474 m^2		
Volume	109.1913 m^2		
Average Density	310.4424 kg/m^3		
Mass	33,897.61 kg		
Center of Gravity	7.52 m		
Moments of Inertia w.r.t. system axes	I_{xx} = 521,241.0 I_{xy} = 0.0	I_{yy} = 30,105.43 I_{yz} = 0.0	I_{xx} = 521,241.0 I_{xz} = 0.0
Rotation Matrix from System axes to principal axes			
row #1	0.0	1.0	0.0
row #2	1.0	0.0	0.0
row #3	0.0	0.0	-1.0
Rotation angles from System to Principal axes			
	angle about x	180.0 °	
	angle about y	0.0 °	
	angle about z	90.0 °	
Principal moments of Inertia	I_{11} = 30,105.43	I_{22} = 521,241.0	I_{33} = 521,241.0

Table 2.3 Center of Gravity (Stage 2 -- Full)

STAGE 2 BURN, EMPTY TANKS

Surface Area	243.0474 m^2		
Volume	109.1913 m^2		
Average Density	118.2324 kg/m^3		
Mass	12,909.94 kg		
Center of Gravity	10.61 m		
Moments of Inertia w.r.t. system axes	$I_{xx} = 271{,}658.3$ $I_{xy} = 0.0$	$I_{yy} = 11{,}465.69$ $I_{yz} = 0.0$	$I_{xx} = 271{,}658.0$ $I_{xz} = 0.0$
Rotation Matrix from System axes to principal axes			
row #1	0.0	1.0	0.0
row #2	1.0	0.0	0.0
row #3	0.0	0.0	-1.0
Rotation angles from System to Principal axes			
	angle about x	180.0 °	
	angle about y	0.0 °	
	angle about z	90.0 °	
Principal moments of Inertia	$I_{11} = 11{,}465.69$	$I_{22} = 271{,}658.3$	$I_{33} = 271{,}658.3$

Table 2.4 Center of Gravity (Stage 2 -- Empty)

STAGE 3 BURN, FULL TANKS, NO PAYLOAD FAIRING

Surface Area	124.0270 m^2		
Volume	52.55912 m^2		
Average Density	171.9172 kg/m^3		
Mass	9,035.816 kg		
Center of Gravity	3.11 m		
Moments of Inertia w.r.t. system axes	I_{xx} = 31,811.37 I_{xy} = 0.0	I_{yy} = 8024.966 I_{yz} = 0.0	I_{xx} = 31,811.37 I_{xz} = 0.0
Rotation Matrix from System axes to principal axes			
row #1	0.0	1.0	0.0
row #2	1.0	0.0	0.0
row #3	0.0	0.0	-1.0
Rotation angles from System to Principal axes			
	angle about x	180.0 °	
	angle about y	0.0 °	
	angle about z	90.0 °	
Principal moments of Inertia	I_{11} = 8024.966	I_{22} = 31,811.37	I_{33} = 31,811.37

Table 2.5 Center of Gravity (Stage 3 -- Full)

STAGE 3 BURN, EMPTY TANKS, NO PAYLOAD FAIRING

Surface Area	124.0270 m^2		
Volume	52.55912 m^2		
Average Density	42.44666 kg/m^3		
Mass	2,230.959 kg		
Center of Gravity	4.53 m		
Moments of Inertia w.r.t. system axes	$I_{xx} = 14,871.43$ $I_{xy} = 0.0$	$I_{yy} = 1,981.378$ $I_{yz} = 0.0$	$I_{xx} = 14,871.43$ $I_{xz} = 0.0$
Rotation Matrix from System axes to principal axes			
row #1	0.0	1.0	0.0
row #2	1.0	0.0	0.0
row #3	0.0	0.0	-1.0
Rotation angles from System to Principal axes			
	angle about x	180.0 °	
	angle about y	0.0 °	
	angle about z	90.0 °	
Principal moments of Inertia	$I_{11} = 1,981.378$	$I_{22} = 14,871.43$	$I_{33} = 14,871.43$

Table 2.6 Center of Gravity (Stage 3 -- Empty)

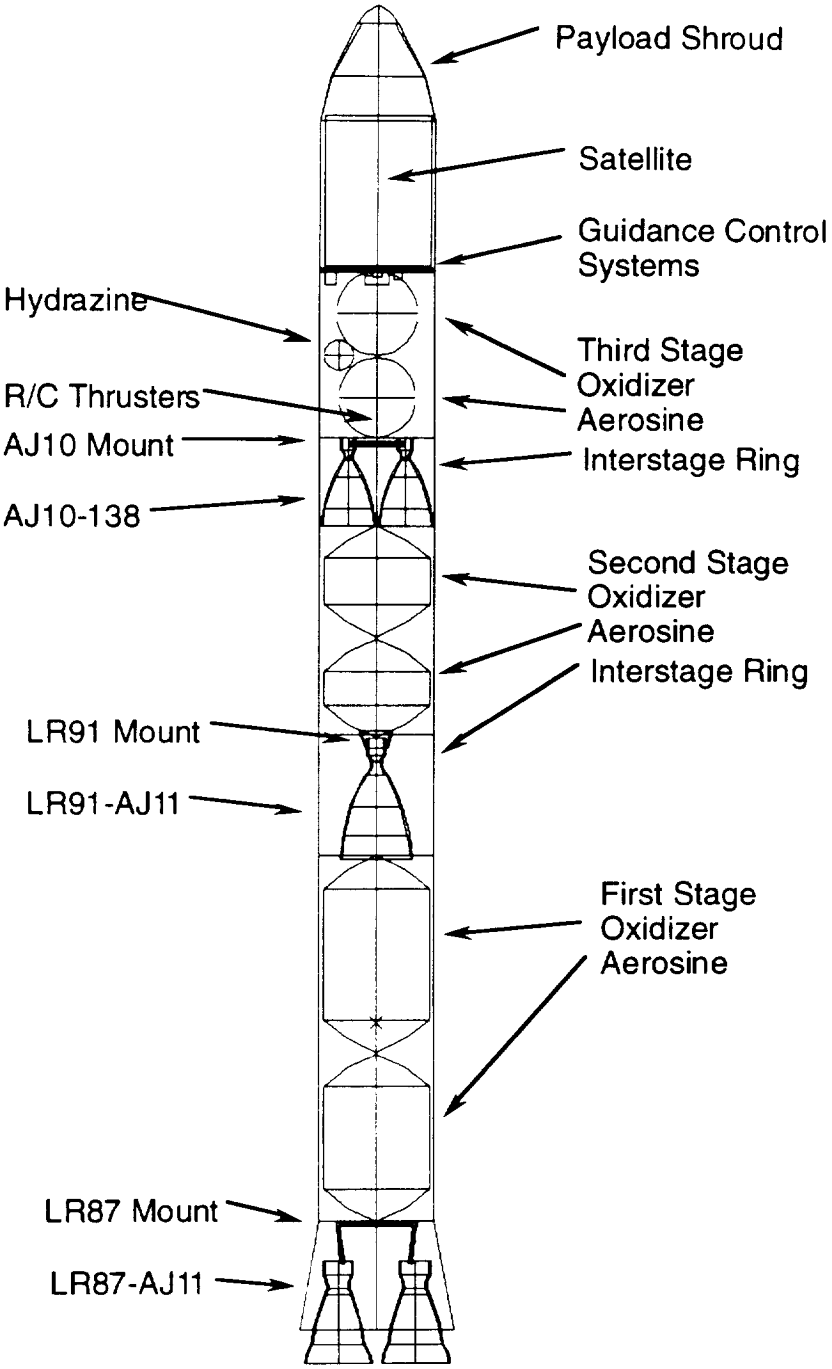
Payload Shroud
Satellite
Guidance Control Systems
Hydrazine
Third Stage Oxidizer Aerosine
R/C Thrusters
AJ10 Mount
Interstage Ring
AJ10-138
Second Stage Oxidizer Aerosine
Interstage Ring
LR91 Mount
LR91-AJ11
First Stage Oxidizer Aerosine
LR87 Mount
LR87-AJ11

Figure 2.4: Booster Configuration

3.0 INTEGRATION TIMELINE

In order to make sure the Athena program runs on time, an integration timeline needed to be designed. The timeline is designed to cover all the major operations going on at Vandenberg Air Force Base from the time the engines and parts show up to the post flight analysis. The timeline designed can be seen in Figure 2.5. It is based on a six launch per year time scale giving approximately eight weeks per launch. If the number of launches is increased or decreased, the time frame can be adjusted accordingly.

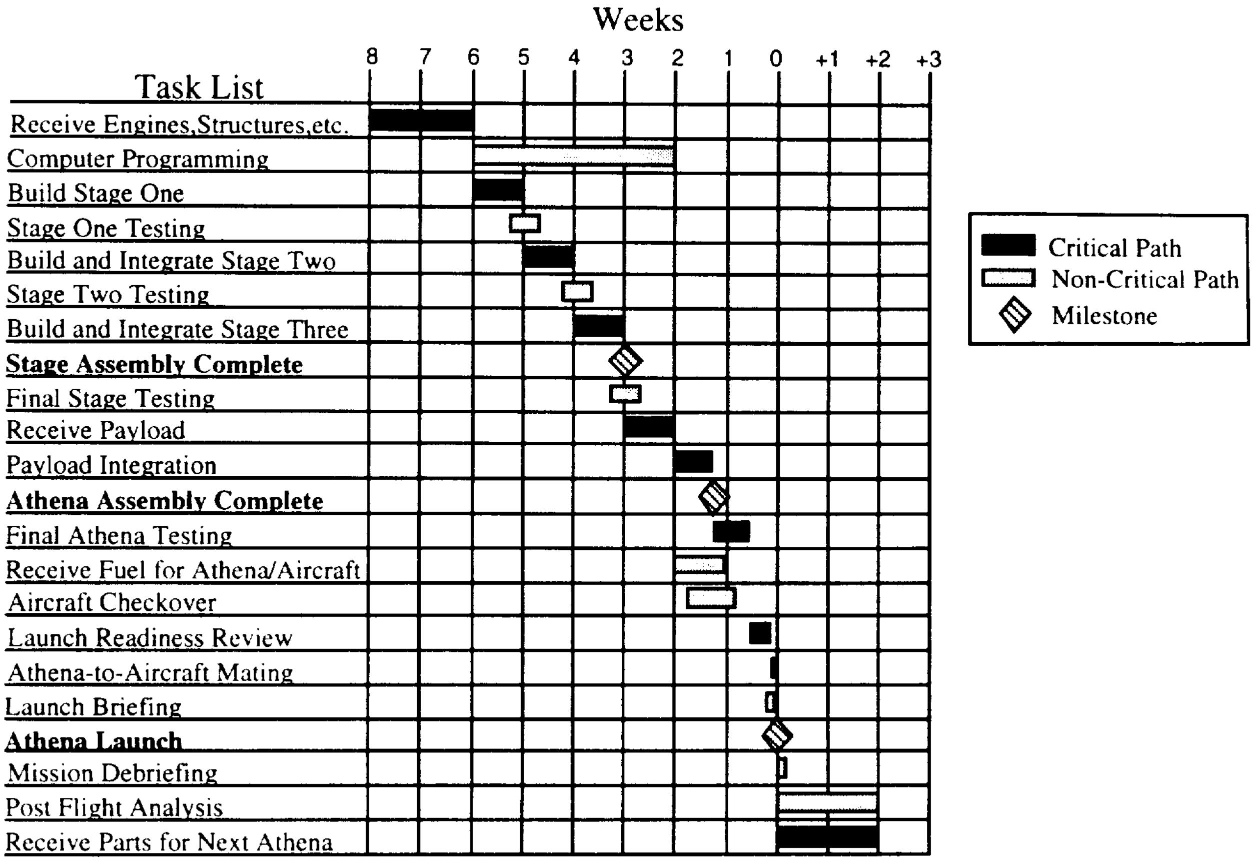

Figure 2.5: Integration Timeline

3.1 Task List Assignments

Figure 2.5 has a long task list of assignments. These assignments will be defined in this section.

3.1.1 Receive Engines, Structures, etc.

A two week period is assigned in which we want to assemble all the engines, structures, fuel tanks, and other parts necessary to assemble the Athena stages. A two week period gives plenty of time for all the parts to be received from the various manufacturers. Once all the parts are verified and accounted for, assembly can begin.

3.1.2 Computer Programming

The navigation and guidance computers will be shipped in the same time as the engines and structure, so programming of the system can begin right when assembly begins. The programming is independent of the actual assembly and extends for four weeks. The programming can get done early, but the four week period would mark the absolute deadline.

3.1.3 Build Stage One, Build and Integrate Stages Two and Three

These three assembly stages require the engines, fuel tanks, structure, and other parts for each stage to be put together and integrated with the other stages. Each stage is allocated a week of assembly time.

3.1.4 Stage Testing and Final Stage Testing

Near the end of each stage assembly, a period of about four to five days is spent testing to make sure each stage is assembled properly, any moving parts work, etc. The final stage testing comes after all the stages have been integrated, and it gives a complete check-over of the staging system.

3.1.5 Receive Payload and Payload Integration

Two to three weeks before Athena launch, a window is set in which we expect to receive the payload satellite. This week gives ample time to handle any delays the satellite manufacturer may have in delivering its package. After the satellite arrives, the payload integration begins and lasts about six days. In this period, the payload is processed, cleaned in a 10K clean room, integrated into the third stage, and encapsulated into the payload fairing.

3.1.6 Final Athena Testing

This testing lasts five to six days and marks the final complete check-over of the Athena booster. All the engines, connections, and mechanics are examined, and the computer programming is evaluated to make sure it works properly.

3.1.7 Receive Fuel for Athena/Aircraft

One to two weeks before Athena launch, the fuel for both the Athena booster and the Chimaera is expected to be shipped into Vandenberg. The fuel would then be stored for the week or two left before launch. Receiving the fuel at this time lessens the fuel storage time, but also gives sufficient time for its arrival before the launch date.

3.1.8 Aircraft Check-over

A week and a half before the launch date, the Chimaera should be at Vandenberg and available for a systems check-over. The aircraft will be evaluated to make sure it is ready for the mission. Having the Chimaera a week before launch guarantees adequate time to prepare for the Athena-to-Aircraft mating.

3.1.9 Launch Readiness Review

The final evaluation. All aspects of the Athena project will be looked over to make sure everything is operating up to standards. If not, the mission launch may be delayed. If everything passes standards, the mission is a go.

3.1.10 Launch Briefing and Mission Debriefing

The launch briefing discusses all the procedures and operations to be done during the launch. The mission debriefing looks over all the actions taken during the launch and evaluates performance.

3.1.11 Post Flight Analysis/Receive Parts for Next Mission

The post flight analysis lasts for two weeks after the Athena launch date. In this two weeks, all the recorded data from the launch is examined and performance is evaluated. If any failures occurred, they are addressed during the post flight analysis. The post flight analysis coincides with the receiving period for the next set of parts for a new Athena booster. While the Athena project waits for the parts to come in, the mission data can be looked over. If the number of launches per year is boosted up to seven, then this period will be cut back to a week.

3.2 Deviations

No booster program will run flawlessly, so deviations and delays need to become an assumed and acceptable factor of any timeline. Some of the deviations and delays and the ways to deal with them are discussed in the sections below.

3.2.1 Safety Concerns

The safety of personnel and the Athena is always of utmost concern. If continuing with a stage of the program is not advantageous to personnel and the Athena, delays will be taken to allow time to rectify the problem. Some of these problems are just faulty parts, and these just require a new part to be ordered or the old part repaired. Other delays are further from our control, like the weather. Launch and transfer of the Athena can be delayed due to inclement weather conditions. There is enough leeway in the schedule to allow for some small weather delays, but if a large disaster like an earthquake strikes, the Athena project may have to be put on hold indefinitely.

3.2.2 Construction Delays

Construction delays will occur when trouble arises when assembling the Athena stages or the stage parts do not arrive on time. Assembly difficulty can be covered by extending the stage assembly time by a few days, but any longer and the launch date will have to be pushed back. The timeline also has tried to give a large enough window for the arrival of stage parts and payload. These windows give two weeks for the arrival of stage parts (engine, fuel tanks, etc.), and a week for the payload to arrive.

3.2.3 Aircraft Limitations

The Chimaera C-5B aircraft can be another source of delay time. The Chimaera needs to be fully operational in order for the Athena launch to happen. The Chimaera is supposed to be acquired a week and a half before the Athena launch date to give plenty of time to check over the entire aircraft.

4.0 CARRIER AIRCRAFT - *THE CHIMAERA*

The Athena booster project requires as its zero stage a large transport aircraft capable of carrying large payloads to high altitudes. The Systems Integration group considered several aircraft to accomplish this mission, including two produced in Ukraine, part of the ex-Soviet Union. After comparing the candidates performance and availability, we decided to use the Lockheed C-5B Galaxy as our launch platform.

4.1 Lockheed C-5B Galaxy Capabilities

The Lockheed C-5B Galaxy is a heavy logistics transport aircraft currently used by the United States Air Force. The current version of the C-5 became operational in 1985. The C-5B was selected as the launch platform for the Athena because of its lifting capabilities, air-drop readiness and availability. Figure 2.6 shows the C-5B Galaxy configuration.

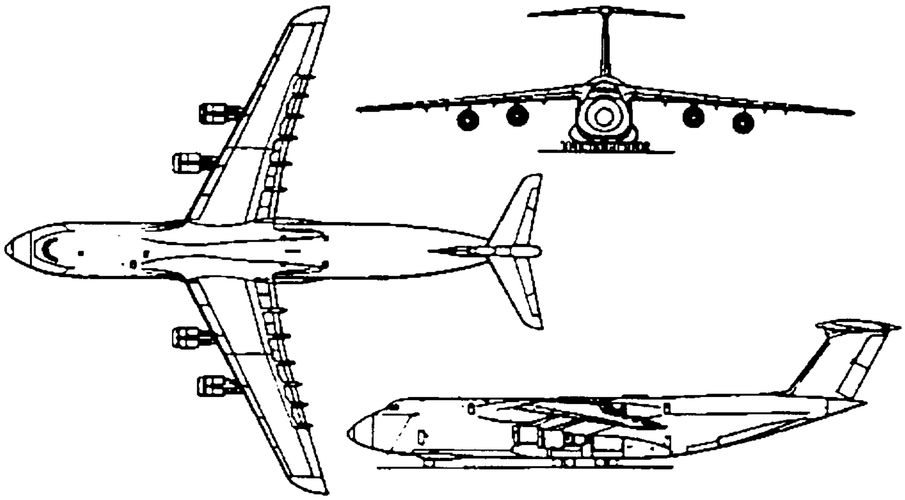

Figure 2.6: Lockheed C-5B Galaxy

4.1.1 C-5B Description

The C-5B is powered by four General Electric TF39-GE-1C turbofans rated at 43,000 lb static thrust each. It has a total fuel capacity of 51,150 US gallons in twelve integral fuel tanks. The C-5B is capable of being refueled in flight, which increases our mission flexibility.

The standard crew of five consists of a pilot, co-pilot, flight engineer and two loadmasters. There is also a seating area for up to fifteen people located at the front of the upper deck. The Athena control center and operator will be located in this area.

The cargo bay is accessed via a 'visor' type upward hinged nose and rear 'clamshell' type doors. This allows for simultaneous loading and unloading of cargo. The rear loading ramp forms the under surface of the fuselage. The cargo bay may be equipped with aerial delivery system (ADS) rails for air-drop missions.

The C-5B is equipped with four 60-80 kVA AC engine driven generators. These generators meet the electrical requirements of the launch control panel computers, and are also capable of supplying the Athena with power during transport to launch site.

4.1.2 C-5B Dimensions

Listed below are some important dimensions of the C-5B.

External:

Wing span	73.30 m (240 ft 5.25 in)
Wing aspect ratio	8.55
Length overall	69.10 m (226 ft 8.5 in)
Height overall	20.78 m (68 ft 2.25 in)
Aft loading opening	
max. height	3.93 m (12 ft 10.75 in)
max. width	5.79 m (19 ft 0 in)

Internal:

Cargo bay	
Max. height	4.09 m (13 ft 5 in)
Max. width	5.79 m (19 ft 0 in)
Length, without ramps	36.91 m (121 ft 1 in)
Length, with ramps	44.09 m (144 ft 8 in)

For airdrop operations, the aft cargo bay doors are partially opened to allow egress of a cargo up to 3.68 m (12 ft 1 in) wide and 3.93 m (12 ft 10.75 in) high. During such an operation, the rear loading ramp partially lowers to become coplanar with the rest of the cargo bay. The ramp is then locked into position using ADS links.

4.1.3 C-5B Weights and Loading

Listed below are some important weights and loading.

Operating weight empty, equipped	169,643 kg (374,000 lb)
Max. payload	118,387 kg (261,000 lb)
Max. fuel weight	150,815 kg (332,500 lb)
Max. takeoff weight	379,657 kg (837,000 lb)
Max. zero-fuel weight	288,030 kg (635,000 lb)
Max. landing weight	288,415 kg (635,850 lb)

4.1.4 C-5B Performance

Listed below is performance data for the C-5B at maximum takeoff weight.

Max. cruising speed at 7,620 m (25,000 ft)	908 km/h (564 mph)
Max. rate of climb at sea level	525 m/min. (1,725 ft/min.)
Service ceiling	10,895 m (35,750 ft)

Takeoff run at sea level	2,530 m (8,300 ft)
Landing run, max. landing weight	725 m (2,380 ft)
Range with max. fuel	10,411 km (6,469 miles)
Range with max. payload	5,526 km (3,434 miles)

4.2 Alternative Aircraft

The C-5B Galaxy was not the only aircraft considered for this mission. Also considered were the Ukrainian-built An-124 and An-225, both of which are larger than the C-5B. However, neither of these aircraft fulfilled all of the necessary requirements as well as the C-5B.

4.2.1 An-124

The An-124 is nearly identical to the C-5B in appearance. The most noticeable difference is its low-mounted horizontal tailplane, compared to the Galaxy's high-mounted tailplane. The An-124 is powered by four ZMKB Progress D-18T turbofans which produce 51,590 lb of static thrust each. Unlike the C-5B, however, the An-124 is 100% fly-by-wire.

Listed below are some important dimensions of the An-124.

External:	
Wing span	73.30 m (240 ft 5.25 in)
Wing aspect ratio	8.55
Internal:	
Cargo bay	
Max. height	4.4 m (14 ft 5.25 in)
Max. width	6.4 m (21 ft 0 in)
Length	36.0 m (118 ft 1.25 in)

Listed below are some important weights and loading.

Operating weight empty, equipped	175,000 kg (385,800 lb)
Max. payload	150,000 kg (330,693 lb)
Max. takeoff weight	405,000 kg (892,872 lb)
Max. zero-fuel weight	325,000 kg (716,500 lb)

Listed below is performance data for the An-124 at maximum takeoff weight.

Max. cruising speed	865 km/h (537 mph)
Max. rate of climb at sea level	525 m/min. (1,725 ft/min.)
Takeoff run at sea level	2,520 m (8,270 ft)
Landing run, max. landing weight	900 m (2,955 ft)
Range with max. fuel	16,500 km (10,250 miles)
with max. payload	4,500 km (2,795 miles)

The An-124, although out-performing the C-5B in some areas, does present some problems to our mission profile. The An-124 is not in-air-refuelable, which limits our capability to launch at any inclination. The An-124 would also have to be purchased for our uses, and we would have to train our own flight crew. The C-5B is in-air-refuelable, and we can contract the U.S. Air Force to conduct our missions, thus reducing our overhead cost.

4.2.2 An-225 Mriya (Dream)

The An-225 the only aircraft in the world designed to take off at a weight of over one million pounds. It is essentially a stretched An-225 with six turbofan engines rather than four. The internal cargo bay height and width remain unchanged. However, the An-225 was designed to carry the Russian space shuttle, and is therefore not equipped to handle payloads internally. More importantly, the An-225 does not have rear cargo bay doors, and thus major modifications would need to be made to the aircraft for it to carry the Athena internally. External transport and launch methods were studied, but these created more problems than they solved. The An-225 also suffers from the same problem as the An-124 in that it is not in-air-refuelable.

All of these problems could be overcome could be overcome to produce a viable launch platform which is larger than the C-5B. However, there is a more important issue which practically eliminates the An-225 from consideration - only one exists. Others could be produced, but the amount of money necessary to purchase the aircraft up front would prohibit the project from ever getting off the ground.

4.3 Air Drop Testing Procedure

In order to determine the safety of the air drop operation and to practice loading and egress procedures, the Systems Integration group developed an air drop test plan.

4.3.1 Test Drop Number 1

The first air drop will be done at 75% of the intended mission launch weight. We begin our testing at this level since the Minuteman air launch test program, conducted by Lockheed in 1978, successfully air dropped a load of approximately 50% of our intended mission launch weight.

This first test will require the construction of a Booster Transport System (BTS) sled. Concrete blocks will be attached to the BTS to achieve the desired weight. The parachutes which will be employed for a normal mission will be used. A chase plane will also be needed to watch for any external abnormalities and also to film the BTS egress.

4.3.2 Test Drop Number 2

The second air drop will be at an increased weight of 105% of the intended mission launch weight. This test is to be done at greater than mission launch weight to allow us a small margin of safety. Other test requirements are identical to test drop number 1.

4.3.3 Test Drop Number 3

The third air drop will test the structural integrity of Athena during egress. This test will be done with a booster shell, with no engines, mounted on the BTS as would be done for a normal mission. The fuel tanks will be filled with an inert liquid of the same density as the rocket propellants to simulate the actual movements of the liquid propellants. This test will be conducted as if it were a real mission, with all safety measures being taken throughout the pre-launch and launch activities. This will allow ground and flight crews to become familiarized with all necessary safety procedures.

4.3.4 Test Drop Number 4

The final air drop test will be done with a near-fully operational booster. Only the first stage of the booster will be equipped with its engine and fueled. The second and third stage fuel tanks will be filled with an inert liquid, as in test drop number 3, to simulate the actual launch weight and movement of the vehicle. Full guidance and navigational equipment will be installed, and Trajectory Tracking and Control (TTC) facilities will be operated. Again, safety procedures will be adhered to as if this were an actual mission.

Following the successful egress and stabilization of the booster, the first stage engine will be ignited. Once the booster has begun upward movement, the self-destruct mechanism will be tested, and the booster destroyed.

Unless difficulties arise during tests 1 through 4, no additional air drop tests will be necessary, and actual mission launches may commence.

4.4 Chimaera Range Capabilities

In order to determine the range the Chimaera could travel with any various payload weight, an analysis was done comparing payload weight to aircraft range. In order to do this analysis, data was taken from *Jane's All the World's Aircraft 1988-1989* on the capabilities of the C-5B. The data recorded is shown in Table 2.7.

Empty Weight =	169643.5kg
Max Payload =	118387.6kg
Max Fuel =	150819.5kg
Max Take-Off Weight =	379656.8kg
At Max Fuel with No Payload, Range=	10411km
At Max Payload, Range =	5526km

Table 2.7: Aircraft Data for Range Analysis

Using the last two pieces of information in Table 2.7 as end points, a linear fit was done to find the slope at which the kilometers per kilogram was changing with payload. Then taking intervals of 2000kg payload masses, data points were amassed to create Figure 2.7.

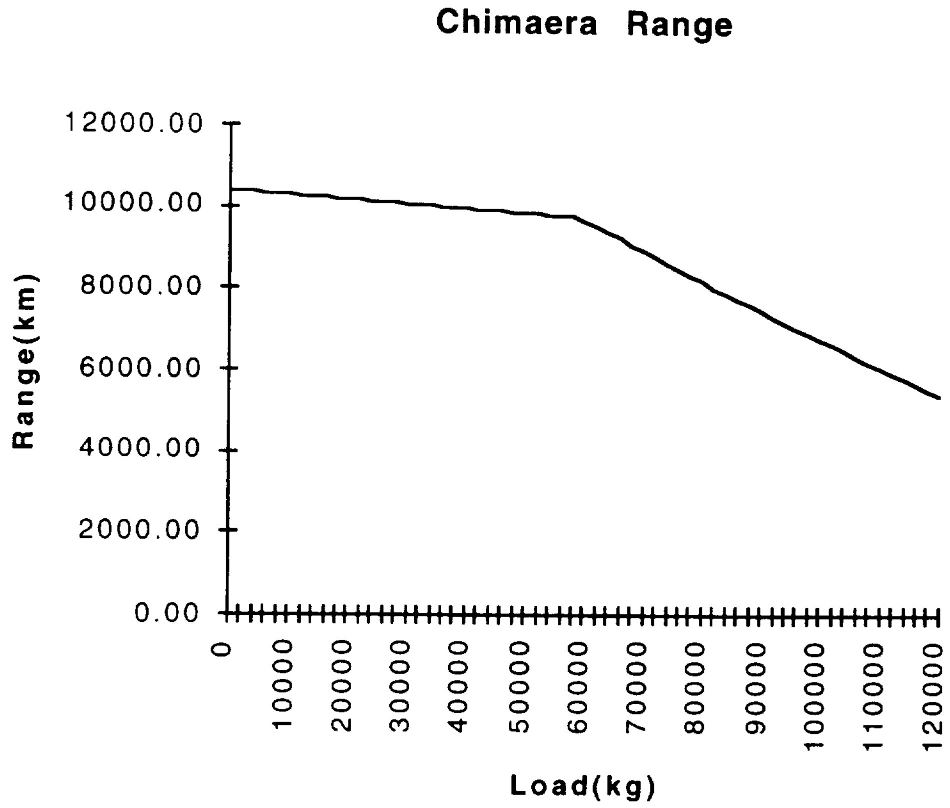

Figure 2.7: Graph of Chimaera Range vs. Payload (raw data for Figure 2.7 can be found in the Appendix A.2)

The final Athena mass along with the carraige is 83379.8kg. At this mass, the Chimaera is carrying:

$$379656.8kg - 169643.5kg - 83379.8kg = 126633.5kg\_fuel$$

With 126633.5kg of fuel, the range of the Chimaera is:

$$126633.5kg \times [0.069030\,km/kg - (\tfrac{83379.8kg}{118387.6kg}) \times 0.008719\,km/kg] = 7963.9km$$

In this equation, 0.069030km/kg is the range per kilogram fuel at zero payload, 83379.8/118987.6 is the mass fraction of total payload, and 0.008719km/kg is the difference in range per kilogram fuel between zero and maximum payload.

4.5 Wing Bending Modes

An approximate EI value for the Chimaera's wings needed to be found in order for the Structures group to do a bending mode analysis. This analysis is necessary to make sure the wing modes are not the same as those of the Athena and its cradle, otherwise disastrous vibrations will occur. The attempt to find an approximate EI value for the Chimaera's wings was started by trying to fit an elliptical lift distribution to the wing, and including a distributed fuel weight and engine weights. Trying to solve for EI this way proved to be very difficult, so a simpler wing model was suggested. A rectangular lift distribution was fit to the wing, and the maximum displacement at the tip of the wing was approximated. Figure 2.8 shows the wing loading and wing length.

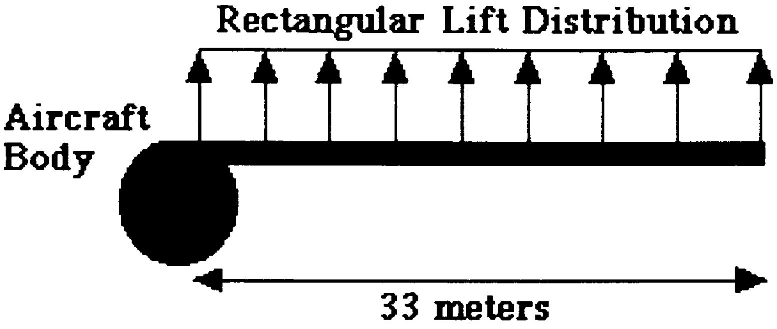

Figure 2.8: Aircraft Wing Lift Distribution

The length of the wing is 33 meters, total lift on the wing is 1.798x10^6 Neutons, and the approximated maximum wing tip displacement is 3.1meters. The following equation is then used to find EI:

$$EI = \frac{FL^3}{8\delta}$$

$$\delta = 3.1m$$

$$L = 33m$$

$$F = 1.798 \times 10^6 N$$

The results are then:

$$EI = 2.605 \times 10^9 N \bullet m^2$$

$$E_{AL} = 72 \times 10^9 N/m^2$$

$$I_{AL} = 0.0362 m^4$$

The E_{AL} is the elastic modulus and I_{AL} is the moment of inertia for the aluminum beam used in modeling the Chimaera wing. The Structures group then used this data to compute wing modes.

5.0 PRE-FLIGHT OPERATIONS

Once all the parts for the Athena are transported to the launch site and assembly area, the pre-flight operations seeing into gear. With the choice of Vandenberg Air Force Base as our assembly and launch point, we will be able to use the facilities and capabilities of the California Commercial Spaceport Inc. (CCSI). Located within Vandenberg Air Force Base, the CCSI facilities consist of the Integrated Processing Facility and the Cypress Ridge Launch Facility. The Integrated Processing Facility, which has already been activated, is capable of providing complete booster and payload processing, payload fairing cleaning and storage, and payload fairing encapsulation. The Cypress Ridge Launch Facility provides total launch services to all customers and should be operational by mid-1995. For the Athena, all we need to use is the Integrated Processing Facility because the Athena will be carried on-board the Chimaera and no ground launch facilities will be needed. There does need to be a process to transport the Athena to the Vandenberg runway from the Integrated Processing Facility. Once the Athena is mated with the Chimaera at the runway, the storable liquid fuels need to be loaded into the Athena, and then a final checklist needs to be evaluated. A contact at the CCSI was made to assist in informing our group of what the CCSI can do for our project. Our contact and source for all CCSI information is listed below.

Dominick R. Barry
Director, Business Operations
California Commercial Spaceport, Inc.
3865 Constellation Road, Suite A
Vandenberg Village, California 93436
(805) 733-7370

5.1 Athena Stage Assembly

Stage assembly will take place in the Integrated Processing Facility (IPF). Once all the various components are delivered to the IPF, a horizontal assembly procedure will be implemented. The Athena is assembled horizontal because this is the way it will be positioned in the Chimaera. The stage segments will be assembled on the support cradle, and then both the Athena and cradle will be placed on a transport trailer to move it over to the Vandenberg runway. Since the stages will not be fueled during assembly and transport, the maximum weight that needs to be lifted is 13257.8kg (during transfer of Athena to transport trailer). The IPF does not normally do horizontal assemblies, so it is cheaper and easier to construct Athena vertically. Once built, Athena will be tipped horizontally and placed on its cradle. The IPF has all the cranes and testing equipment necessary in Athena assembly. The IPF will also assist in the construction and fabrication of any additional structures needed in our assembly operation.

Assembly begins with the first stage LR87-AJ-11 engine and fuel tanks. The engine and fuel tanks are mated with the structure, and then testing of the first stage begins. Before this testing is done, the second stage LR91-AJ-11 engine and fuel tanks are brought into alignment with the first stage. The second stage engine and fuel tanks are mated with their structure and then mated to the first stage. Further testing is done, and then the third stage AJ10-138 engines and fuel tanks are brought into alignment with the first and second stage. The third stage engines and fuel tanks are mated with their structure and then mated to the first and second stages. The third stage computer equipment and navigation tools are then integrated into the system. Final testing is done on the stages, and then the payload is configured and integrated.

5.2 Payload Integration

The Integrated Processing Facility is one of the most capable payload processing facilities ever constructed. The IPF can handle large Shuttle-sized satellites in its 100K clean conditions. The IPF maintains a complete watch of temperature, humidity, and particulate levels in order to create the necessary environment for any satellites used as our payload. Our payload will arrive two the three weeks before launch. The payload will then be processed, cleaned in a 10K clean room, integrated into the third stage, and encapsulated into the payload fairing. Testing is run over the entire Athena booster. When done, the Athena is ready for transportation.

5.3 Athena Booster Transport

The Athena is assembled at the Integrated Processing Facility (IPF) and launched from the runway, which are approximately two miles apart. This distance requires the assembled booster to be transported, which causes safety concerns. The assembled, unfueled booster will be transported from the IPF, by truck, to the runway where it will be loaded onto the C-5B and fueled just prior to takeoff.

5.3.1 Athena - Truck Integration

The Athena will be loaded onto a standard trailer capable of carrying 14,200 Kg. The sled will be loaded onto the trailer prior to booster integration and, since the Athena is assembled vertically, the booster will be lowered onto the sled and bolted to the sled while both are sitting on the trailer. This allows for proper alignment between the sled and booster and also ensures that the booster and sled are loaded on the trailer properly. The top of the booster (nose cone) will face the rear of the trailer so the booster can be loaded from the front of the C-5B. A system of rollers similar to the C-5B's Air Delivery System (ADS) rails will be installed on the trailer to ease the transport from the trailer to the aircraft. The minimum personnel needed for this stage in the mission is 9: 1 crane operator and 8 people to guide the booster into place on the sled.

5.3.2 Athena Transport

The transport from the IPF to the runway is of great concern due to the large booster size and weight. The decision to carry an empty booster was based on two major factors: (1) the booster would be two heavy for any commercial truck and trailer to carry and (2) the hazard of carrying the extremely flammable fuel on a populated road. Figure 2.9 shows the coastline section of Vandenberg AFB and the travel path of the Athena from the IPF to the runway. All pertinent roads will be closed during transportation in order to insure a safe booster transport and to keep all personnel clear of the Athena during this crucial stage. The minimum personnel needed for this stage in the mission is 4: 2 to drive the truck, 1 to lead the convoy, and one to follow the convoy.

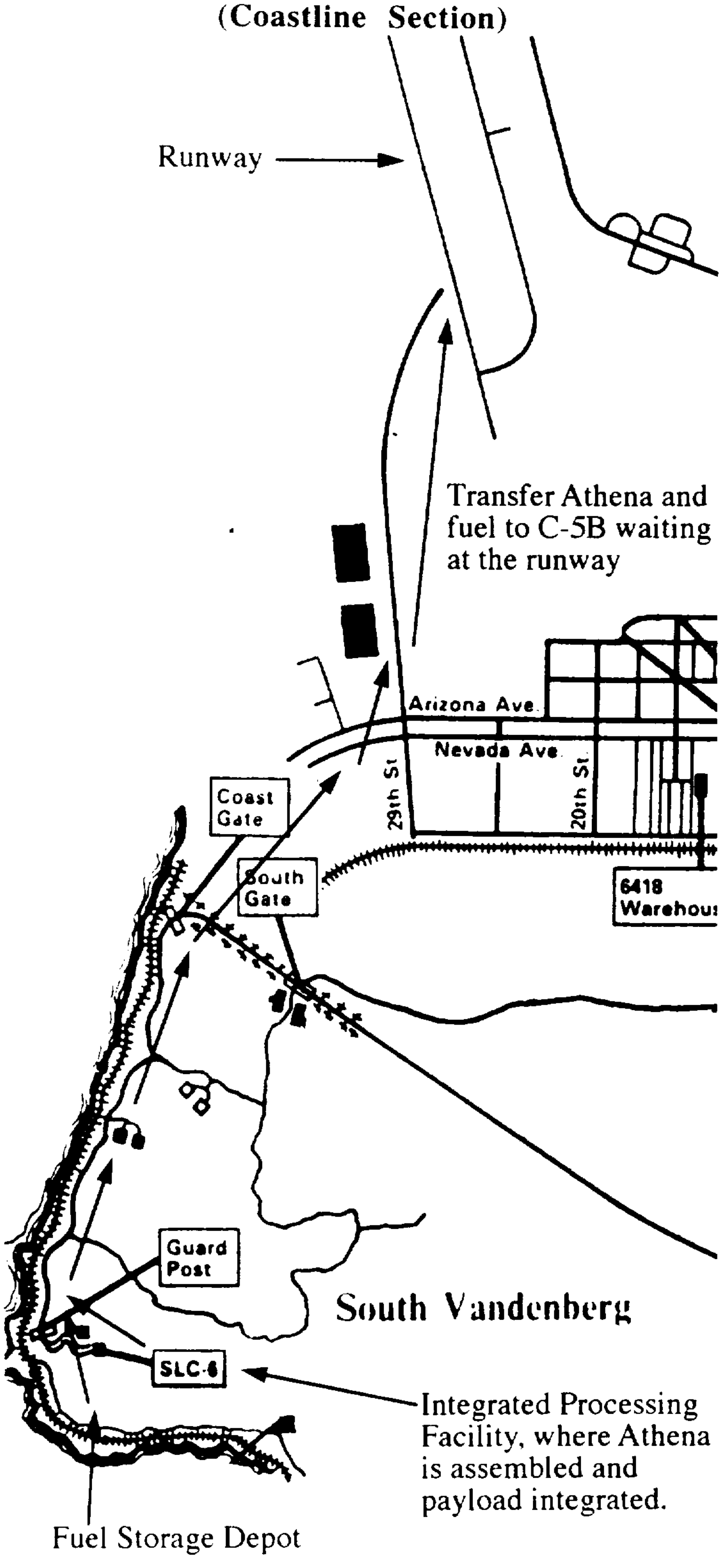
(Coastline Section)
Runway
Arizona Ave
Nevada Ave
29th St
20th St
Coast Gate
South Gate
6418 Warehous
Guard Post
South Vandenberg
SLC-6
Fuel Storage Depot

Transfer Athena and fuel to C-5B waiting at the runway

Integrated Processing Facility, where Athena is assembled and payload integrated.

Figure 2.9: Vandenberg Air Force Base

In Figure 2.9, the Integrated Processing Facility, fuel storage depot, and the runway the C-5B will take-off from can all be seen. There is a long transfer path between the assembly facility and the runway, but the California Commercial Space Inc. has said they can assist in the transfer process. The transfer of Athena to the runway will be done via a transport on wheels, and the storable liquid fuels will be transferred to the runway by either railway or tanker trailers. The C-5B will be waiting for the Athena at a predetermined site where the two will be integrated, the booster will be fueled, and all systems finalized. This predetermined site needs to be able to handle all the safety precautions surrounding the storable liquid fuels, such as having all fueling operations take place on a concrete platform.

5.4 Aircraft Mating

The Athena and Chimaera are both at the designated safety site near the runway and the Athena is ready to be transported onto the Chimaera. Proper booster alignment is essential to a successful booster extraction at altitude.

5.4.1 Trailer to Aircraft Transfer

The following is the procedure to properly load Athena onto the C-5B:

1. Align the trailer with the front cargo doors of the C-5B.
2. Release the attachments between the sled and the trailer.
3. Roll the booster and sled from the trailer to the C-5B.
4. The booster will lock into place using four custom locking mechanisms (discussed later).
5. Two secondary locking mechanisms are attached.
6. Taxi the C-5B to the end of the runway where the booster will be fueled.
7. Cut all C-5B engines.
8. Fuel the booster.
9. Connect the cooling unit to the booster payload bay.
10. Connect power cables for booster interface during flight.
11. Conduct a final systems check.
12. Ignite the C-5B engines and prepare for takeoff.

The booster is being loaded through the front of the C-5B to avoid any problems with the tail section of the airplane during loading.

5.4.2 Primary and Secondary Locking Mechanisms

Two locking mechanisms were developed in order to keep the booster from shifting during flight to altitude. The primary mechanisms will consist of four separate clasps each connected to the floor and restricting the sled motion in both the longitudinal and transverse directions. Together, they will also prevent any sled rotation. The secondary mechanism consists of two separate clasps connected to the floor at the rear of the booster (front of the plane) which will only prevent movement in the longitudinal direction. The secondary mechanism is used after the cargo doors are opened and the primary locks are released. The sole purpose of the secondary system is to prevent the booster from rolling out of the aircraft before the launch is initiated.

5.4.3 Payload Cooling Unit

The payload needs to stay within a certain temperature and humidity range during the entire mission. During the aircraft flight stage (stage 0) a pressurized nitrogen tank will be used to keep the payload bay cool and within the specified humidity. This will be connected during the systems interface procedure described above.

5.5 Athena Fuel Safety and Storage

The Athena uses storable liquids fuels for all three stages. The oxidizer is nitrogen tetroxide, and the fuel is aerozine-50 (a 50/50 mixture of hydrazine and unsymmetrical dimethylhydrazine). These storable liquid fuels needs to be handled with extreme care due to their toxic and corrosive nature. Nitrogen tetroxide and aerozine-50 are hypergolic, so contact between the two must be avoided. Proper storage containers and fuel carrying vehicles are required in order to maintain safety. The Athena will be fueled right before it is loaded into the Chimaera, so these fuel carrying vehicles will be needed to transport the fuel from the storage area to the designated site near the runway where the C-5B and Athena will both be fueled.

5.5.1 Fuel Safety

Nitrogen tetroxide and aerozine-50 are both extremely toxic and corrosive. As such, each has a long list of safety procedures in order to keep anyone from being injured. A book called *Handling and Storage of Liquid Propellants*, from the Director of Defense Research and Engineering, gives a through list of the safety concerns for storable liquid fuels. This book does not contain information on aerozine-50, but the book does list out safety concerns for hydrazine and unsymmetrical dimethylhydrazine (the two components of Aerozine-50). The exact characteristics of aerozine-50 are a mix of its two components, but the listed precautions for hydrazine and unsymmetrical dimethylhydrazine should adequately describe the concerns with aerozine-50. The following list highlights the important hazards and safety precautions of the Athena's storable liquid fuels.

Nitrogen Tetroxide

Hazards:
- Skin contact causes severe burns.
- Breathing of vapor may cause poisoning
- Spills may cause fire and may liberate toxic gas.
- Contact with fuels may cause explosions.

Safety Precautions:
- The nature and characteristics of nitrogen tetroxide shall be explained to all persons working with this material.
- Persons engaged in operations involving handling or transfer of nitrogen tetroxide shall wear approved boots, gloves, acid hood and protective suit. In addition, a protective mask shall be worn by all persons exposed to the vapors of nitrogen tetroxide.
- Operations requiring the handling or use of nitrogen tetroxide shall be performed by groups of two or more persons.
- Before beginning to use equipment, make sure the system is not pressurized. Avoid trapping nitrogen tetroxide between closed valves. Do not operate pumps against closed valves.

Check lines, valves and receiving tank before starting to transfer nitrogen tetroxide.

- Use care when opening cylinders (transfer container for nitrogen tetroxide). Cylinders not connected to a receiving system must not be opened unless contents are below the boiling point (21.1°C at pressure of 101,324 Pascals).
- Avoid spills. If nitrogen tetroxide comes into contact with organic materials such as sawdust, excelsior, wood scraps, cotton waste, etc., it may cause fire. Toxic fumes are generated from such spills, and color is not a reliable indication of toxicity.
- Protective clothing, hand tools and other equipment shall be flushed with water immediately after contact with nitrogen tetroxide.

Hydrazine

Hazards:

- Contact with liquid may cause burns, severe eye damage and general poisoning.
- Breathing of vapor may cause lung damage and irritation of the eyes, nose and throat.
- Spills represent an immediate fire and explosion hazard.
- Contact with acid causes fire and possibly explosion.

Safety Precautions:

- All personnel must be familiar with the nature and characteristics of hydrazine.
- Persons handling Hydrazine must wear fuel-resistant gloves, shoes or overboots, a face shield, wrist and arm protectors, and a rubber-type apron.
- Respiratory protection must be available when working in hydrazine-contaminated atmospheres.
- Storage, transfer and operating areas shall be kept clean of organic matter and oxidizers. No electrical sparks or open flames shall be permitted.
- Leaks and spills must be immediately flushed away with large amounts of water.
- Transfer, handling and storage must be performed by at least two persons.
- An atmosphere of nitrogen must be maintained over the hydrazine.
- An adequate supply of water must be available for flushing and decontamination.
- Storage drums and containers shall be grounded.

Unsymmetrical Dimethylhydrazine (UDMH)

Hazards:

- Contact with liquid UDMH may cause eye damage and general poisoning.
- Breathing UDMH vapor may cause lung damage and may irritate the eyes, nose and throat.
- Spills create immediate fire and explosion hazards.

- Contact of UDMH with oxidizing agents causes fire and possibly an explosion.

Safety Precautions:

- All personnel shall be instructed in the nature and characteristics of UDMH.
- Persons handling or transferring UDMH shall wear approved boots, gloves, hood and clothing.
- Operations requiring the handling or use of UDMH shall be performed by persons working in groups of two or more.
- When opening UDMH storage drums, personnel shall stand to one side, opening the bung slightly to relieve pressure and leaving bung in place until hissing stops.
- Avoid spills of UDMH; the resulting vapors present a fire hazard. Wash all spills with water immediately.
- Protective clothing , wrenches, and all other equipment that has been contaminated shall be flushed with water as soon as practicable.
- At no time shall storage drums of UDMH be left at the test site after a fueling operation has been completed.

5.5.2 Fuel Storage Facilities

The nitrogen tetroxide and aerozine-50 will arrive at Vandenberg Air Force Base by barge about a week before the Athena launched, so the nitrogen tetroxide and aerozine-50 need to be stored. Proper safety must be maintained at the storage site in order to reduce the risk of accident or injury. The storage requirements for nitrogen tetroxide and aerozine-50 are listed below.

Nitrogen Tetroxide

- Store in aluminum or stainless steel (300 series) tank cylinders.
- Tanks shall be mounted on reinforced-concrete saddles over a reinforced-concrete drainage basin.
- Each tank, or group of tanks, shall be surrounded by a dike high enough to contain at least 10 percent more than the storage capacity.
- A nitrogen tetroxide detection and alarm instrument should be provided to warn personnel operating indoors when the concentration of nitrogen tetroxide in the air gets too high.
- All buildings in the main fuel storage area shall be constructed of materials not readily affected by nitrogen tetroxide or its fumes.
- All electrical lines and wires shall be installed in rigid metal conduits, and all electrical controls, junction boxes, and panels shall be vaporproof and weatherproof.
- An adequate water supply needs to be on hand for flushing, showers, and eye baths.
- Storage and transfer sites must be kept clean of any organic materials to avoid any reaction with nitrogen tetroxide.
- A complete drainage system, flowing to a limestone decontamination pit, shall be provided at each storage and transfer facility.

- A system of ventilation is required in all storage and transfer structures.

Aerozine-50

- Store in stainless steel-304 containers.
- Storage of aerozine-50 should be maintained at a temperature below 48.9°C to avoid boiling.
- Store in isolated area, away from any oxidants.
- The storage building should have fire extinguishers of a type approved for use against hydrocarbon-fuel fires, and it should also have safety showers and eye baths.
- All aerozine-50 storage tanks shall be surrounded by a dike high enough to hold 10 percent over the tank's maximum storage capacity.
- All aerozine-50 storage and transfer areas shall be kept clear of any organic material and oxidizers.
- Closed areas storing aerozine-50 must be ventilated, and open-sided storage buildings are recommended where possible.
- All areas of aerozine-50 operation shall be properly drained so that all spills can be flushed with large quantities of water.

5.5.3 Fuel Transfer

The storable liquid fuels used with the Athena, nitrogen tetroxide and aerozine-50, are brought in by barge to Vandenberg Air Force Base a week before launch. The fuel storage depot is right off the coast, just east of the fuel barge harbor, and it is well away from any of the populated areas of Vandenberg. The fueling of Athena will take place at a specified area near the Vandenberg runway, about 2-3 miles from the fuel storage depot. The nitrogen tetroxide and aerozine-50 will need to be transferred using the guidelines listed above. The fuel transfer can either be done by tank trucks or by train storage cars. If the railway is used, there will still need to be transfer tank trucks to get the storable liquid fuels from the railway to the exact fueling site.

5.5.4 Fueling Procedure

Once the booster is loaded onto the C-5B, and the C-5B is in the designated site for fueling procedures, the fuel trucks will transport the fuel to the C-5B. The first stage will be fueled first, followed by the first stage oxidizer; the second stage will be fueled second, followed by its oxidizer; and the third stage will be completed last. It is crucial that all personnel be evacuated from the immediate area during fueling with the exception of the personnel needed to fuel the booster. The minimum personnel needed for the fueling is two for each fueling vehicle. All other personnel, including the C-5B crew, are to be evacuated until the fueling is complete.

6.0 FINANCIAL ANALYSIS

The main financial goals of Project Athena were to beat the cost of the competition by 50%, on a cost per kilogram of payload basis, in order to insure investors that they would be able to receive a 15% return upon their investment. This proved to be a very elusive goal as the booster size decreased, along with the payload capability, due weight constraints imposed by the carrier aircraft.

The financial analysis of Project Athena includes the following:

- Comparison of Athena with other launch vehicles
- Detailed analysis of launch costs
- Budget determination for project lifetime

6.1 Comparison with Competition

In general, launch systems are compared by the amount, in kilograms, of payload that they can deliver to various orbits, and launch costs are divided by that amount to determine a comparable cost per kilogram. The goals of this project were to beat other systems costs by 50% in order to insure that satellite makers would be persuaded to choose Athena over other more established launch vehicles. See Figure 2.10 for a comparison of payload capabilities with other launch vehicles. All information on competitors has been obtained from Jane's Space Directory (Wilson, pp. 209-327)

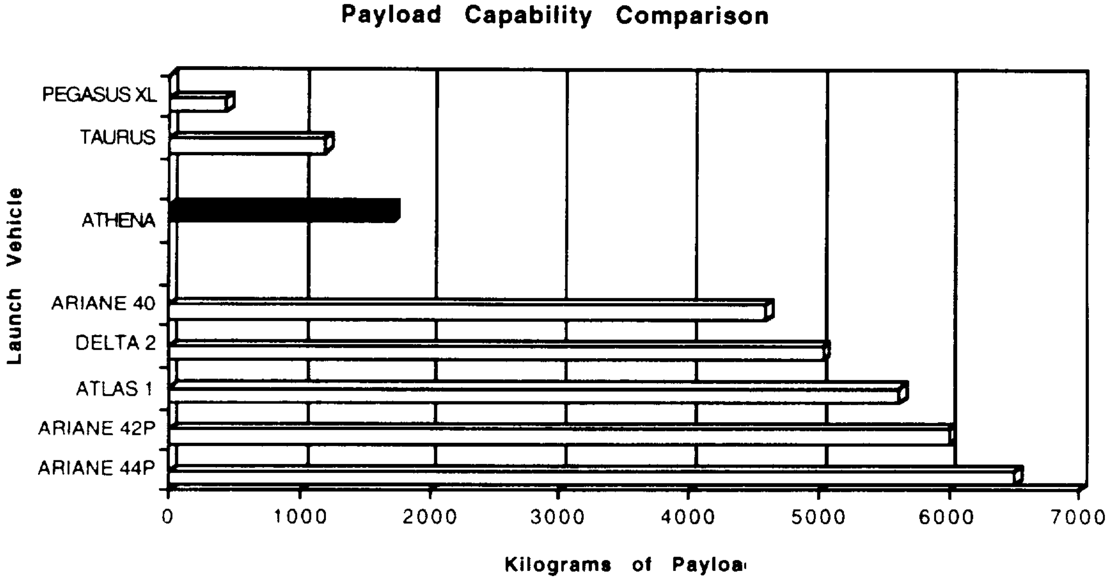

Figure 2.10: Payload Capability Comparison

The main competitor of Project Athena is the Taurus produced by Orbital Sciences Corporation. The Taurus is capable of taking 1,200 kilograms to Low Earth Orbit (LEO), while the Athena can take 1,715 kilograms to LEO. In Addition, Athena costs slightly less than the Taurus on a cost per kilogram basis. Refer to Figure 2.11 for a cost comparison of Athena with other launch vehicles.

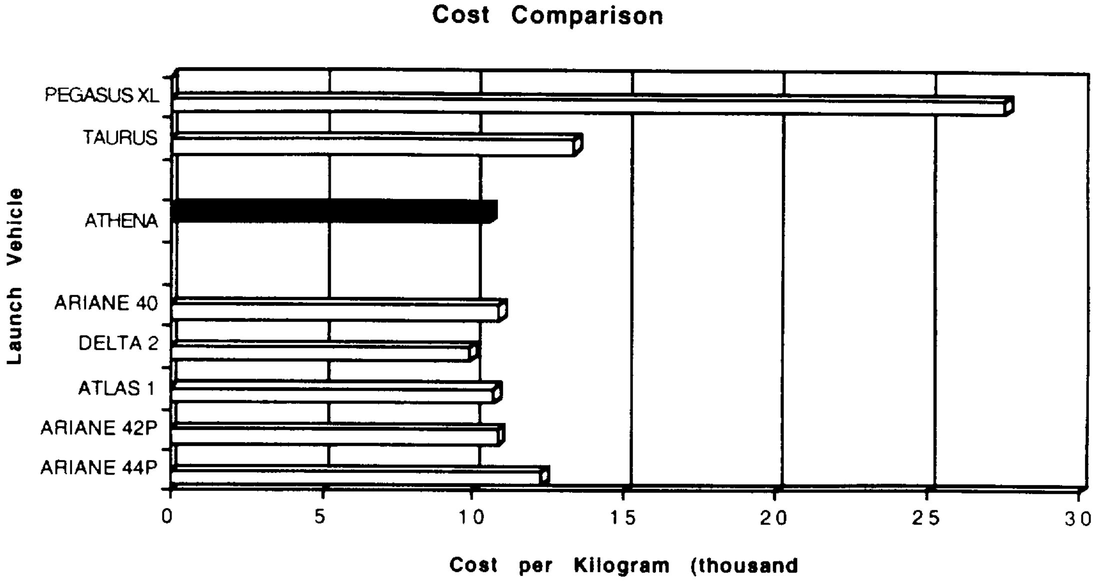

Figure 2.11: Vehicle Cost Comparison

Other competitors of Athena include Pegasus, made by Orbital Sciences Corporation, Delta 2, made by McDonnell Douglas Space Systems Company, Atlas 1, made by General Dynamics, and the Ariane 4 series, made by Arianespace Incorporated. The Pegasus is a much smaller booster, capable of only 435 kilograms using the new XL model, and costs far more on a cost per kilogram basis. Athena costs only 50% compared to the Pegasus per kilogram of payload. On the other hand, the Delta 2 is capable of almost four times the amount of payload as Athena and as a result, Athena costs about 40% more per kilogram. This is also true of the Atlas 1 and the Ariane series which are capable of three to five times as much payload. For a complete detail of the costs and capabilities of Athena and other launch vehicles, refer to Appendix A.4.

6.2 Detailed Launch Cost Analysis

The costs for the Athena booster launch system were determined by working with the respective groups and attempting to obtain costs from industry sources, and by making estimates where sources were unavailable or declined to provide cost information. Financial details about the booster can be seen in Appendix A.5, where the booster costs are shown on a cost per launch basis. This detail of the costs also shows when costs are incurred by the notes in the left column. In general, propulsion systems incur the greatest costs as can be seen in Figure 2.12. This section will explain in detail the costs associated with each group.

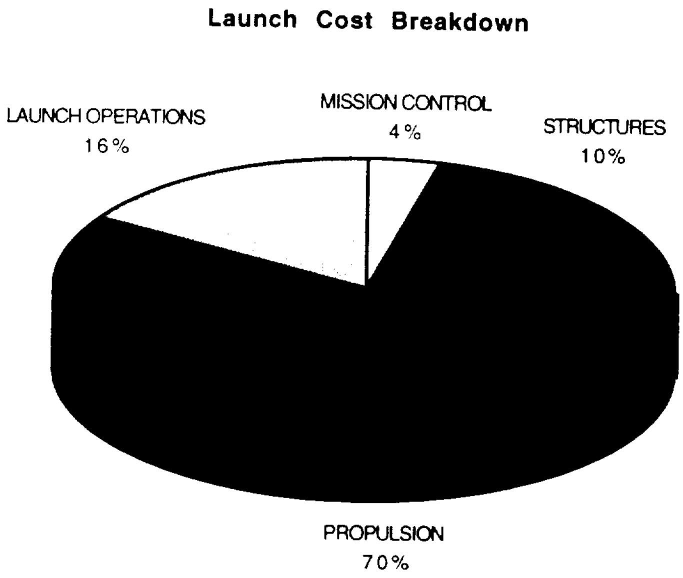

Figure 2.12: Launch Cost Breakdown

6.2.1 Launch Operations

Launch operations includes all costs incurred in construction, testing, and the actual drop out of the C-5B. Liability insurance coverage is also included in launch operations and accounts for more than half of the costs accounted for by this category.

There are two one-time costs associated with the C-5B. Modifications are required on the wheels in the cargo bay as they have not been designed to handle the amount of weight that will be required in order to drop the booster. In addition, several tests need to be conducted to insure that the C-5B will be able to successfully drop such a large mass out of the cargo bay without further modifications. A cost schedule can be seen in Appendix A.6 for the drop tests. These one-time charges have been divided by 60, the total number of launches performed by the project, in order to determine their costs on a per launch basis. Though expensive due to interest considerations, these costs are believed necessary to insure that the launch system will be successful and to show satellite makers that this system will be safe and reliable. The final drop will be fully functional and will show whether or not the booster can be safely dropped and ignited.

Each mission in the C-5B will be flown by the Air Force at an approximate cost of $75,000 per hour, with an average mission time of about six hours. Furthermore, a chase plane will be employed at a rate of about $7,000 per hour in order to watch and film the launch procedure. Fuel for the C-5B are not included in the rental costs and thus have been included separately here.

The sled on which the booster will be mounted in the cargo bay will have to be constructed and it's costs have been estimated here. Construction costs had to be estimated because it is difficult to determine how many hours will be required to actually perform the construction. Booster assembly costs have also been estimated based upon the launch timeline (see Section 3.0) but are still rough estimates. The liability insurance has also been estimated based upon findings from Space Economics, (Greenberg, p. 3-319) but actual insurance costs could not be determined until an insurance company actually evaluated the risk and made an agreement.

6.2.2 Mission Control

The one-time costs required by mission control involve the software development for the mission control program which will guide the booster to the required orbit. Also, LPO (Launch Panel Operator) equipment is required to be mounted on-board the C-5B in order for the LPO to monitor the booster during flight, from inside the carrier aircraft.

The equipment required by mission control in the form of onboard computers and guidance and navigation equipment is included in Appendix A.5. In addition a mission specialist is required to program each launch for its particular mission. The use of Vandenberg's tracking center will be approximately $550,000 and is the major portion of the mission control group's costs.

6.2.3 Power/Thermal/Control

The power/thermal group is responsible for the power systems and the control systems required to guide the booster along its desired trajectory. The power/thermal group also designed the system to pull the Athena out of the C-5B cargo bay by using extraction chutes. The cost of these components are shown in Appendix A.5.

6.2.4 Propulsion

The majority of the costs incurred by the propulsion group were in the form of engines. The first stage engine costs approximate $3 million dollars. The second and third stage engines cost approximately $2.5 million each and two engines were required on the third stage. The fuel tanks, and the cost of the fuel and oxidizer are also included in the cost of the propulsion systems and are all listed in Appendix A.5. The fuel tanks were estimated to cost four times the cost of the materials in order to account for manufacturing costs. This was confirmed to be a good estimate by the structures group.

6.2.5 Structures

In general the cost of the structure would be impossible to determine without having a company actually perform the manufacturing and arrive at a cost. As this is impossible for the project to do in a conceptual design, manufacturing costs are estimated as some multiple of the material costs. For the first and second stages, the total cost was estimated to be five times the material costs. The third stage and payload bay were estimated independently on a total cost of $1.5 million since the manufacturing will be more expensive due to the use of composites.

6.3 Budget Determination

The overall budget consisted of three main items, launch costs, interest payments, and taxes. The launch costs were covered in detail in the previous section, but a further analysis of whether or not Athena could compete in a business setting is not entirely determined by that information. It was necessary to consider the project as if it was a business and pay interest on its debts to investors at a rate of 15% per year.

In order to determine what the project would need to charge per launch, it was necessary to come up with an overall project plan and budget. To accomplish this, a budget spreadsheet (see Appendix A.7) was developed based upon the following parameters:

- 60 total launches during a 10 year period
- 1 year start-up time and 2 years for carrier aircraft drop testing
- Maximum of 7 launches during any year
- 2 year satellite launch contracts
- All booster materials purchased 1 year prior to launch excluding fuel
- 15% interest paid on debt to investors per year
- 35% taxes paid on net profits
- Minimum cash balance of $5 million

A chart of the financial position of the project can be seen in Figure 2.13, which is based upon the results of this analysis.

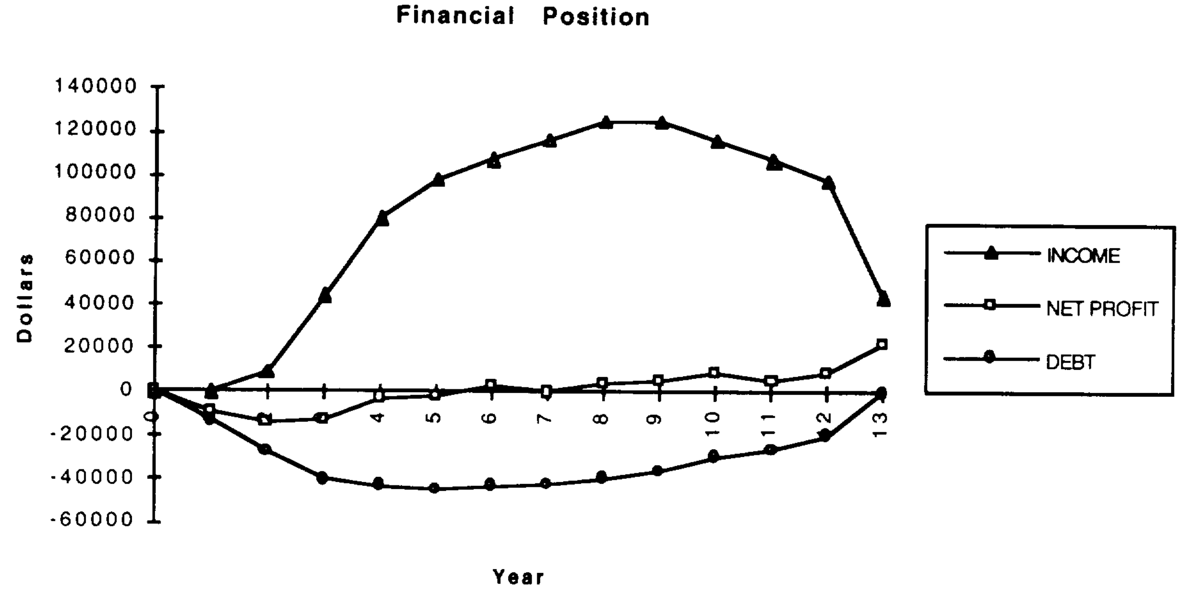

Figure 2.13: Graph of Project Financial Position

6.3.1 Project Lifetime

It was determined that the project should be limited to ten years of use based upon the fact that the booster would be made using "off-the-shelf" components, and that these components would not be efficient for use after about fifteen years. After fifteen years the project should be reconsidered as factors change over time and this particular launch system may no longer be practical, nor cost effective after such time.

6.3.2 Start-up Time

The "start-up" year would be necessary to acquire the use of the construction facilities offered by CCSI, as well as to contract with the Air Force for the use of the Lockheed C-5B. The next two years would consist mainly of drop tests conducted in order to gain experience and to insure that there were no problems dropping such a large mass out of the C-5B, as that much weight has not been dropped as a single object to the best knowledge of the project.

6.3.3 Yearly limits

A maximum of seven launches per year was determined after establishing a booster construction timeline. The timeline is based upon six launches per year which is what the project would average, but it also includes two weeks of slack time per launch, of which less than one week per launch would be needed in order to launch seven times during one year. Slack time of about week or so is required in order to insure that launches do not fall behind schedule as penalties are often placed in launch contracts for delays. This is all that is required by this project since weather will generally not be a factor for the C-5B, and the vehicle assembly should not take very long since it consists entirely of established technologies.

6.3.4 Contracts with Satellite Manufacturers

Contracting with satellite makers is complicated and often incentives are included in the contracts in order to make a particular launch service seem more attractive than another. For example, General Dynamics offers a free second launch if the Atlas fails to properly place the satellite in orbit. Arianespace allows a certain portion of the launch charge to be withheld until after the launch vehicle has successfully placed the satellite in orbit. There are various other incentive methods by which launch services use in order to compete for business, but these have been excluded and replaced with a shorter two year contract rather than the normal three to four year contract required by other launch services. What this means is than the satellite maker does not have to begin making payments to the launch service provider until two years prior to the launch date.

6.3.5 Pre-purchasing of Materials

All of the materials for the Athena booster would be purchased one year before launch in order to insure that all the parts would be available at the time when construction was supposed to begin. Furthermore, this will help to insure that launch delays will not be due to the launch vehicle not being prepared. All other costs, such as insurance, booster fuel, tracking facilities, and other services, such as the use of the C-5B, will be paid for within one year of the actual launch date as these services and supplies should be available by scheduling them properly. Refer to Appendix A.6 for a detailed list of when launch costs will be paid.

6.3.6 Interest to Investors

The design of the project calls for a 15% return to investors on all money they lend to the project. As such, 15% interest on all debt will be paid, on an annual basis. The overall budget spreadsheet (see Appendix A.7) calculates interest during any given year by taking 15% of the debt balance at the end of the previous year. Thus interest is not compounded, but simplified to a one-time charge each year. This simplification is justified by the maintenance of a minimum cash balance on which no interest is earned.

6.3.7 Taxes

It is difficult to say what tax rates will actually be like for businesses in the future, but based on current rates, taxes have been taken as 35% of net profits earned by the company. No taxes have been paid in years which the company shows a net loss. This would seem to be a reasonable approximation since there are some incentives for private industry in the space launch business, the extent of which are not known to the project as such a constant tax rate has been assumed throughout the lifetime of the project.

6.3.8 Minimum Cash Balance

Although no exact formula exists for how much cash must be held on hand, it is clearly a function of cash flow. In any given year the cash flow of the company could be as high as $125 million dollars, with an average of about $105 million per year. Because of this it was decided that the cash balance of the company should at least be close to 5% of the average cash flow in order to avoid times when the company would face a "cash crunch." Although payments on the debt are rather relaxed in favor of the project according to the budget spreadsheet, this minimum cash balance offsets that leniency somewhat by not giving the project such a flexible cash supply.

Chapter 3

Mission Control

Mission Control's Symbols

Dv	change in velocity
w	rate of rotation

1.0 GROUP OVERVIEW

The Mission Control Group had the following tasks during the design process:

- Selecting the airport for takeoff of the plane carrying ATHENA
- Determining the location of mission control
- Guidance, navigation, and control (GNC) of the booster .
- Selecting the on-board computer
- Tracking, telemetry and command (TTC) during the mission.
- Determining the airborne support equipment on board the carrier aircraft
- Addressing the various safety issues and concerns while preparing to launch and while in the process of launching
- Deriving abort scenarios for the various phases of the launch
- Outlining the flight termination system (FTS)
- Create a launch sequence for deployment of ATHENA

The completion of these tasks involved the familiarization with the various systems and components of mission control and the evaluation of the different options based on their appropriateness in ATHENA missions. In selecting the various components, it required that the performance and cost were weighed against each other. In an attempt to come up with the most cost efficient components that were capable of satisfying our requirements.

2.0 AIRPORT SELECTION

Location from which to launch from was a serious concern since one of the mission goals was to beat the competition's price by 50%. In order to do this, it was decided that we could afford only one launch center and not the two, one on each coast, that most launch companies use.
This led us to believe that a site in the midwest, possibly at one of the C-5B bases would suit our needs. As safety problems involving flying over land with 80,000 kg. of liquid fuel became a serious concern, it was decided that we would have to launch from near the coast.

The next choice was Edwards AFB in California which would offer the same facilities that the Pegasus uses along with an airport capable of handling the C-5B. Edwards also offered a location which was away from the coast and therefore sea spray posed no threat. Edwards was eventually passed over because this site also posed a threat to the public because it is over a hundred miles inland and would require a significant amount of flight over land. To add to the time of flight, the C-5B wouldn't be able to fly out to sea until it had reached a safe altitude to fly over the mountains.

PRECEDING PAGE BLANK NOT FILMED

The options were now either Kennedy Space Center in Florida or Vandenberg AFB in California. KSC is the primary launch site for equatorial launches and VAFB is the primary launch center for polar orbits. KSC was eventually discarded because although it could handle equatorial launches, polar launches would require that the C-5B fly an extraordinary far distance away in order to avoid hitting any of the Caribbean islands. Vandenberg, however, could handle equatorial launches, given that the C-5B flew approximately 2500 km. away since there are relatively few islands off the west coast of the United States and Mexico. VAFB also offers both an airport and the Southern Pacific Railroad to transport our materials in to be assembled and silos for liquid fuel.

During our search, we were told of the California Commercial Spaceport, Inc. This private company will use the facilities at Vandenberg AFB to integrate boosters and launch them. This information came to us at the same time that we had selected Vandenberg as our launch center, therefore, CCSI changed the launch site minimally but could have a huge impact on the cost of the launch. Although they could not give a price due to the fact that they are just developing and won't be operational until 1997, they stated that their company goal was to offer the launch facilities for the lowest cost available. We would use the Cypress Ridge Launch Facilities which are located at the southern end of VAFB. The launch site itself is built on the proposed SLC-7 Titan IV/Centaur launch site and it has an Integrated Processing Facility (IPF) nearby where our booster can be assembled. CCSI has facilities for vertical integration. This would lead us to construct Athena upright and then lay it down onto the sled. Should this prove to be unfeasible or cause unforeseen problems, CCSI does have contacts with Martin Marietta who own a horizontal integration facility at Vandenberg that we might be able to make use of.

It should be noted that after selection of VAFB and CCSI, Payloads decided that it might not be feasible to launch polar satellites, and at the same time Mission Analysis was having problems getting into polar orbit. This would have pushed us back to the east coast which was closer to the equator, thereby reducing third stage propellant, the correct launch site for equatorial orbits (VAFB is for polar. The reason that we decided to remain at VAFB and CCSI was cost. CCSI has stated that they will give us their facilities for the lowest possible price since they will be commercial. An additional incentive, given our 1997 planned launch date will be the Space Commercialization Act which could lower our cost by a third and even up to one half of today's current costs.

CCSI will allow us to assemble and launch Athena much cheaper than anywhere else and it gives us access to some of the world's best space facilities.

2.1 Mission Control Location

Once VAFB and CCSI were selected to be the airport location, it was necessary to determine where Mission Control could be located. Since VAFB is the location of the Western Missile and Space Range, and VAFB is also the secondary launch center for the Space Shuttle, there is a Mission Control Center present. There is also a host of tracking stations located nearby. CCSI has stated that these control facilities can be used through them.

A problem occurs, however, when we launch. Until the point of deployment, the Goldstone tracking station, located at Vandenberg, can track Athena on an S-band. After deployment, however, the booster goes out of Goldstone's tracking range, therefore, it will be necessary to get several other sites. It might be worthwhile to get one of NASA's tracking ships which can be deployed anywhere either in the Pacific or the Atlantic to track a launch.

3.0 GUIDANCE, NAVIGATION, AND CONTROL (GNC)

The most important responsibility of Guidance, Navigation, and Control (GNC) is to ensure that Athena follows a predetermined path as closely as possible in order to accomplish its mission and deliver the payload to its destination (i.e. insert the satellite into the desired orbit). This is accomplished through the three main processes of GNC. More specifically:

1) Guidance is the process of generating maneuver commands to control the vehicle's motion and guide it to its destination. This is done after taking into account inputs of the current position and motion of the vehicle.

2) Navigation is the process of determining the exact current position of the vehicle.

3) Control is the process of determining what actions need to be taken by the flight control mechanisms to set the vehicle in the desired motion that is prescribed by the guidance process.

Just like most other launch vehicles Athena relies on inertial navigation to determine its position, velocity and attitude during flight. Inertial navigation is a method of dead reckoning that uses the outputs of two types of sensors - accelerometers and gyroscopes, accelerometers being used for measuring components of the linear acceleration of the vehicle and gyroscopes being used for measuring angular rates. It is termed "inertial" navigation because it makes use of Newton's fundamental laws of motion. The navigation starts off by entering the initial position and alignment of the vehicle into the Inertial Measurement Unit (IMU). After the vehicle has been set into motion the signals from the accelerometers and the gyroscopes are continuously compared with a timing signal over which they are integrated once to obtain the current velocity of the vehicle and twice to obtain the current position of the vehicle. Thus, navigational data is obtained which in turn is compared with the mission data load software in the auto-pilot processor and control commands are sent to the flight control mechanisms on the exterior of the vehicle.

Before the advent of digital computers the accelerometers that were being used were mounted on gimbals so that each one of them would maintain a constant orientation in inertial space enabling it to constantly measure the component of the vehicle's acceleration along that axis. However, the advancement of computers made possible the use of strapdown systems. These are systems in which analytic (computed in real time) gimbals replace the hardware gimbals of older IMU's. Thus, the accelerometers and the gyro's are mounted directly on the vehicle frame with the outputs being produced first in terms of body fixed coordinates and then being transformed into inertial space coordinates.

There are some sources of error in the IMU's. Two of those are temperature fluctuations and the gyro drift which is the angular deviation of the spin axis of a gyro away from a fixed reference in space. In the case of Athena, the long captive carry to the point of drop presents a significant gyro drift problem which may lead to inaccuracies in the output of the IMU. Athena must be a low cost vehicle and low cost IMU's do not maintain high accuracy for extended periods of time. The solution is to provide external aids to the inertial navigator such as Global Positioning System (GPS) navigational data which continuously updates the vehicle's position and velocity.

Three strapdown IMU units were considered for Athena. Two of these were Litton models, the LP-81 and the LN-200 and the third one was the Honeywell GG1320. The LN-200 was chosen as the IMU unit for Athena based on comparisons of accuracy, reliability, cost, and weight of the three units. A comparison of the three units is presented in the table below.

	LP-81	LN-200	GG1320
Weight(kg)	3.4	0.7	1.63
Power (watts)	26.2	10	17.5
Activation Time (sec)	9	0.8	2.25
Operating Range (g's)	5	40	30
Reliability (hrs)	7,646	22,345	11,380
Cost ($)	50,000	30,000	275,000

Table 3.1: Comparison between the three primary IMU selections

The LP-81 is the IMU that is used aboard the Pegasus. The LN-200 uses fiber optic gyros while the GG1320 uses ring laser gyros. Both fiber optic gyros and ring laser gyros are optical sensors that sense changes of transit time along clockwise and counterclockwise closed optical paths. The difference in the two transit times is a measure of the applied rotation rate. Both types of gyros provide great accuracy. Fiber optic gyros are a recent development that have contributed a great deal to the reduction of the cost and the weight of IMU's. Today's IMU technology is dominated by the ring laser gyro strapdown mechanization but the rapid progress and unique characteristics of fiber optic gyros will replace ring laser gyros in the next generation of IMU's.

The LN-200 IMU uses three orthogonal fiber optic gyros for measuring angular rate and three silicon accelerometers for measuring vehicle acceleration. These devices comprise the sensor assembly. The LN-200 also contains two printed circuit cards (PCBs), the analog PCB and the digital/I/O PCB. The analog PCB provides the analog electronics and optical interface to the inertial instruments. The digital/input-output PCB contains the digital signal processor that compensates the gyro and accelerometer data and provides the output data. The unit outputs incremental angle and velocity changes that have been compensated for temperature and other parameters. The data is output over an RS-485 serial data bus. Some further information on the LN-200 is given in the table that follows.

Size	8.9 cm diameter by 8.5 cm high
Cooling	conduction to mounting plate
Digital Processor	TMS 320C26
Output Data Rate	400 Hz
Data Latency	less than 1 ms
Temperature	-54°C to +85°C operating range

Table 3.2: Additional Features of the LN-200 IMU

To provide navigation data (in inertial space coordinates), i.e., latitude, longitude, and altitude, the IMU outputs are further processed by a navigation processor. The main component of this processor is a sophisticated Kalman filter. The Kalman filter uses Global Positioning System velocity updates to infer the attitude of the gyro triad. The Kalman filter is also used to calibrate the inertial instruments by providing estimates of a number of other error sources. These estimates lower the effective drift of the gyros and accelerometers. Thus, by using the Kalman filter the performance of a more expensive inertial navigation system can be achieved with the relatively inexpensive Athena unit. A system block diagram of the IMU is shown in the figure that follows.

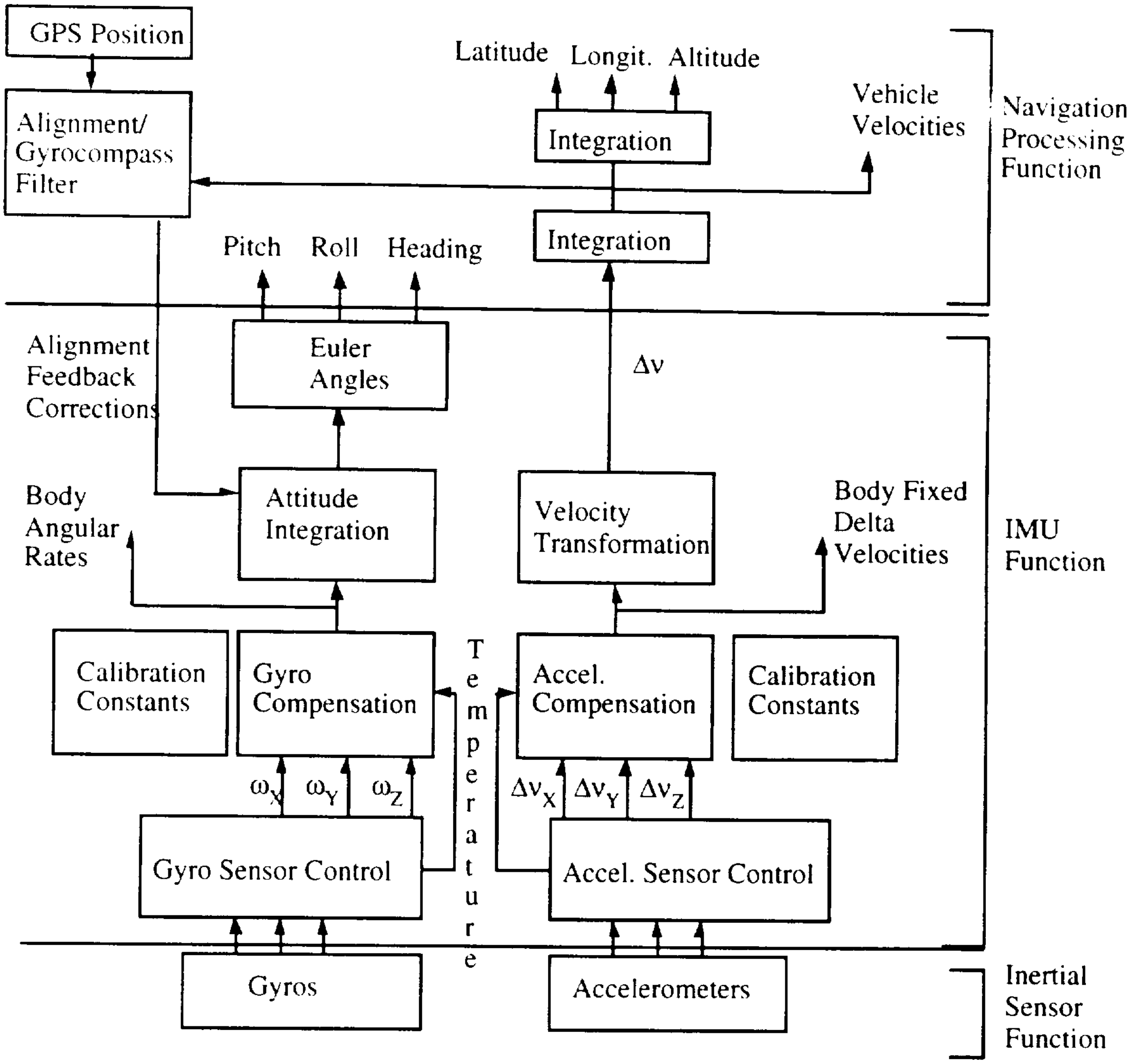
GPS Position
Alignment/ Gyrocompass Filter
Latitude
Longit.
Altitude
Integration
Vehicle Velocities
Navigation Processing Function
Pitch
Roll
Heading
Integration
Alignment Feedback Corrections
Euler Angles
Δv
Body Angular Rates
Attitude Integration
Velocity Transformation
Body Fixed Delta Velocities
IMU Function
Calibration Constants
Gyro Compensation
Temperature
Accel. Compensation
Calibration Constants
ωX
ωY
ωZ
ΔvX
ΔvY
ΔvZ
Gyro Sensor Control
Accel. Sensor Control
Gyros
Accelerometers
Inertial Sensor Function

Figure 3.1: System Block diagram of the ATHENA IMU

A second IMU in the Launch Panel Operator (LPO) console of the carrier airplane is also used. The purpose of this second IMU is to communicate with the LN-200 aboard Athena so that the Athena IMU is continuously updated from the time of take off up until the point of deployment. Just prior to deployment the carrier aircraft must perform a series of maneuvers to provide the Kalman filter with a information-rich stream of measurements.

3.1 Global Positioning System

Navigational data from the GPS is used to provide external aids to the LN-200. The GPS is a system that was originally developed by the Department of Defense (DoD) for exclusively military purposes. However, the DoD was soon directed by the Congress and the President to promote its civil use, thus, allowing civilians to take advantage of the system. The GPS is an accurate and inexpensive way to obtain the position and velocity of a vehicle and the exact time at which the position and velocity are measured anywhere on the globe. Civilians however are denied full use of the system. There are two GPS codes, the C/A-code also designated as the Standard Positioning Service (SPS) which is available for civilian use and the P-code, also designated as the Precise Positioning Service (PPS) which has been reserved for use by the U.S. military and other authorized users. In the SPS full system accuracy is denied.

The GPS receiver that was chosen to obtain the signals from the GPS satellites was the Trimble Quadrex 6-channel Advanced Navigation Sensor (TANS) which is a GPS SPS receiver. The TANS provides worldwide, day-and-night, all-weather position and velocity data. Three fixed-pattern antennas are used to receive the GPS satellite signals. These signals are then sent to the Receiver Processor Unit (RPU). The RPU utilizes six processing channels to compute three-dimensional position and velocity and to maintain the satellite tracking process. The primary output of the TANS is time-tagged position and velocity at intervals of approximately one second. This output is sent to the Kalman filter of the inertial navigator via two RS-422, 9600 baud data channels. Some of the characteristics of the TANS are given in the table that follows.

Weight (kg)	1.59
Power (watts)	1.94
Operating Range (g's)	7
Position Accuracy	25 m spherical error probability
Reaction time	less than 2 minutes
Operating Temperature	-40^{0}C to $+71^{0}$C
Cost ($)	10,000

Table 3.3: Characteristics of the Trimble Quadrex GPS Sensor

4.0 ON-BOARD COMPUTER SYSTEM

Any type of space booster requires an on-board computer system in order to handle the processing of Tracking, Telemetry and Command (TTC) information. Athena is no different in this respect. The only limitations placed upon the Athena on-board computer system is that it must be a pre-existing space ruggedized system requiring little to no modification of the current hardware. For this reason we have chosen the AITech C130 68030 - Based Single Board Computer (SBC) and the AITech C401 Multi-Protocol Communication Controller Board.

All software used will have to be written specifically for Athena. The fact that we are attempting something unique with Athena does not allow us to use presently existing flight control software. A conservative estimate for the price of software development is one time, up front cost of $125,000 paid out in one year to a two person programming team. After this we will need to keep one software engineer on retainer to write the mission specific programming for our computer system.

4.1 On-board Computer Hardware

The on-board computer system hardware selected for Athena is manufactured by AITech Defense Systems, Inc. We will be using AITech's C130 SBC and C401 Communication Controller Board. All computer hardware will be mounted in the third stage between the payload and the third stage engines.

The C130 SBC from AITech is based on Motorola's 68030 32-bit microprocessor. We will need to use the Series-500 full MIL-SPEC space ruggedized system in Athena. This system was used on Orbital Science Corporations Pegasus air launched space booster and can work equally well with Athena.

In order to maintain our compatibility in terms of cost we will be using the C130 SBC in its standard configuration. The standard configuration of the C130 board includes: (1) a Motorola 68030 CPU operating at 16 MHz; (2) a memory bank with 0.5 MB SRAM and 256 KB boot EPROM; (3) VIC/VAC VMEbus interface; (4) two serial ports (RS-232 or RS-422 interfaces); and (5) timers of either general purpose, tick or watchdog type.

The C130 SBC has a host of optional features that can be chosen on a mission specific basis should the need arise. For example the Motorola 68030 CPU can be upgraded to operate at 32 MHz, the SRAM of the system can be upgraded up to 2 MB, or an additional memory bank can be added to the system. All optional features would be used on a need only basis and their costs are not reflected in the budget given in previous chapters.

Figure 3.2 is a model of the C130 board with all its standard hardware. As can be seen there is ample room for expansion on the board.

Athena also requires a communications controller board in order to handle the transfer of data between Athena and mission control. For this purpose we will be using AITech's C401 Multi-Protocol Communications Controller Board as part of our on-board computer system. Once again we will be using the full military specifications (MIL-SPEC) space ruggedized series-500 model.

The C401 Communication Controller Board is based on Motorola's 68000 microprocessor operating at 12.5 MHz. The C401 Board can support a maximum of 12 jumper selectable RS-232/422/423 serial ports. The standard board we will be using includes three(3) 68564 Serial Input/Output peripherals allowing six(6) serial communication channels. This will allow us to control the two(2) transmitting and two(2) receiving antennae.

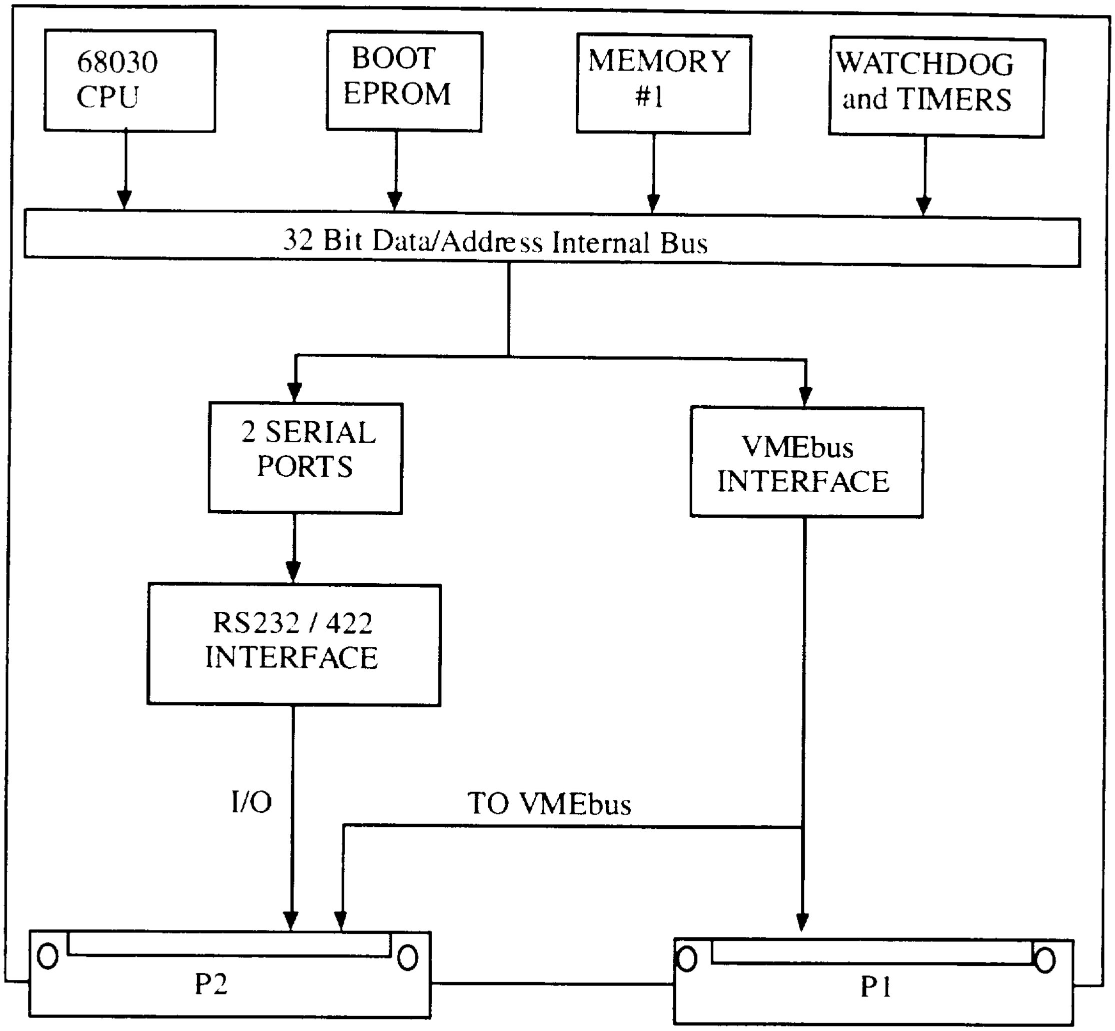
68030
CPU
BOOT
EPROM
MEMORY
#1
WATCHDOG
and TIMERS
32 Bit Data/Address Internal Bus
2 SERIAL
PORTS
VMEbus
INTERFACE
RS232 / 422
INTERFACE
I/O
TO VMEbus
P2
P1

Figure 3.2: The C130 68030 - Based Single Board Computer

Figure 3.3 is a model of the C401 board with all its standard hardware.

The C130 Single Board Computer and the C401 Communication Controller Board will be mounted in AITech's E101 VME Board Enclosure. The E101 Board enclosure is designed to house the VME boards produced by AITech. The enclosure is made of aluminum alloy and screws and captive screws are made of stainless steel. The enclosure is designed to resist severe vibration and shock. The E101 is sold standard with its own power supply which we will not be using due to the manner in which it was chosen to power Athena's electrical systems. For the purposes of Athena we will need to use the E101 series MIL-E-16400 space ruggedized enclosure board.

Table 3.4 is a chart of the overall specifications of Athena's on-board computer system. As can be seen the entire hardware package costs only $85,000 which is a reasonably competitive rate.

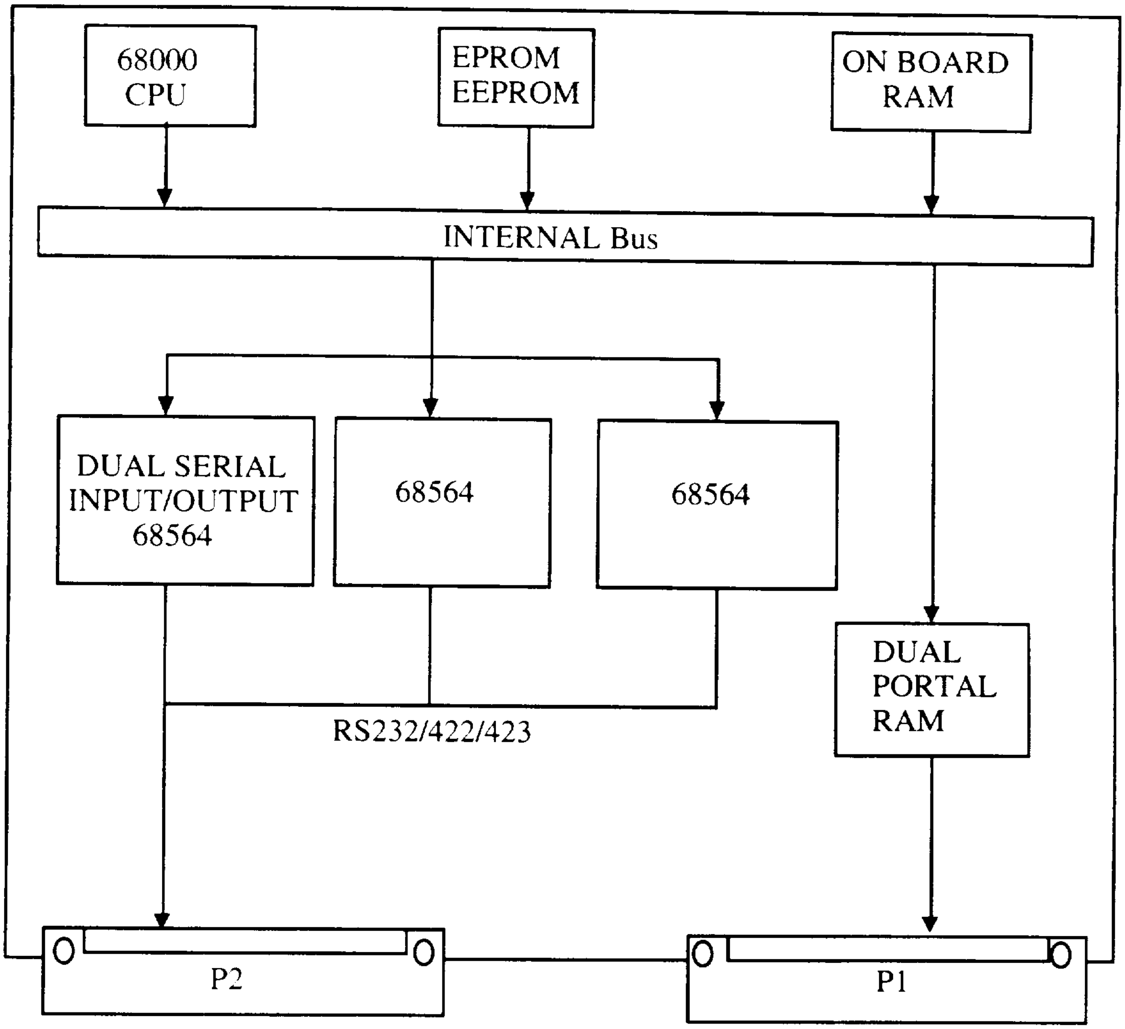
68000
CPU
EPROM
EEPROM
ON BOARD
RAM
INTERNAL Bus
DUAL SERIAL
INPUT/OUTPUT
68564
68564
68564
DUAL
PORTAL
RAM
RS232/422/423
P2
P1

Figure 3.3: C401 Multi-Protocol Communication Controller Board

	C130	C401	E101
Dimensions (mm)	N/A	N/A	124x193.5x562.1
Power Requirements	+5V 2.2A 2.6A ±12V 80mA 120mA	+5V 2.2A 2.6A ±12V 200mA 250mA	N/A
Mass (kg)	N/A	N/A	14.10
Temperature Range (°C)	N/A	N/A	-55 to 85
Overall Cost ($US)	$85,000		

Table 3.4: Overall Characteristics of The ATHENA Computer System

4.2 On-board Computer Software

The on-board computer software system of Athena needs to be developed from the beginning. An entirely new software package must be created for use by Athena. The software for Athena will need to handle the integration of the inertial measurement and global positioning telemetry data. Athena software must integrate the engine controller designed specifically for Athena by the Power, Thermal and Control team. It is also necessary that the software package that is developed for Athena should operate the communication controller board and handle the processing of data that is transmitted and received.

According to our research it would take two(2) software engineers a maximum of one(1) year to write Athena's software package. The cost of this work should only be $125,000. This price is an optimum cost for software development. A team larger than two(2) members would be able to create the software quicker but would cost more. A lone software engineer would require a greater amount of time to write Athena software and would not be monitored or supervised for proper results.

Once the system software has been created it is then necessary to retain the services of one(1) software engineer or programmer. It would be this persons job to write mission specific code to handle whatever type of payload we are attempting to place into orbit. The estimated recurring cost per mission of this programmer would be, at most, $10,000 per mission.

5.0 MISSION TRACKING

All satellite launchers must be tracked throughout their flight. Athena presents a special situation in that it is necessary to launch Athena over 2500 km from land. Athena must therefore be tracked and controlled through multiple means. First off Athena will require the use of chase planes to track its flight. Athena also will use its own internal guidance, navigation and control equipment to monitor its own position. Both the chase plane's data and own guidance information will be relayed to ground control at the Western Missile and Space Range at Vandenberg Air Force Base (AFB).

5.1 C-5B Flight Path

The C-5B used to deploy Athena will take off from Vandenberg AFB at a true course of 225° with a speed of 500 knots. Roughly 3 hours after takeoff the C-5B will be approaching the drop sight heading westward. At this point the flight speed will decrease to approximately 230 knots (200 miles/hour - Note: at the drop height of 10 km, the C-5B has a stall velocity of 200 knots). The inertial Measurement Unit calibration is fed down by the C-5B. After all pre-launch checks are made Athena will be deployed at 20° 00"N latitude and 128° 00"W longitude with a heading east-south-east along the Mexican coast. At this point the C-5B returns to Vandenberg and Mission tracking begins. This is all illustrated in Figure 3.4 showing the entire C-5B flight path.

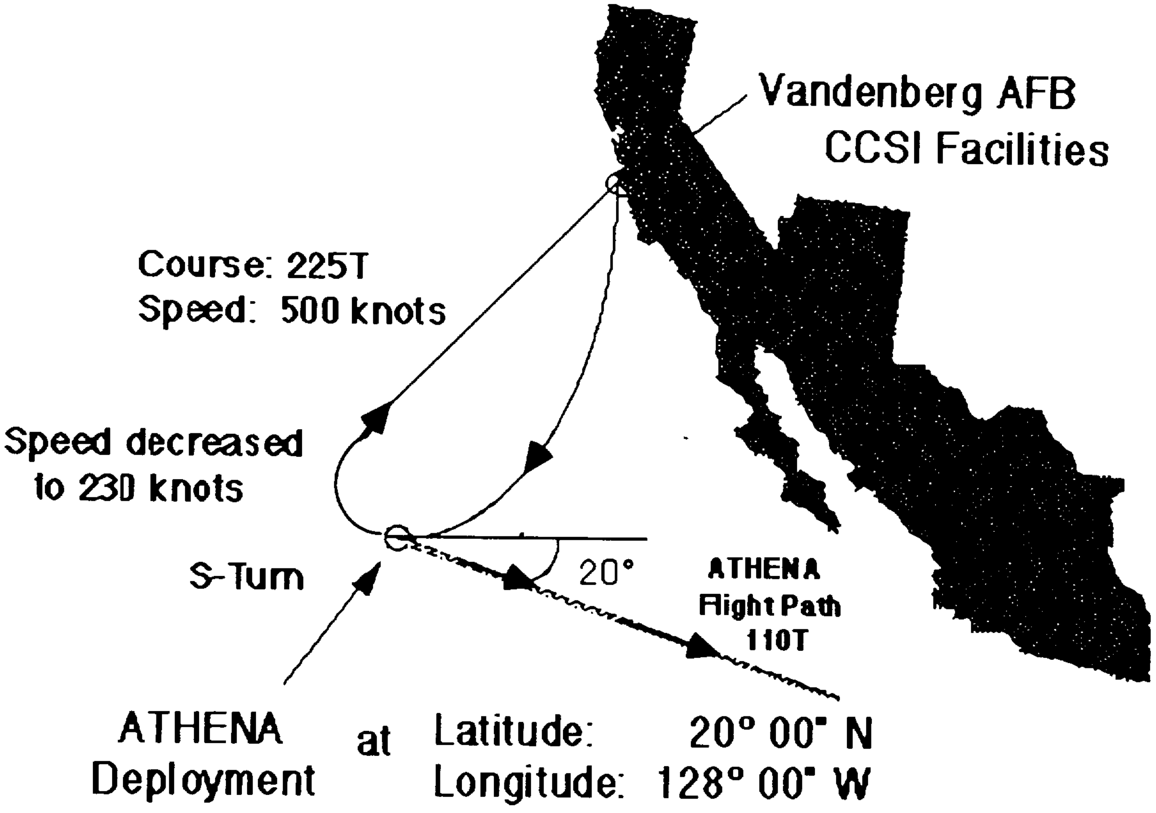

Figure 3.4: C-5B Flight Path

5.2 External Tracking

In order to track Athena 2500 km. from land we will have to use a chase plane. We can rent the services of an ARIA chase plane at a rate of $7,000 per hour for the entire 6 hour flight time of the C-5B for a total cost of $42,000 for chase plane tracking. All tracking data obtained from the ARIA will be transmitted back to mission control at Vandenberg AFB where flight path and trajectory will be analyzed.

The Vandenberg mission control facilities will be used to interpret telemetry and flight path data obtained about Athena in flight. All ground monitoring will be done in the control room at Vandenberg. Data will be received and interpreted at this site and all mission control information that needs to be sent to Athena will be done from here (see section on Flight Termination System in this chapter).

The cost for use of Vandenberg's mission control facilities is difficult to determine precisely. At the present time it would likely cost Athena $550,000 per launch for the use of the facilities. By our startup date in the year 1997 though the California Commercial Space Industry (CCSI) facilities are due to be under way. None of our contact people at CCSI right now could be sure of what it would cost to track and monitor Athena using their facilities rather than the Air Force. It is believed though that CCSI in order to be competitive, and with the new Space Commercialization Act, that the cost for mission control and tracking from Vandenberg will decrease by the time Athena goes into production. Although this amount might go down a third or even one half of the current cost, this is not certain and that is why our working budget for Vandenberg's facilities is $550,000.

5.3 Internal Tracking

As has already been shown Athena possesses its own means of monitoring its position through the use of an IMU and a GPS receiver. All this information is fed into the C130 SBC and interpreted with respect to the pre-established information within its mission programming. All necessary course corrections should be done automatically by Athena with no input from mission control at Vandenberg.

All the tracking information taken in by Athena will be sent back to mission control at Vandenberg by means of the C401 communication controller board and two transmitting antennae on Athena. These two transmitting antennae are located 180° from each other within Athena next to the receiving antennae. They are so placed so that Athena may transmit and receive telemetry information regardless of its spin orientation. Information can be broadcast back to mission control at a rate of 1 Mb/sec, keeping mission control fully aware of what Athena perceives as its trajectory and flight path.

The two receiving antennae are sheets 152.4 mm. x 152.4 mm. Each antennae weighs 0.5 kg and costs $5,000. The two transmitting antennae are 50.8 mm x 76.2 mm x 50.8 mm. Each antennae also weighs 0.5 kg and costs $5,000. This gives us a total transmitting and receiving cost of $20,000.

6.0 AIRCRAFT SUPPORT

After the launch of the C-5B and prior to the booster extraction, the booster will need to be monitored closely to ensure that all safety concerns are being adhered to and that the extraction will take place under safe conditions. In order to monitor the status of the booster during flight, an individual, henceforth called the Launch Panel Operator (LPO), will monitor the booster via a special console. The console will be located near the rear compartment of the upper deck and will be connected by shielded pairs of pass-through cables to the cargo bay. The cables will be connected to the booster at the third stage avionics section.

The console in front of the LPO will contain the following instruments:

- Ruggedized PC with a hard wire telemetry link to vehicle
  The PC unit can be nearly any kind, we have been looking at an IBM as the most likely choice, however, after software development, should another suit the projects needs better it would be selected.

- Four (4) Display Monitors
  The LPO console will be connected to four(4) video cameras mounted in the cargo bay. These will allow the LPO to monitor the booster visually to determine if there is any major damage to the booster before extraction. The LPO will have the ability to zoom in close enough to see the stage connections in detail and in focus. Two of the four monitors will be reserved for this purpose.

  The display monitors will also be connected to four(4) 8 mm video recorders so that all the flight data can be recorded for future analysis. This also ensures that should communication between the LPO and Mission Control falter, the LPO will have a complete recording of the video of the booster.

- LN-200 IMU
  During flight, the LPO console will not only have its own IMU, but will also receive data from the aircraft's IMU. This is for triple redundancy. The booster's IMU will be initialized prior to launch and will be tested prior to launch to ensure that it is working properly. During prolonged captive carry, however, navigation accuracy is lost due to inertial drift, therefore, the IMU will be on the console so that the LPO can compare the value from the two and correct the IMU onboard the booster.

- Mass data storage device
  This will record all nonvisual data.

- Uninteruptable power supply
  The LPO console will be connected to the C-5B's power supply for this purpose. Until minutes before launch, the aircraft will supply all power to the booster. To ensure that there is no problem when power is transferred, a "make-before-break" relay is used to ensure uninterrupted power to all electronic boxes.

- Transmission of all data to Mission Control
  Since an entire team cannot be placed onboard the C5-B, all information will be transmitted back to Mission Control so that a larger audience may review the data.

- Air percent monitoring
  Should there be a fuel leak which is so small that it cannot be seen visually on the monitors, the air will be tested to see what elements are present and in what amounts. The results will be compared against previous test flights to determine what 'normal' is.

- Communications with both the flight crew and Mission Control
  Communication with both the flight crew and Mission Control is vital. Should either be lost, the project would have to be aborted. Communication with the flight crew will be done via the C-5B's internal communication net. Since the pilot is the one who finally releases the booster, proper communication is imperative.

- Control Panel for air-conditioning to payload fairing
  This is in order to ensure that the payload is not damaged thermally prior to egress.

- Telemetry receiver

- Oxygen supplement for the LPO

- Payload required equipment

- Main switch panel
  Control of booster release mechanisms
  In order to release the booster, a series of steps will be required to ensure that it cannot be released accidentally. The final release lies with the pilot.

  The main panel will also allow the LPO to control what will be seen on the video monitors.

In essence, the LPO should be able to:

Monitor booster and payload status;
Provide conditioned external power to the payload;
Update the vehicle IMU prior to release;
Switch between internal and external power;
Download mission data to the flight computer and verify the mission data load;
Prepare and enable the vehicle for drop;
Capture, record, and display data from the vehicle and payload prior to launch.

Prior to extraction, the pilot may abort the mission for any reason s/he feels endangers the aircraft or the lives of those onboard. If the LPO wishes to abort, the decision must be seconded by either Mission Director or the pilot. See the section on Aborts.

7.0 SAFETY FACTORS AND CONSIDERATIONS

During every phase of the Athena program, from assembly of the booster until safe insertion of the payload in its orbit, there are many problems which could arise and must be prevented. This section will go through each step of the booster program and attempt to identify most of the major problems facing the program and how these threats are to be avoided.

- Fuel for the Athena booster
  Storage requirements of the fuel - Aerozine-50:
    Store in closed systems under a blanket of nitrogen;
    Avoid contact with the atmosphere;
    All mixing, blending, and transferring to be done in a closed system;
    All possible sources of flames and sparks must not be present;
    Stored in open and well ventilated storage spaces only;
    Must not be placed near flammable items.

  Storage requirements of the oxidizer - Nitrogen Tetroxide:
    Stored in open and well ventilated storage spaces only;
    Must not be placed near flammable items;
    Storage tanks must not be exposed to direct sunlight;
    A personnel shower should be available in case of spillage.

  Safety of the attitude control fuel - Hydrazine:
    Being poisonous, it is extremely important that this fuel be handled carefully.

  For more information on the safety of fuel to be used by Athena, see the Propulsion Report - Chapter 6, Section 6.1.

- Fueling of the Athena booster
  All possible sources of flames and sparks must not be present.

- Aircraft/Booster Integration
  As the booster (on the carriage) is placed inside the C-5B, precautions must be taken so that the vibrations don't become too bad.
    Limits of the payload with respect to vibration frequency:

>30 Hz	Longitudinal
>10 Hz	Latitudinal

Temperature and humidity levels must be watched at all times so that complications don't arise.
Low end limits of the temperature range:
0°C - 40°C (32°F - 104°F)

Aircraft, booster, and towing vehicle must all have engines and electrical systems off along with the aircraft being grounded so as not to have any sparks.

- On the Runway - Aircraft Engines and both Aircraft and Booster Electrical Systems are Running
  Towing vehicle is safe distance from aircraft.

  All aircraft systems have been previously checked during flight preparation in hanger.

- En Route to Deployment
  Must ensure that both vibrational and temperature requirements are adhered to.
  Ensure that there are no leaks.

- Deployment
  All umbilical connections must be removed and out of the way.
  Aircraft must be flying at approximately 230 knots (200 miles/hour - Note: stall speed at an altitude of 10 km for a C-5B cargo plane is 220 knots).
  Disengagement of main locks must have gone without a hitch.
  Rear Doors must open without any problems.
  The 3 G-11c Cargo Extraction Chutes must deploy and fill properly (Note: one of the three can fail and the parachutes will still work).
  Booster slides out of cargo bay properly.

- Miscellaneous
  Should the mission be aborted and payload bay need to be repressurized, precautions would need to be taken.
  Contamination of the shroud must be prevented.
  Due to the unsafe situations that might result from fuel spillage, all precautions must be taken to prevent a spill of any kind, on the ground, in the aircraft, and even to minimize the spill in the ocean should there be one.

7.1 Abort Scenarios

All craft, whether spacecraft, aircraft, or experimental, must ensure that all possibilities that could result from a launch are covered. As the Athena booster attempts to do what has previously been seen as impossible there are many factors which could lead to an abort. This section will attempt to identify possible situations in every step of the process of getting the payload up to proper position in orbit.

The three charts below will detail abort scenarios for the following three cases:

- Prior to launch while both the aircraft and booster are on the ground.
- After launch of the C-5B but prior to the extraction.
- After extraction.

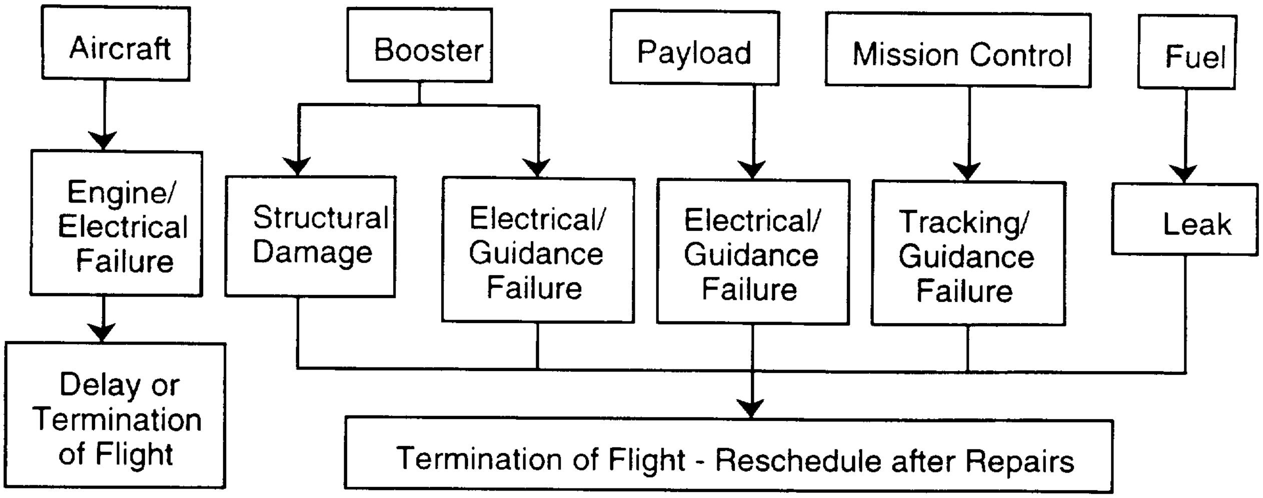
Aircraft
Engine/ Electrical Failure
Delay or Termination of Flight
Booster
Structural Damage
Electrical/ Guidance Failure
Payload
Electrical/ Guidance Failure
Mission Control
Tracking/ Guidance Failure
Fuel
Leak
Termination of Flight - Reschedule after Repairs

Figure 3.5: Abort Scenarios Prior to Launch

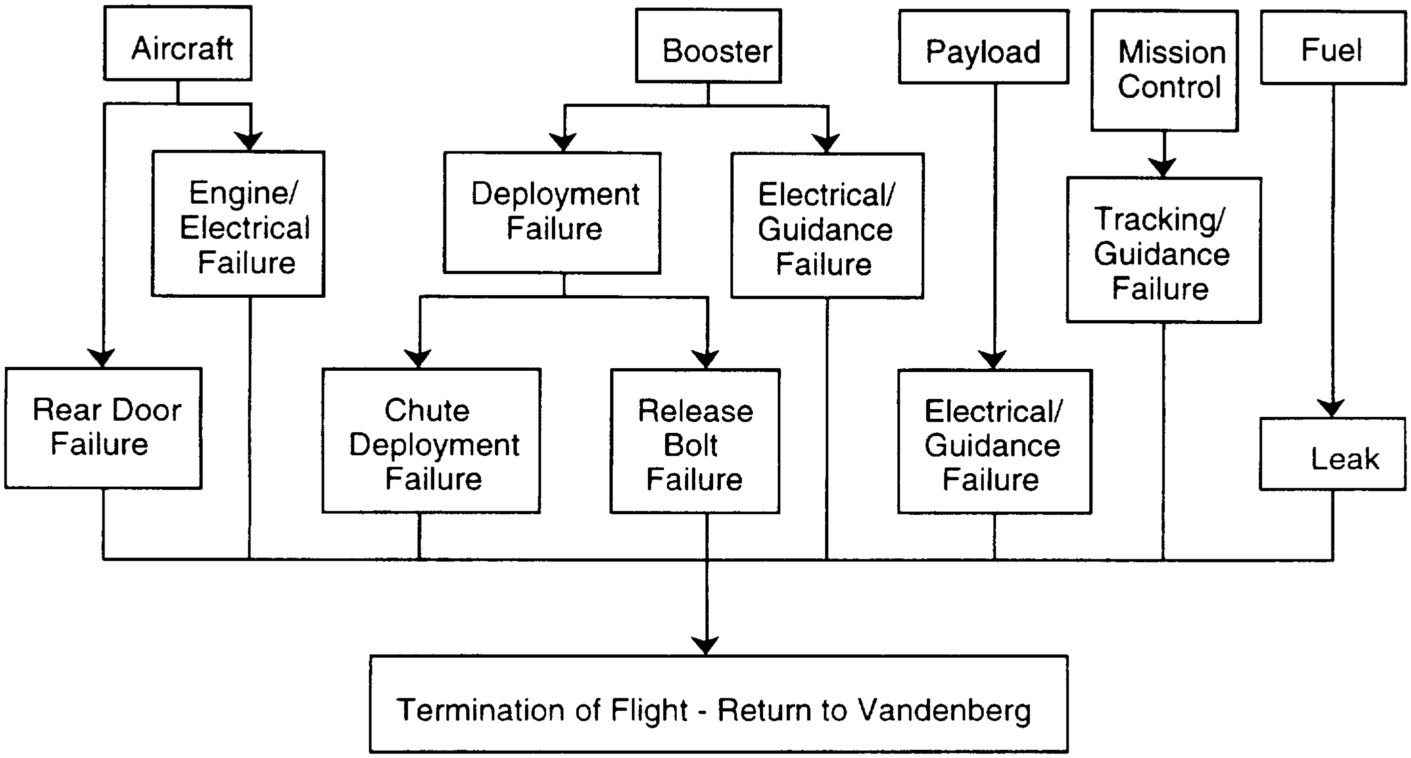
Aircraft
Engine/ Electrical Failure
Rear Door Failure
Booster
Deployment Failure
Electrical/ Guidance Failure
Chute Deployment Failure
Release Bolt Failure
Payload
Electrical/ Guidance Failure
Mission Control
Tracking/ Guidance Failure
Fuel
Leak
Termination of Flight - Return to Vandenberg

Figure 3.6: Abort Scenarios After C-5B Launch and Prior to Extraction

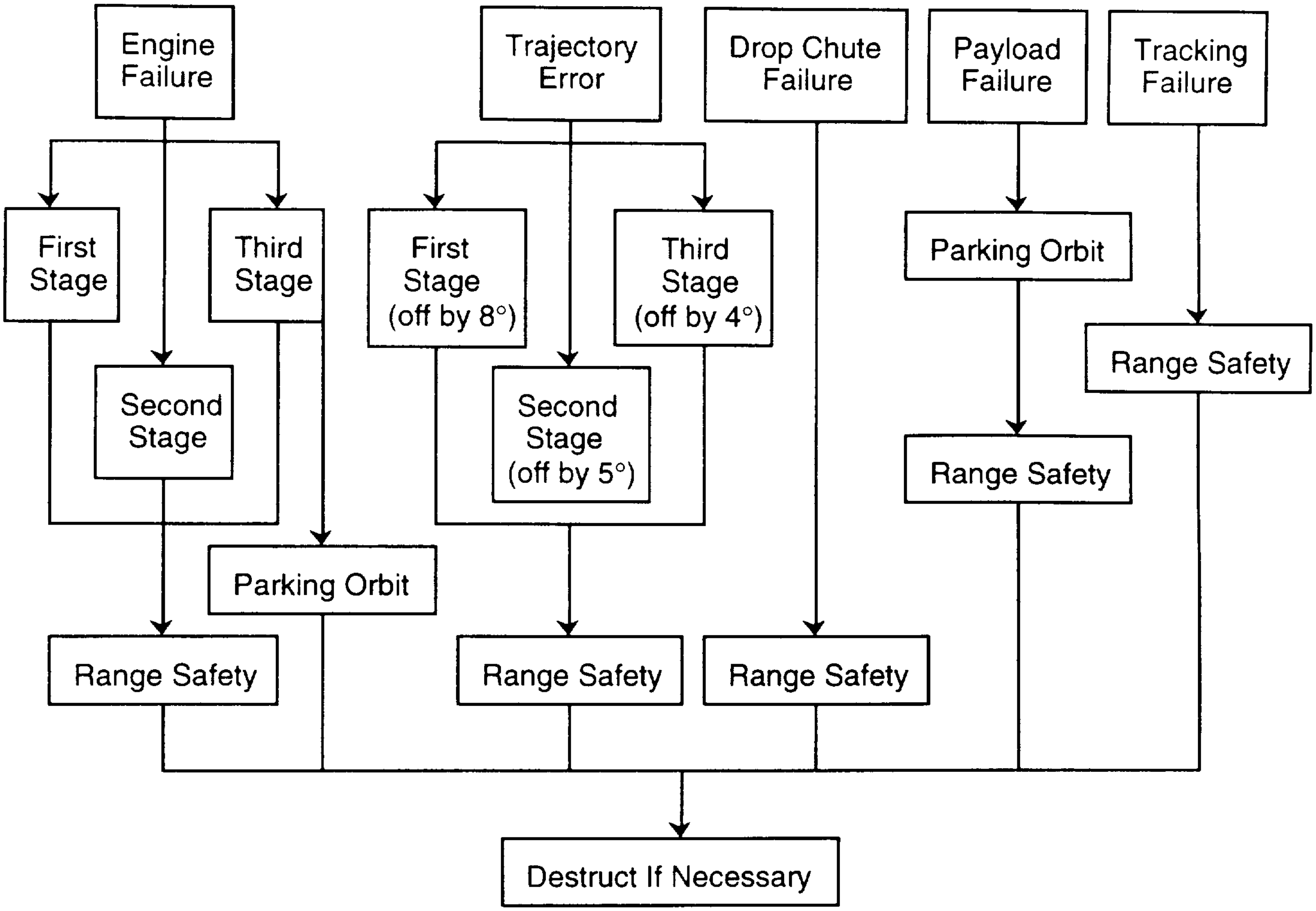
Engine Failure
Trajectory Error
Drop Chute Failure
Payload Failure
Tracking Failure
First Stage
Third Stage
First Stage (off by 8°)
Third Stage (off by 4°)
Parking Orbit
Range Safety
Second Stage
Second Stage (off by 5°)
Range Safety
Parking Orbit
Range Safety
Range Safety
Range Safety
Destruct If Necessary

Figure 3.7: Abort Scenarios After Extraction

8.0 FLIGHT TERMINATION SYSTEM(FTS)

The FTS is a system composed of small redundant explosive charges located at strategic junctures around the booster. Their purpose is to deactivate the propulsion system without complete annihilation of the booster. The reason an incapacitated falling booster is preferred over annihilation is due to the propellant used. Should the booster be exploded at a high altitude, the propellant would most likely dispense greatly, and should it catch fire, would pose a major environmental, political (being in the ocean), and clean-up problem. As it is, should the booster be simply disabled it would still be ripped apart upon impact with the ocean and would need special treatment due to the hazardous and even poisonous fuel that would remain, but this is the best method.

While in captive carry mode, all ordinance is in the safe condition. It is not until after complete egress and just prior to first stage burn that the ordinance is armed by the flight computer. This is to ensure that the ordinance poses no threat to either the booster or the aircraft prior to egress. Exact arming procedures will vary for each flight.

The system can be commanded by Mission Control or can be automatic in the case of premature stage separation. No FTS support would be needed from the payload. The FTS system, which is independent of the flight computer can receive signals from the ground which are encoded so that the system isn't accidentally tripped by a false signal.

The FTS system contains the following elements:

- Flight Termination Logic Unit (FTLU)
- Break Wires
- Receivers
- Antennae

9.0 LAUNCH TIME SEQUENCE

T	-15 hrs	-0:00.0	min	C-5B Present and Fueled Athena-to-Aircraft Mating Begun
T	-9	-0:00.0		Aircraft Preflight Preparations Begun
T	-7	-30:00.0		Range Set-up
T	-7	-0:00.0		Mating Complete Athena on aircraft power Reference IMU initialized Athena fueling begun
T	-6	-30:00.0		LPO Entry
T	-6	-25:00.0		LPO Power-On
T	-5	-50:00.0		Range-Safety Checks
T	-5	-25:00.0		LPO Verification
T	-5	-15:00.0		Payload Verification
T	-4	-30:00.0		Crew Boarding
T	-4	-0:00.0		Preflight Preparations Complete
T	-3	-30:00.0		Engine Starts Taxi
T	-3	-0:00.0		Launch of C-5B Galaxy
T	-0	-3:00.0		Payload/Booster Check (Initial)
T	-0	-2:40.0		Turn on IMU/S-Turn
T	-0	-0:45.0		Rear Doors Open
T	-0	-0:30.0		Payload/Booster Check (Final) Switch to Internal Power
T	-0	-0:10.0		Fill and Bleed Complete Detach Umbilicals
T	-0	-0:01.0		Deployment of the 3 G-11c Cargo Chutes
T	+0	0:00.0		Carriage Deployed; Pilot Engaged
T	+0	0:06.7		Egress of Booster Complete
T	+0	0:11.0		Arming Sequence Begins

		Flight Termination System(FTS) Armed
T +0	0:11.4	Ignition of First Stage
		Deployment Chutes Detached
T +0	0:12.9	Full Burn Achieved
T +0	0:17.9	Ascent Begins
T +0	0:59.4	First Stage Burnout/Separation
		Stages 1/2 Coast
T +0	1:02.4	Second Stage Ignition
T +0	3:18.4	Second Stage Burnout/Separation
		Stages 2/3 Coast
T +0	3:21.4	Third Stage Ignition
T +0	8:01.4	Third Stage Burnout/Separation
		Payload Placed into Orbit
T +0	8:02.0	Payload Events as Required
T +3 hrs	0:00.0	C-5B Touchdown at Vandenberg AFB

10.0 CONCLUSION

After researching many available options, and making multiple contacts throughout the professional field, the Mission Control Team gained a better understanding of what it takes to get a booster into orbit. Due to the lack of assistance from many contacts it is unknown whether the system Mission Control put together is the optimal choice. Therefore this system should be considered preliminary and future options should be looked into.

Chapter 4

Mission Analysis

Mission Analysis' Symbols

a	acceleration	R_e	Earth radius
a_t	semi-major axis of transfer orbit	r	radius
C_d	drag coefficient	S	reference area
D	drag	T	thrust
E_t	transfer energy	Δt	time increment
F_c	centripetal force	V	velocity
g	local gravitational field strength	ΔV	velocity increment
g_o	standard surface gravity	V_{cs}	circular velocity
i	inclination	v	velocity
I_{sp}	specific impulse	v_o	initial velocity
M	mass	W	weight
M	Actual payload mass	x, z	axes of a reference frame
M_c	dry mass		
M_f	final mass		
M_i	initial mass	q	pitch angle
M_o	sub-rocket mass	q	inclination change
M_p	(useful) propellant mass	q'	pitch rate
M_t	mass at time t	q_f	final pitch angle
M_u	payload mass	q_i	initial pitch angle
m_f	propellant mass	m	gravitation parameter
m_f'	propellant mass flow rate	r	atmospheric density
p	position	F	phase lag
p_o	initial position	Y	angular velocity

Earth Constants

Standard surface gravity $g_o = 9.80665$ m/s^2
Mean equatorial radius $R_e = 6378.140$ km
Gravitation parameter $m = 3.986013 \times 10^5$ km^3/s^2

75-76

PRECEDING PAGE BLANK NOT FILMED

1.0 GROUP OVERVIEW

The Mission Analysis group for the Athena project was responsible for two phases of the mission. The first phase involved the design of a satisfactory vehicle ascent trajectory including all staging operations. This had to be done while remaining within given maximum structural parameters such as the vehicle g-loading, and taking into account an approximation of the vehicle's drag profile. The goal of the trajectory was to get the payload up to an altitude outside of the atmosphere, while imparting sufficient velocity to maintain an orbit. Further, analysis of the ascent trajectory downrange distances were crucial in determining the position of the launch site for range safety purposes.

The second phase of the mission was to determine the best method for transferring the satellite to a final orbit, as well as finding the position of the satellite over the earth for geosynchronous orbits. The goal of this was to find a method that required the least energy to be added to the vehicle. The result of using the least energy maneuver would be to enable the most weight to be taken to the final orbit.

2.0 SATELLITE SELECTION

The goal of the Athena project is to allow the maximum range selection of satellites to be put into orbit by the launch vehicle, while maintaining cost competitiveness with other industry vehicles. The three circular orbits obtainable by Athena are Low Earth Orbit (LEO), Middle Earth Orbit (MEO) and Geosynchronous Earth Orbit (GEO). These orbits and their altitudes are outlined in Table 4.1. A third type of orbit mentioned is a Geosynchronous Transfer Orbit (GTO). This is an elliptical orbit used to transfer the vehicle from a parking orbit (LEO) to GEO. This is discussed more thoroughly in Section 5.

Orbit	Altitude (km)
Low Earth Orbit (LEO)	200 - 400
Middle Earth Orbit (MEO)	400 - 3000
Geosynchronous Earth Orbit (GEO)	35,723

Table 4.1: Definition of Earth Orbits

One of the most likely future uses for this vehicle is for the Iridium satellite system. This system is a network of satellites in MEO which provided communications services to users on the ground. Since the system includes a number of satellites, care had to be taken to ensure that the cost remained feasible. This was accomplished by using minimum energy transfer orbits. This results in the maximum weight to be taken to the final orbits. Other possible missions include scientific payloads to LEO and communication satellites to GEO.

3.0 DESIGN CONSTRAINTS

The mass and dimensions of Athena were determined by its carrier aircraft, the C-5B Galaxy. The associated constraints and their implications follow:

- Maximum booster weight of 80,000 kg
  90,000 kg was determined to be the maximum safe lifting weight of the C-5B and the egress sled was estimated to be 10,000 kg.
- Inside diameter of 2.7 m
  The back doors of the C-5B are 2.8 m in height and 3.5 m in width. It was decided that an elliptical cross-section was not cost effective compared to a circular section with a diameter of 2.7 m. Skin thickness and stringers put the inside tank diameter at 2.5 meters. (Structures)
- Total length of 30 m
  It was determined that 30 m was the greatest length the C-5B Galaxy could safely deploy. (Systems Integration)

Using these constraints, suitable engines were chosen from the list provided by the Propulsion Team. Along with weight and dimensional limits we had to keep the g-loading below 7 to protect our payload. Applying these guidelines to available rocket engines proved to be a complicated process.

The first stage engine had to be very powerful yet fit into the 2.5 m diameter constraint. Since two or more moderate-thrust engines would not fit, a single powerful engine had to be used. The LR87-AJ-11, the most powerful liquid engine listed, was chosen. The most powerful solid rocket booster that fit the diameter constraints was the Castor 120GT which, unfortunately, weighed more and had less thrust.

The second stage engine should have been about half as strong as the first for optimal g-loading. Again, solid rocket engines did not work. Thrust was too low or burn times were too short. Unfortunately, there was no ideal liquid rocket engine available either. The LR87-AJ-5's thrust exceeded the g-load limit and the next closest engine was the LR91-AJ-11. The LR91-AJ-11 had very low thrust, and two of these engines would not fit. An elliptical cross-section would fit two engines and take up more payload, but the extra payload revenue would not cover the cost of the extra engine and structure. Therefore only one LR91-AJ-11 was used at the cost of an extensive second stage burn.

The third stage engine had to have a low enough thrust to stay under the 7 g limit. For orbital maneuvering, restart capability was needed. Therefore solid rocket engines could not be used. Unfortunately, there was no ideal liquid rocket engine available. The LR-105's thrust exceeded the g-load limit and the next closest engine was the AJ10-138. Two of these engines fit within the diameter constraint, so a higher but less than ideal thrust was attained. The final engine configuration and specifications are given in Table 4.2.

	Engine	Number Used	Thrust per Engine (N)	Isp (seconds)
Stage 1	LR87-AJ-11	1	2 437 504	301
Stage 2	LR91-AJ-11	1	467 040	316
Stage 3	AJ10-138	2	35 584	310

Table 4.2: Athena Engines

4.0 ASCENT TRAJECTORY

Athena was modeled as a point mass in order to calculate the ascent trajectory. We assumed a nominal trajectory for our vehicle, that is, a purely two-dimensional motion. This means that all forces acting on the vehicle lie in its plane of motion. This is not the case in practice, since it does not allow for aerodynamic forces, gravitational forces, or thrust forces that may be acting perpendicular to the instantaneous plane of motion. However, a three dimensional model would require extensive numerical methods for solution, whereas the two dimensional model allows the motion of the vehicle to be solved for analytically.

Finding a set of equations for a two dimensional model of an ascent trajectory is simple for a flat earth with constant gravity and a constant density atmosphere. However, a more accurate model was needed. The rocket equations (Cornelisse) which integrate the changing mass over each time step seemed like a good place to start, but including centripetal acceleration into these equations was not possible with our program. Programs we tried using the full round earth equations never gave us realistic results. The equations we decided to use were derived from basic physics and the equations of motion for a flat earth. They included variable gravity, variable atmospheric density, and a centripetal acceleration term to simulate a round earth.

4.1 Forces and Equations of Motion

Figure 4.1 shows the Free Body Diagram for our vehicle. Assuming a flat earth (as is common), X is parallel to the surface of the earth, and Z is perpendicular to it (i.e., in the direction of gravity). Since a spherical, rotating earth is not nearly the same as a flat, stationary earth, we had to make compensations. To account for the spherical earth, a centripetal force was added. The rotation of the earth was accounted for with an initial X velocity corresponding to the speed of rotation at our drop altitude of 10 km.

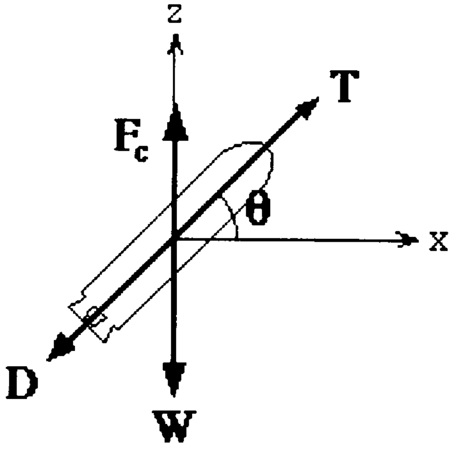

Figure 4.1: Athena Free Body Diagram

The derivation is as follows:

Where:

q = Pitch Angle
T = Thrust
D = Drag = $\frac{1}{2}$ r V^2SC_d (Eqn. 4.1)
r = density of the atmosphere
V = vehicle velocity
S = reference area
C_d = drag coefficient

W = Weight = Mg (Eqn. 4.2)
F_c = Centripetal Force = $\frac{MV^2}{R_e + z}$ (Eqn. 4.3)
R_e = mean radius of the earth

The sum of the forces is then:

$$F = T - D - W + F_c \quad \text{(Eqn. 4.4)}$$

From Newton's Second Law :

$$F = Ma$$
$$a = \frac{F}{M}$$
$$a = \frac{T - D}{M} - g + \frac{V^2}{R_e + z} \quad \text{(Eqn. 4.5)}$$

From this the directional accelerations are:

$$a_x = \frac{T - D}{M} \cos q \quad \text{(Eqn. 4.6)}$$

$$a_z = \frac{T - D}{M} \sin q - g + \frac{V^2}{R_e + z} \quad \text{(Eqn. 4.7)}$$

From Physics, we know that the velocity of a particle is a function of its acceleration at any given time:

$$v = v_0 + aDt \quad \text{(Eqn. 4.8)}$$

Likewise, the position is just a function of velocity:

$$p = p_0 + vDt \quad \text{(Eqn. 4.9)}$$

4.2 Iteration Technique

These equations are for a constant mass vehicle traveling in a constant gravity field, constant density atmosphere, with a constant pitch angle, which is not the case. To solve this problem, a Matlab program (see Appendix A) was developed in which these forces were solved for in time steps over which the aforementioned terms could be held constant. Each time step is exactly 1 second, so the Δt terms in the equations effectively drop out. The total time is the burn time of the engine. Over each step, gravity and atmospheric density (Hill & Peterson) were calculated from the previous step's position using the following equations:

$$g = g_0\left(\frac{R_e}{R_e + z}\right)^2 \quad \text{(Eqn. 4.10)}$$

$$r = 1.2 \exp[(-2.9\times10^{-5})\, z^{1.15}] \quad \text{(Eqn. 4.11)}$$

The mass and pitch angle were slightly more complicated. The pitch rate was calculated from:

$$q' = \frac{q_i - q_f}{\text{burn time}} \quad \text{(Eqn. 4.12)}$$

q_i = initial vehicle pitch angle

q_f = final vehicle pitch angle

Then, the pitch angle over any given time step is:

$$q_t = q_{t - D_t} - q'Dt \quad \text{(Eqn. 4.13)}$$

The mass is calculated similarly by:

$$M_t = M_{t - Dt} - m_f'Dt$$

$$m_f' = \frac{T}{g_0 I_{sp}} \quad \text{(Eqn. 4.14)}$$

where M_t is the total vehicle mass at time t and m_f' is the propellant mass flow rate. Using these equations the program calculates the acceleration, velocity, and position of the vehicle over each time step, thereby determining the final values for each of these functions at the end of the engine burn.

4.3 Multi-stage Rocket

Because Athena is a three stage booster, each stage drops off after it is done firing. This means the trajectory analysis had to be done in several steps. To aid in understanding this, some nomenclature must be introduced. Figure 4.2 is a diagram detailing the multi-stage rocket booster (Cornelisse, 263).

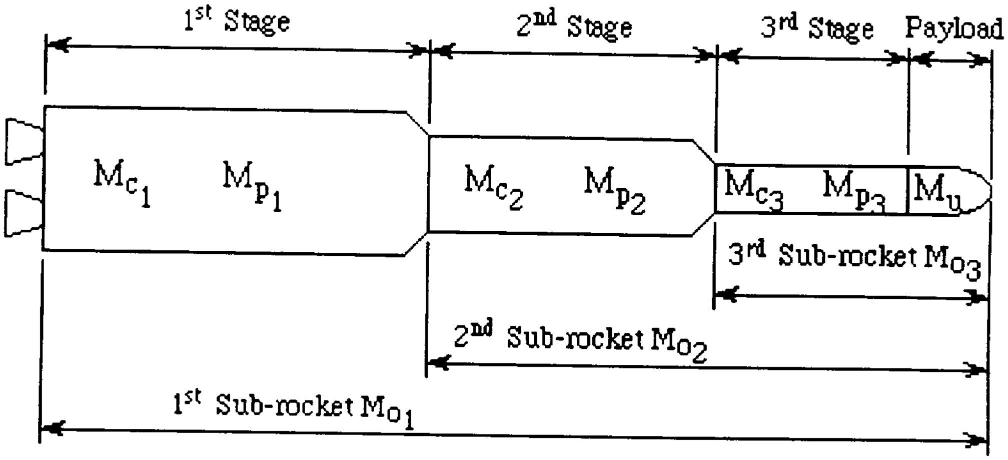

Figure 4.2: Nomenclature for a Three-Stage Rocket

In figure 4.2:

M_{c_i} = Dry mass of Stage i
M_{p_i} = Propellant mass of Stage i
M_u = Actual payload mass
M_{o_i} = Initial mass of Sub-rocket i

From this we can define the initial mass of sub-rocket i as:

$$M_{o_i} = M_{c_i} + M_{p_i} + M_{u_i} \quad \text{(Eqn. 4.15)}$$

where:

$M_{u_i} = M_{o_{i+1}}$; $i = 1 \ldots N - 1$
$M_{u_N} = M_u$

This means that the "payload" of *Sub-rocket i* is effectively the mass of everything above *Stage i*, since it sees the other stages as dead weight. For example, the effective payload of Sub-rocket 1 is Stage 2 + Stage 3 + Payload.

4.4 Fuel Mass Distribution

Determining the best mass distribution was complicated by the fact that we did not have the best engines for the mass of our booster. Methods we found included mass ratios calculations, proportional velocity changes, and maximum g-load calculations. A summary of our trial and error follows:

First, burn times were calculated to obtain maximum allowable g-load at engine burnout using a 5000 kg payload. With these burn times the amount of fuel needed was much higher than 80,000 kg. Reducing the fuel mass to 80,000 kg meant that the rocket did not reach orbit even with minimal payload. We tried to use mass ratios between the stages but the combined mass and size constraints made this method unusable. Next we tried to have each stage contribute an equal change in velocity. This approach proved ineffective because it made the first stage too powerful and heavy. Decreasing first stage burn time made the weak second and third stage engines burn longer than the engines were rated for.

The best results we found were by combining these methods. Setting the second stage to maximum g-loading and then using the mass ratio for an estimate of the first and third was nearly correct. Then the first and third stages were adjusted to lower the weight to 80,000 kg. Then it was a trial and error process to find the best thrust angles for each stage. Because of our weak second and third stage engines, we could not keep the first stage near vertical. Arcing the first stage over to use some of its thrust for horizontal velocity means that the rocket loses all its vertical velocity before the end of the third stage burn. Pitching first stage up more means that we don't get enough horizontal velocity. Cutting the inter-stage coast times down to the minimum time for safe stage separation gave the best use of the first stage vertical velocity.

4.5 Ascent Trajectory Program

This section deals with the program listed in Appendix C.1. The program does six separate time iterations:

1) First stage burn
2) First coast
3) Second stage burn
4) Second coast
5) Third stage burn
6) Third "coast" (to confirm orbit)

The data given in Table 4.3 was used to determine Athena's dry mass.

	Structural Mass (kg)	Tank Mass (kg)	Engine Mass (kg)
Stage 1	1050	1827.7	2285
Stage 2	450	803	584
Stage 3*	450	310.9	2 x 110

*Since we have two engines on third stage, the engine mass is doubled

Table 4.3: Athena Mass and Engine Data

The burn times, initial and final pitch angles, and fuel consumed per stage are given in Table 4.4.

	Burn time (sec)	qi (°)	qf (°)	Usable Propellant (kg)	Safety Propellant (kg)
Stage 1	58	60	20		
Coast 1	3	20	18	0	0
Stage 2	111	18	10		
Coast 2	13	10	7	0	0
Stage 3	205	7	4		

Table 4.4: Burn Times, Pitch Angles and Fuel Consumed

This input gave the results in Figures C.2.1 and C.2.2 (see Appendix C.2). A list of this output is given in Table 4.5.

Event	Time from Deployment (sec)	Velocity (m/s)	Altitude (km)	Downrange Distance (km)
First Stage				
Ignition	11	-50.0	10.0	0.0
Burnout	69	2415.7	32.525	66.862
Second Stage				
Ignition	72	2402.5	34.925	73.668
Burnout	183	5005.9	106.2	453.18
Third Stage				
Ignition	196	4998.8	113.28	517.82
Burnout and Orbit Insertion	401 / 1011	7787.6 / 7787.5	151.36 / 214.26	1782.8 / 14328

Table 4.5: Key Trajectory Results

5.0 ORBIT TRANSFERS

The second phase of the mission begins after the third stage engine has shut off. At this point, the payload has reached a parking orbit of 200 km above the surface of the Earth. This is not likely to be the final orbit altitude for the vehicle since many payloads require a higher orbit (MEO or GEO).

5.1 Hohmann Transfer Orbits

An orbit transfer between two circular coplanar orbits is the most basic orbital maneuver. The procedure involves the ascent into a low altitude parking orbit, followed by a transfer to a high circular orbit using an intermediate elliptic orbit that intersects both circular orbits.

The method which requires the least speed change (ΔV) requires a doubly-tangent transfer orbit. This elliptical orbit has the special feature of being tangent to the low altitude parking orbit at its perigee, and tangent to the final high altitude circular orbit at its apogee (see Figure 4.3). The maneuver was first realized by Hohmann in 1925, and is called the *Hohmann transfer orbit* (Bate, Mueller and White, 163).

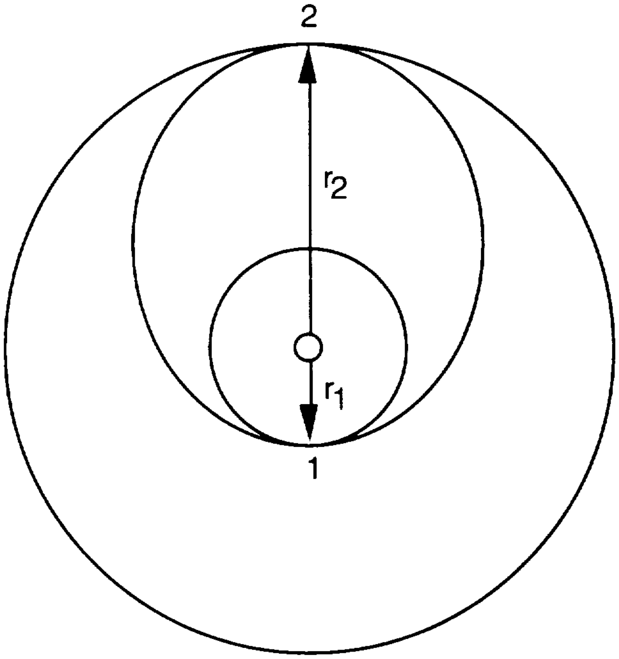

Figure 4.3: Hohmann Transfer Orbit

Point 1 is the perigee of the Hohmann transfer orbit and is also the point of tangency to the low altitude orbit. The speed of the vehicle at this point is the circular orbit speed of the parking orbit:

$$V_{cs} = \sqrt{\frac{\mu}{r}} \quad \text{(Eqn. 4.16)}$$

Athena lifts its payload up to a circular parking orbit of 200 km. The value r in Equation 4.16 is the radius of the orbit *from the center of the earth*.. The radius of the earth is 6378.14 km. Thus, the radius of the orbit is the radius of the earth plus the orbit altitude, or 6578.14 km. Using Equation 4.16, with $r=r_1=6578.14$ km, the vehicle speed in the parking orbit was calculated to be:

$V_{cs} = 7.78$ km/s

The vehicle speed must be increased at this point to equal the perigee speed of the elliptical transfer orbit. To calculate the required speed for insertion into the transfer orbit, the transfer orbit energy must be calculated using:

$$E_t = \frac{-\mu}{(r_1 + r_2)} \quad \text{(Eqn. 4.17)}$$

Then, using the energy equation for the elliptical orbit, the required speed can be calculated:

$$V_1 = \sqrt{2\left[\frac{\mu}{r_1} + E_t\right]} \quad \text{(Eqn. 4.18)}$$

This speed, V_1, is the speed which the vehicle must obtain to follow the path of the doubly-tangent transfer orbit. However, when the vehicle is at Point 1, its speed is less than the required speed. The vehicle must then commence an orbit insertion burn to attain this velocity. The speed increase required from the insertion burn is found using:

$$\Delta V_1 = V_1 - V_{cs1} \quad \text{(Eqn. 4.19)}$$

Once the vehicle attains the required velocity for the transfer orbit, it will coast following the elliptical trajectory. Point 2 is the apogee of the elliptical transfer orbit, and the vehicle has a velocity corresponding to:

$$V_2 = \sqrt{2\left[\frac{\mu}{r_2} + E_t\right]} \quad \text{(Eqn. 4.20)}$$

This velocity is less than the velocity required to maintain the desired circular orbit. The velocity which must be obtained can be calculated using Equation 4.16 with $r=r_2$. Here, r_2 corresponds to the final orbit altitude of the vehicle. To obtain this required speed, a rocket engine is fired to increase the speed by the amount:

$$\Delta V_2 = V_{cs2} - V_2 \quad \text{(Eqn. 4.21)}$$

This final impulse is provided by the stage 3 engine (after a restart) after a transfer to MEO, or by an apogee kick motor if the final orbit is in GEO.

5.2 Orbit Inclination Change

The orbit inclination is the angle which the satellite's flight path makes with the equator of the Earth (see Figure 4.4). This angle corresponds to the latitude of the vehicle's launch site. Athena is to be launched, ideally, from 20° N latitude, 128° W longitude, which means that any satellite put into orbit by Athena will have an orbit inclination of 20°. Also, it should be noted that the maximum extremes of latitude of the satellite's flight path will be between 20° N and 20° S latitude.

The most likely cause for a change of inclination for the payload would be if the payload was going to GEO. In this case, the payload must be brought to an inclination of 0°. This is done by applying thrust in the plane perpendicular to the plane of the orbit. This maneuver is best done at the apogee of the transfer orbit, either just after or coincidental with the recircularization burn. The reason for doing it at this point can be seen by looking at the equation for the ΔV for the inclination change:

$$\Delta V = 2V\sin\frac{\theta}{2} \quad \text{(Eqn. 4.22)}$$

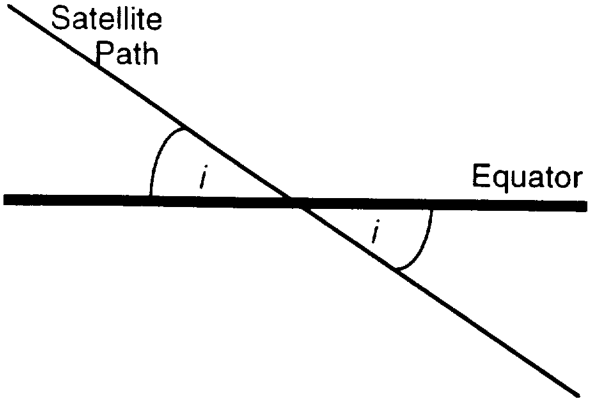

Figure 4.4: Orbit Inclination *i*

As can be seen in Equation 4.22, the ΔV is a function of the orbital velocity. The orbit velocity decreases as the orbit altitude increases. Therefore, the velocity is smallest at the apogee of the elliptical transfer orbit. If the purpose of the inclination change is to "equatorialize" the orbit, care must be taken to initiate the velocity change at one of the points where the satellite is directly over the equator. The apogee of the GTO satisfies both of these requirements, and thus is the most ideal point for the inclination change. The payload aboard Athena will have to undergo and inclination change of 20°. The Athena payload must apply

$$\Delta V = 2V\sin\frac{\theta}{2} = 2(7.78)\sin\frac{20^\circ}{2} = 1.07\,\mathrm{km/s}$$

in the plane perpendicular to the 20° inclination orbit.

5.3 Mass Fraction Computation for Transfer

The total mass which Athena lifts into the 200 km parking orbit is 1715 kg. This value should not be confused with the effective mass of the satellite, which, depending on the final orbit altitude, could be substantially less. The value of 1715 kg includes the actual satellite *plus* the mass of the fuel and rocket engines used in the orbit transfer.

The total mass that can be inserted into the transfer orbit is a function of the ΔV required to insert the payload into the elliptical transfer orbit. The relation to determine the final mass, after transfer orbit insertion, is:

$$\frac{M_i}{M_f} = e^{\frac{\Delta V}{gI_{sp}}} \quad \text{(Eqn. 4.23)}$$

A new value of the acceleration of gravity, g, must be calculated since this value changes with distance from the center of the Earth. The equation for gravitational acceleration is given in Equation 4.10. With the new value for gravity at the 200 km orbit, Equation 4.23 can be used to calculate the fraction of the total mass that will be in the transfer orbit. The following chart (Table 4.6) shows the mass ratios for various MTO burns and a GTO burn.

Final Orbit Altitude (km)	Transfer Orbit Insertion Mass Ratio (initial/final)
500	1.032
800	1.062
1000	1.082
35,723	2.365

Table 4.6: Transfer Orbit Insertion Mass Ratios

Equation 4.23 can also be used to calculate the mass of the final satellite. The final mass is that which is left after the transfer orbit apogee burn. Care must be taken to use the value of the gravitational acceleration at the desired orbit altitude, since this value varies from as much as 9.2 m/s at 200 km to 0.22488 m/s at GEO altitude. The following chart (Table 4.7) shows the mass fraction values for various recircularization burns.

Final Orbit Altitude (km)	Recircularization Burn Mass Ratio (initial/final)
500	1.0335
800	1.0709
1000	1.0989
35,723	1589884064

* Assumes apogee kick motor I_{sp} is 310 sec.

Table 4.7: Recircularization Burn Mass Ratios

5.4 Phase Changes

A major concern in transferring satellites to geosynchronous orbits is determining the point over the earth at which the satellite will be stationed upon final orbit burn. Figure 4.3 shows that the GTO insertion point and the GEO insertion point are 180° apart from each other. However, the satellite position with respect to the earth will lag by a certain amount due to the fact that the Earth is rotating.

The magnitude of this phase lag is dependent on the time of flight during the transfer orbit. The time of flight is dependent on the magnitude of the semi-major axis of the elliptic transfer orbit:

$$a_t = \frac{r_1 + r_2}{2} \quad \text{(Eqn. 4.24)}$$

We can see from Figure 4.3 that the transfer orbit consists of one-half the total elliptical orbit. As a result, the time of flight (TOF) for the orbit transfer is one-half the period of the total transfer orbit:

$$TOF = \pi\sqrt{\frac{a_t^3}{\mu}} \quad . \text{ (Eqn 4.25)}$$

The Athena payload going to GEO has:

$r_1 = 6578.14$ km (200 km orbit)
$r_2 = 42101$ km (GEO)
$a_t = 24339.57$ km
TOF = 18895.132 sec (5.2486 hr)

The Earth spins through a full 360° of longitude every day, or 23h 56m (Bates, Mueller and White, 160). This corresponds to an angular velocity of Y=0.00417827 °/s. Therefore, during the time elapsed while the satellite is in GEO, the earth precedes the satellite by:

$\Phi = \Psi \times TOF$ (Eqn.4.26)

The phase lag of the Athena payload to GEO is 78.949° using the above values of Y and TOF. In other words, the satellite will be 78.949° behind the insertion latitude (or equivalently, 101.051° ahead of the insertion latitude). The insertion latitude depends on the position where the satellite crosses the equator.

6.0 SUMMARY

Time constraints did not permit us to perform the number of iterations required for a more optimum trajectory. The results, as of this time, are that Athena can achieve a low earth parking orbit of 200 km with a payload of 1715 kg. A downrange distance of 2500 km over open water will be needed to launch safely into orbit. Analysis of the transfer orbit shows that the vehicle can place 888kg into GTO. Analysis of the GTO recircularization shows that Athena may not be feasible for launch of payloads to GEO. Further, Athena will not have the capability of placing a payload in a polar orbit.

Chapter 5

Payload

CHAPTER 5 -- PAYLOAD

Payload's Symbol

Δm: change in mass
Δp: change in pressure
ΔT: change in temperature
g: standard gravitational acceleration
m: mass
p: pressure
Pi: 3.14159265
R: specific gas constant
T: temperature
v: volume

1.0 GROUP OVERVIEW

The available payloads and payload requirements are of the utmost importance in the design of a space booster. This is especially true since there are many launch vehicles on the market and a new one would have to attract payload owners and investors. For these reasons, Athena had to keep payload concerns in mind throughout its design.

A general understanding of the current and future payloads was of importance initially. As changes were made in the booster design and capability, the payload market was readjusted to keep this area of the design in perspective. Athena also had to keep payload concerns in mind. Of importance were concerns such as:

- Mass and size capabilities
- Market (Current and Future)
- Payload mission capability
- Payload protection

All these concerns were considered and used in the design of Athena.

2.0 ATHENA PAYLOAD CONFIGURATION

Athena's payload configuration has changed, as has the whole booster, many times over the course of the term. This section will focus on the designing process and how the final payload capability was reached. Athena's final payload capability is:

- 1715 Kg to LEO
- 1143 Kg to MEO (specifically 800 km)
- 888 Kg to GTO

2.1 Initial Design and Adjustments

Athena originally was expected to be capable of taking over 5000 Kg to Low Earth Orbit. However, due to limitations in the C-5B and other limiting factors, this capability was not feasible. Before the payload capabilities were reduced, there were many designs for the

PRECEDING PAGE BLANK NOT FILMED

payload bay. Most importantly, we had a payload bay designed to be structurally capable of taking two satellites if necessary.

There were three original payload bay configurations. Booster length became a concern and more elliptical body structures were considered. A design for a side by side dual payload was considered. All four of these designs can be seen in Appendix D.1. During the development of the new designs for the payload bay, the payload capability was reducing. The market was considered at every step down. 4000 kg., 3000 kg., 2000 kg. were all expected capabilities to LEO during Athena's design. The payload decrease throughout the design process continually decreased Athena's available market. Most steps were not drastic, Athena just moved into a new market niche. In the end, the concern for our decreasing market was heard and understood but deferred in importance to other factors in the design.

2.2 Final Configuration

The final payload configuration was decided by booster capability at its limited total mass. Athena proved to be less efficient at the decreased mass and therefore less capable in its payload mass. The final payload capability of Athena is 1715 kg. to LEO and the payload bay utilized has been decreased as well. Athena can take payloads up to 4.5 m. in height and 2.7 m. in diameter. More detail on the payload bay can be found in section 4.

3.0 PAYLOAD MARKET

The payload market concerns are of major importance in designing a booster like the Athena. If no market can be found, the system is unlikely to find use and therefore will never be profitable. The market concerns come down to what types of payloads are available and how our design fits the needs of the current and future market. Since we plan on launching by 1997, current payloads become of utmost concerns because the trends are not likely to change that drastically.

3.1 Payloads Available

Payloads currently available and available in the near future are a starting block for the design of a space launch system like Athena. Since our payload was unlikely to ever be much over 5000 kg. and our size was limited by the C-5B, satellites had to be our major market right from the start.

3.1.1 Communications Satellites

Communications are our only real means of sending data over long distances. Wires produce too much distortion as do other types of relays. They can also be very slow in transmission of data. Satellites overcome these problems and are therefore a major industry. Of all satellites launched, communications satellites are by far the most common. They tend to represent the majority of the market for space launchers like Athena. Figure 5.1 shows a typical communications satellite configuration.

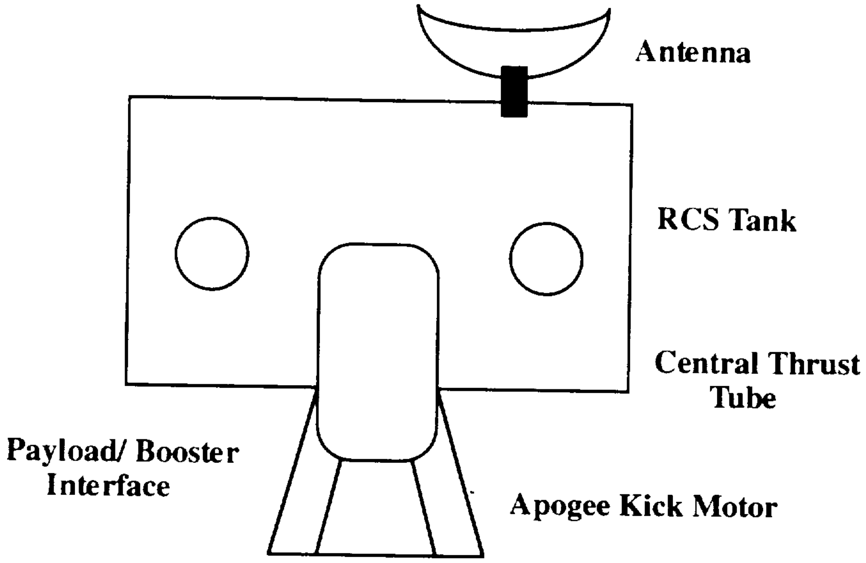

Figure 5.1: Typical Communications Satellite

3.1.2 Other Satellites

Small Satellites

Because of our reduced payload capability, smaller satellites had to be analyzed. They prove to be a very important part of our market niche along with the communications satellite. Although communications satellites are far more common, they are typically in GEO and with our small payload capability, our percent share of the communications market will be small.

Note that small satellites are typically in LEO and weigh less than 220 kg. They are becoming increasingly popular in recent years. Information on a 76 of these small satellites was available and useful in proving the availability of smaller payloads.

Tethered Satellites

The upper atmosphere has proven to be very difficult to gather data in as it is to high for balloons and to low for satellites to gather much data before they reenter. Tethered satellites are an attempt to gather information in this area. The Space Shuttle attempted one tether mission with a satellite named TSS-1. It was fairly successful in the data it gathered but full deployment was not reached. TSS-2 was recently launched as well. However, it was sent on an expendable booster like Athena. TSS-AVM is another satellite designed specifically for expendable tether missions. It is lighter and does single specific studies during its mission. The specifications for the TSS-AVM satellite are presented in Figure 5.2. The mass of the structure needed to tether to the booster can vary but typically the payload is under 1715 Kg. Athena would be capable of performing future expendable tether missions.

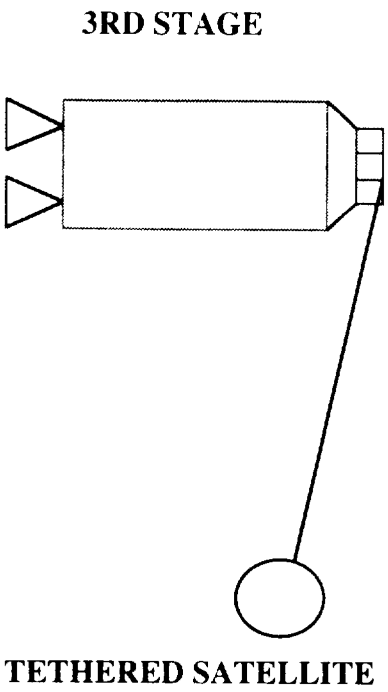

MASS : 900 - 1300 KG

DIAMETER : 1.5 m

TETHER : 25 m (length)

ORBIT : 200 km

Figure 5.2: Tethered Satellite System

3.2 Orbits

Satellites are typically put into varying orbits around the Earth depending on the goals to be accomplished. Small satellites are typically placed in Low Earth Orbits (LEO) since there power capabilities tend to be somewhat limited. Weather, remote sensing, and scientific satellites have varying orbits ranging from under 200 km. (LEO) to over 36000 km. in altitude. These satellites are typically placed into circular orbits. There are some common elliptical orbits such as the Moliniya but they will not be discussed as they do not prove to be an expected market for Athena.

3.2.1 Low Earth Orbit (LEO)

Low Earth Orbit is the term typically used to represent circular orbits at altitudes of 200 to 2000 km. However, the lower altitudes in this range are not typically utilized due to atmospheric drag being of major concern to holding the orbit. Inclination angles for these orbits normally range from 30 to 90 degrees, though others can be utilized.

In the past this orbit has been commonly used for remote sensing and other scientific purposes. It has had limited use with regards to communications satellites. However, there are many advantages to use of this orbit by communications systems. First, the power requirements to relay information are reduced tremendously by only having to transmit 200 - 1000 km. rather than 36,000 km (The altitude of most current communications systems). This allows for the satellites to be smaller and simpler than the current methods. Another advantage that hits directly with the public is the fact that the delay in current systems is .5 seconds. In LEO this would be reduced to .02 seconds.

However, there is good reason for which this orbit has not been utilized for communications. In particular, the orbital period is only a few hours so the satellite is moving into and out of a certain location's sight often during a day. That means that one satellite cannot cover any area throughout a day. The other major problem with these low altitudes is that satellites cannot cover as great an area on the Earth.

LEO may have disadvantages but its advantages have made it an area of great interest to current satellite system designs. As was mentioned before, at least one LEO communication system is already being funded and others are being designed.

3.2.2 Geosynchronous Earth Orbit (GEO)

Geosynchronous Earth Orbit has been the location commonly used for communication and weather satellites for quite some time now. Two concepts which relate to this orbit are Geostationary orbits and the transfer orbit required to attain Geosynchronous orbit. Geostationary orbits refer to a GEO orbit with inclination very close to zero (stays near the equator). The advantages of these two orbits will be discussed, but first to be addressed is the transfer to these orbits.

Geosynchronous Transfer Orbit (GTO) refers to the elliptical path traveled from LEO to GEO. Typically this is performed by a low energy Hohmann Transfer. The important aspect for the payload is the time of transfer. This transfer typically takes about 5.3 hours. This time becomes important in areas such as the power requirements of the payload as well as payload deployment. Mission Analysis covers this area in greater detail.

Once GEO is achieved communications and weather satellites have a great overhead view of the Earth as they are at an altitude of nearly 36,000 km. All circular orbits at this altitude have a period equal to the period with which the Earth rotates (synchronous). With this being true it is possible to hold the same position above the equator with little adjustment of the orbit (stationary). Stationary orbits can only exist at zero inclination so this orbit tends to be rather limited in its usefulness since many populated countries or cities lie at latitudes well above or below the equator. Those GEO orbits at inclination however do not stay above one location on the Earth. They actually traverse a figure eight around the equator.

This pattern takes the full day period of the orbit. (See Fig. 5.3)

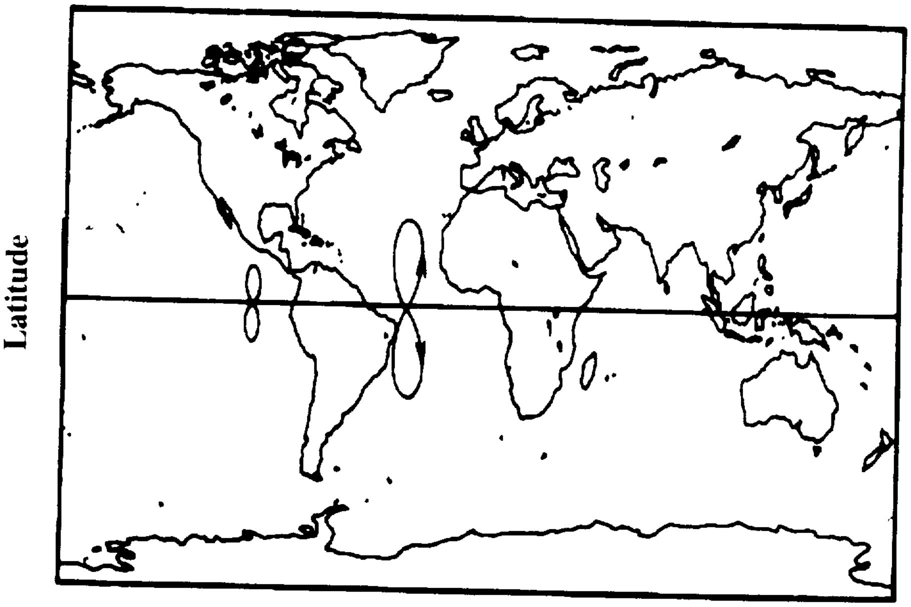

Figure 5.3: Inclined GEO Tracing

The advantages found in GEO are with regards to three major aspects. First, the high altitude allows for coverage of large areas of the Earth's surface (or atmosphere for weather satellites). Second, the fact that they stay above the same area of the Earth allows for easy tracking from the ground. Finally, since they stay in relatively the same area for a long time they prove to be quite easy to use for systems of satellites. These systems can easily cover a specific area of the Earth (like the United States) without a large number of satellites or complicated relays.

GEO has its disadvantages though. In particular, the power requirements to relay a signal from that distance are quite great. The equipment needed becomes more complicated, and in turn more sensitive to interference. As mentioned before the delay time at this altitude is also much greater than at a lower orbit. However, more important than these other reasons is the fact that this orbit is very specific. There are a finite number of satellites which can occupy this orbit. The attainment of station (getting the satellite to its correct position above the Earth) becomes more difficult due to the fact that attitude adjustment thrusts cannot occur within one degree of any satellite. As more and more satellites find themselves in this orbit, the mission and placement of satellites becomes much more difficult.

3.3 Athena Payload Market

The target market of the Athena has changed dramatically throughout its design. As was mentioned before Athena has a 1715 kg. payload capability to LEO, an estimated 888kg. to GEO and 1150 kg. to orbits between LEO and GEO (specifically 800 km.). Information on well over 500 payloads was compiled to get an understanding of the market. Future satellite missions can be found in Appendix D.2. This section is split into payloads Athena is capable of taking and those it is not. Appendix D.3. presents compiled data on recent payloads (primarily since 1990 and NASA since 1985) for reference. The data from these two Appendices are summarized in Figure 5.4.

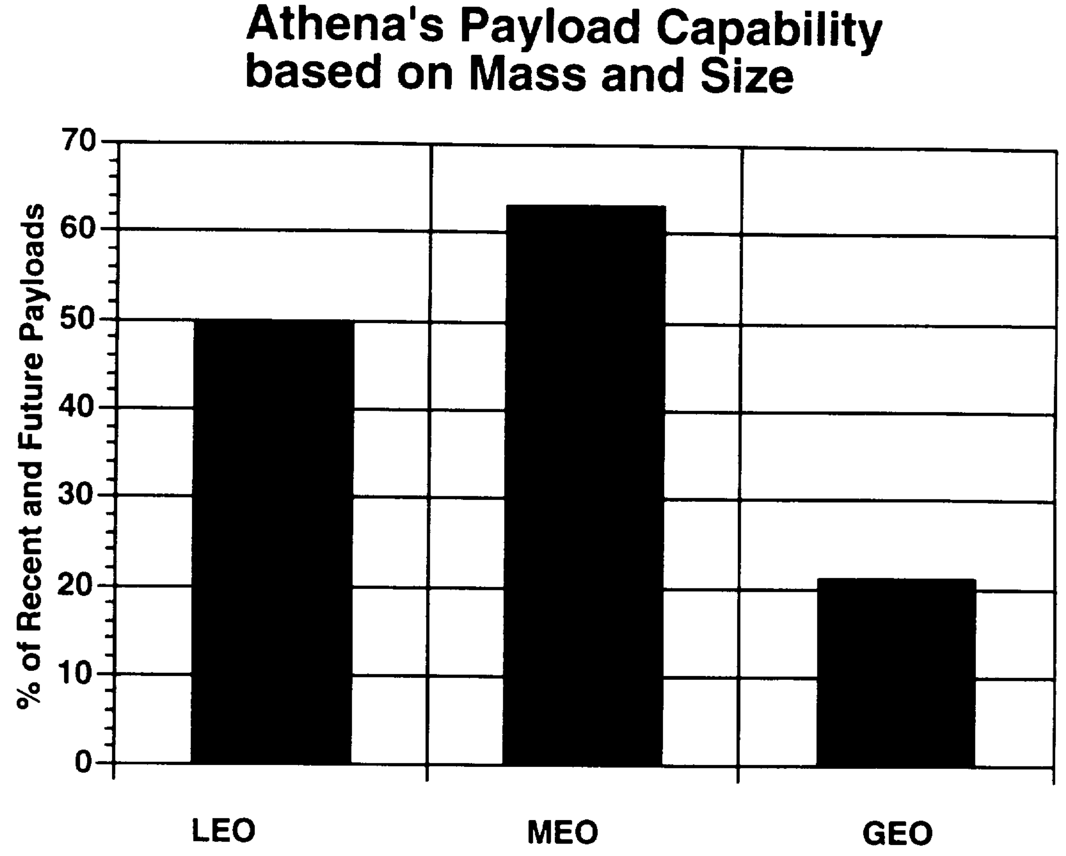

Figure 5.4: Athena % Payload Capabilities

Again, this graph was based on a survey of over 500 payloads, mostly satellites. It can be seen that our capability to send payloads to GEO is quite limited. LEO and orbits in the 500-2000 km range seem to be our best market opportunities. The MEO data primarily depends on the availability of the Iridium system in the near future.

4.0 PAYLOAD BAY DESIGN

The payload bay is 3.5 m. long with a nose cone attachment of 2.5 m. The outer diameter is 2.7 m., with the diameter of the static envelope being 2.5 m., these numbers are at the base of the payload bay. We will be using 1 m of the nose cone for payload use also, the outer diameter at the top is 2.15 m. and the static envelope diameter is 1.95 m. The static envelope allows some vibration of the satellite, without the satellite coming into contact with the payload fairing.

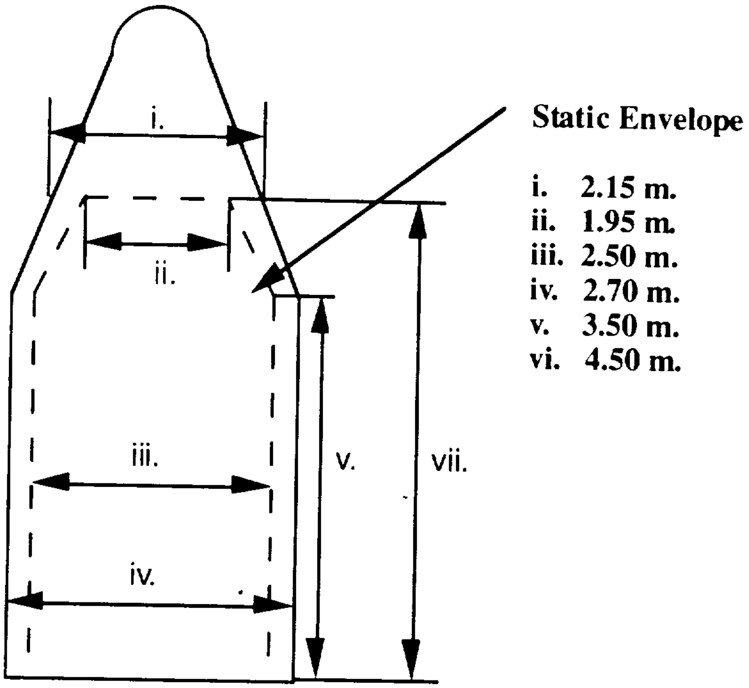

Figure 5.5: Payload Static Envelope

5.0 PAYLOAD STRUCTURAL INTERFACE

Since Athena payloads have been determined to be satellites, the structure of the payload fairing and interface have been designed with the specific purpose of protecting and deploying satellites. The payload bay has some specific requirements that must be met by the structural support and covering.

The primary structural requirements relate to the fairing and payload interface. Thermal requirements must also be met by the surrounding structure during ascent through the atmosphere. These thermal concerns will be addressed later. This section will focus specifically on the payload fairing requirements and the deployment of satellite payloads.

5.1 Fairing and Fairing Separation

The fairing is the structure which covers and protects the payload during ascent. This section is also known as the payload bay. However, that terminology can become confusing since the fairing is actually attached to the second stage. The fairing consists of two halves, with a nosecap bounded to one of the halves, and a separation system. Each half is composed of a cylinder and ogive section. We will be using two cones in th figure instead of the ogive section. It is held together by two titanium straps around the cylinder section, one near its midpoint and the other just aft of the ogive section. An internal retention bolt secures the two halves together at the surface where the nosecap overlaps the top surface of the fairing half. The base of the fairing contains a linear shaped charge to sever the aluminum attach ring allowing each half to rotate on hinges mounted on Stage 2 side of interface.

Athena initiates separation by a simultaneous firing of a Linear Shaped Charge (LSC) at the fairing base and at six bolt cutters. The LSC severs the aluminum fairing base attach ring and the bolt cutters release two titanium fairing retaining straps and the nosecap retention bolt. A gas generator drives two hot gas thrusters which separates the fairing halves. Athena will be using compressed springs near the hinge at second stage instead of the gas thrusters. However, the use of nitrogen gas stored in bottles in the forward end of the cone should also be utilized. The explosives release the nitrogen into the bay during separation and should force all particles away from the payload at separation. Fall away hinges and forcing cams at fairing base control fairing separation to eliminate the possibility of contact with the payload. The fairing halves rotate through a total of 30°, then deploy completely off the hinges and fall clear of the vehicle. Figure 5.6 shows a schematic for illustration of fairing separation. It should be noted that the fairing actually separates completely in under one second.

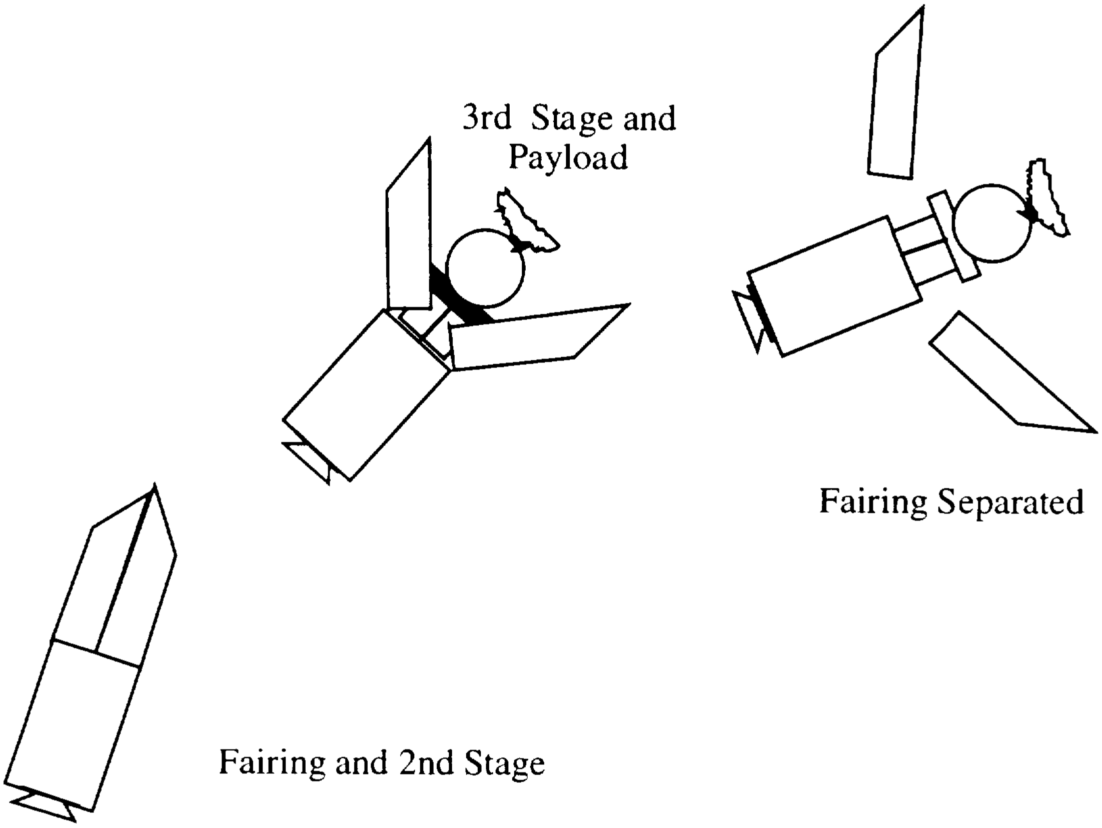

Figure 5.6: Payload Fairing Separation

It is likely that the forward momentum of the vehicle and the force of the explosives would actually swing the fairing back into the second stage. This is of little concern since the fairing is not jettisoned until after second stage burnout. At this time the fairing has been planned to jettison just before second stage drop and third stage ignition. This is far from optimal. Once exact understanding of the time at which the booster reaches 120 - 130 km. has been determined, we will take advantage of the opportunity to jettison the fairing at that time. This will drop nearly 900 kg. at a much earlier point in Athena's trajectory. This would hopefully improve our payload capabilities as well.

5.2 Payload Separation and Interface

The payload interface is the top portion of the payload adapter. This is the structural connection between the payload and Athena. The avionics section is located here but the payload separation mechanism is the structure of major importance to the payload. This is not to infer that the electrical interface in this section is not important. In fact this interface is necessary for prelaunch checkout as well as returning any other necessary payload data. However, the structural requirements of the interface are the focus of this section.

The separation mechanism has two main structural requirements. First, it must support the payload during launch and ascent. Second, it must deploy the payload upon reaching the correct altitude and velocity.

Payload separation is an important part of any satellite mission. Upon reaching the desired orbit, the satellite needs to separate from the third stage to go on with its mission. A schematic of payload separation can be seen in Figure 5.7.

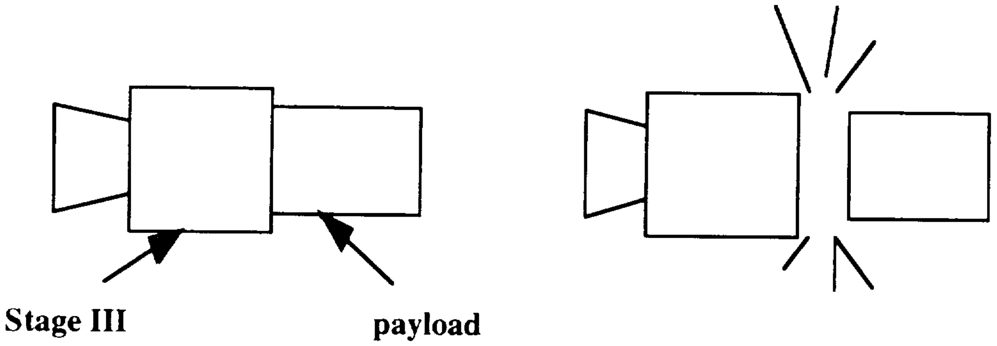

Figure 5.7: Payload Separation

Payload separation is accomplished through the use of the separation mechanism within the payload interface. Redundant bolt cutters are activated which allow a titanium clampband and its aluminum shoes to release. The band and clamp shoes remain attached to the avionics structure by seven retention springs. The payload is ejected by four matched push-off springs with sufficient energy to produce the required relative separation velocities (about 1 m/s). These springs can also be utilized for imparting spin to the payload if necessary. Figure 5.8 is a schematic showing the separation mechanism and clampband for payload connection.

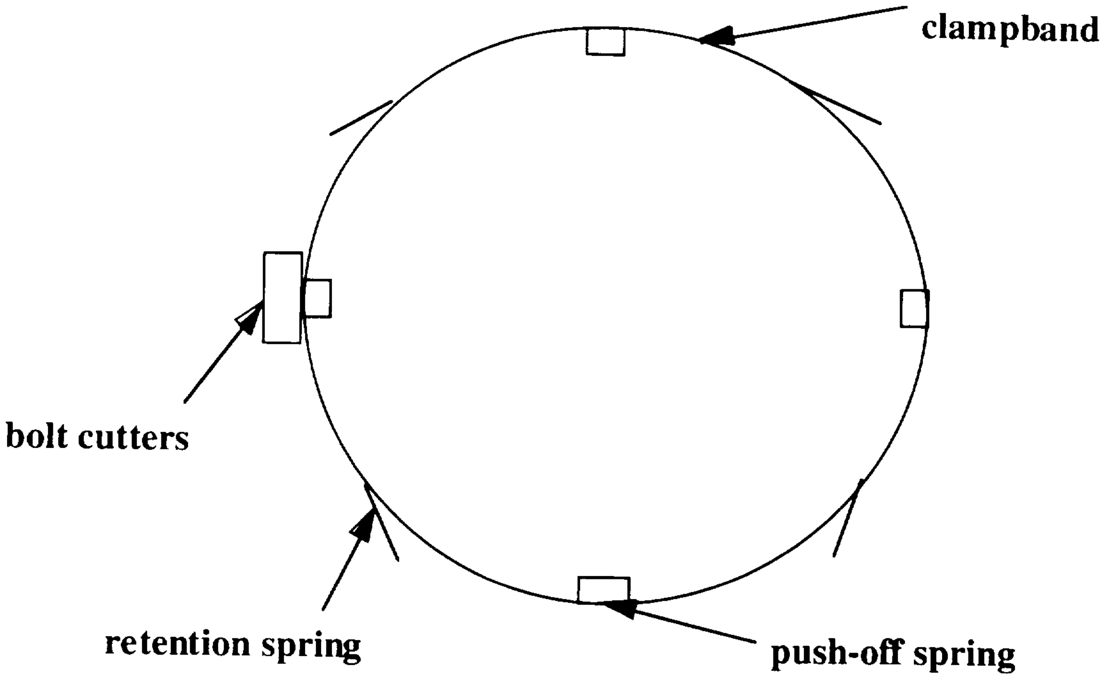
clampband
bolt cutters
retention spring
push-off spring

Figure 5.8: Payload Interface and Deployment Mechanism

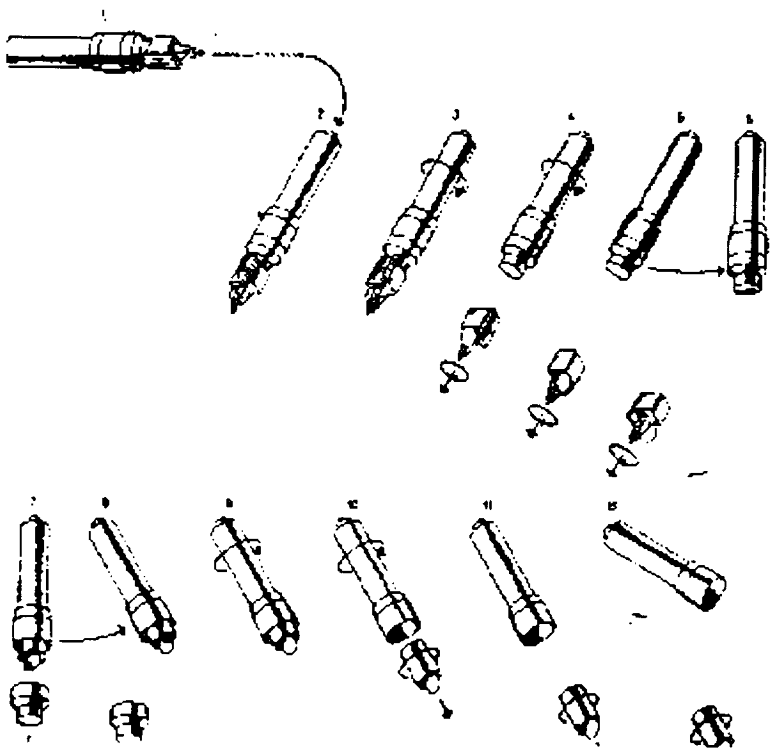

Figure 5.9: Double Payload Deployment

In a typical mission, deployment occurs only once. However, since our goal initially was to be capable of taking 5000 kg. to LEO, double payload deployment was considered. There are two methods which can be used for double payload deployment. The first method is to pass through GTO apogee twice. The Athena would reach GTO apogee and deploy one of the payloads and then make a complete orbit and release the second payload when it passes through GTO apogee the second time. The other method would occur the first time Athena reaches GTO apogee. The first satellite would be released heading in one direction and the Athena would change the direction it is facing and release the second payload in a different direction with Athena going in a third direction so as not to collide with the two payloads. Double deployment is shown in Figure 5.9.

6.0 PAYLOAD CONCERNS

A lot of concerns arise in regards to the payloads during a mission. Essentially it is important that Athena not cause any damage to the payload (satellite) during integration or launch. The possible concerns of the payload before in orbit are addressed in the following section.

6.1 Cleanliness During Integration

Athena payloads will be integrated with the fairing in a class 10,000 clean room. This will assure that the payload and payload bay are not contaminated. The integration should provide and air tight payload bay so as to avoid contamination later. The clean room will also be environmentally controlled. This will assure that the humidity stays at a low level to avoid damage to the payload electronics. The payload bay should be kept in this environmentally controlled state until launch. A portable air conditioner will provide this service.

6.2 Pressure in Payload Bay

Pressure scenarios in the payload bay becomes a concern in two ways. First, having a pressure inside the bay much higher than that outside. Second, having a pressure inside lower than the outside pressure. The reasons these scenarios are a concern are that the payload bay may collapse or leak damaging the payload itself.

6.2.1 Higher Pressure Inside Payload Bay

During flight and ascent, the atmosphere outside the bay will be decreasing. Since the payload bay has been constructed in the clean room to be air tight, a mechanism for reducing pressure inside the bay is necessary. The reason for this necessity is to avoid imparting a force on the fairing due to the pressure difference being created.

Athena utilizes a simple solution for this problem. A one way valve will be located in the lower portion of the payload bay. This will allow gas to escape but no unclean air will be allowed to enter.

6.2.2 Higher Pressure Outside Payload Bay

Depressurization concerns are solved by means of a release valve attached to the payload bay. The questions which then arose were i) what gas to carry and ii) how much?

Solution:

i) Compressed Nitrogen was chosen because it is inert and relatively cheap.

ii) Assume that the gas behaves ideally in the payload bay.

$\therefore \Delta m = \Delta p * v / R * T$

Sea-level pressure, p_o = 101 323.7 Pa

Pressure at 40 000 ft, p_1 = 18 822.59 Pa

pv= mRT $\Rightarrow$ $\Delta p * v = \Delta m * R * T$

For Payload Bay, volume = Pi(2.89/2)^2(15*0.3048)
R = 296.93 J/kg k
T = 223 K (Assume worst case scenario)

$\therefore \Delta m = \Delta p * v / R * T$ = 37.37 kg = **50 kg** (Safety factor included)

Assuming compression to 2500 psi., and that the Ideal Gas law is still valid, vol. of tank = 0.3 m^3.

This small volume of nitrogen gas will be stored on board the C-5B and will be used to repressurize the payload bay in case of an abort before egress from the plane.

6.3 Electrical and Power Requirements

The electrical requirements for the satellite are typically met by battery and solar power. The concern for satellite missions is what power is needed before launch and how soon they need to be able to utilize solar power to recharge their batteries.

Athena will be able to power the satellites with 28 volts DC and 5 Amps (140 Watts). This power will be provided both on ground and continued in flight in order to keep the satellite fully powered until launch. Typically, the satellite will switch to its batteries for power at that point but the Athena should be able to continue power if necessary during launch and ascent. Once the desired orbit is reached, the satellite is deployed and power requirements are met by solar arrays or batteries onboard.

GEO missions might normally be of concern since there is a 5.3 hour transfer occurring. This is of little concern since solar arrays are deployed during the transfer giving power in addition to the batteries. Once released in GTO or LEO, the satellites are self sufficient.

6.4 Launch Environment

Problems faced by Satellites during launch:

1) Violent Acceleration
2) Thermal
3) Vibration
4) Shock
5) Acoustic shock
6) Decompression

These concerns will be addressed in order.

6.4.1 Loading

Violent acceleration refers to the acceleration loads or g-loading that may be imparted on the payload during egress, launch, or ascent. Satellites are tested find out if they have adequate structural design to withstand the most severe acceleration loads they might encounter during launch. This in addition to booster structural concerns provided one of Athena's goals. That goal was to stay below 7 g's transverse load. Athena's final configuration actually stays below 6 g's which is below most other launch vehicles.

6.4.2 Temperature

The temperature concerns of the payloads within the payload bay are important but they do not top the concerns presented by the electrical systems connecting the avionics section and the payload. The electrical interface should be kept in a nominal temperature range. The standard for this is 0 - 40° Celsius. Thermal control of satellites and temperature limits follow, but the major concern imparted on thermal control of the payload bay was not from the payloads themselves but the aforementioned controls and electronics.

Thermal Control Techniques of Satellites :

a) Passive Control
- thermal coatings, insulation, heat sinks, phase-change materials.

Examples of thermal coatings include white paint and mirror coating. Thermal insulation includes an outer skin of 25 micrometers of Aluminized Kapton. Remaining layers are of Aluminized Mylar separated by Dacron Mesh.

Kapton - max. temp = 343° Celsius
Mylar - max. temp = 123° Celsius
Titanium - max. temp = 1400° Celsius (Used for Motor insulation)

b) Active Control
- heat pipes, louvers and electric heaters

Two types of thermal testing are done on satellites.
1) the qualification thermal vacuum test, at 10° Celsius beyond expected extreme.
2) acceptance thermal test, at 5° Celsius beyond expected extreme.

Basically, satellites are tested to withstand temperatures between -200° and 150° Celsius.

6.4.3 Other Environmental Concerns

Vibration refers to violent low frequency sinusoidal vibration during lift off and flight on some launch vehicles (Pogo Effect). It is caused by a resonance phenomenon in fuel lines, resulting in the satellite being stressed to the limit. Satellites are once again designed and tested to withstand these types of stresses. They are tested to survive sine and random vibration frequencies of 5 to 5000 Hz. Another important aspect of satellite design is that they typically have no fundamental resonant frequencies below 30 Hz. in the longitudinal axis or below 10 Hz. in the lateral axis.

Shock refers to bouncing, bumping, or hitting of the payload by other object or payload against the fairing wall. Satellites are tested to withstand these types of occurrences, but Athena has been designed in an attempt to avoid these occurrences. The static envelope of the payload bay should allow for any displacement of the payload during launch and the interface should provide adequate support to hold the satellite down. Nothing inside the bay will have freedom to move or fall. In particular this just refers to the nitrogen tanks in the nose for fairing separation.

Acoustic shock refers to the high frequency sound produced by the engines or possibly atmosphere on the booster. These engines have all been commonly used for satellite deployment in other vehicles. The safety tests done for typical high frequency acoustic excitation would surpace the levels of current launch vehicles. Athena, using of the shelf hardware would easily fit these specs.

Decompression refers to the same problems previously addressed in Section 6.2.

6.5 Tracking and Communication

Athena has tracking and communications systems on board in the avionics section above third stage. The payload interface allows room for connection of electronics, power, and air conditioning umbilicals. As mentioned earlier, communication is an important aspect of all satellite missions because it allows for all inflight disconnections, changes, and data relay.

7.0 CONCLUSION

Launch vehicles can only survive as long as someone wants to put something in space. Communications systems are well established, giving consistent reason for space launches and more importantly improving the capabilities of these launches. Athena helps fill a new medium range payload launch vehicle gap. Other than Orbital Sciences Corporation's Taurus, no launch vehicles fit smaller satellites in the 1000-2000 kg. range. There is definitely a market for these sized payloads and more importantly this market is increasing. Small communications satellites are planned to be placed in lower orbits. Iridium is a funded project fitting this range. Much larger vehicles may prove inefficient for smaller payloads of this type. Athena will be capable of the smaller satellite market on the grow.

1715 kg. to LEO and 888 kg. to GEO might not seem an ideal capability when other launch vehicles are considered, but the capability fits a large market and Athena takes full care of the concerns coming from launching satellite payloads.

Chapter 6

Propulsion

PRECEDING PAGE BLANK NOT FILMED

CHAPTER 6 -- PROPULSION

Propulsion's symbols

Qty	Quantity
O/F	Oxidizer/Fuel [ratio]
Oxid	Oxidizer [mass]
hp	Horsepower
cc	Cubic Centimeters
PSV	Pressure Sequencing Valve
MW	Molecular Weight
ML	Metal Loading
t	Thickness
P	Pressure
a	radius
e	weld efficiency
S	Safety Factor
[mdot]	total mass flow rate
TankA	Tank area
Payload	Payload ratio
U	Exhaust Velocity (aka ìcî)
n	number of ...
DV	Change in velocity
r	density
b	tank end hemisphere radius
W	Total Weight
R	fireball radius

1.0 GROUP OVERVIEW

The main purpose of the Propulsion group was to find a suitable set of engines and support systems to use on the Athena booster. This entailed choosing engines from a set of pre-existing engines to meet the needs for the mission set forth: an air-launched space booster under 150,000 kg in weight, and suitably affordable enough to entice investors. In addition to choice of engines for the mission, propellant choice, tank design, and final configuration of the Athena booster were all within the Propulsion group's responsibilities. These responsibilities required this group to be in constant communication with other groups and industry as well. This section of the Athena report will follow through with the Propulsion group's selection process and final results. These results will show a system that maximizes the amount of payload that Athena may insert into orbit while maximizing safety of the drop aircraft, the C-5B Galaxy -- cargo aircraft, and its crew, while maintaining a tight budget.

2.0 SELECTION OF ATHENA BOOSTER SYSTEM

The selection of the final propulsion configuration can be broken down into four main areas, namely:

1) the selection of the type of propellant.
2) the selection of the integrated booster configuration
3) the selection of engines.
4) the selection of propellant tanks.

PRECEDING PAGE BLANK NOT FILMED

2.1 Selection of Type of Propellant

In general, propellants can come in two main forms, namely solid and liquid. The liquid propellants can be further subdivided into storable and cryogenic. On top of these two main types of propellant, a third and promising form of propellant (still under research) is the gelled propellant.

2.1.1 General Propellant Requirements

It is usually desirable for a propellant to have the following characteristics (Kit, 13):

1. A high specific impulse so that as little propellant is required to produce a specific amount of thrust.
2. Low molecular weight so that the propellant can be as light as possible. Since propellant mass usually make up 90% of the total mass of a launching system, it would be advantageous to have a relatively light propellant so that a heavy payload maybe launched.
3. A high heat of combustion per unit volume in order to permit reducing the size of the launching system. This is especially true for the case whereby the volume of the system is a limitation (as with Athena).
4. Combustion product should be in gaseous form in order to ensure satisfactory conversion of the heat energy into kinetic energy. Furthermore, solid product does not transfer heat rapidly enough. This may hasten the corrosion and wear of the nozzle due to localized heating.

On top of those characteristics mentioned above, propellants should preferably meet several operational requirements. Some of these requirements are:

1. Chemical and physical stability to permit storage over long periods under widely varying climatic conditions without specialized storage facilities and precautionary measures, and to avoid unusual transportation requirements.
2. High self-ignition temperature to prevent accidental ignition.
3. Stability towards mechanical impact.
4. Should not be toxic or present a health hazard. Also, disposal of the exhaust should not pose a problem.

2.1.2 Special Requirements for Liquid Propellants

Besides the requirements as cited above, it is usually desirable for liquid propellants to meet other requirements (Kit, 19).

1. Storage and transfer of liquid propellants require that freezing and vapor pressure be low so as to permit operation in extreme climatic conditions.

2. The necessary cooling of the combustion chamber and nozzle of a liquid engine requires at least one of the following properties:

   a. High boiling point or decomposition temperature.
   b. High heat capacity.
   c. High thermal conductivity.

3. The design characteristic of the liquid propellant feed systems and the mixing of fuel and oxidizer before or after injection requires the following:

   a. A low viscosity to permit easier pumping and engine calibration. In addition, the viscosity differential between fuel and oxidizer should be as low as possible and should change as little as possible with temperature.
   b. A low coefficient of surface tension to permit easier mixing of propellant in the combustion chamber.
   c. A low vapor pressure to facilitate handling of propellants and simplify pump design.

4. The ignition and combustion of the propellant requires the smallest possible ignition delay (period of time between ignition and steady combustion). Furthermore, non-hypergolic propellant requires as low a temperature of ignition as possible .

2.1.3 Final Selection of the Propellant Type

One of the early tasks of the Propulsion group was to look into and decide on the type of propellant to be used for the booster. The advantages and disadvantages of the different forms of propellants were weighted.

It was decided that the group would go with storable liquid and/or solid propellant. The selection was based on the reasons that:

1. Restriction of space.
   The total system has to be able to fit into a dimension of at most 3m x 5.5m x 30m. Hence, the propellant would have to be as dense as possible so that a greater amount of potential energy may be packed into a smaller space. Cryogenic, though more efficient than both solid and storable liquid, lose out in this due to its low density and hence large amount of space taken.

2. Handling and safety
   Unlike conventional launchers, Athena involves a greater amount of booster transportation and handling. In order to survive the frequent disturbance and rough ride on the aircraft, a relatively stable propellant has to be chosen. The cryogenic propellant, though not much more dangerous than storable liquids, are nevertheless more susceptible to leakage due to its highly volatile nature. Flying an aircraft with a leaking hydrogen booster would, after all, sound repulsive to most pilots.

3. Storage
   As with handling, storage of the propellant is also a prime concern. The propellant has to be preferably stable at normal storage condition and does not require special alteration to the aircraft to provide such a condition. The

cryogenic, having a low boiling point, would require special refrigeration system in the aircraft to keep it at a liquid state at low altitude. Installation of such a system would be expensive and not economically wise. Hence, once again, storable liquid and solid propellants are preferred to cryogenic.

Incidentally, gelled propellant happens to meet all the above selection requirement for Athena. Though suffering from a slight lost in Isp, the gelled version is as dense as storable liquid and solid propellant. However, the clear advantage of the gelled propellant over its liquid and solid counterpart is in its stability. It is safer, easier to handle and requires less stringent storage condition. Regrettably, the gelled propellant is still in its research phase and no known commercially produced version is available in the market.

2.2 Selection of Athena Booster Configuration

After deciding on the use of storable liquid and solid propellant, various possible combinations of liquid engines and solid motors were investigated to determine their viability of sending the target payload weight of 8000 kg to LEO (approx. 200 km). The 7 configurations that the Propulsion group came out with are named configuration A to G. A brief description of the configuration and schematic drawing is attached as Appendix E.3.

The system performance spreadsheet was used to give an initial analysis of the performance of the different configurations. In the case where strap-on solid motors were used, both parallel burning (i.e. the case whereby the strap-ons and the main engine have the same burn time) and unparallel burning (i.e. the case whereby the strap-ons burn shorter than the main engine and are separated from the booster once expended) were considered.

It was found from the initial analysis that the strap-ons that could be used, due to the restriction of dimension, are too small to contribute positively to the first stage of the booster. Hence, the idea of having strap-on solid motors was discarded.

It was found that configuration C, with 2 liquid first stage engines, was the most suitable configuration to handle a payload weight of 6000 kg. However, the deadly flaw of the configuration is that at about 120 000 kg, it is 50% above the weight limit imposed on the launching system. In fact, this is near the lifting capability of the Galaxy C-5.

The group finally settled on configuration A after the target payload mass was cut down to about 2000 kg (though the final payload mass is 1715 kg to LEO).

2.3 Selection of Engine Systems

With the elimination of cryogenic engines, only storable liquid engines and solid motors were considered for the booster. The relative advantages and disadvantages of solid motors over liquid engines were taken into consideration. These include:

Advantages:

1. Solid motors are simpler by comparison. They have no moving parts, no tanks, no injection system and require, as a general rule, no cooling.

2. As a result of their simplicity, solid motors are easily stored, handled and serviced. Their field equipment is much simpler and they are ready for launching any moment.

3. The lack of pumps, valves, and control facilitates operation and minimize failures. In fact, the reliability of solid motor is as high as 99%.
4. The absence of pumps, valves and other parts found in liquid engines increases the obtainable mass ratio beyond that of the latter.
5. The over-all cost of the solid motors is usually far below that of the liquid engines.

Disadvantages:

1. Solid motors usually have a lower specific impulse and performance.
2. Thrust control and termination is usually difficult in solid motors. Unlike liquid engines, they are also not restartable.
3. The burn time of solid motors are lower than most liquid engines. Hence, their total impulses are lower than the latter.
4. The performance of solid motors is quite sensitive to variations in temperature, whereas liquid engines are, within a wide range, insensitive to temperature changes.
5. The manufacturing of solid propellant grain is always very involved and the entire motor has to be replaced at times of malfunction.

Bearing the differences in mind, a list of possible solid motors and liquid engines, with their performances and physical statistics, was complied along with the cryogenic engines that were researched early in the selection process (Interavia Space Directory 1992-93). The list is attached as Appendix E.1.

2.3.1 Final Engine Configuration Choices

Several possible motor/ engine combinations from configuration A and B were submitted to the Mission Analysis for a detail consideration. This includes:

Conf	Description.
A	1 X LR-87-AJ-11 1 X LR-91-AJ-11 1 X AJ10-138
B1	1 X LR-87-AJ-11 + Castor 1 1 X LR-91-AJ-11 1 X AJ10-138
B2	1 X LR-87-AJ-11 + Castor 2 1 X LR-91-AJ-11 1 X AJ10-138
B3	1 X LR-87-AJ-11 + Castor 4A 1 X LR-91-AJ-11 1 X AJ10-138
B7	1 X LR-87-AJ-11 + Orbus 7 1 X LR-91-AJ-11 1 X AJ10-138

Table 6.1: Initial Engine Configurations

After the analysis by Mission analysis and Mission Control, it was finally decided that the engine combination to be used for Athena is as follows:

Stage 1 - 1 x LR-87-AJ-11 with a thrust of 2437 kN
Stage 2 - 1 x LR-91-AJ-11 with a thrust of 467 kN
Stage 3 - 2 x AJ10-138 with a thrust of 36 kN each

The selection was based on the consideration of:

1. Thrust and restriction of maximum g-force on system.
   The prime restriction on the type of engine that can be used is that the thrust of the engine must not propel the system beyond the maximum allowable g-force. The restriction is most visible at the third stage where the mass is small, and hence more powerful engines are not suitable. With a pre-selected g-force limit of 7g and a payload mass of 2500 kg, the third stage engine has to have a thrust of less than 150 kN.

2. Flexibility of burn time.
   Since the performance and weight of the booster is pretty much determined by the burn time, the liquid engines (which come with variable burn time) are preferred to the solid motors (which have fixed burn time) for use as the main propulsion system. This would enable the realization of a more flexible booster that can better cater to the specific need of the target payload and orbit. The solid motors, however, can be used as strap-ons for the first stage.

3. Availability of gimbals.
   In order to maneuver the system into the required orbit and to adjust for small disturbance along the flight, it is desirable for the engines to come together with gimbals capability. Most liquid and some solid engines (e.g. Orbus 7S), come with this capability.

4. Availability of engines and service support.
   The engines chosen are all produced by American companies. This provides easy communication with the supplier and ready service support when malfunctions occur.

5. Reliability of engines.
   The engines selected for the Athena is identical to those used by the Titan III. With a success rate of 92.3% (Jane's Space Directory) and numerous launches, the engines have proven to be reliable.

3.0 CALCULATIONS FOR CONFIGURATION CHOICES

A spreadsheet was developed by the Propulsion group to calculate the performance of the various configurations. Unlike the model used by Mission Analysis which considers the actual flight dynamics with changing flight angles, the preliminary model used by the Propulsion group assumes that the booster is fired vertically against the gravity. Using this model, a common basis was established for the comparison of the propellant requirement, velocity, burn time, altitude at burnout, cost and approximate tank dimension of the different configurations. The burn time of each possible engine combination within a configuration was then optimized through trial and error to obtain as high a velocity and altitude at burnout as possible for a total weight of less than 80,000 kg. The best possible model of each booster configuration was then submitted to Mission Analysis for a more realistic simulation and analysis. Hence, Propulsion acted as a screening agent for Mission Analysis by reducing the number of feasible configurations that had to be analyzed by the group.

3.1 Explanation of Calculations

Instead of going through the similar type of calculation for every trial configuration, the spreadsheet automatically made the necessary changes in the calculations and gave the desired results for the configuration. The user need only enter the following vital information and the rest of the work was taken care of by the computer:

1) the quantity of the type of engine used and its properties.
2) the burn time of each stage.
3) the desired payload mass.

The following is a step by step explanation of how the spreadsheet works and how the final calculated results are obtained.

1. Enter quantity (Qty) and description/ properties of the engines used.

2. The fuel mass (Mf) of a stage alone is calculated from the dry mass of the constituent engines.

$$M_F = (Qty)(DryMass)$$

3. The total mass flow rate ($\dot{m}$) of a particular type of engine is calculated from the maximum thrust produced and the I_{sp}.

$$\dot{m} = \frac{Thrust}{I_{sp} g}$$

4. The mass of propellant used (M_p) is calculated from the burn time (t_b), which is input into the spreadsheet by the user, and the flow rate ($\dot{m}$) of the engine.

$$M_p = \dot{m} t_b$$

5. The initial mass of a stage alone is calculated from the final mass (Mf) and the propellant mass (M_p).

$$M_{stage} = M_F + M_P$$

6. The fuel mass (Fuel) is calculated from the propellant mass (M_p) and the oxidizer to fuel ratio (O/F).

$$Fuel = M_P - \frac{M_P}{O/F}$$

7. The oxidizer mass (Oxid) is then calculated from the propellant mass (M_p) and the fuel mass (Fuel).

$$Oxid = M_p - Fuel$$

8. With a pre-selected tank area (Tank A), the length of the oxidizer and fuel tank (L_{oxid} and L_{Fuel}) required may be estimated from the oxidizer and fuel density (ρ_{oxid} and ρ_{Fuel}) stated(a more detail calculation is done separately, taking into consideration the actual shape and arrangement of the tanks).

$$L_{oxid} = \frac{Oxid}{(\rho_{Oxid})(TankA)}$$

$$L_{Fuel} = \frac{Fuel}{(\rho_{Fuel})(TankA)}$$

9. The total length of the tank (L_{Tank}) is calculated from the length of the oxidizer and fuel tank (L_{oxid} and L_{Fuel})

$$L_{Tank} = L_{oxid} + L_{Fuel}$$

10. The total length of a stage alone is derived from the length of the propellant tank (L_{Tank}) and the length of the engine (L_{engine})

$$L_{stage} = L_{engine} + L_{Tank}$$

11. Mass of each stage ((M_{stage})i) is calculated from the mass of each stage alone (M_{stage}).

$(M_{stage})1 = M_{stage1} + M_{stage2} + M_{stage3} + M_L$ (first stage)
$(M_{stage})2 = M_{stage2} + M_{stage3} + M_L$ (second stage)
$(M_{stage})3 = M_{stage3} + M_L$ (third stage)

where M_L = payload mass

12. The final mass of each stage ((M_f)i) is calculated from subtracting the propellant mass of that stage alone (M_p) from the initial mass of that stage ((M_{stage})i)

$(M_f)1 = (M_{stage})1 - M_{p1}$ (first stage)
$(M_f)2 = (M_{stage})2 - M_{p2}$ (second stage)
$(M_f)3 = (M_{stage})3 - M_{p3}$ (third stage)

13. The mass ratio of each stage ((M_{stage}/M_f)i) is then obtained.

14. The payload ratio (Payload ratio) is then calculated.

$$Payload = \frac{M_L}{M_{stage}}$$

15. The effective exhaust velocity (c) of the propellant is calculated from the Isp.

$$U_e = I_{sp} g$$

note that if engines of different I_{sp} are used in a single stage, the effective I_{sp} has to be used, where

$$I_{sp} = \frac{\sum (I_{sp})_i}{n}$$

16. The change in velocity for a stage (ΔV) is calculated from

$$\Delta V = I_{sp} g \ln \frac{M_{stage}}{M_f}$$

note that the effect of gravity is taken into consideration.

17. The vertical height (H) attained by a stage is calculated.

$$H = U_e \left(1 - \frac{\ln \frac{M_f}{M_{stage}}}{\frac{M_f}{M_{stage}} - 1} \right) t_b - .5 g t_b^2$$

18. The maximum g force at a stage (G_{max}) is calculated from the final mass at that stage ($(M_f)_i$)

$$G_{max} = \frac{Thrust}{M_f g}$$

19. The prices of the fuel and oxidizer are calculated from their mass and the unit price of \$13(US) per lb of fuel and \$3.15(US) per lb oxidizer.

3.2 Assumptions and Limitations

There are several assumptions made when developing the spreadsheet. Also, there are limitations to what the spreadsheet can do.

1. As mentioned earlier, the spreadsheet made the assumption that the system was launched vertically and stayed so throughout the whole duration of the flight. Although this

assumption is unrealistic, it nevertheless provides a common basis for the comparison of various systems.

2. The spreadsheet made the assumption that all the propellant tanks were lined up one on top of the other and were all of cylindrical shape. This is not the case in actual fact. Combination of shapes and arrangement usually results in a lower length required by the tanks.
3. The spreadsheet took into consideration the weight of the engines, propellants and payloads only. The weight of the structure, tanks and other equipment, which usually make up about 5-10% of the total mass, was not taken into consideration. Hence, a lighter final payload mass may be realized.
4. The spreadsheet made the assumption that the performance of the engines was constant and that the fuel/ oxidizer densities were constant.

3.3 Results

Using the spreadsheet, it was found that with a payload mass of 2500 kg, the final configuration would have a total mass of about 76 000 kg, giving a V of about 5000 m/s at a vertical height of 173 km.

Note, once again, that these results are for the unrealistic case of a vertical flight and would be quite different from the more detail analysis by Mission Analysis.

4.0 ENGINES

The choice of engines was made difficult by the fact that there were a great number of engines that were researched. However, by tightening the search parameters, many engines were removed from consideration. Cryogenic fuels are useful in many applications, Isp is high, but the need for refueling while in flight and refrigeration while in the C-5 removed these engines from consideration. Thus, storable liquid fueled engines and small solid fueled engines were the choices that were most closely scrutinized. Of these engines, the engines for the Titan launch vehicle were best suited for the needs of the missions that the Athena booster was designed for.

The LR87-AJ-11, the LR91-AJ-11, and the transtage engines (2 AJ10-138 engines in tandem) are the engines used for Titan series of launch vehicles and are all produced by Aerojet Corp. These engines were first used in 1955, and have gone through an extensive series of refits and refinements throughout the years. Reliability and experience gained in the over 400 Titan series rockets makes these engines good choices for the Athena booster. The availability of the engines is very high, and they are being produced today. In addition, price breaks may be garnered from Aerojet Corp. because of the need for a great number of engines.

4.1 Stage One Engine: LR87-AJ-11

The LR87-AJ-11 engine is a storable liquid fueled turbopump-fed engine that produces a maximum of 2,437,504 Newtons of thrust and has an Isp of 301 seconds. The LR87-AJ-11 is in actuality two separate engines attached to a single steel frame which is mounted to the Athena booster. The two separate engines operate simultaneously under a single control system. Together, the engine is 3.84 meters from the bottom of the nozzles to the top of the mounting truss, and 1.85 meters at the widest part of the modified truss. The engine has a dry mass of 2,285 kg.

The LR87-AJ-11 is fueled by a 1.91:1 ratio of Nitrogen Tetroxide and Aerozine-50 which are fed separately to the engine subassemblies (each separate engine) by way of suction lines to the turbopump assemblies which are driven by turbines which are rated at over 5000 hp. Pressure is increased in the pumps by over 6.9E7 Pa (1000 psi), forcing the propellant (Aerozine-50) and the oxidizer (Nitrogen Tetroxide) through the discharge lines and are atomized into a gas as they are fed into the thrust chamber of each engine. Thrust chamber valves control the engine start and shutdown. When the hyperbolic propellant and oxidizer mix in the thrust chamber, combustion takes place, producing gas at pressures over 5.5E7 Pa (800 psia) and temperatures above 2700°C (5000°F). This gas is then expanded through a convergent-divergent DeLaval-design nozzle and exhausted at supersonic velocities to produce thrust. Thrust vector controls for pitch, yaw, and roll motion is achieved by pivoting the thrust chambers on gimbal bearing mounts, which is provided by hydraulic actuators and can produce 4.5° of thrust vectoring. The maximum lifetime of the LR87-AJ-11 is 200 seconds (Titan III Propulsion Systems, 2-1 - 2-3).

4.2 Second Stage: LR91-AJ-11

Like the LR87-AJ-11 engine, the LR91-AJ-11 is a storable liquid fueled, turbopump-fed engine that uses Nitrogen Tetroxide as an oxidizer and Aerozine-50 as a propellant. The LR91-AJ-11 produces a maximum thrust of 467,040 Newtons of thrust, has an Isp of 316 seconds, and is rated for a maximum lifetime of 247 seconds of thrust. The engine is 2.81 meters from nozzle to engine frame and is 1.62 meters at its widest point, fitting nicely into the confines of the cargo bay of the aircraft. The engine's dry mass is 584 kg.

The LR91-AJ-11 engine is very much like the LR87-AJ-11 engine in construction and operation, the main differences being that the LR91-AJ-11 is somewhat smaller than the LR87-AJ-11, having only one engine to produce thrust, and requiring an ablative skirt on the nozzle which provides a 49.2:1 expansion ratio since this engine is designed to operate at higher altitudes than the LR87-AJ-11. The LR91-AJ-11 is fueled by a 1.86:1 ratio of Nitrogen Tetroxide and Aerozine-50 which are fed separately to the engine by way of suction lines to the turbopump assembly which is driven by a turbine which is rated at over 2000 hp. Pressure is increased in the pumps by over 6.9E7 Pa (1000 psi), forcing the propellant (Aerozine-50) and the oxidizer (Nitrogen Tetroxide) through the discharge lines and are atomized into a gas as they are fed into the thrust chamber the engine. Thrust chamber valves control the engine start and shutdown. When the hypergolic propellant and oxidizer mix in the thrust chamber combustion takes place, producing gas at pressures over 5.5E7 Pa (800 psia) and temperatures above 2700°C (5000°F). This gas is then expanded through a convergent-divergent DeLaval-design nozzle and exhausted at supersonic velocities through the ablative skirt to produce thrust. Thrust vector controls for pitch and yaw motion is achieved by pivoting the thrust chambers on gimbal bearing mounts, which is provided by hydraulic actuators and can produce 3.5° of thrust vectoring. Roll control is achieved by ducting turbine exhaust through a roll control nozzle which is swiveled by a hydraulic actuator controlled by the launch vehicle control system. This nozzle produces 3,825 Newtons of thrust and swivels 35° in two directions (Titan III Propulsion System, 3-1 & 3-2).

4.3 Stage 3: The Transtage

The Transtage engine is in actuality a set of two AJ10-138 engines working in tandem, much like the LR87-AJ-11 engines used for the first stage, but much smaller. The AJ10-138 engine is a multiple restart, pressure-fed, storable liquid fueled engine using the same fuel tandem as used in the previous stages (a 1.9:1 ratio of Nitrogen Tetroxide oxidizer and Aerozine-50 propellant). This engine produces a maximum thrust 35,584 Newtons as a single engine, and 71,168 Newtons as a tandem. The AJ10-138 has an Isp of 310 seconds and is rated at 500 seconds for a maximum lifetime. The length of the engine is 2.07 meters from nozzle to engine mount and has a maximum width of 1.2 meters. Dry mass of one engine is 110 kg.

The AJ10-138 is a pressure fed engine and requires a sphere of Helium filled to a pressure of 2.48E8 Pa (3600 psia) to maintain tank pressure at approximately 1.1E7 Pa (160 psia)to force propellants from the tanks into the engine. The propellants (Nitrogen Tetroxide and Aerozine-50) are fed into the thrust chamber in an atomized form where they ignite upon contact with each other. The gas in the thrust chamber has a pressure of 7.24E6 Pa (105 psia) and is ejected through a convergent-divergent DeLaval nozzle and an ablative skirt with an expansion ratio of 40:1 to produce thrust. The engine may be shut down and restarted an unlimited number of times to modify an established orbit or to achieve a higher orbit by shutting off valves for the propellants by way of the launch vehicle control system. Pitch and yaw control are achieved through a gimbal ring which pivots the engine a maximum of 6.5° by way of mechanical systems (Titan III Propulsion Systems, 4-1 & 4-2).

5.0 OPERATIONS OF THE ENGINES

5.1 Stage One Engine: LR87-AJ-11

Prior to the operation of the LR87-AJ-11, the prevalves in the propellant tank lines immediately above the engine interface prevent propellant from entering the engine system. This not only allows the propellant tanks to be loaded long before the scheduled launch, but also protects the engine systems from long-term exposure to the propellants. During the countdown within the aircraft, prior to cargo bay door opening, an arming signal is supplied to the Athena booster. This signal opens the prevalves, allowing the engine to enter the fill and bleed cycle, and readies the electrical starting circuits to receive the firing signal.

Opening the motor-operated prevalves places the engine into a fill and bleed cycle. The fill and bleed cycle uses the tank pressure to fill the fuel lines with fluid and to purge as much air as possible from the system. This cycle bleeds about 1200 cc/min of both Nitrogen Tetroxide and Aerozine-50 from drain ports located between the nozzles. This bled propellant and oxidizer are siphoned into receptacles built into the carriage mounting for the Athena, and are kept separate for safety of the aircraft and crew. This cycle must take place for a minimum of 30 seconds prior to engine start.

After completion of the fill and bleed cycle, the engine is armed and ready for operation. Because of this reason, as little electronic signal output from the aircraft as possible is necessary until the Athena booster is ready to be detonated. When engine start is desired, the start signal, Fire Switch 1, applies 28 Volts DC to the initiator charges of a solid propellant start cartridge mounted on the turbine inlet manifold of each subassembly and initiates separation of the exit closure from the thrust chamber ablative skirt. The start cartridge ignites and supplies gas to the turbines causing them to accelerate. The turbine shaft of each subassembly is connected through a gear train to the fuel and oxidizer pump causing pump operation to begin. Since the thrust chamber valves are closed, no propellant flows and pump acceleration produces only an increasing pressure in the discharge lines and the valve actuation system. When fuel discharge pressure reaches approximately 2.1E7 Pa (300 psig), the pressure on the opening end of the pressure sequencing valve (PSV) spool produces a force which exceeds the spring force on the PSV spool closing end, causing the spool to shuttle from the bleed position to the operation position. This occurs about .25 seconds after Fire Switch 1.

This stops the flow of fuel to the bleed orifices, and opens the valves to the thrust chamber. These valves begin to open about 0.3 seconds after the signal is given and continues until the valves are fully open at about 1.1 seconds after the signal. Propellants begin to flow into the thrust chamber as soon as the valves begin to open after flowing through toroidal chambers surrounding the chamber in order to cool the temperatures. As soon as the valves are open, and both Aerozine-50 and Nitrogen Tetroxide enter the thrust chamber, the engine starts, and thrust levels begin to rise. Only 1.1 seconds after the Fire Switch signal, the engine reaches its operating level. Engine shutdown occurs when either Aerozine-50 or Nitrogen Tetroxide is depleted (Titan III Propulsion Systems, 2-3 -2-5).

5.2 Second Stage: LR91-AJ-11

The LR91-AJ-11 works very much like the LR87-AJ-11, and uses the same firing signal to start operation of the engine. Prior to the operation of the LR91-AJ-11, the prevalves in the propellant tank lines immediately above the engine interface prevent propellant from entering the engine system. This not only allows the propellant tanks to be loaded long before the scheduled launch, but also protects the engine systems from long-term exposure to the propellants. During the countdown within the aircraft, prior to cargo bay door opening, an arming signal is supplied to the Athena booster. This signal opens the prevalves, allowing the engine to enter the fill and bleed cycle, and readies the electrical starting circuits to receive the firing signal.

Opening the motor-operated prevalves places the engine into a fill and bleed cycle. The fill and bleed cycle uses the tank pressure to fill the fuel lines with fluid and to purge as much air as possible from the system. This cycle bleeds about 1200 cc/min of both Nitrogen Tetroxide and Aerozine-50 from drain ports located between the nozzles. This bled propellant and oxidizer are bled into receptacles built into the carriage mounting for the Athena, and are kept separate for safety of the aircraft and crew. This cycle must take place for a minimum of 30 seconds prior to engine start, and works concurrently with the first stage fill and bleed cycle.

After completion of the fill and bleed cycle, the engine is armed and ready for operation. Because of this reason, as little electronic signal output from the aircraft as possible is necessary until the Athena booster is ready to be detonated. Once the first stage is jettisoned, the second stage firing signal is given. The start signal, Fire Switch 1, applies 28 Volts DC to the initiator charges of a solid propellant start cartridge mounted on the turbine inlet manifold and initiates separation of the exit closure from the thrust chamber ablative skirt. The start cartridge ignites and supplies gas to the turbine causing it to accelerate. The turbine shaft is connected through a gear train to the fuel and oxidizer pump causing pump operation to begin. Since the thrust chamber valves are closed, no propellant flows and pump acceleration produces only an increasing pressure in the discharge lines and the valve actuation system. When fuel discharge pressure reaches approximately 2.1E7 Pa (300 psig), the pressure on the opening end of the PSV spool produces a force which exceeds the spring force on the PSV spool closing end, causing the spool to shuttle from the bleed position to the operation position. This occurs about .25 seconds after Fire Switch 1. This stops the flow of fuel to the bleed orifices, and opens the valves to the thrust chamber. These valves begin to open about 0.3 seconds after the signal is given and continues until the valves are fully open at about 0.9 seconds after the signal. Propellants begin to flow into the thrust chamber as soon as the valves begin to open after flowing through toroidal chambers surrounding the chamber in order to cool the temperatures. As soon as the valves are open, and both Aerozine-50 and Nitrogen Tetroxide enter the thrust chamber, the engine starts, and thrust levels begin to rise. Only 0.9 seconds after the Fire Switch signal, the engine reaches its operating level. Engine shutdown is initiated when either Aerozine-50 or Nitrogen Tetroxide are depleted (Titan III Propulsion Systems, 3-3 -3-5).

5.3 Stage Three: Transtage

The engine start sequence for the AJ10-138 engines is initiated by applying 28 Volts DC to the pilot valve solenoid. With the pilot valve energized, fuel is ported through the pilot valve to a cavity behind the bipropellant valve power piston. The force resulting from the fuel pressure on the power piston is sufficient to overcome the spring and friction forces holding the valve in the closed position. This force moves the common fuel poppet and oxidizer piston stem assembly to the open position allowing propellants to flow through the bipropellant valve to the injector. Opening time is controlled by an orifice between the pilot valve and bipropellant valve. Propellants from the bipropellant valve flow into the fuel and oxidizer manifolds of the injector and are injected into the thrust chamber where hypergolic ignition takes place. Propellant flow rates to maintain the design mixture ratio for the engine system are controlled by balance orifices located at the bipropellant valve inlets. Ninety percent of the thrust is achieved within .4 seconds after the receipt of the electrical signal. The pilot valve draws approximately 1.6 amps to sustain engine operation. Engine shutdown is initiated when a signal is given to the pilot valve to close, this shuts off the flow of fuel and oxidizer, stopping the combustion process (Titan III Propulsion Systems, 4-2 & 4-5).

6.0 PROPELLANTS

The biggest safety concern for the Athena project is the danger posed by the liquid propellants. This danger was accepted because of the undesirable weight of solid propellants and the difficulty in maintaining cold temperatures for cyrogenic propellants. All three engines used in the booster burn the same oxidizer and fuel. The oxidizer is Nitrogen Tetroxide while Aerozine 50 is used for the fuel. This section will address the needed precautions and some of the properties for the propellants.

6.1 Nitrogen Tetroxide, The Oxidizer

Nitrogen Tetroxide (N_2O_4) is the oxidizer of all three stage of the Athena booster. Its most desirable property is that it is in liquid form when stored at room temperature. This eliminates the problem of maintaining a temperature control system for the propellant tanks. N_2O_4 is usually stored in 375 lb (170 kg) drums. These drums and any other storage container may be made of almost any type of metal and even some non-metals such as Teflon, graphite, and pyrex glass. But if the Nitrogen Tetroxide absorbs a small amount of water (approximately 0.1% of the total mass) it becomes corrosive with the metal. N_2O_4 contains no more than 0.17% water in the propellant grade so this may be a problem for extended storage. Nitrogen Tetroxide also readily absorbs moisture from surrounding air which increases the probability of corrosion. The plastics also start to degrade with extended exposure to the oxidizer but pyrex glass and graphite are unaffected.

Some of the more important properties are listed in the Table 6.2 below. As seen in the table the appearance of N_2O_4 at room temperature is a red-brown liquid. At slightly lower temperatures it appears to have a yellowish tint and as the water content increases it becomes a blue-green color. Nitrogen Tetroxide has a very strong acidic odor. It is a liquid at room temperature but will become a gas at any temperature over 21°C (70°F). This means that in most applications the liquid will start to boil away. But as long as the oxidizer is kept above -11°C (12°F), it will not freeze. It is also a very dense material because of its liquid state. The cost of one 375 lb (170 kg) drum is the same as if N_2O_4 were purchased in bulk at $3.15 /lb ($6.94 /kg) ("Standard Prices for Missile Fuels Management Category Items", 3-4).

Appearance: Red-Brown Liquid
Odor: Pungent Acid Odor

Properties	English Units	Metric Units
Boiling Point	70.1°F	21.2°C
Freezing Point	11.8°F	-11.2°C
Density	11.96 lb/gal	1450 kg/m^3
Cost	$3.15 /lb	$6.94 /kg

Table 6.2: Properties of Nitrogen Tetroxide at room temperature (77 °F or 25°C)

Nitrogen Tetroxide will not spontaneously combust without any other chemicals but it is a strong oxidizer and can cause hazardous fires. A N_2O_4 fire should be extinguished using large amounts of water but the fumes released are very toxic and appropriate precautions should be made. Nitrogen Tetroxide is also very toxic when in human contact. It will cause severe pain if plashed in an eye and can burn the skin with prolonged contact. Both of these effects can be treated by flushing the area with water. A safety shower should be nearby anywhere the oxidizer is stored along with personal wearing protective clothing. Inhalation of N_2O_4 causes irritation of the lungs and nasal passages and can cause sickness not noticeable up to 24 hours after exposure. In order to avoid the build-up of toxic gases, storage areas should be well ventilated. Monitoring equipment must be present in areas where Nitrogen Tetroxide might settle. This equipment, along with portable devices, should be able to detect a threshold limit value of 5 ppm. The area must also be free of any debris and should not be exposed to direct sunlight. Filling the storage tanks, whether in the wherehouse or onto the booster, should be done by gravity. But before this is done the tanks should be free of air by flushing it with nitrogen (Titan III Propulsion Systems, 7-9 - 7-12).

6.2 Aerozine 50, The Fuel

The fuel used in the booster is Aerozine 50 (A-50). It is also a liquid at room temperature like N_2H_4, but A-50 is has a more complex molecular structure. It is a 50-50 mixture of Hydrazine (N_2H_4) and Unsymmetrical Dimethylhydrazine (UDMH). This means A-50 performs better than pure N_2H_4 but has utilizes the stability of UDMH to make it more safe. Again like Nitrogen Tetroxide, Aerozine 50 is non-corrosive with most metals but water contamination will cause it to be more corrosive. A-50 can be stored in tanks made from aluminum, cobalt, nickel, and titanium alloys and stainless steels. It can also be kept in Teflon and Polyethylene lined containers but Nylon tanks are only safe for 90 - 120 days. The most practical material for storage is stainless steel. Some recommended types are AISI 3030, 304, 321, 327, and 440. As stated above the lifetime of these materials is decreased as the water content of Aerozine 50 is increased. Water will also degrade the engine performance of the fuel and if more that 5% of the solution is water it is hazardous to engine materials. Aerozine 50 is flammable in air because of the vapor produced above the liquid. Any ignition source is able to initiate combustion and if enough A-50 is exposed to air it can self-ignite.

Table 6.3 shows the properties of Aerozine 50 at room temperature. The characteristics of A-50 are a combination of Hydrazine and UDMH. The solution becomes uniform with sufficient agitation. The liquid has no color but it has a fishy smell characterized by UDMH instead of Hydrazine's ammonical odor. Although the boiling point of A-50 is much higher than room temperature the solution is highly unstable. This instability comes from the properties of

Hydrazine. Caution must be used so that Aerozine-50 does not come into contact with a catalyst of Hydrazine. A-50 will not freeze until a very low temperature of 22°F (-5.6°C) which should not be a problem. The fuel is less dense than water but it is in liquid form giving it a relatively high density. Aerozine 50 may also be purchased in 375 lb (170 kg) drums or in bulk at a rate of $13.00 /lb ($28.66 /kg) ("Standard Prices for Missile Fuels Management Category Items", 3-4).

Appearance:	Red-Brown Liquid	
Odor:	Pungent Acid Odor	
Properties	**English Units**	**Metric Units**
Boiling Point	158°F	70°C
Freezing Point	22°F	-5.6°C
Density	7.5 lb/gal	960 kg/m^3
Cost	$13,00 /lb	$28.66 /kg

Table 6.3: Properties of Aerozine 50 at room temperature (77°F or 25°C)

As stated above large amounts of spillage of Aerozine 50 in direct contact with air can generator enough heat to self-ignite. This can be remedied by always covering it by a blanket of nitrogen gas. If A-50 should catch on fire, large amounts of water should be used to extinguish the flames. However, if a solution of A-50 and water contains less than 65% water, it will still be flammable. An alternate method is to use Carbon Dioxide extinguishers. The Carbon Dioxide causes the UDMH to solidify and therefore cleans the surrounding air of UDMH vapor. Hydrazine may ignite in the A-50 if a proper catalyst is present. One such catalyst is rust. It causes an oxidation process to occur and will spontaneously combust on contact with sufficient amounts of rust. The area surrounding A-50, like Nitrogen Tetroxide, should be free of debris and well ventilated. Aerozine 50 is very toxic to humans. Precautionary equipment similar to that needed for N_2H_4 must be present at all times. If personal do come in contact with Aerozine 50, they should be washed completely with large amounts of water and taken to an area with fresh air. Detection devices also must be placed in regions of stagnant air to monitor the level of A-50 (Titan III Propulsion Systems, 7-9 to 7-12).

6.3 Propellant Additives

In the future of Athena it is proposed to make the booster much more safe. Current research at NASA Lewis under Bryan Palaszewski claims that an additive to the propellants will transform them from the liquid state to a gelled state. In the gelled form, the propellants are much less likely to spread after a spill. This decreases the chance of detonation. If a leak did occur where N_2O_4 and A-50 came into direct contact the oxidizer and fuel would not immediately explode but would merely burn at the interface. This makes it easier to detect a leak. It also makes the mission much more safe, especially for the crew of the C5.

The propellants are mixed with an additive to gel the liquid. It has been proven that the gelled propellants can be pump fed. This means that the same engines and pumps can be used with only one added component (the gelling agent). Since the propellants are atomized in the engine before they are ignited, they can be detonated by the atomic interaction. Unfortunately, a study of gelled propellants were shown to have a lower Isp when compared to the ungelled form (Launch Vehicle Performance Using metallized Propellants, 1 (presumably from Advanced Gel Technology Program, Giola,et.al.)). To correct for this problem, the propellants are metallized by adding micron-sized particles of metals to the gelled state. A study of this subject is included in "Launch Vehicle Performance Using Metallized Propellants" by Palaszewski and

Powell. The I_{sp} is proportional to the combustion temperature (T_c) and the molecular weight (MW) by the relation:

$$I_{sp} \propto \left(\frac{T_c}{MW} \right)^{.5}$$

The metallic additives increase the molecular weight of the propellants and therefore increase the I_{sp}. This correction means that the propellants are more dense and therefore take up less room in the form of storage tanks. The density of the metallized fuel($\rho_{p,m}$) can be calculated from the equation shown below using the propellant density (ρ_p), the metal density (ρ_m), and the metal loading (ML).

$$\rho_{p,m} = \frac{1}{\frac{(1-ML)}{\rho_p} + \frac{ML}{\rho_m}}$$

This higher density means a decrease in propellant tank volume on the order of 20 - 25%. The recommended metal additive is aluminum. A study of the Titan IV first and second stage engines showed that the optimal metal loading was 35 - 40%. These engines use the same propellants as the engines used in the Athena booster. This means the metal loading should be on the same order as for the Titan IV. The metal loading also decreases the mixture ratio by more than half. For example the first stage Titan IV engine has a ratio of oxidizer to fuel of 1.91 (LR87-AJ-11). This was decreased to .69 with the aluminum added. These figures should give the reader an idea of how the gelled/ metallized propellants would increase the performance of the rocket while still adding safety in the form of a gel (Launch Vehicle Performance Using Metallized Propellants, 1-14). Unfortunately, this technology is not currently available in industry. It has been predicted that about 5-7 years of research and development must be done before metallized, gelled fuels are available. With additional funding from the Athena project, it is relatively certain that gelled propellants should be usable sooner than 1999. At this time, the gelled propellants will be integrated into the booster design, making missions more safe and reliable.

7.0 Propellant Storage Tanks

The Athena booster was designed to be deployed from the C-5B Galaxy aircraft. This put a large size constraint on the booster. The structure of the booster was sized by the dimensions of the rear door of the aircraft. This in turn determined the diameter of the fuel tanks. This diameter was found to be 2.5 m (8 ft 2 in). The tanks could also be designed to be different shapes. The volume could be spherical or cylindrical. The volume needed determines which shape is the best design, from a length viewpoint, from the dimensions of the tanks. These possible designs and constraints lead to the final design of the propellant tanks. This section will go into the detail of the tank design process.

7.1 Calculations

The easiest design for the propellant tanks is to use a spherical volume. The radius of the sphere could be set by the volume of the propellant or by size constrains on the booster. The volume equation for the sphere is shown below along with the calculation for the thickness of the walls. The walls must be thick enough to hold the pressure inside the sphere but be light enough to keep a low mass. The thickness (t_s) is found from knowing the tank pressure (P_t), the radius desired (a), the efficiency of the weld (e_w), assumed to be .75, and the yield strength of the material divided by a safety factor of 1.2 (S_w) (Design of Liquid Propulsion Rocket Engines, 332-341).

$$V = \frac{4}{3}\pi a^3$$
$$t_s = \frac{P_t a}{S_w e_w}$$

Because of the severe size constraints on the C5, it is more practical to use propellant tanks of a cylindrical shape. These tanks must have rounded ends so that they can hold the pressure of the propellant. The volume can be determined from the radius and length of the cylinder. But the wall thickness will vary on the ends as compared to the cylinder itself. The equations are shown below using the same notation as above plus wall thickness of the cylinder (t_c) and of the ends (t_e).

$$V = \frac{4}{3}\pi a^3 + \pi a^2 l_c$$
$$t_c = \frac{P_t a}{S_w e_w}$$
$$t_s = \frac{P_t a}{S_w e_w}$$

where l_c is the length of the cylindrical section.

A more efficient way to design the propellant tanks is to use ellipsoidal end caps. Ellipses still can withstand the high pressures within the tank but decreases the overall length. The dimension listed as b in Figure 6.1 below. Since this width dimension is shorter than the total diameter it saves length which was another constrain of the C-5. Again the end and cylinder wall thicknesses are different and the equations for each are listed.

$$V = \frac{4}{3}\pi b^3 + \pi a^2 l_c$$
$$t_c = \frac{P_t a}{S_w e_w}$$
$$t_e = \frac{\frac{K P_t a}{S_w e_w} + \frac{P_t b}{2 S_w e_w}}{2}$$

Where $K = .5\left(\frac{a}{b}\right)$ is from Fig.8-7 in "Design of Liquid Propulsion Rocket Engines" by Huzel & Huang, and where b is the semi-minor axis of the ellipsoidal tank end (Design of Liquid Propulsion Rocket Engines, 332-341).

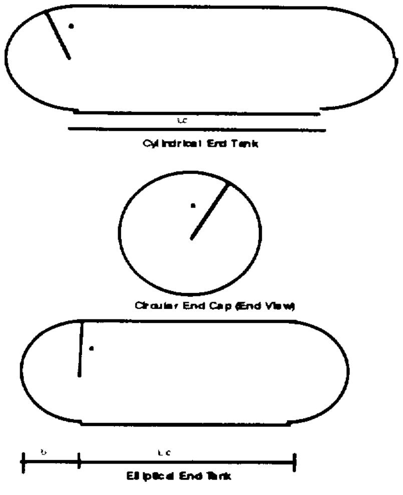

Figure 6.1: Diagrams of the various shapes of propellant tanks.

7.2 Tank Configurations

The volume of fuel and oxidizer is set given the burn time of the engines and the radius is known from the size constraints. This means that the equations can be solved for the length of the tank. It is seen that there is a point where the spherical tanks are no longer practical and cylindrical tanks are needed. If the radius of the tank is about the same diameter as the specified size constraint or less (i.e. approximately 2.5 meters), spherical tanks are used. On the other hand, if the radius is larger, cylindrical tanks with elliptical end caps are needed. The following equations are used to compare the length of the cylinder to the diameter of the radius. (L indicates the overall length of the tank whereas l_c is for the length of the cylinder itself.)

$$a = \left(\frac{3V}{4\pi}\right)^{\frac{1}{3}}$$

$$L = \frac{V}{\pi a^2} + \frac{2b}{3}$$

It became obvious in initial calculations that the overall length of the Athena booster was too large for the C-5 carrying capabilities. This prompted consideration for putting the fuel tanks side by side in the first stage instead of the end to end configuration. However, since the oxidizer mass is larger than that of the fuel, booster's mass distribution would be uneven. To correct this the side by side tanks would have to each have half of the oxidizer and half of the fuel. After a couple of iterations of propellant masses from the Mission Analysis team, it seemed obvious that the booster would be short enough so that splitting the tanks would not be necessary. In the end the tanks were placed end to end in all of the stages. Cylindrical tanks with elliptical end caps were used for the first and second stages while the third stage was comprised of spherical tanks (Design of Liquid Propulsion Rocket Engines, 332-341).

7.3 Overall Volume and Mass Calculations

Before specific numbers can be given in the final calculation of the propellant tanks some additional mass and volume must be added. The additional mass comes from the safety fuel needed for small corrections in the trajectory due to conditions such as wind and for inefficiencies in the propulsion systems. This extra fuel was determined to be 5% of the total propellant mass. This mass was then converted into a total volume given the densities and oxidizer to fuel ratio of each engine. An extra 5% was added to this volume to account for ullage within the tanks. The final calculations for the propellant masses and volumes are included in Table 6.4.

Stage	**Mox/Mf**	**Total Stage Mass (kg)**	**+ 5% Safety Fuel (kg)**	**Propellant Vol (m^3)**	**+ 5% Ullage Vol (m^3)**
First (Ox)			27335		19.79
First (Fuel)			14312		16.59
Sub-Total	*1.91*	*39664*	*41647*	*34.65*	*36.38*
Second (Ox)			14006		10.14
Second (Fuel)			7530		8.73
Sub-Total	*1.86*	*20511*	*21537*	*17.97*	*18.87*
Third (Ox)			4546		3.77
Third (Fuel)			2392		3.17
Sub-Total	*1.90*	*6560*	*6938*	*6.61*	*6.94*
Totals		**66735**	**70122**	**59.23**	**62.19**

Table 6.4: Final masses and volumes of propellants per stage

Now that the volumes have been calculated the actual tank dimensions and weights can be determined. It turns out that the first and second stage tanks are most efficient lengthwise as cylinders with elliptical ends, while the third stage is most efficient as spheres. The actual dimensions are listed in Table 6.5.

	a (meters)	**b (meters)**	**Length Ox. Tank (m)**	**Length Fuel Tank (m)**	**Total Tank Length (m)**
Stage 1	1.25	.75	4.53	3.88	8.41
Stage 2	1.25	.75	2.57	2.28	4.85
Stage 3	1.25	---	1.93	1.82	3.75
				Total Tank Length	17.01

Table 6.5: Final tank lengths and geometry

Notice that the third stage tanks were designed to hold enough fuel for the **GTO** mission. This mass is calculated from: the mass to LEO (6560 kg) plus the extra fuel for **GTO** (387 kg).

The lengths and diameters can then be used to find the total weights of the tanks. From the following equations, the tank masses were able to be calculated. These tanks were designed from AISI 304 stainless steel, which has a density of 2.16E-6 kg/m^3 (.29 lb/in^3).

$$W_s = 4\pi a^2 t_s \rho$$

$$W_c = 2\pi a l_c t_c \rho$$

$$W_e = \frac{\pi a^2 t_e E \rho}{2\frac{a}{b}}$$

Where $E = 1.5\left(\frac{a}{b}\right)$ is from Fig.8-7 in "Design of Liquid Propulsion Rocket Engines" by Huzeli Huang. In order to alleviate tank sloshing, baffles must be added to the tanks. A baffle is a metal ring in the tank, extending from the tank wall toward the center of the tank a set distance, approximately .61 m (2 ft). These are places at set intervals throughout the tanks. For the Athena, the 1st stage tanks each have 4 baffles, the 2nd stage tanks have 2, and the 3rd stage has one baffle. Table 6.6 shows the final masses for the tanks using AISI 304 stainless steel for the material of the tanks.

Tank	**Baffle Mass (kg)**	**Total Tank Mass (kg)**
Ox. 1st Stage	135.35	1407.3
Fuel 1st Stage	135.35	420.5
1st Stage Total	*270.69*	*1827.7*
Ox. 2nd Stage	67.67	467.5
Fuel 2ndStage	67.67	335.5
2nd Stage Total	*135.35*	*803.0*
Ox. 3rd Stage	33.84	177.9
Fuel 3rd Stage	33.84	133.0
3rd Stage Total	*67.67*	*310.9*
Total	**473.71**	**2941.6**

Table 6.6: Final baffle and tank masses

***Note** that the baffle calculations were only a simple approximation of rather complex systems, and the weights for these are only an estimation.

The following chart, Figure 6.2 shows the mass allocation of propulsion systems for each stage.

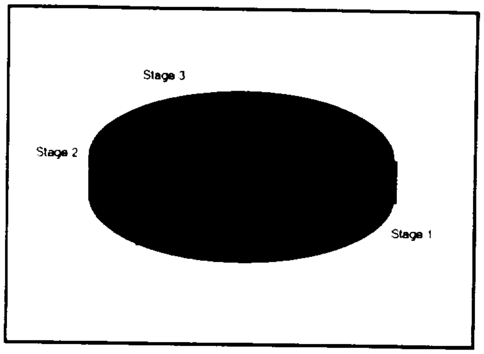

Figure 6.2: Mass Allocation for Each Stage

7.4 Fireball Radius

The equation relating the weight of propellant to the fireball radius is:

$$R = zW^{\frac{1}{3}}$$

where by z (units of ft/ lb^0.33) is the parameter related to the over-pressure of the fireball (Stull). It was found that an over-pressure of 1 psi is sufficient to knock down a person. Taking this as the limit, the chart in "The Handbook of Pyrotechnics" by Stull was consulted and a value of z = 50 was obtained. The fireball radius was figured to be about 800m. This means that if there were to be a catastrophic failure, and the Athena booster were to explode, the radius of maximum destruction would be the fireball radius. The C-5 carrier aircraft should be at least this distance away from the booster when all systems are activated in order to maximize the safety of the crew and aircraft.

8.0 COSTS

8.1 The Final Costs

The original goal of the Athena project was to maintain a cost at about half that of the closest competitors, Titan, Delta, and Pegasus. As data began to be collected, this goal was found to be nearly impossible for the propulsion systems to meet. The following table, Table 6.7, shows the Propulsion group's estimates on the systems chosen for the Athena booster.

Stage	**Propellant Costs ($M)**	**Engine Costs ($M)**	**Tank Costs ($)**	**Total Costs ($M)**
Stage 1 Oxid.	.190		5805	
Stage 1 Fuel	.410		1735	
Sub total	*.600*	*3.00*	*7539*	*3.61*
Stage 2 Oxid.	.097		1928	
Stage 2 Fuel	.216		1384	
Sub total	*.313*	*2.50*	*3312*	*2.82*
Stage 3 Oxid.	.036		734	
Stage 3 Fuel	.078		549	
Sub total	*.115*	*5.00*	*1282*	*5.12*
Totals	**1.027**	**10.50**	**12134**	**11.54**

Table 6.7: Final Cost Estimates

The cost estimates for the engines were from Bill Sprow at Aerojet Corp. and were for a moderate launch schedule (i.e. 3-4 launches per year). These costs would be reduced with more launches per year. As time passes, these prices will become smaller due to advances in manufacturing, and reduction in initial research and development money placed on each engine will reduce Athena's costs a great deal.

The propellant prices were estimates from the Air Force Logistics Center. These prices would be reduced by using private fuel companies for propellant procurement.

The tank cost estimates were based on an estimate of $1.13 / kg for AISI 304 stainless steel from Advanced Aircraft Material Corp. These costs were then added to a labor estimate of $3 / kg to assemble the tank systems that are required for the Athena booster. This estimate was decided on by the Propulsion group to arrive at a reasonable cost estimate for the tanks.

The following chart, Figure 6.3 shows the cost allocations for each stage of the Athena booster.

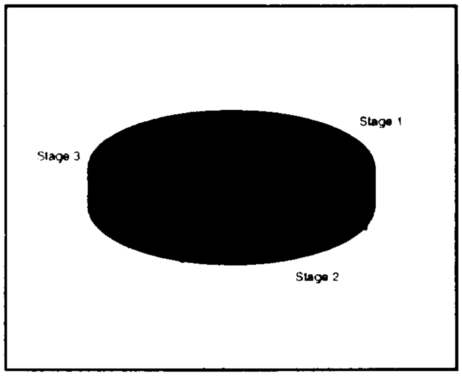

Figure 6.3: Cost Allocation for Each Stage

9.0 CONCLUSION AND FUTURE PLANS

The Athena booster consists of one LR87-AJ-11 engine, one LR-91-AJ-11 engine, and two AJ10-138 engines, along with tanks and support equipment for each engine. Thus, since the engines are currently available, and being used in this same configuration for the Titan family of launchers, this is a very well tested and reliable system. The fact that the Athena booster is in effect a small Titan rocket, dropped from an aircraft gives the Athena project the viability in the marketplace that is desired. The added enhancements that an air-launched vehicle affords to the Titan system makes the Athena an attractive space launch system.

The future is wide open to the Athena booster from a propulsions standpoint. Once gelled propellants are widely available, the stored liquids become exceedingly safe for use in this type of mission, further enticing investors. The addition of new, small, low-weight solid boosters would increase the payload available to LEO and GTO. A larger cargo aircraft, or one that could lift more weight would also add much more weight to the payload available. Already, the Athena may be able to launch up to 50% of existing satellites, and these advances would only increase this number.

Chapter 7

Structure

PRECEDING PAGE BLANK NOT FILMED

~~ORIGINAL PAGE~~
~~BLACK AND WHITE PHOTOGRAPH~~

CHAPTER 7 -- STRUCTURES

Structure's Symbols

Al: aluminum
A_s: shroud surface area
B: global buckling coefficient
b: length of panel between stringers
g: standard gravitational acceleration
J: torsional constant
mm: millimeters
ν: Poison's Ratio
π: 3.14159265
ρ: material density
r: radius
ρ: radius of gyration
σ: stress
t: thickness
t: thickness of skin
t_c: composite thickness
t_m: material thickness
W: weight / mass

1.0 GROUP OVERVIEW

The structures group is responsible for the overall structural design of the booster which includes a static analysis and dynamic analysis. The constraints imposed on the structures group are material cost and manufacturing and also structural weight. Below is a list of the primary booster elements investigated in this report:

- Main booster structure design
- Payload shroud
- Booster egress assist cradle design

2.0 STRUCTURAL DESIGN OF BOOSTER EXTERIOR

The booster structure in handling operations and flight maneuvers is subjected to tensile, compressive, bending and torsional load systems. The structure may be pressurized or unpressurized. The structural design of such structures thus requires a knowledge of the buckling strength under the various load systems, acting separately and in combination. The following sections will focus on the design algorithm used in constructing the main booster components:

- Exterior Skin
- Stringers
- Lateral Buckling Rings

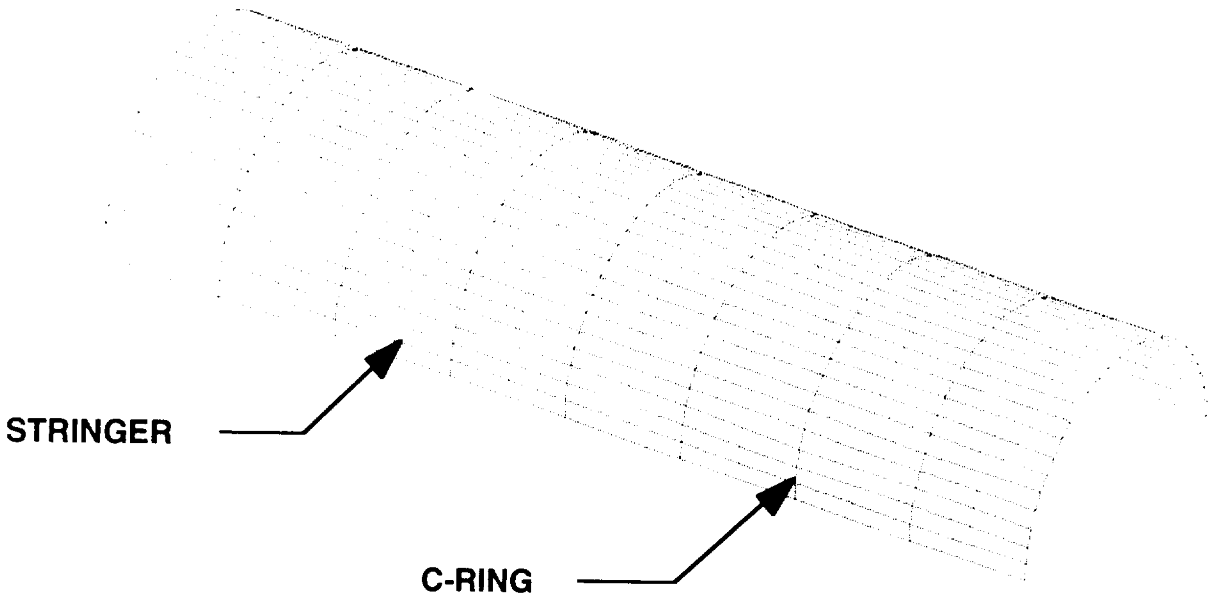

Figure 7.1: First Stage Design Cut-Away

The figure above is a cut-away of the first stage design configuration. The stringers and c-rings make up the interior diameter. The skin is attached to the outside face of the stringers.

The booster is designed with a factor of safety set at 1.4. The maximum g-loading the booster is able to withstand is approximately 7 in the longitudinal direction and 2.5 g's in the lateral direction.

2.1 Materials Selection and Properties

Material selection is a major design requirement for flight vehicle structures. The materials must provide a high degree of structural integrity against failure, with as light a structural weight as possible.

The material selected for the main structural components, i.e. stringers, c-rings, and skin, is 7075-T6 Aluminum. 7075 Al was selected for high strength, low weight, low cost, and availability.

Material	E_c (MPa)	s_{ty} (MPa)	s_{cy} (MPa)	n
7075-T6 Al	72	516	482	.33

Table 7.1 Material Properties of 7075-T6 Aluminum

2.2 Exterior Skin Design

The exterior skin is basically a curved sheet panel. Curved sheet panels represent a common part of flight vehicle structures. If the curved sheet has no longitudinal stiffeners, failure will occur when buckling occurs. If the curved sheet has stiffening elements attached, then the combined unit has an ultimate strength much greater than the load which caused initial buckling of the curved sheet panel. In this section we will determine what stress will cause the curved sheet panels to buckle and also what external loads will cause the stiffened sheet panel to fail.

The skin is made of 7075-T6 Al sheets 0.08 cm thick. The sheets are attached to the stringers through rivets.

The expression for the critical buckling stress under axial compression is (Bruhn C9.1),

$$\sigma_{crit.comp.} = \frac{K_C\pi^2 E}{12\left(1 - \upsilon^2\right)}\left(\frac{t}{b}\right)^2$$

where:

b = length of panel between stringers
t = thickness of skin

For Athena the stringer spacing on the first stage is 15.14 cm and skin thickness is 0.79375 ≈ 0.8 mm.

$$\Rightarrow \sigma_{crit.comp.} = \frac{9.6\pi^2(72\cdot 10^9)}{12(1-0.3^2)}\left(\frac{8\cdot 10^{-4}}{0.1514}\right)^2 = 17.44 \text{ MPa}$$

K_C is the buckling coefficient and is determined from the theoretical curves (Bruhn C9.2). The resulting critical stress is in compression. The actual compression stress the skin will be subjected to, if stringers are not used is,

$$\sigma_{act.comp.} = \frac{\text{Force}}{\text{Area}_{\text{skin}}}$$

$$\sigma_{act.comp.} = \frac{3.39\cdot 10^6 N}{6.78\cdot 10^{-3} m^2}$$

$$\Rightarrow \sigma_{act.comp.} = 500 \text{ MPa}$$

Since,

$$\sigma_{act.comp.} >> \sigma_{crit.comp.}$$

it can be understood that the skin carries a very minimal portion of the compression load. With the skin not taking much of the axial compressive or bending loads, the longitudinal stringers had to be designed to function as the major load carrying components.

2.3 Longitudinal Stringer Design

A cylindrical structure composed of a thin skin covering and stiffened by longitudinal stringers and transverse frames or rings is a common type of structure for space vehicles. Such structures are often referred to as semi-monocoque structures.

The internal rings in a semi-monocoque structure divide the longitudinal stringers and their attached skin into lengths called panels. The stringers act as columns with an effective length equal to the panel length which is the ring spacing.

In general, thin curved sheet panels buckle under relatively low compressive stress and based on the design requirement of no buckling of the sheet, the sheet would have to be relatively thick or the stringers placed very close together.

In design of the stringers, several iterations were done to determine the final selection of stringer and stringer spacing. The type of stringer selected for stages one, two, and three is a standard Z-section #68 with a cross-sectional area of 2.48 cm^2 (Bruhn A3.12). Below is the stringer configuration,

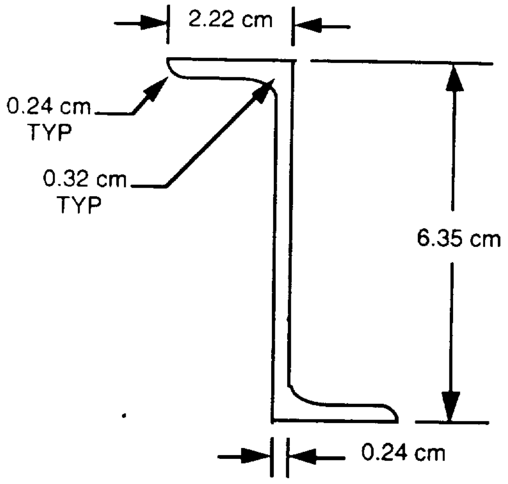

Figure 7.2: Stringer Configuration

LOCAL BUCKLING

The local buckling strength of the stringer is determined by the expression (Bruhn C6.2),

$$\sigma_{local.crit.} = \frac{K_W \pi^2 E}{12(1-\upsilon^2)}\left(\frac{t_w}{b_w}\right)^2$$

K$_W$, the stringer buckling coefficient, is dependent upon the geometry of the stringer and determined from the theoretical buckling curve to be 4.1 (Bruhn C6.3).

$$\Rightarrow \sigma_{local.crit.} = \frac{4.1\pi^2(72\cdot 10^9)}{12(1-0.3^2)}\left(\frac{0.094}{2.406}\right)^2 = 426.9\text{MPa}$$

GLOBAL BUCKLING

The global buckling stress of the stringer is determined by the following expression (Bruhn C7.22),

$$B = \frac{\left(L'/\rho\right)}{\pi\sqrt{\dfrac{E}{\sigma_{local.crit}}}}$$

where:

B : global buckling coefficient

$L' = \frac{L}{\sqrt{c}}$: c = 1.5 for pinned end conditions

$\rho =$ radius of gyration

therefore;

$$\Rightarrow B = \frac{(36.24)}{\pi\sqrt{\frac{72 \cdot 10^9}{426.9 \cdot 10^6}}} = 0.888$$

from Johnson's Parabola (app. 1) and B, S is found to be 0.8. The value for the global buckling stress of the stringer is calculated from,

$$\sigma_{global.crit.} = S \cdot \sigma_{local.crit}$$

$$\Rightarrow \sigma_{global.crit.} = 0.8 \cdot (426.9 \text{ MPa}) = 341.52 \text{ MPa}$$

The maximum stress on the stingers created by the maximum loading on the booster is,

$$\sigma_{act.str.} = \frac{\text{Force}}{\text{Area}_{str}}$$

$$\Rightarrow \sigma_{act.str.} = \frac{60.53 MN}{0.2484 \cdot 10^{-3} mm} = 243.7 \text{ MPa}$$

which places the safety factor of the booster design at 1.4.

Stages 2 and 3 were designed using the stringer section. Material costs can be reduced by ordering a bulk amount of material. The number of stringers needed for stages 2 and 3 were reduced from that of stage 1, due to different maximum loading conditions.

Stage	# of Stringers	Spacing (cm)
1	56	15.15
2	36	23.56
3	28	30.29

Table 7.2 Number of Stringer per Stage & Stringer Spacing

2.4 Internal Compression Rings

The internal rings in a semi-monocoque structure must act as structural units to support inward loads, produced by the stringers, which puts the rings in *hoop* compression. There are two types of rings, those attached to the skin and those not attached to the skin, called *floating rings*, which support, and are therefore loaded only by, the stringers (Bruhn C11.34).

The Athena booster was designed with floating rings, referred to in this report as c-rings. The cross-section and dimension of the c-rings is shown figure 7.3.

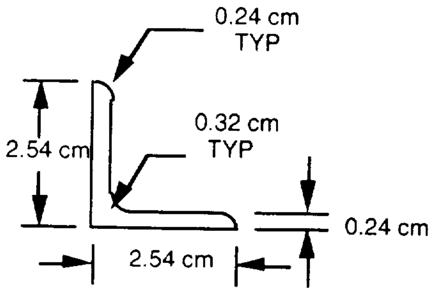

Figure 7.3: Cross Section of C-Rings

All rings are standard L-channels manufactured out of a 7075-T6 AL. The cross-sectional area of each c-ring is 1.16 cm^2 and the mass is 2.68 kg. Each stage was designed so that a minimum number of c-rings are needed to prevent the stringers from buckling. This minimizing will keep material costs and structural weight below expected values.

Table 7.3 Number of C-Rings per Stage & C-Ring Spacing

Stage	# c-rings	Spacing (cm)
1	14	87.5
2	8	95.6
3	6	97

3.0 PAYLOAD SHROUD MATERIAL SELECTION AND DESIGN

In order to protect the payload during the atmospheric portion of the Athena's ascent, the booster was fitted with a payload shroud. Several different options of material and design were looked at in an attempt to minimize structural mass, while avoiding high cost and labor intensive projects. Additionally, great pains were taken to select a material profile that would provide the necessary thermal protection, yet was neither too costly nor difficult to manufacture. This portion of the report will present the initial structural and thermal material options that were investigated, the reasoning behind the final material selections and the geometry of the payload shroud.

3.1 Initial Material Options

There are two areas where material options were investigated: structural materials and thermal protection materials. The primary driver for the material selection for the payload shroud is the structural mass. This is due to the fact that the payload shroud will remain with the booster throughout the first and second stage burns. Therefore, the amount of fuel required for the first and second stage is largely affected by the mass of the shroud. In regards to the thermal material, the driver is maximum service temperature, availability and ease of manufacturing.

3.1.1 Structural Materials

The structures group analyzed five different options for the material to be used in the structure of the payload shroud. Each of these configurations is shown in Figure 1 (on page 144). These include aluminum skin with stringers, aluminum honeycomb within a composite sandwich, integrated J-stiffened composites, Kevlar composite skin with composite reinforcements and boron reinforced compression panels. Each of these materials will be discussed individually concerning their benefits and/or disadvantages.

An aluminum skin and stringers configuration was considered for several good reasons. The skin was to be made of 7075-T6 aluminum, primarily because of its excellent strength to weight ratio compared to other aluminum materials, its historical performance, good availability and low cost, and it s use for the rest of the booster skin which may help to reduce the cost of materials over the long run. The stringers were also to be made of 7075-T6. It was proposed that they be designed to the same dimensions as those in the lower stages for simplicity. There are, however, two clear disadvantages tend to hinder the use of an aluminum skin. The first, and perhaps most important, is excessive weight. As mentioned earlier, the primary design consideration for the shroud is minimized mass. The aluminum skin configuration is the heaviest of those available. The other disadvantage of the aluminum is that it can be difficult to form. 7075-T6 is a very stiff type of aluminum so processing costs could be high.

The second option is an aluminum honeycomb core with a sandwich of pre-preg carbon composite laminates. The aluminum core would be either 7075-T6 or 5056-H3. The composite would consist of a carbon fiber applied unidirectionally within an epoxy that would be determined based on thermal protection value, as well as several other criteria. (see section 3.2 for an explanation of the choice of composite matrix material). The critical advantages of this configuration are the fact that it is proven technology and has relatively low cost and low weight. It does have several disadvantages, however. The manufacturing of this configuration, while not technologically advanced, can be highly labor intensive because of the unusual shape of the shroud. Additionally, there is a risk of debonding between the composite laminates and the honeycomb core. This fact could lead to a thermal breakdown of the shroud during flight, not to mention catastrophic failure.

Another option is that of integrated J-stiffened composite panels. This technology was developed in the late 1980's by companies like McDonnell Douglas to produce lighter and stronger aircraft fuselages. This configuration consists of a graphite composite with stiffeners that are shaped by fiberglass fibers. The most significant advantage for this configuration is that it has a very high strength to weight ratio. Additionally, this configuration can be shaped into the desired geometry rather easily. It has several disadvantages, however. The technology is very recent and may not prove reliable enough. This last fact leads to the further conclusion that this configuration is also expensive.

Yet another option was a Kevlar-49 skin with stringers made of graphite fiber composite. The stringers are manufactured into a skeleton of the structure onto which the Kevlar skin is bonded. This design provides excellent strength with low weight, and is rather easy to manufacture. The critical disadvantage is, however, that it is very costly. In addition, this is very recent technology and, like the integrated composite stiffeners, may not be reliable.

The final option that was investigated was that of boron reinforced compression panels. It consists of an aluminum 7075-T6 skin with stringers of the same material that are reinforced with columns of boron. This configuration offers tremendous strength, particularly under compression, at relatively low weight. In addition, the majority of the structure consists of aluminum making it readily available and easy to manufacture. The trouble with this configuration, however, is its extremely high cost and untested performance.

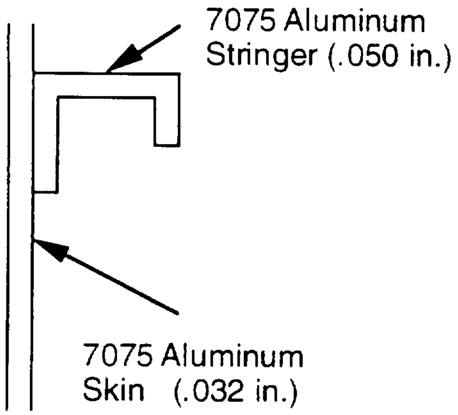
7075 Aluminum
Stringer (.050 in.)
7075 Aluminum
Skin (.032 in.)

Conf. 1: All Aluminum Structure

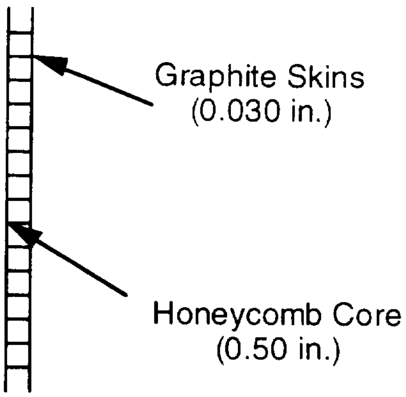
Graphite Skins
(0.030 in.)
Honeycomb Core
(0.50 in.)

Conf. 2: Honeycomb Sandwich Structure

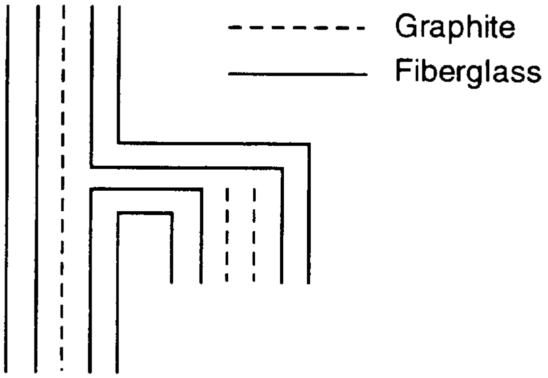
Graphite
Fiberglass

Conf. 3: Integrally Stiffened Laminate Structure

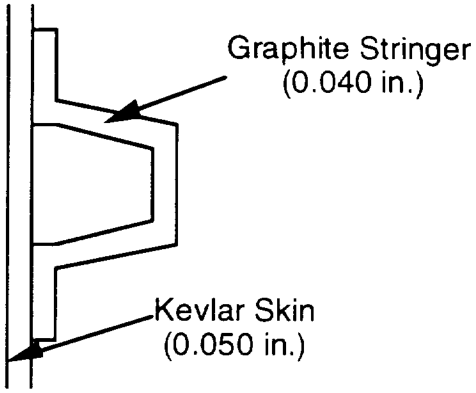
Graphite Stringer
(0.040 in.)
Kevlar Skin
(0.050 in.)

Conf. 4: Skin-Skeleton Structure

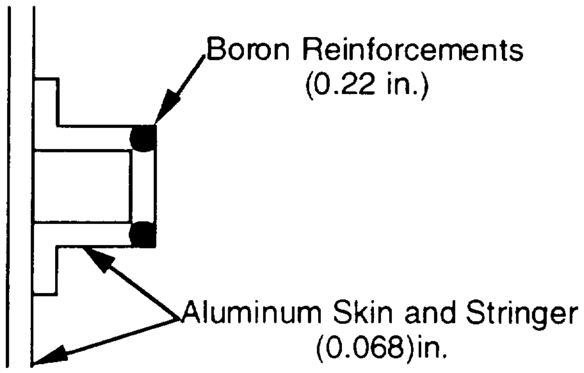
Boron Reinforcements
(0.22 in.)
Aluminum Skin and Stringer
(0.068)in.

Conf. 5: Boron-reinforced Compression Panels

Figure 1: Booster Skin Configurations

3.1.2 Thermal Materials

The most important factor in determining which material to choose for a thermal protection system was maximum heat resistance (or emissivity) for minimum cost and weight. There are two areas on the Athena booster on which thermal protection is critical. The nose cone requires thermal resistant materials in order to protect the structure, and the avionics bay requires additional protection to maintain a safe service temperature for the electrical components.

Therefore, two approaches must be taken. The outer surface of the shroud will experience temperatures around 1700°C, particularly near the nose. The allowable temperature is dependent upon Seville temperature of the structural material and that of the payload. The service temperature of the structure will vary greatly depending on the material that is chosen. The payload, however, must be maintained at a temperature below 250°C. For the avionics bay, temperatures must be maintained below 40°C.

There are a wide range of materials available for thermal protection ranging from black and white enamel paints, to ablatives and ceramic tiles. Paints tend to be the cheapest, add the least amount of weight and are the easiest to apply; however, they are not practical at temperatures near those experienced at the nose cone. Ablative materials are good thermal protection materials even at very high temperatures, and they are very easy to apply. On the other hand, they tend to be very expensive and often quite heavy. Ceramic tiles (like those used on the space shuttle) are by far the best insulating materials. Unfortunately, they are also the most expensive and require that the structure of the shroud be specifically designed for integration of the tiles.

3.2 Final Materials Selected

The following will discuss the materials that were selected for the payload shroud and give some of the reasoning behind those selections.

3.2.1 Structural Materials

An aluminum honeycomb core with a carbon composite sandwich was selected as the final structural materials. This material is available from the Hexcel Co., a world leader in honeycomb production. The aluminum core is type 5056-H3 and the carbon composite will consist of unidirectionally oriented graphite fibers at 35 % by volume within a polyimide matrix, PMR-15. The cells within the aluminum core will be filled with a polymeric foam so as to reduce vibration in the shroud, providing a better dynamic envelope for the payload.

This configuration was chosen over the others for three reasons. First, it is lighter in weight than the aluminum skin based configurations. Secondly, the honeycomb is much cheaper than all of the other configurations, with the exception of an aluminum skin with aluminum unreinforced stringers. And lastly, the honeycomb sandwich is more readily available and easier to make than the other composite configurations.

The aluminum 5056-H3 was chosen because it has superior compressive strength and lower density, when compared to the other aluminum materials that are available. A list of the properties of this material is found in Tabel 7.6. The dimensions for the honeycomb are a cell diameter of 0.64 cm, a gage of 0.0025 cm and a height of 0.00503 cm. This material is designated as 1/4 - 5056 - .001 in the Hexcel Co. brochures.

Property	5056 Hexagonal Aluminum Honeycomb
Compressive Strength (Mpa)	1.82
Compressive Modulus (GPa)	0.40
Crush Strength (MPa)	0.69
Shear Strength L Direction (MPa)	1.24
Shear Modulus L Direction (GPa)	0.22
Shear Strength W Direction (MPa)	0.69
Shear Strength W Direction (MPa)	0.11
Density (kg/m^3)	36.84

Table 7.4: Selected Properties of Hexagonal 5056 Aluminum Honeycomb

To determine the mass of this material we use the following equation:

$$W = (\ A_s \times t_m\ ) \times \rho$$
$$W = (\ 44.88 m^2 \times 0.0159 m\ ) \times 36.84\, kg/m^3$$
$$W = 26.25 kg$$

where tm = material thickness, A_S = shroud surface area, and r = material density.

The carbon composite consists of a reinforced polyimide matrix. The fibers are graphite fibers that will be oriented unidirectionally parallel to the axis of the shroud. Graphite fibers were chosen because of their low density, high strength and good availability. The matrix will be made of a polyimide thermoplastic, designated PMR-15 and produced by DuPont. This material was chosen because it has historically been used as a material for composite matrices in high temperature applications. Polyimides can withstand temperatures up to 500°C. Table 7.5 contains some of the properties for this material.

Property	PMR - 15
Density (kg/cm^3)	1320
Strain-to Failure Ratio	1.5
Fracture Toughness (m kg/m^2)	1163.31
Shear Strength at 316°C (MPa)	51.71
Flexural Strength at 31°C (MPa)	1103.2
Maximum Service Temperature (°C)	500°C

Table 7.5: Properties of PMR-15

The composite will be placed over the honeycomb in the form of laminates that are 0.014 cm thick. There will be 18 plies placed on each side of the honeycomb. The mass of the composite material can be determined from the following:

$$W = (A_s \times t_c \times N) \times \rho$$

$$W = \left(44.88 m^2 \times 0.0050 m \times 36\right) \times 1300 kg/m^3$$

$$W = 293.41 kg$$

where A_S = shroud surface area, t_C = composite thickness, N = no. of plies and r = material density.

3.2.2 Thermal Materials

The thermal protection system that is being used can be broken into two parts: nose cone area and avionics bay.

The protective material chosen for the nose cone is an ablative material called Haveflex T.A. - 117, produced by Ametek Co., Haveg Div. It will be layered on the shroud until a maximum thickness of 2.9 cm is achieved. Haveflex is a two component modified phenolic ablative coating and adhesive, that was originally developed for U.S. Navy ships for protection of missile launch systems from high temperatures (up to 2760°C). This material will adhere to almost all surfaces, including composites. The surfaces may need some sandblasting, however, no primer is needed. Haveflex can be applied with normal serrated trowels and will set within 24 - 36 hours at 20°C. The properties of Haveflex T.A. - 117 are listed in Table 7.6.

Property	**Haveflex T.A.-117**
Tensile Strength, (MPa)	4.31
Elongation, %	12.5
Density, (kg/m^3)	1288
Thermal Conductivity (Watts/m^2/°C/m of path)	569.7
Max. Service Temperature (°C)	2760

Table 7.6: Selected Properties of Haveflex T.A.-117

The weight of the ablative would be given by:

$$W = (A_n \times t_a) \times \rho$$

$$W = (15.20 m^2 \times 0.029 m) \times 1288 kg/m^3$$

$$W = 567.84 kg$$

Because of Haveflex's ease of application and good thermal properties it was chosen over other ablatives, such as Thermalag and Firex. Additionally, paints and ceramic tiles were not chosen because they were not practical for this application and were too costly respectively.

The remainder of the payload shroud will be protected by a white enamel paint. The lower portions of the shroud will not experience the same high temperatures that the nose cone will. Therefore, a material could be selected that did not have a very high service temperature, but was lightweight, inexpensive, and easy to apply. The white enamel paint was chosen because it displayed outstanding emmissivity, is very low weight and is very easy to apply to a surface such as the shroud. Calculations will not be used to determine the mass of the paint because it will have a negligent contribution.

The avionics bay must be maintained at a temperature of 40°C. The white enamel paint will provide much of this paint; however, further protection must be used to protect the sensitive electronics. For this purpose alumina insulating cylinders with refractory silica bonds will be used. This material is provided by Zircar Co. and is designated as AL 30 in its brochures. Alumina fibers offer some of the greatest hot strength and dimensional stability available in a rigid refractory fiber structure. Table 7.7 shows some of the important properties of AL 30.

Property	Alumina Al 30 Insulator
Weight Percent Al_2O_3,%	85
Weight Percent SiO_2	15
Density (kg/m^3)	480
Max. Service Temperature Continuous (°C)	1540
Max. Service Temperature Intermittent (°C)	1650
Linear Shrinkage at Max. Service Temperature, %	3.0

Table 7.7: Selected Properties of Alumina Insulating Board, AL 30

Another good feature of the AL 30 is its low thermal conductivity in comparison to other insulating alumina materials. This fact is particularly true at temperatures in excess of 1350°C. Figure 7.5 shows the relationship of thermal conductivity and temperature for several alumina insulating materials including AL 30.

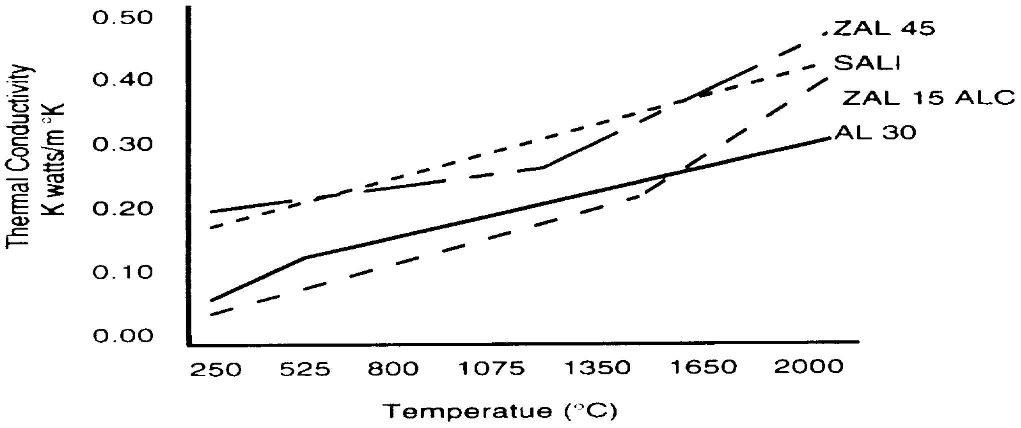

Figure 7.5: Comparison of Thermal Conductivity for Various Fibrous Ceramics Over a Varying Temperature

4.0 FREQUENCY RESPONSE OF BOOSTER STRUCTURE

The frequency response and mode shapes of the Athena Booster Rocket were necessary for modeling of the control systems. The modal analysis of the booster also serves as a delimiter for payload construction as coupling of payload and booster frequencies may be detrimental to the payload. This section describes the model used to simulate the frequency response and the results of the analysis.

Modal analysis was accomplished using a MSC/NASTRAN code that was developed to model the structure of the booster. Several assumptions and estimations about the booster were needed to complete the model. Length estimates and physical properties were modeled using data given about the configuration and reference material on component properties. The assumptions were carefully chosen to accurately depict the booster.

4.1 MODELING

Since a rocket is a complex system, numerous assumptions were made to simplify the actual system into an analytic model. The assumptions used in the NASTRAN model were based on the role of all components and the importance of each component to the structure of each section. The assumptions are as follows.

- Each stage can be modeled as a CBAR element. All members contributing to the bending or torsional stiffness of the section either are assumed to be incorporated in the moment of inertia calculations.
- All parts of the propulsion system offer negligible contributions to the structural integrity of the booster. The fuel tanks and rocket motors should not bear any of the structural loads.
- Large masses were considered to be either point or distributed mass. High density masses were modeled as point masses, and lower density masses were modeled as distributed masses.

The hull of the booster was modeled as CBAR elements due to the location of the load-bearing members. For the CBAR element, the moment of inertia, torsional constant, and element lengths were needed for the model. Only the skin and stringers were considered to contribute to the bending stiffness of the structure. The cross sectional geometry was modeled using UniGraphics II. Using the cross-section model, the moment of intertia was calculated using the solver provided in UniGraphics II. Since only closed section geometries like the skin offer resistance to twisting, the torsional constant was calculated by assuming the torsion to be suppressed only by the skin of the booster. The stringers offer little torsional resistance as the are open Z cross-section beams. The torsional constant for a circular cross-section with thickness t is given by

$$J = 2\pi r^3 t$$

The lengths of each section were set by the amount of fuel needed for each section. Given the amount of fuel needed and the density of the fuel, a length for each section was set. Table 7.8 list the length of each stage as set by the fuel volume as well as structural constants necessary for modal analysis.

Section	CBAR #'s	Length (m)	Moment of Inertia (mm^4)	Torsional Constant
Payload	1	4.572	9.6E+11	1.2E+11
3rd Stage	2,3	6.120	9.6E+11	1.2E+11
2nd Stage	4,5	7.360	1.1E+12	1.2E+11
1st Stage	6	11.050	1.4E+12	1.2E+11

Table 7.8: Model Data

The propulsion system was assumed to add little to the stiffness of the structure. The fuel tanks were considered to be thin-shelled pressure capsules that should not be subjected to the stresses inherent in the structural members as a structural load may cause the vessels to rupture. The tanks were therefore not used to calculated the moments of inertia or added to the hull structure for added stiffness. The rocket motors were also excluded from the moments of inertia calculations. Since the moments of inertia of the motors could not be found in text or by inspection, the mass was treated as a singularity at the end of each stage. Also, the engine mounts serve to isolate the motor from the structure thereby preventing structural loads on the engine. Thus, the motors do not add stiffness to the structure.

The fuel, fuel tanks, and motors were considered to be masses along the model. Point and distributed masses were distinguished by the density of the mass. The engines were considered to be point masses as they are dense mass concentrations. The payload was also modeled as a point mass for the same reason. These point masses were modeled using the concentrated mass (CONM2) card in NASTRAN. Although moments of inertia could have been added to the model in the CONM2 card to make the simulation more accurate, insufficient data prevented such an upgrade. The fuel and fuel tanks were modeled as non-structural mass along each section of the booster. The addition of the mass-per-unit-length field on the bar property (PBAR) card provided the necessary addition to add the fuel and fuel tanks in the NASTRAN file. A PBAR card was needed for every stage and interstage. Since the interstage areas do not house fuel tanks or mass that can affect the modes, these areas were modeled as bars without the added non-structural mass.

4.2 Results

Using the 103 solver for dynamic response, the results of the NASTRAN simulation produced the bending modes which are critical to the placement of the control system. The first bending modes was found at a frequency of .962 Hertz. However, the bending mode was not the first non-rigid body mode. Further review of the output file shown the first modes to be axial modes. Since this an unusual occurance, further analysis of the problem and iterations of the analysis with better models may produce better answers.

Analysis of the output data showed the maximum displacement to be at the tip of the payload for this mode as expected by inspection of the problem. As a result, the control sensor should be placed away from the tip to prevent sensor error due to a modal response. The low modal frequencies may present a problem as small, infrequently occuring disturbances may cause the system to destabilize.

Unfortunately, due to a software problem, a picture of the first mode could not be shown in this report.

5.0 ENGINE MOUNT DESIGN

When configurations for the booster were being debated, the engine mount for the LR-87-AJ-11 used for the first stage of the booster was found to conflict with the geometry set for the exterior hull. Upon further calculation, the diagonal distance for the motor mount was found to exceed the 2.7 meter diameter of the booster as seen in Figure 7.6. As a result, an engine mount was designed to match the LR-87 and the Athena configuration. This section outlines the design process and the finite element model and analysis used to test the new design.

The new design is similar to the previous design aside from the geometry of the mount and the sectional area of each member. The new design matches the hull configuration of the booster and the engine configuration. Since structural integretity at high temperatures was a deign concern, the mount was modeled using a titanium alloy. Titanium also helps reduce the overall mass of the booster due to its high strength-to-weight ratio.

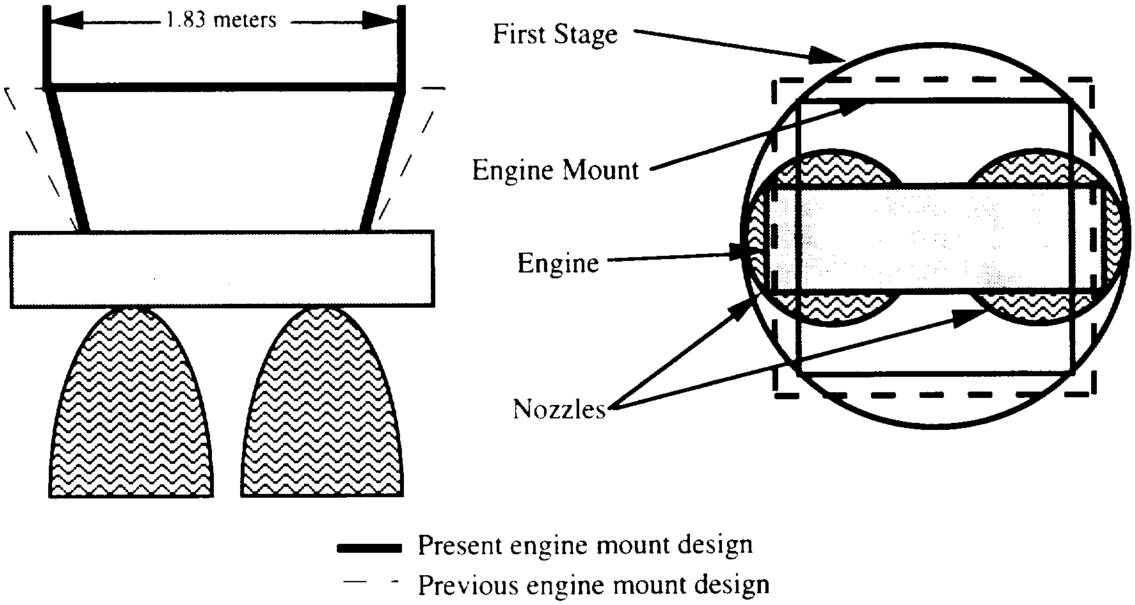

Figure 7.6: Problem Schematic

5.1 Material Selection

Material selection and total loading were set by the engine. The material selection was crucial to the design. The material had to be able to withstand high temperatures and have a low density to maximize payload. Aluminum 7075-T6, structural steel, and a titanium alloy were considered. The total load is dependent on the thrust provided by the engine. Since the rest of the booster can only react with a force equal to or less than the thrust, the maximum thrust was considered as the maximum loading of the engine mount.

An alpha-beta titanium alloy composed of titanium, 6% aluminum and 4% vanadium (Ti-6Al-4V) was selected as the engine mount material for thermal and mass reduction reasons as seen in Table 7.9. Since the LR-87 operates at high temperatures, aluminum may not be suited for the task as it tends to lose a substantial percentage of its strength at high temperatures. Steel was considered but not used due to its high density. The titanium alloy was selected due to its extensive use in present aerospace technologies and its welding capabilities. Unlike most other titanium alloys, Ti-6Al-4V is easily shaped and welded. Although the cost of titanium is high compared to steel and aluminum, the low weight and high strength at high temperatures of the titanium alloy make it ideal for the engine mounts.

Material	Elastic Modulus (Pa)	Density(kg/m^3)
Ti-6Al-4V	125E+06	4900
Aluminum	70E+06	2720
Steel	217E+06	7810

Table 7.9: Material Properties

5.2 Modeling

5.2.1 Physical Model

The total loading on the engine mounts were determined by the performance of the rocket. The LR-87 is capable of producing a maximum thrust of 2.4 million Newtons. The loading capacity of the new engine mount was set to match the overall maximum thrust from the engine multiplied by a factor of safety of 1.25 which set the maximum load at 3 million Newtons. This load was divided evenly between the two engine attachment points to set the equivalent nodal load equal to the maximum load.

The final design incorporates pipe cross-section beams with the sectional area varied according to the loads received by member of the engine mount. Both sectional areas are shown in Figure 7.7 . The horizontal members have the smaller cross-section of the two section types. The attachment struts have a much larger cross-section in comparison as to receive the direct force of the engine without encountering a material or buckling failure.

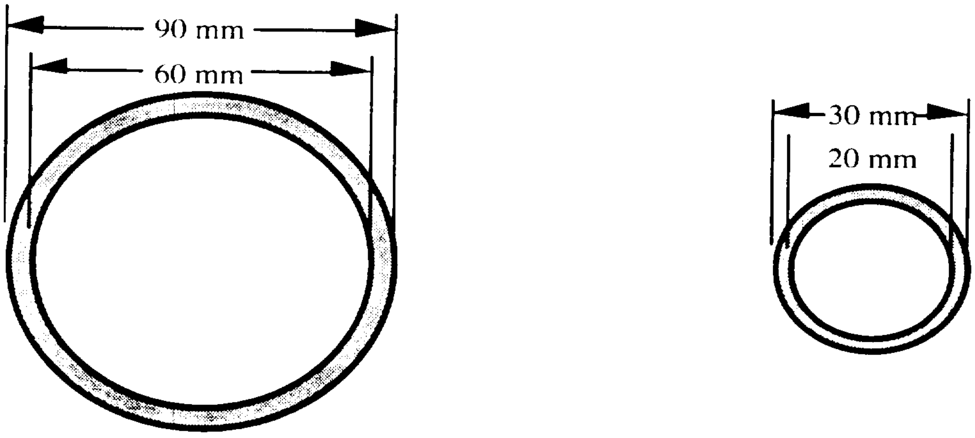

Attachment struts

Horizontal members

Figure 7.7: Sectional Areas of Engine Mount Members

5.2.2 Finite Element Model

With the material properties and loading set for the engine mount, a finite element model of the mount was created. The model consists of six beams configured to resemble the motor mount. The geometry as shown in Figure 7.8 was taken from scale drawing estimations and dimensions given in the Titan III Hankbook. Each beam is composed of ten beam elements of equal length.

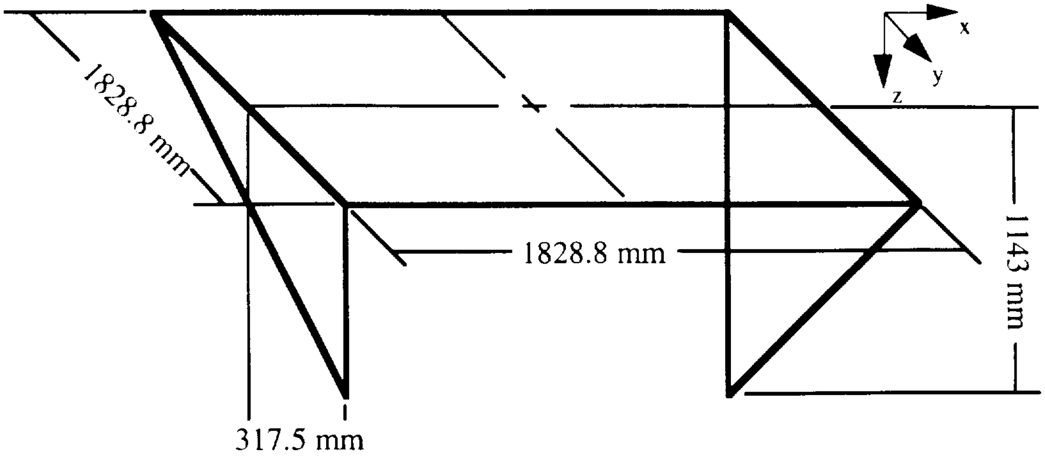

Figure 7.8: Engine Mount Configuration

SDRC I-DEAS was used to produce a model given the geometry of the engine and the booster shown in Figure 7.9. The model is basically a simple truss structure designed to hold the engine in place with respect to the booster. The ends of the attachment struts were restrained in displacement in all directions but were allowed to rotate freely in all directions. The material properties were set to match the Ti-6Al-4V alloy.

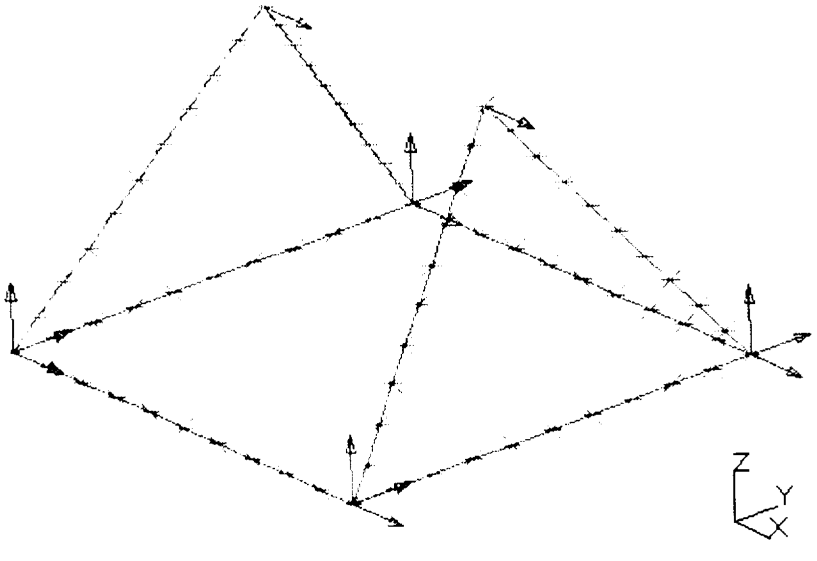

Figure 7.9: Finite Element Model of Engine Mount

5.2.3 Testing

Tests were conducted on the finite element model to determine if the finite element model met the required design specifications. Failure possibilities and static displacements constraints were set, and the testing of the finite element model progressed in two stages.

1) The buckling load for the engine mount was established to ensure the engine mount could withstand the thrust of the engines without experiencing a structural failure.

2) The design was tested using a linear-static solver and the maximum thrust case to provide the maximum displacement.

The design parameters were set to allow only slight deviations. No structural failures were permitted. The minimum buckling load was set at 4 million Newtons to ensure a structural sound engine mount. The static displacement was also set to a high degree of accuracy. If the buckling load was less than 4 million Newtons or the maximum displacement of the linear-static solution exceeded 1% of the overall height of the engine mount, the process was repeated using a new model of the same geometry but different sectional areas.

A -1.0 Newton force was applied to the point where the engines are attached in the z-direction. The engine was modeled by restraining the engine attachment point as to simulate a rigid member between the two points. The model showed that the horizontal members that space the attachments struts were in tension while the attachment struts were in tension. The beam sections were changed until a configuration that could withstand the loading without buckling was established. The buckling load of the model is calculated by multiplying the load by the buckling load factor.

As seen in Figure 7.10 the mount design buckles for a load of 2.17 million Newtons applied at the engine attachment points. Since this load is much higher than the maximum engine thrust, the engine mount will not buckle under working conditions.

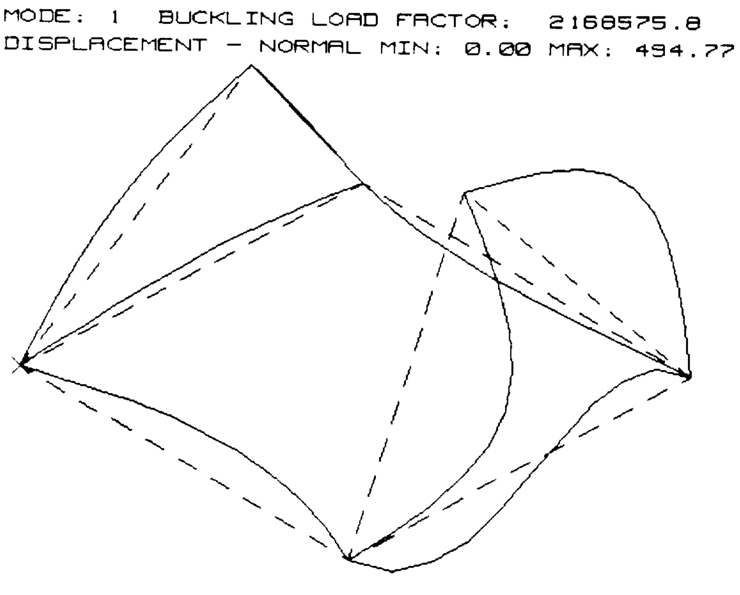
MODE: 1 BUCKLING LOAD FACTOR: 2168575.8
DISPLACEMENT - NORMAL MIN: 0.00 MAX: 494.77

Figure 7.10: Linear-Static Displacement of Engine Mount Model

The next part of the analysis used the linear-static solver in I-DEAS to find the displacements of the engine at the maximum thrust. A large displacement is not desirable for this design as it affects the overall thrust angle for the booster. The linear-static solution gave a maximum displacement for the engine mount of 4.36 millimeters at a load of 1.5

million Newtons as seen in Figure 7.11. This displacement is acceptable as it is less than 1% of the length of any member of the engine mount. The effects of the displacement are negligible.

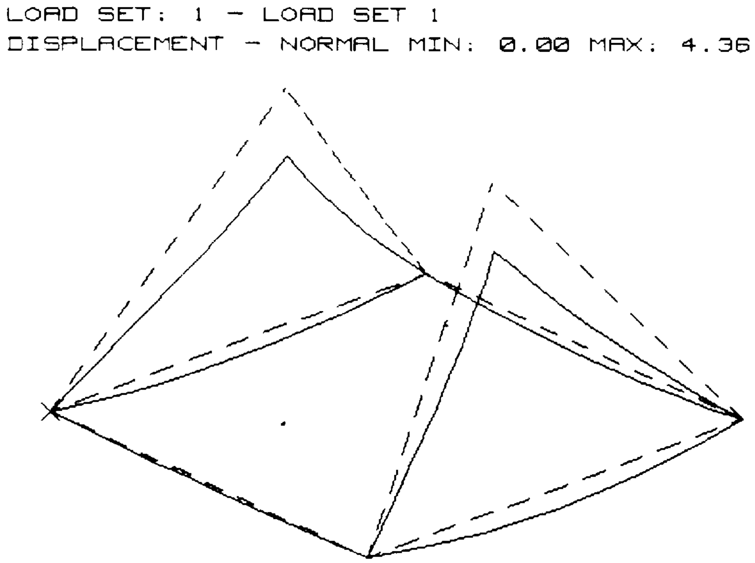

Figure 7.11 Linear Static Displacement of Engine Mount

5.2.4 Conclusion

The engine mount design is capable of withstanding maximum thrust from the motor without experiencing a structural failure. Using the Ti-6Al-4V titanium alloy allows the mount to be used at high temperatures as well as reducing the mass of the booster. This design will serve as the new design for the first stage engine mount and meets the design specifications for the Athena Booster.

6.0 BOOSTER TRANSPORT STRUCTURE (BTS)

A structure was needed to help stabilize the booster while in transport, in the carrier aircraft, and during the egress from the aircraft. Since takeoff weight was restricted by the performance characteristics of the C-5B and safety concerns, the mass of the "sled" design was set below 10,000 kilograms. This section outlines the design process and the modeling used to finalize the design for the transport structure.

The BTS is basically a truss system designed to encompass the Athena Booster. Special consideration was given to offer support without restricting the separation of the truss. The truss reaches the midline of the booster and runs along the sides for the length of the hull excluding the nose cone and the aft engine skirt as seen in Figure 7.12.

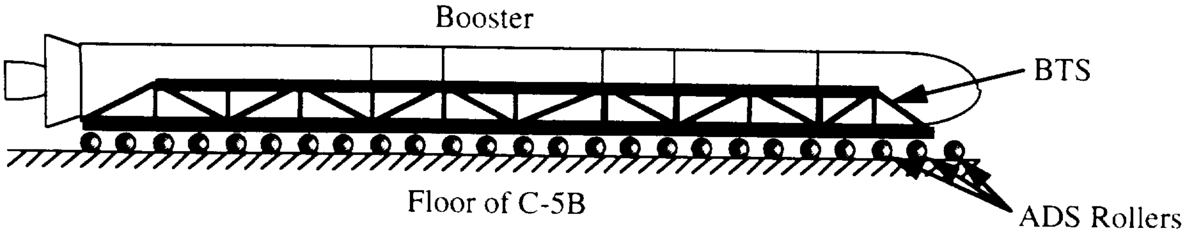

Figure 7.12: Schematic of BTS

The weight of the booster is supported by three points of contact at each interstage ring and motor attach point and at five points of contact at the third and first stage interface as seen in Figure 7.13. This helps to distribute the weight along the three main floor beams of the sled which serve as the runners of the "sled." The floor beams are placed on the Air Deployment System (ADS) rails mounted to the floor of the C-5B. A finite element model was created to test the structure.

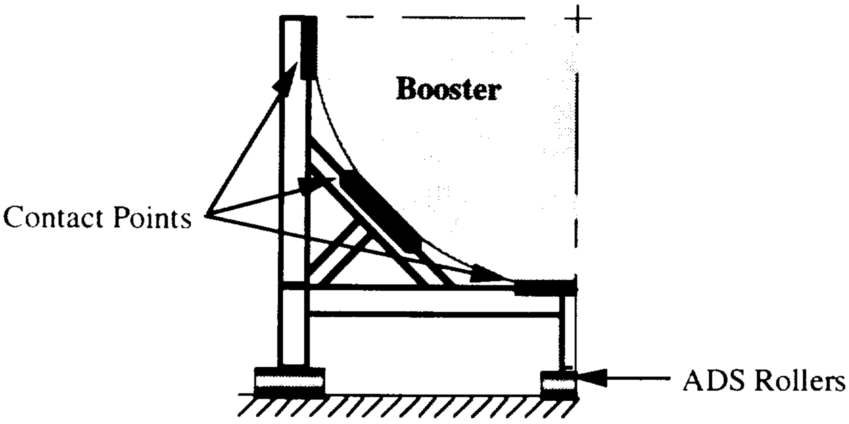

Figure 7.13: BTS Cross Section with Contact Points

6.1 Modeling of Cradle

Several iterations were required to complete the design of the cradle. Aside from the analysis of the final configuration which required several iterations, numerous design iterations helped select the final design.

Initially, the design consisted of two large box beam along the hull length with smaller box beams spanning the distance between the two main beams. A curved plate that matched the curvature of the skin was suggested for supporting the weight of the booster. This design was too heavy and was replaced with curved bracket to support each compression ring. After further review of this design, the supports were still too heavy to match the mass restriction of 10,000 kg for the BTS. At this point a redesign was suggested, and a truss structure was designed to support the Athena. Although the truss system was not as stiff as the previous design in bending, the considerable weight saving made the truss structure acceptable for the design.

Although several different beam sections would have optimized the design by reducing weight, the model was simplified to use only two beam sections as shown in Figure 7.14. The larger of the two sections was used in designing the three beams to serve as the runners of the BTS as well as the two beams which run along the midline of the Athena. These beams run the length of the structure excluding the nose cone and first stage engine skirt. These sections were specifically designed to provide bending stiffness to the overall structure. The smaller sections were used as webbing between the five beams that run the length of the booster. This section was also used as bracing to support against a torsional load if any were applied.

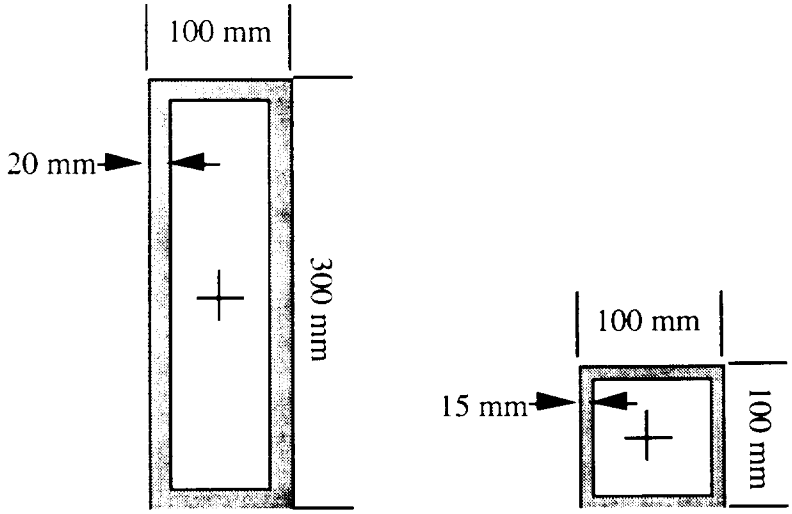

Figure 7.14: BTS Beam Cross Sections

Points of contact were determined by examining the booster. The Athena is designed to have compression rings at each stage and interstage interface. Since these points along the booster will be reinforced, all points of contact were placed at the interfaces to prevent damaging the booster as seen in Figure 7.15.

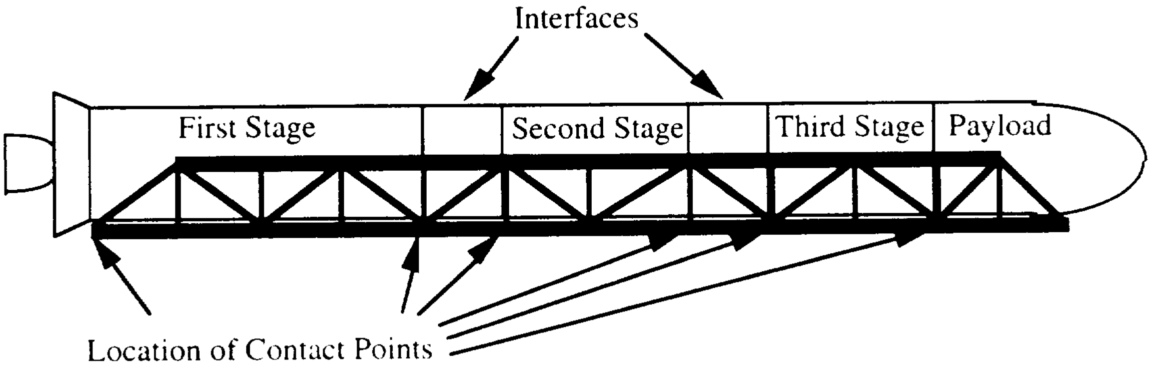

Figure 7.15: Placement of Contact Points

Once the configuration had been set, a finite element model was constructed using SDRC I-DEAS. The booster was assumed to be rigid and was modeled using the rigid bar elements in I-DEAS. The complete node and element set are shown in Figure 7.16.

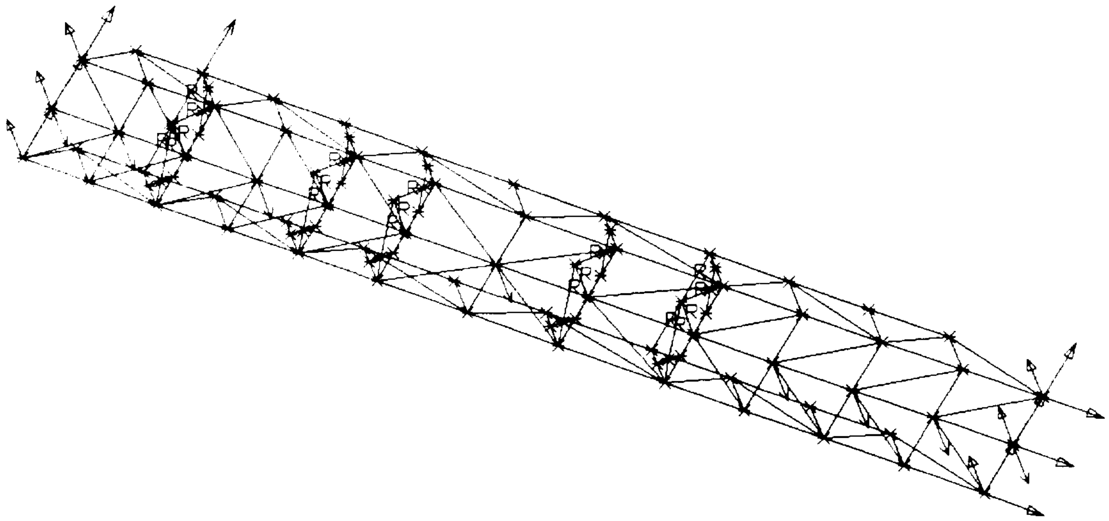

Figure 7.16: Finite Element Model

The loading was established to be greatest when the booster had egressed to the end of the cradle since the moments created by the gravitational and applied load are the greatest at this point. A worst-case gravity load was set at 2g's and a safety factor of 1.1 set. The safety factor was reduced for the sled to help keep the weight down without seriously affecting the structural integrity of the truss. The parachute was not modeled as a load as it offers little or no lateral loading and a negligible longitudinal load at the point of worst case loading. The finite element load set was modeled as a distributed load equivalent to the weight of the fuel for each stage and the weight of the engine for each interstage. The load was then adjusted using the worst-case load and the safety factor.

The boundary condition was set to resemble the classical beam problem. One end was only allowed to rotate while the other end was free to rotate as well as translate in the longitudinal direction. These conditions simulate the pull of the parachutes during egress and the forces applied by gravity and any pilot corrections. A model where both ends are constrained for all displacements does not accurately simulate the problem as it creates a tensile force in the bottom members which adds stiffness.

6.2 Testing Procedure

Most of the testing was concentrated on finding a usable design that met the design specifications. The testing for the BTS resembles the procedure used to design the engine mount. Testing was divided into two distinct procedures.

1) Beam sections were modeled in I-DEAS.

2) A linear static deflection was calculated using the solver provided in I-DEAS.

Since large displacements relative to the booster diameter should be avoided, a criterion was set for the deflection of the BTS. If the maximum displacement exceeded 5% of the diameter of the booster, the testing process was repeated. Several iterations were performed to find a suitable configuration with a mass lower than 10,000 kg.

6.3 Results

After the design had been set, dimensions of the beam sections and mass calculations were performed. The final configuration for the BTS was 7300 kg total mass. This number is acceptable as the BTS was originally allotted 10,000 kg. Table 7.10 shows the final mass data.

Cross Section	Area	Total Length	Total Mass
100x100x15	5100 mm^3	185.64 m	2600 kg
300x100x20	14400 mm^3	119.42 m	4700 kg
		Σ mass=	7300 kg

Table 7.10: BTS Specifications

The static displacement was found to be acceptable for the 2g loading. The maximum displacement of the BTS was calculated to be .109 meters. This value is acceptable as it is only 4.04% of the diameter of the booster. A greater value may jeopardize the structural integrity of the booster by excessive loading on the booster structure. The I-DEAS drawing of the deformed BTS is shown in Figure 7.17.

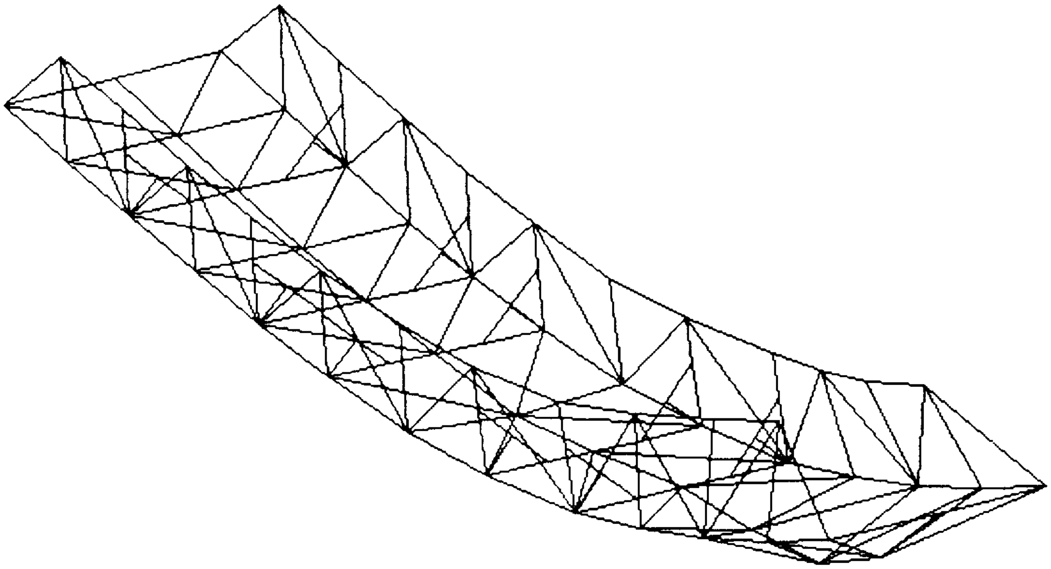

Figure 7.17: Deformed BTS for 2g Loading

6.4 Conclusion

As this section has detailed, the present design for the BTS meets the maximum displacement and mass restrictions necessary for the Athena Booster design. Although more time is necessary to optimize the BTS, the present design is both usable and practical for the purpose of an air-launched vehicle.

Chapter 8

Power / Thermal / Control

PRECEDING PAGE BLANK NOT FILMED

Power / Thermal / Control Symbols

α: angle of attack
C_g: center of gravity
C_p: center of pressure
D(s): Laplace Transform Denominator
D: drag
δ: gibal angle
d_p: distance between C_p and C_g
d_T: distance between gimbal and C_g
γ: ratio of specific heats
I: current (amperes)
I_{yy}: Moment of intertia about the y-axis at C_g
L: lift
M: local Mach number
M_T: moment about center of gravity due to thrust
N(s): Laplace Transform Numerator
θ: pitch angle
q_α: lift gradient
R: resistance (ohms)
s: Laplace Transform variable
T: stagnation temperature
T: thrust of gimbal engine
t: atmospheric temperature
Ω: Ohms

1.0 GROUP OVERVIEW

This is the Power/Thermal/Controls section of the Athena Project report. This section deals with five topics:

- Booster Egress
- Power Source
- Attitude Control Systems
- Thermal Analysis and Shielding
- Nose Cone Analysis

2.0 SELECTION OF DEPLOYMENT SYSTEM

Pulling the booster out of the C-5 nose first on 3 G-11c 30.5 meter diameter cargo chutes was the selected deployment system for Athena.

PRECEDING PAGE BLANK NOT FILMED

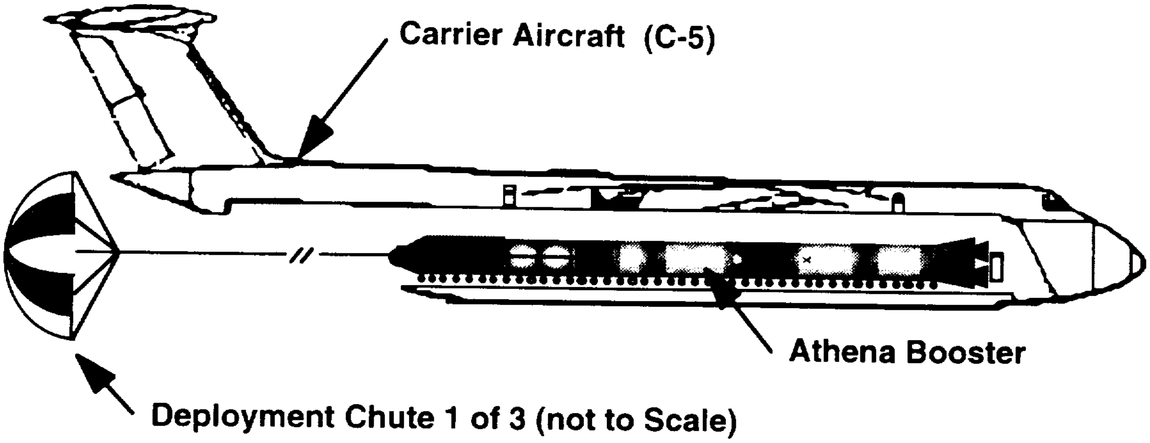

Figure 8.1: Booster Egress

2.1 Criteria For Selection

1. The deployment system should extract the booster and have it ready to launch at a distance of 800 meters from the carrier aircraft, with a minimal loss of altitude and a minimal downward velocity.
2. The deployment system should require limited modifications to the carrier aircraft.
3. The deployment system should not be too expensive.
4. The deployment system should not create a risk to the carrier aircraft and crew.
5. The deployment system should not put excessive strain on the pilot.
6. The deployment system should work on proven technologies, and use "off the shelf" equipment as much as possible.

2.2 Answers to Criteria

1. The parachute system selected safely extracts the booster in 1.7 seconds, and has the booster ready for ignition 808 meters from the carrier aircraft in 7.2 seconds. At this time the booster has a downward velocity of 36.8 m/s and it has dropped a total of 116 meters.
2. The parachute deployment system only requires adding a deployment routine to the C-5 auto pilot.
3. The parachutes are made of cheap materials, with a cost of only $3,500 each and a total cost of $10,500
4. The only risk to aircraft and crew would be if there were multiple chute failures early in extraction. The use of three extraction chutes eliminates this risk.
5. The auto pilot on the C-5 could be programmed to handle the deployment of the booster, so pilot strain would be minimal.

6. Parachutes have been used to air drop equipment for years, and the chutes have been used in clusters of up to 12, so the parachute deployment system is definitely a proven technology.

2.3 Alternatives to Parachutes

1. Lift booster off top with wing or lifting surface.
2. Push booster out of cargo bay with spring, or spinning tire.

2.4 Reasons for Rejection

1. In order to lift the booster off the top you would need a very large wing. The booster weighs about half of the weight of the C-5 so the wing would have to have a wing with about half of the surface area of the C-5's wing. Such a large added wing would cause tremendous drag on the carrier aircraft. This deployment system would be very expensive, and would have a good probability of colliding with the carrier aircraft. A collision would most likely result in a loss of the booster, carrier aircraft, and possibly the aircraft crew.

2. Pushing the booster out of the cargo bay with a spring or spinning tire, would require significant modifications to the cargo bay. This deployment system would impart momentum to the aircraft necessary to extract the booster. The added momentum would cause a sudden acceleration to the aircraft which would be a nuisance to the pilot and crew.

2.5 Analysis of Extraction System

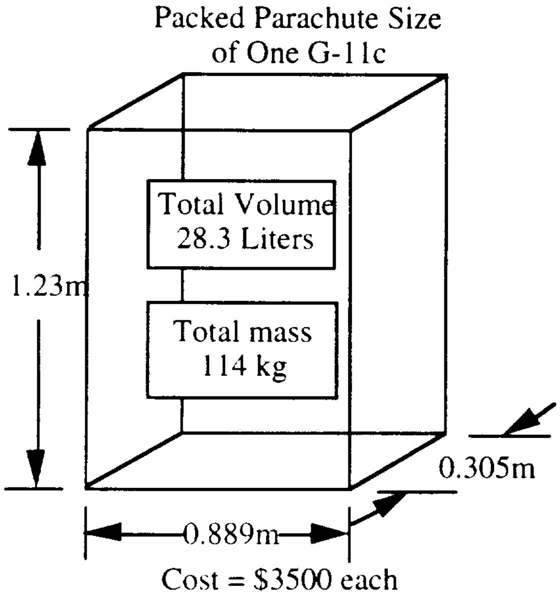

Figure 8.2: Extraction Chute Packaging

Deployed -- these chutes have a 30.5 meter diameter each

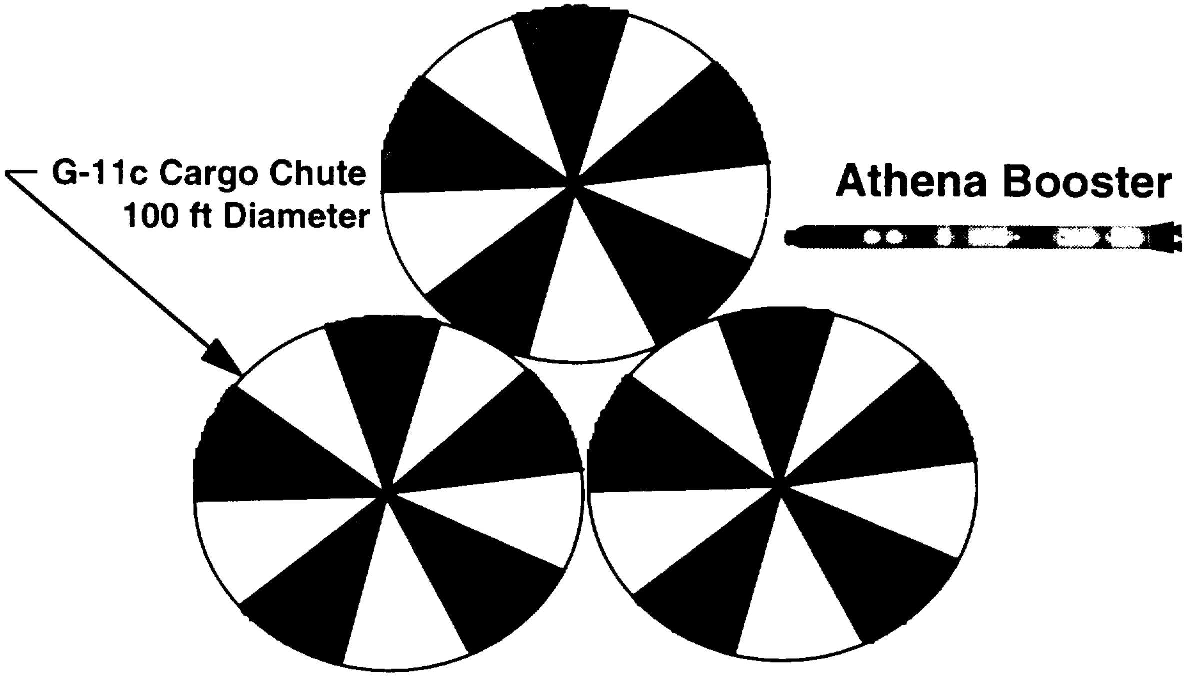
G-11c Cargo Chute
100 ft Diameter
Athena Booster

Figure 8.3: Chute size comparison with Athena

These chutes produce the following G-Forces on the Booster during extraction and descent.

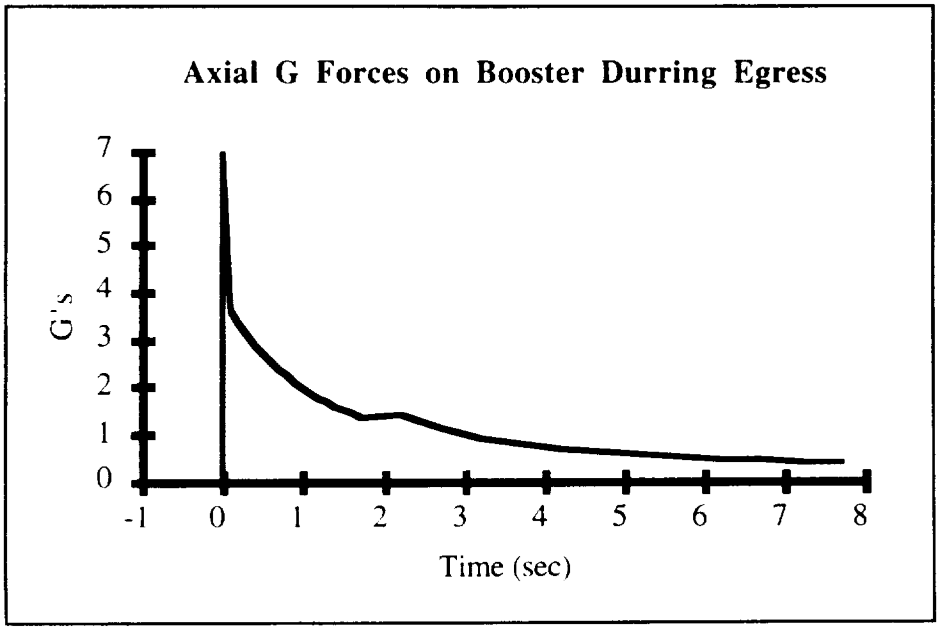

Figure 8.4: Axial g-forces during extraction

This graph was based on the following parameters

Deployment speed	70 m/s (5% above fully loaded stall speed at altitude)
Deployment altitude	11,000 m
Deployment chutes	3 G-11c 30.5 meter diameter solid conical

The initial spike in this graph is caused by the chutes opening. This opening force is very short term ≈ 1/10 of a second.

Once the booster has rolled out of the cargo bay of the C-5 the booster transporter is separated by detonating the explosive bolts used to fix it to the booster. After a 5.5 second descent the booster is 808 meters from the C-5, which is the fireball radius calculated by the Propulsion group. At this time the descent chutes are separated by detonating their explosive bolts and first stage ignition is started. The booster then free falls for 1.5 seconds as the first stage engines build up to full thrust. This time allows the parachutes to clear the booster, and at this point the booster is 1058 meters from the C-5, has fallen 178 meters from its initial altitude, has attained a pitch angle of 66.8° from horizontal and is rotating at 4.6 °/s angular velocity.

The attitude control system can change the boosters attitude from 66.8° with a 4.6°/s angular velocity to 67° with zero angular velocity in ≈ 2 seconds. The next graph shows the timeline of booster deployment and corresponding pitch angles.

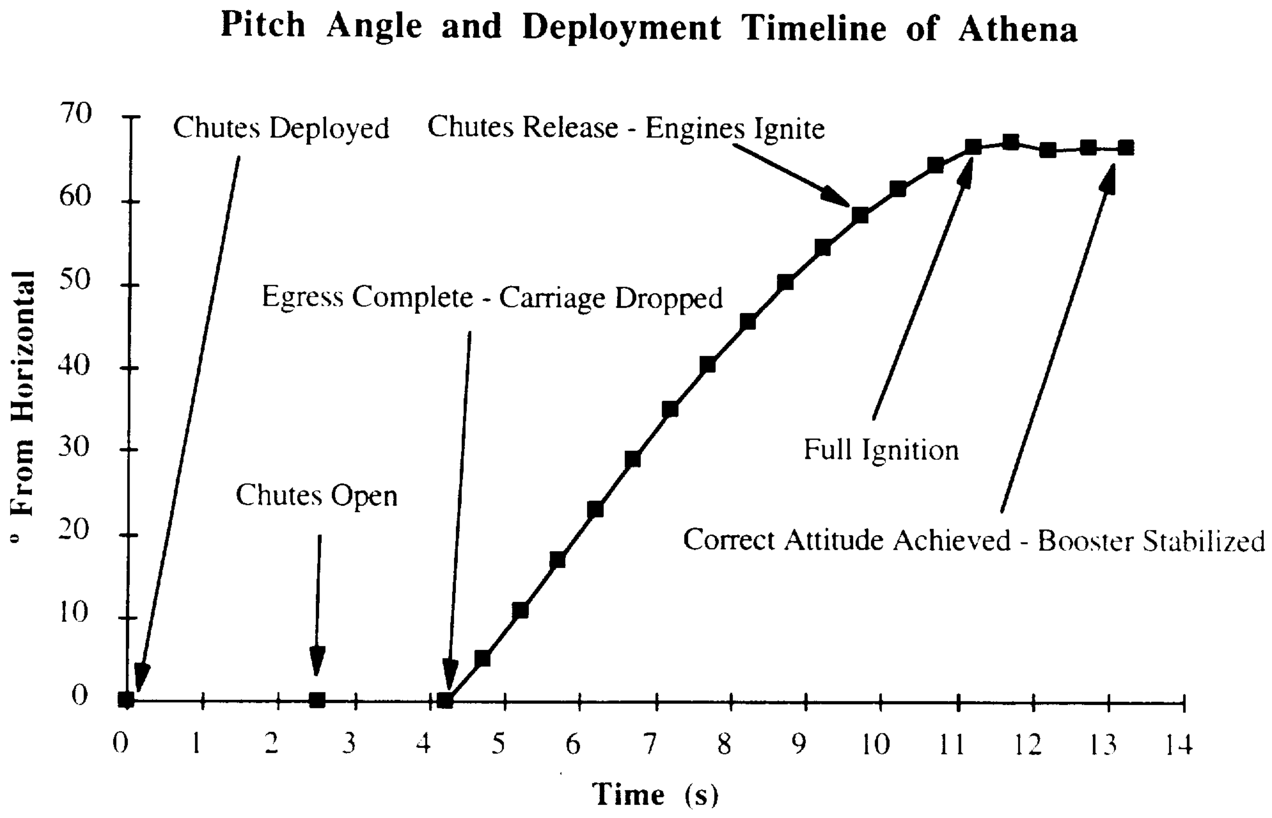

Figure 8.5: Pitch angle during extraction

3.0 SELECTION OF POWER SYSTEM

In order to size Athena's power system the power that needed to be supplied was first determined, and the following table lists the requirements.

Table 8.1: Power Requirements

System	Power	Time Length	Energy	
Engine Starts	560 Watt total	2 seconds	0.3	Watt/hrs
Reaction Thrusters	420 Watt	300 sec	35	Watt/hrs
Payload	140 Watt	6 hour mission	840	Watt/hrs
Computer	1 Watt	6 hour mission	6	Watt/hrs
Gps Receiver	2 Watt	6 hour mission	12	Watt/hrs
Communications	3 Watt	6 hour mission	18	Watt/hrs
IMU	26.2 Watt	6 hour mission	157	Watt/hrs
Cable Power Loss	9.6 Watt	6 hour mission	57.6	Watt/hrs
Total	1160 Watt		1130	Watt/hrs

Lithium Thionyl Chloride Cells were chosen for Athena's power system because of their relative high energy density and low cost. Each cell has an open circuit voltage of 3.63 volts and a total energy of 1798 Watt/hrs each. Eight of these cells connected in series would have an open circuit voltage of 29.04 volts and a total energy of 14.38 kW/hrs. This is enough energy for a full 6 hour GTO Mission plus 12 hours of wait time. This extra time would be needed if the mission were aborted after switching to internal power, and to allow for a factor of safety in case any other equipment requiring power would need to be added to the booster such as extra sensing equipment, (strain gages, cameras, etc.), or for a payload requiring extra power. The mass of the batteries and casings would be ≈ 32 kg.

The wiring selected for Athena was 14 gage copper wire. This wire can carry a maximum of 15 amps, while the maximum current needed by Athena is 5 amps. The resistance of 45 meters of 14 gage copper wire is 0.384 W and the resulting power loss would be $IR^2 = 0.385 \times 5^2 = 9.6$ Watts. The weight of 45 meters of 14 gage copper wire is ≈ 5 kg.

The total mass of the batteries, casings, and wiring would be ≈ 37 kg.

The total cost of a space rated system described above would be ≈ $800.

4.0 CONTROL AND STABILITY

4.1 Introduction

This section focuses on the control and stability of the longitudinal dynamics of the booster. Since the booster is multistage, a controller is necessary for each stage. The actuators for control system in each stage are listed as follows:

STAGE I	Gimbal Engines
STAGE II	Gimbal Engines
STAGE III	Reaction Control Systems (RCS)

Later, we will look at the control and stability of Stage I and Stage III. Real time simulation is run on MATLAB/SIMULINK to give all time response and phase plots of teh systems. Stage II is not included since the control maneuvers for Stage II and Stage I are basically the same.

Also, the roll control is beyond the scope of this report because of its typical design. The performance of corresponding systems are discussed in the following sections.

4.2 Longitudinal Dynamics And Stability

This section develops the longitudinal dynamics of Stage I and Stage III. Also, it includes the Laplace' Transform of the dynamic equations for simulation.

4.3 Longitudinal Dynamics Of Stage I

As described in previous sections, Stage I corresponds to low-altittude flight within the atmosphere. So the aerodynamic effect on the booster must be taken into account in studying the dynamics of the system. Due to the fact that the center of pressure (2% behind booster center) is always in front of the center of gravity, lift acting at the center of pressure creates a positive moment on the booster and tends to tilt up its nose. As the angle of attack or the pitch angle increases, lift increases. Hence, the nose is tilted up even more by the positive moment acting at the center of pressure. Thus pitch angle diverges. In other words, any disturbances in pitch angle will lead to instability in the longitudinal dynamics of the booster. Therefore, we need a controller to stabilize it. However, there are no control surfaces such as horizontal stabilizers and elevators in our design. The reason is that the moment of inertia of the booster is very large as compared to the unstable aerodynamic effect. Hence, we are able to control the longitudinal dynamics without using any control surfaces which tend to make the structure of the booster more complex. After a thorough investigation, we decided to use gimbaled engines for the control of the first stage.

Under the certain loading, the booster will deform slightly. The controller will also consider the first few bending modes as well as the mode shapes of the booster. So we can always avoid vibration at the natural flexible mode frequencies which can lead to serious damage in case of resonance.

Basically, the dynamics of Stage I can be modeled in the following equations,

Rigid Body Modes,

$$I_{yy}\ddot{\theta} + q_\alpha d_p \theta = M_T = T d_T \sin\delta - L d_p \cos\alpha + D d_p \sin\alpha$$

where

C_g......Center of Gravity

C_p......Center of Pressure

I_{yy}......Moment of Inertia about the y - axis at C_g

q_α......Lift Gradient $\equiv \partial L / \partial \alpha$

θ.......Pitch Angle

T.......Thrust of Gimbal Engine
d_T......Distance between Gimbal and C_g
d_P......Distance between C_p and C_g
L.......Lift
D......Drag
δ.......Gimbal Angle
α......Angle of Attack

Applying the theory of small perturbation

$$I_{yy}\ddot{\theta} + q_\alpha\theta = M_T = Td_T\delta$$

Taking the Laplace' Transform,

$$\frac{\delta(s)}{\alpha(s)} = \frac{Td_T}{I_{yy}s^2 - q_\alpha d_P}$$

Now consider the transfer function with other bending modes,

$$\frac{\delta(s)}{\theta(s)} = \frac{Td_T}{I_{yy}s^2 - q_\alpha d_P} + \sum_{i=1}^{\infty} \frac{\gamma_i\beta_i}{s^2 + 2\zeta_i\omega_i s + \omega_i^2}$$

The initial conditions (t=0, main engine fires) for the system is:

$$\theta(o) = 66.47501^\circ$$

$$\dot{\theta}(o) = 4.58904^\circ/s$$

4.4 Longitudinal Dynamics of Stage III:

Apart from Stage I, Stage III corresponds to high altitude trajectory where aerodynamic effect can be neglected. In this case, the dynamics is not as complicated as that in Stage I. Since lift is assumed to be zero, the unstable term in the dynamics equation is removed. However, the system still requires a controller for disturbance-rejection. The Reaction Control System(RCS) is chosen for this purpose.

The rigid body mode dynamics of the system is similar to that in Stage I,

$$I_{yy}\ddot{\theta} = M_T = T_t d_t$$

where all symbols carry the same meaning as those of Stage I except that T_t represents the thrust of the RCS thruster.

Transfer function including other bending modes,

$$\frac{N(s)}{D(s)} = \frac{T_t d_t}{I_{yy}s^2} + \sum_{i=1}^{\infty} \frac{\gamma_i\beta_i}{s^2 + 2\zeta_i\omega_i s + \omega_i^2}$$

4.5 Design Configuration And Performance of System

Since all constraints such as masses, thrust and modes are set by other groups, the controller has to be designed so as to optimize the performance of the systems. The design features and performance of systems are described as follows.

4.6 Design For Stage I

Stage I is an error-rejecting feedback controller with the following configuration.

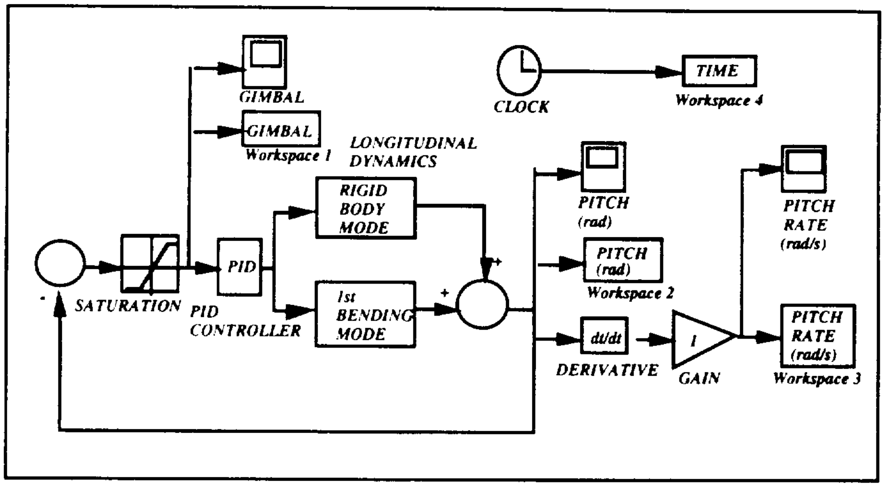
GIMBAL
GIMBAL
Workspace 1
CLOCK
TIME
Workspace 4
LONGITUDINAL
DYNAMICS
RIGID BODY MODE
PITCH (rad)
PITCH RATE (rad/s)
PID
PITCH (rad)
Workspace 2
-
SATURATION
PID CONTROLLER
1st BENDING MODE
+
+
du/dt
DERIVATIVE
1
GAIN
PITCH RATE (rad/s)
Workspace 3

Figure 8.6: System Configuration for Stage I using Gimbaled Engines

Gimbaled Engine:

The two gimbaled engines used in Stage I are LR-87 installed with gimbal mechanism with a maximum gimbal angle is of 6°. Using any gimbaled engine with larger gimbal saturation limits will improve the performance by reducing the decaying time of error. However, increasing in gimbal saturation limit means to increasing in complexity of the whole gimbal mechanism and hence increases the weight of the propulsion system. Moreover, the torque required for gimbaling can be very large and has a very large power requirement.

Proportional Integral Differential (PID) controller:

From root locus plots, both P and PI controllers cannot give BIBO stability. The proposed PID controller for Stage I has a combination of [1 0 1]. Increasing the type number of the controller may speed up the error-rejecting time. However, it may also drive the system into instability. The optimal type number of the system is 2.

Sensor Locations:

Pitch sensors which measure the pitch angle of the whole booster must always line up with the relative wind direction of the booster. Due to the natural flex modes of the structure, the center line of the booster does not usually line up with the its principal axis. Hence, we need to decide where to put our pitch sensors. Though the controller is able to avoid the first few natural bending modes, it is secure to locate more than one sensors at antinodes of each corresponding mode. Pitch sensors work with a frequency detector of the same sensitivity. When the bending frequency of the booster falls within a particular range, the pitch sensor located at the corresponding antinode is activated. This requires another controller with simple logic which is beyond the scope of the report. From the bending modes of the booster, the locations of antinodes and sensors as well as the corresponding frequency range are summarized in the following table.

Sensor	Antinode (m) from tip	Frequency Range (Hz)
1	15.16	0.4170944
2	7.65	0.7345331
3	15.10	0.9620926

Table 8.2: Pitch Sensor Locations for Stage I

4.7 Performance of Stage I

From the steady state error plot in **Appendix G.3**, the system has a zero steady state error. The controller is able to die down the initial condition down to zero within 5 seconds. Also, the phase plot shows that the final conditions always converge to zero. In other words, the system always remains stable. The main difficulty for designing the controller is that the gimbal saturation limits tend to drive the problem non-linear. However, it works linearly when error is comparatively small.

4.8 Control of Stage III

The main difference in control system of Stage III from Stage I is that Stage III does not use gimbaled engines. Instead, RCS thrusters are used as a 'ping ping' control maneuver. Stage III is a disturbance-rejecting controller with the following configuration.

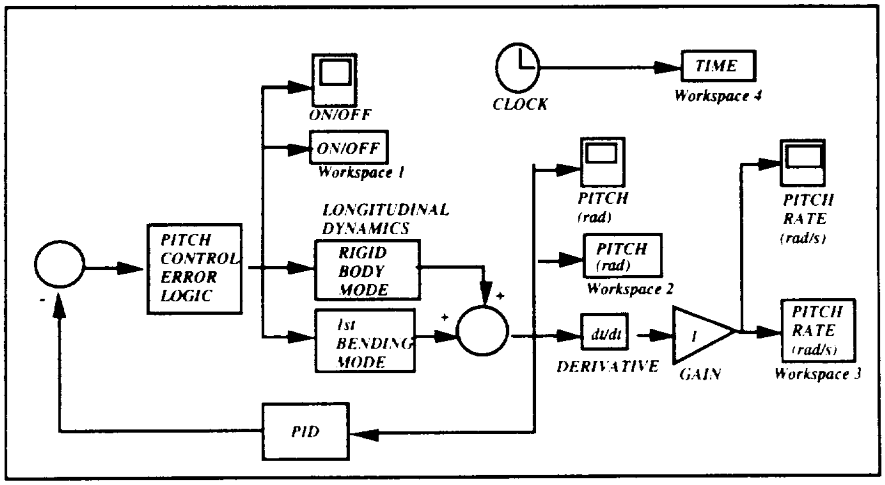
ON/OFF
ON/OFF
Workspace 1
CLOCK
TIME
Workspace 4
LONGITUDINAL DYNAMICS
PITCH CONTROL ERROR LOGIC
RIGID BODY MODE
1st BENDING MODE
+
+
-
PITCH (rad)
PITCH (rad)
Workspace 2
du/dt
DERIVATIVE
1
GAIN
PITCH RATE (rad/s)
PITCH RATE (rad/s)
Workspace 3
PID

Figure 8.7: System configuration for Stage III using RCS

RCS Thruster:

The model for RCS thruster is MR-104. It is chosen among other candidates such as MR-107K since it has a much larger thrust with similar power requirements. The following are some important specifications of MR-104 thruster. Eight thrusters are required for the RCS of Stage III. Four of them are used for pitch control while the rest are used for roll control.

Properties	Specifications (English units)	Specifications (SI units)
Thrust (steady)	147-78 (lbf)	653.89-346.96 (N)
Feed pressure	445-220 (psia)	30.692-15.173 (10E+5 Pa)
Chamber pressure	280-149 (psia)	19.311-10.277 (10E+5 Pa)
Expansion ratio	50:1	
Flow rate	0.639-0.341 (lbm/s)	0.291-0.155 (kg)
Valve power	58W @ 28 VDC & 70F	
Weight	4.18 (lbm)	1.90 (kg)

Table 8.3: Summary of MR-104 Thruster Characteristics

Pitch Error Correction Logic:

The thruster logic is based on the pitch error correction. Whenever the system has a pitch angle error greater than 2.5°, the controller will signal a thruster pair to turn on which generates a negative moment on the system. Hence, the error is retarded. Once the pitch angle error is less than 2.5°, the controller will shut down the thruster pair. However, the system may continue to rotate beyond the equilibrium orientation and cause another pitch angle error of 2.5°. In this case, the controller will turn on an opposite pair of thrusters so as to retard the error.

PID controller:

Similar to Stage I, a PID controller with a combination of [1 3 20]. A non-zero integral PID is used because the thrust generated by the RCS thrusters are very small as compared to the moment of inertial of Stage III. This may give a very large steady state error. Hence, the steady state error has to be reduced by using integral type controller. Also, a much larger differential factor is used so as to reduce the decaying time of the disturbance. However, the steady state error never goes to zero in finite time interval because the 'ping ping' maneuver always keeps the system oscillating about the equilibrium condition..

Sensor Locations:

Similar to Stage I, pitch sensors have to be located at antinodes. Also, they are activated by another controller with a frequency detector. Basically, a pitch sensor at a particular antinode will be activated when Stage III is vibrating within a certain frequency range of that corresponding antinode.

4.9 Performance of Stage III

From the plots shown in **Appendix G.3**, it takes about 80 sec for a disturbance which makes a pitch error of 20° and a pitch rate of 5° per second. The time response has already been speeded up by using a PID controller of [1 3 20]. Actually, as compared to the burn time of Stage III (280 seconds), it is reasonably to have a decay time of 80 seconds for such a huge disturbance. Also, the phase plot shows the final condition always converged to a confined region based on the pitch error correction logic. The advantage of using thruster instead of gimbaled engine is that a lot of unnecessary mechanisms can be avoided in the propulsion system of the last stage. Though the 'ping-ping' response can never attain a zero steady state error, we can always change the criteria of the pitch error correction logic so that it has a pitch error margin as small as we desired. Again, due to the nature of the pitch error always remains non-linear. The controller is designed to limit the non-linear disturbance within the linear decay curve.

Time response plots and phase plots are included in Appendix G.3.

5.0 THERMAL CONTROL SYSTEMS

The purpose of the thermal control systems is to maintain an acceptable temperature environment for the various components which make up Athena. This environment is to be established with a minimum of cost and complexity while being completely reliable and consistent. The challenge lies in the various temperature envelopes at which the separate components operate. The nose cone of Athena experiences temperatures in excess of 1,000°C, while the payload bay must be kept between 0-40°C in order for the deployment and control systems to function properly. Accordingly, it was first necessary to outline a thermal profile for an Athena mission. After the standard operating temperatures were determined, the Structures Group then determined the best configuration and material for the heat shielding.

There are three primary areas of interest regarding temperature:

- The Stagnation Point
- The Payload Bay
- The Exterior

After these primary areas had been analyzed it was then possible to establish the heat shielding configuration. The Structures section contains the actual materials and dimensions used as shielding. The thermal analysis used to design the heat shielding follows.

5.1 Temperatures at the Stagnation Point

The stagnation point is the region in which the speed of the airflow is zero. Due to conservation of momentum, the energy contained in the flow is transferred directly to the stagnation point, making it the hottest part on Athena. The stagnation point is located at the end of the nose cone, and the relationship between the stagnation temperature T and the atmospheric temperature t is as follows:

$$T = t\left[1 + \frac{\gamma - 1}{2} M^2\right]$$

where:
T = stagnation temperature (K)
t = atmospheric temperature (K)
γ = ratio of specific heats
M = local Mach number

The following graph displays the stagnation point temperatures as a function of altitude:

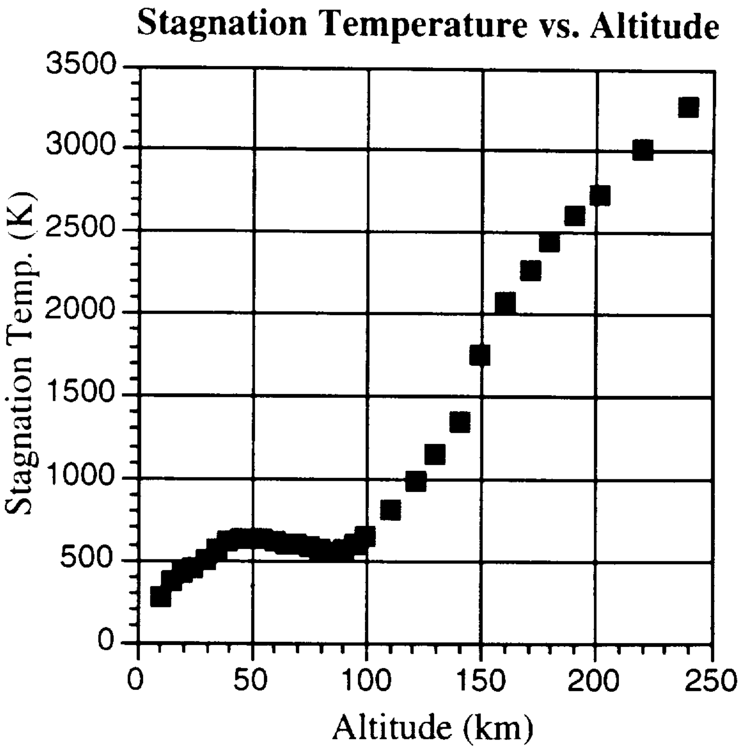

Figure 8.8

A short summary of the stagnation point temperatures is contained below in Table 8.4.

Altitude (km)	Temperature (K)
10	275.19
20	410.28
30	488.78
40	606.76
50	619.46
60	616.45
70	583.64
80	568.15
90	561.96
100	646.37
110	807.7
120	981.02
140	1335.82
160	2063.54
180	2433.95
200	2738.03

Table 8.4: Stagnation Temperature at Altitude

With such extreme temperatures occuring at the stagnation point, the nose cone must be heavily shielded in order to withstand the heat. See the Structures section for a more detailed description of the heat shield materials used.

5.2 The Payload Bay

The payload bay houses the satellite as well as vital electronic components. This region is the most sensitive to temperature fluctuations and extremes. Typically, the payload bay must be kept between 0-40 °C (273-313 K). The steady state heat conduction equation for a hollow cylinder is:

$$Q = \frac{2\pi k L(T_1 - T_2)}{\ln\left(D_o / D_i\right)}$$

where: k = thermal conductivity of the material $\left(W/m - K\right)$
L = length (or height) of the cylinder (m)
T_1 = temperature of the cooler surface (K)
T_2 = temperature of the hotter surface (K)
D_o = outer diameter of cylinder (m)
D_i = inner diameter of cylinder (m)

To find Q, we can integrate the following equation:

$q = \varepsilon\sigma T(t)^4$ = energy transfer per unit time per unit area (Wertz & Larson, p. 377)

where ε = emissivity of the material
σ = Stefan-Boltzmann constant = 5.67×10^{-8} $\left(W/m^2 - K^4\right)$
$T(t)$ = absolute temperature function (K)

Integrating this function over the duration of the trajectory will calculate Q.
For our trajectory, $Q = 197.785 \times 10^6$ J

5.3 The Exterior of Athena

The shell of the booster receives thermal energy from friction as well as conduction. Frictional heating occurs as the booster passes through the atmosphere. Heating due to friction is reduced by forming a strong shock wave around Athena. This shock wave reduces the velocity of the air which passes through it, thereby decreasing the heat caused by friction. Conductive heating occurs as thermal energy flows from hot spots such as the stagnation point to cooler areas on the structure. Conductive heating cannot be stopped entirely, but it is minimized by using materials with a low conductance as heat shielding. Conductance is a property of the material itself, and indicates how well a material conducts or insulates energy. Ideally the material will conduct poorly, insulating the rest of the skin from high temperature regions. Hot spots on the skin can also be caused by the absorption of solar radiation. A good shielding material will reflect most of this thermal radiation into space while absorbing very little of it. An economical reflector is white paint or epoxy.

6.0 NOSE CONE ANALYSIS

The nose cone is one of the most important components of Athena. The nose cone acts as both a heat shield and as an aerodynamic shroud. The nose cone designed for Athena seeks to provide maximum thermal protection with the minimum amount of drag. The fore body is mathematically modeled by a parabola of the form:

$$y = \sqrt{0.69299x}$$

Figure 8.9 is a schematic of the Athena nose cone:

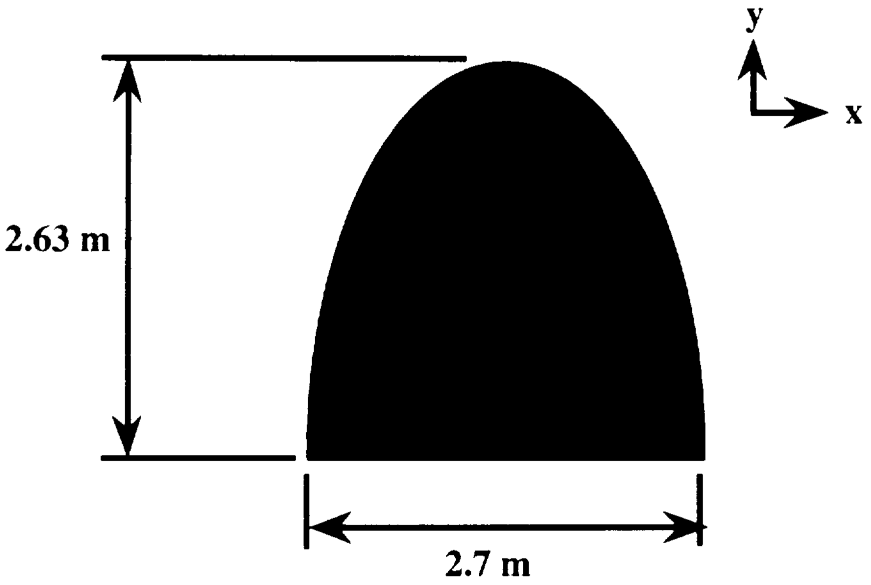

Figure 8.9 Athena Nose Cone

As mentioned in section 5.1 of this chapter, the stagnation point occurs at the apex of the parabola. This particular shape produces a strong normal shock wave ahead of the stagnation point. This shock wave slows the airflow to subsonic speed, greatly reducing the momentum of the flow and thereby the stagnation point temperature as well.

After the mathematical shape was generated it was necessary to determine its characteristics. Using simple integral formulas, the surface area and drag were calculated. The drag was computed from the following equation:

$$D = 2\pi q \int_{0}^{l} \left[\frac{2y\dot{y}^3}{\left(1+\dot{y}^2\right)} \right] dx \text{ (Miele,p. 253)}$$

where: q= dynamic pressure

$y = \sqrt{0.69299x}$

$\dot{y} = {}^{dy}\!/_{dx}$

The values are as follows:

Surface Area (m^2)	C_D
16.1143	0.13032

Table 8.5: Nose Cone Characteristics

Figure 8.10 is a plot of total drag vs. altitude:

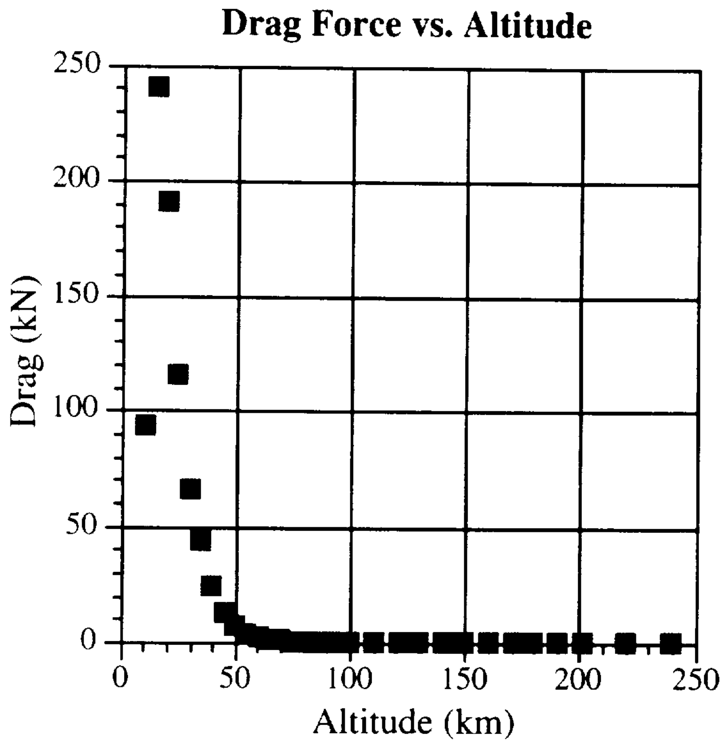

Figure 8.10

Table 8.6 lists several values of drag at altitude:

Altitude (km)	Drag (kN)
10	93.87
15	240.30
20	190.60
25	116.00
30	66.04
40	24.46
50	6.29
60	2.01
80	0.16
100	0.007

Table 8.6: Drag vs. Altitude

As can be seen from Table 8.6, the drag is very high early in the trajectory and quite small at the end. The large initial drag is due to the relatively high density of the air (compared with later in the flight) and the huge amount of thrust produced by the first stage. However, the overall coefficient of drag is quite low. For more detailed information on the construction and composition of the fore body, see the structures report in Chapter 7.

C-3.

Appendix A.1

Configuration Data

PRECEDING PAGE BLANK NOT FILMED

APPENDIX A.1 -- Configuration Data

ATHENA CONFIGURATION CHART

BOOSTER CONFIGURATION

	Engine Type	Length (m)	Mass (kg)	Fuel Type	Spent Fuel (kg)	Total Mass (kg)
Stage 1	LR87-AJ11	3.84	2285	Aerosine 50	50323	52608
Stage 2	LR91-AJ11	2.81	584	Aerosine 50	17577	18161
Stage 3-GTO	AJ10-138	2.07	220	Aerosine 50	5869	6089
-LEO					5042	5262
	R/C Engines	0.05	66.8	Hydrazine	191.2	258

	Tank Length (m)	Mass (kg)	Structure Type	Mass (kg)	Stage Length (m)	Burn Time (s)
Stage 1	8.41	1827.7	56Str., 8Comp	1050	12.25	58
Stage 2	4.84	8.3	36Str., 4Comp	450	7.65	111
Stage 3	3.75	310.9	24Str., 6Comp	450	5.82	205
R/C Engines	0.45	76				50 (max)

Total Mass

Fuel	72,942
Tanks	2,943
Engines	3,089
Structure	1,271
Shroud	885
Avionics+Misc	390
	81,520

Overall Dimensions (m)

Length	31.72
Inside Diameter	2.5
Outside Diameter	2.7

Payload Capacity (kg)

LEO	1715
GTO	888

PRECEDING PAGE BLANK NOT FILMED

Appendix A.2

Overall Mass Allocation

PRECEDING PAGE BLANK NOT FILMED

OVERALL MASS ALLOCATION

5.22%	**SLED**				**4341.00**
	Sled Allocation			4341.00	
		Structure:	4000.00		
		Extraction Materials:	341.00		
2.06%	**PAYLOAD**				**1715.00**
0.02%	**MISSION CONTROL**				**18.69**
	Navigation Computers			18.69	
		IMU:	0.70		
		GPS:	1.93		
		Computer:	14.06		
		Antennae:	2.00		
0.45%	**POWER/THERMAL**				**371.00**
	Miscellaneous Equipment			371.00	
		Batteries and Cables:	37.00		
		Reaction Thrusters:	334.00		
94.88%	**PROPULSION**				**78974.00**
	Stage One			54438.00	
		LR87-AJ-11:	2285.00		
		Fuel:	17293.51		
		Oxidizer:	33029.49		
		Fuel Tanks:	1830.00		
	Stage Two			18964.00	
		LR91-AJ-11:	584.00		
		Fuel:	6145.46		
		Oxidizer:	11431.54		
		Fuel Tanks:	803.00		
	Stage Three			5572.00	
		AJ10-138:	220.00		
		Fuel:	1738.32		
		Oxidizer:	3303.68		
		Fuel Tanks:	310.00		

PRECEDING PAGE BLANK NOT FILMED

2.59%	**STRUCTURES**				**2156.00**
	Stage One			715.00	
		Shell:	154.94		
		Stringers:	319.89		
		Stage Rings:	240.17		
	Stage Two			326.00	
		Shell:	88.54		
		Stringers:	117.49		
		Stage Rings:	119.97		
	Stage Three			230.00	
		Shell:	61.59		
		Stringers:	78.20		
		Stage Rings:	90.21		
	Payload Bay			885.00	
		Shell:	318.60		
		Other:	566.40		
100.00%	**TOTAL LAUNCH MASS**				**83234.69**
105.22%	**TOTAL ROLLING MASS**				**87575.69**

Appendix A.3

Figure 2.7 Raw Data

PRECEDING PAGE BLANK NOT FILMED

Figure 2.7 Raw Data

Load (kg)	km/kg fuel	kg fuel	range (km)
0	0.069030	150819.5	10411.07
2000	0.068883	150819.5	10388.85
4000	0.068735	150819.5	10366.64
6000	0.068588	150819.5	10344.42
8000	0.068441	150819.5	10322.21
10000	0.068293	150819.5	10299.99
12000	0.068146	150819.5	10277.77
14000	0.067999	150819.5	10255.56
16000	0.067852	150819.5	10233.34
18000	0.067704	150819.5	10211.12
20000	0.067557	150819.5	10188.91
22000	0.067410	150819.5	10166.69
24000	0.067262	150819.5	10144.48
26000	0.067115	150819.5	10122.26
28000	0.066968	150819.5	10100.04
30000	0.066820	150819.5	10077.83
32000	0.066673	150819.5	10055.61
34000	0.066526	150819.5	10033.40
36000	0.066379	150819.5	10011.18
38000	0.066231	150819.5	9988.96
40000	0.066084	150819.5	9966.75
42000	0.065937	150819.5	9944.53
44000	0.065789	150819.5	9922.32
46000	0.065642	150819.5	9900.10
48000	0.065495	150819.5	9877.88
50000	0.065347	150819.5	9855.67
52000	0.065200	150819.5	9833.45
54000	0.065053	150819.5	9811.23
56000	0.064906	150819.5	9789.02
58000	0.064758	150819.5	9766.80
60000	0.064611	150013.3	9692.50
62000	0.064464	148013.3	9541.47
64000	0.064316	146013.3	9391.04
66000	0.064169	144013.3	9241.19
68000	0.064022	142013.3	9091.93
70000	0.063874	140013.3	8943.27
72000	0.063727	138013.3	8795.19
74000	0.063580	136013.3	8647.70
76000	0.063432	134013.3	8500.80
78000	0.063285	132013.3	8354.49
80000	0.063138	130013.3	8208.77
82000	0.062991	128013.3	8063.63
84000	0.062843	126013.3	7919.09
86000	0.062696	124013.3	7775.14

88000	0.062549	122013.3	7631.77
90000	0.062401	120013.3	7489.00
92000	0.062254	118013.3	7346.81
94000	0.062107	116013.3	7205.21
96000	0.061959	114013.3	7064.20
98000	0.061812	112013.3	6923.78
100000	0.061665	110013.3	6783.95
102000	0.061518	108013.3	6644.71
104000	0.061370	106013.3	6506.06
106000	0.061223	104013.3	6368.00
108000	0.061076	102013.3	6230.53
110000	0.060928	100013.3	6093.65
112000	0.060781	98013.3	5957.35
114000	0.060634	96013.3	5821.65
116000	0.060486	94013.3	5686.53
118000	0.060339	92013.3	5552.00
120000	0.060192	90013.3	5418.07

Appendix A.4

Comparison With Competition

PRECEDING PAGE BLANK NOT FILMED

Comparison with Competition

LAUNCH SYSTEM	BOOSTER MASS (kg)	LAUNCH COST (Millions)*	PAYLOAD MASS (kg) (GTO)	PAYLOAD MASS (kg) (LEO)	COST PER KILOGRAM (GTO)	COST PER KILOGRAM (LEO)
PEGASUS XL	22,583	$12	146	435	$82,192	$27,586
TAURUS	68,430	$16	430	1,200	$37,209	$13,333
ATHENA	**80,680**	**$18**	**888**	**1,715**	**$20,270**	**$10,496**
DELTA 2	229,730	$50	1,819	5,039	$27,488	$9,923
ARIANE 40	243,000	$50	1,900	4,600	$26,316	$10,870
ATLAS 1	164,290	$60	2,336	5,624	$25,685	$10,669
ARIANE 42P	320,000	$65	2,600	6,000	$25,000	$10,833
ARIANE 44P	355,000	$80	3,000	6,500	$26,667	$12,308

* **December 1993 U.S. Dollars**

Appendix A.5

Overall Dollar Allocation

PRECEDING PAGE BLANK NOT FILMED

Overall Dollar Allocation

16.11%	**LAUNCH OPERATIONS**			**$2,673,339**
	One-Time Costs		$280,877	
[1]	C-5B Modifications:	$100,000		
[1]	Drop Testing:	$16,752,602		
	Aircraft Operations		$520,463	
[3]	C-5B Usage:	$450,000		
[3]	Fuel:	$28,463		
[3]	Chase Plane:	$42,000		
	Sled Construction		$122,000	
[2]	Materials:	$72,000		
[3]	Construction:	$50,000		
	Booster Assembly		$250,000	
[3]	Construction:	$200,000		
[3]	Sled Mounting:	$50,000		
	Insurance		$1,500,000	
[3]	Liability:	$1,250,000		
[3]	Other:	$250,000		
4.27%	**MISSION CONTROL**			**$708,750**
	One-Time Costs		$3,750	
[1]	LPO Equipment:	$100,000		
[1]	Software Development:	$125,000		
	Navigation Computers		$145,000	
[2]	IMU:	$30,000		
[2]	GPS:	$10,000		
[2]	Computer:	$85,000		
[2]	Communication Link:	$20,000		
	Mission Tracking		$560,000	
[3]	TTC:	$550,000		
[2]	Mission Specialist:	$10,000		
0.10%	**POWER/THERMAL**			**$16,150**
	Equipment		$5,650	
[2]	Batteries and Cables:	$750		
[2]	Reaction Thrusters:	$4,900		
	Extraction Materials		$10,500	
[2]	Main Chutes:	$10,500		

PRECEDING PAGE BLANK NOT FILMED

69.54%	**PROPULSION**				**$11,539,133**
	Stage One			$3,607,539	
[2]			$3,000,000		
[2]		Fuel Tanks:	$7,539		
[3]		Fuel:	$410,000		
[3]		Oxidizer:	$190,000		
	Stage Two			$2,816,312	
[2]		LR91-AJ-11:	$2,500,000		
[2]		Fuel Tanks:	$3,312		
[3]		Fuel:	$216,000		
[3]		Oxidizer:	$97,000		
	Stage Three			$5,115,282	
[2]		AJ10-138:	$5,000,000		
[2]		Fuel Tanks:	$1,282		
[3]		Fuel:	$78,000		
[3]		Oxidizer:	$36,000		
9.97%	**STRUCTURES**				**$1,655,000**
	Stage One			$92,500	
[2]		Shell:	$17,500		
[2]		Stringers:	$37,500		
[2]		Compression Rings:	$37,500		
	Stage Two			$62,500	
[2]		Shell:	$12,500		
[2]		Stringers:	$25,000		
[2]		Compression Rings:	$25,000		
	Stage Three			$250,000	
[2]		Shell:	$250,000		
	Payload Bay			$1,250,000	
[2]		Shell:	$500,000		
[2]		Nose Cone:	$750,000		
100.00%	**TOTAL LAUNCH COST**				**$16,592,372**

Key:

[1] : One-time up front charge
[2] : Purchase 1 year ahead for assembly
[3] : Paid during launch year

Appendix A.6

Drop Test Cost Allocation

PRECEDING PAGE BLANK NOT FILMED

Drop Test Cost Allocation

12.91%	**DROP TEST ONE**		**$2,162,963**
	Aircraft:	$520,463	
	Chutes:	$10,500	
	Concrete:	$10,000	
	Insurance:	$1,500,000	
	Sled:	$122,000	
12.94%	**DROP TEST TWO**		**$2,167,963**
	Aircraft:	$520,463	
	Chutes:	$10,500	
	Concrete:	$15,000	
	Insurance:	$1,500,000	
	Sled:	$122,000	
24.22%	**DROP TEST THREE**		**$4,057,963**
	Aircraft:	$520,463	
	Assembly:	$250,000	
	Chutes:	$10,500	
	Insurance:	$1,500,000	
	Sled:	$122,000	
	Structure:	$1,655,000	
49.92%	**DROP TEST FOUR**		**$8,363,713**
	Aircraft:	$520,463	
	Assembly:	$250,000	
	Chutes:	$10,500	
	Engines:	$3,000,000	
	Fuel:	$600,000	
	Insurance:	$1,500,000	
	Miss Control:	$705,750	
	Sled:	$122,000	
	Structure:	$1,655,000	
100.00%	**FINAL TOTAL**		**$16,752,602**

Appendix A.7

Budget Analysis Spreadsheet

APPENDIX A.7

BUDGET ANALYSIS SPREADSHEET

		$17,961	**$16,592**							
Year	#	Charge per launch	Cost per launch	15% Interest	Pre-Tax Profit	35% Taxes	Post-Tax Gain	Payments on Debt	Cash Balance	Debt Balance
0		$0	$0		$0	$0	$0		$0	$0
1		$0	$8,539	$0	($8,539)	$0	($8,539)	($13,539)	$5,000	$13,539
2		$8,981	$20,949	$2,031	($13,999)	$0	($13,999)	($13,999)	$5,000	$27,538
3	1	$44,903	$53,539	$4,131	($12,767)	$0	($12,767)	($12,767)	$5,000	$40,305
4	4	$80,825	$77,641	$6,046	($2,863)	$0	($2,863)	($2,863)	$5,000	$43,168
5	5	$98,786	$93,949	$6,475	($1,639)	$0	($1,639)	($1,639)	$5,000	$44,806
6	6	$107,766	$97,846	$6,721	$3,199	$1,120	$2,079	$2,079	$5,000	$42,727
7	6	$116,747	$110,257	$6,409	$81	$28	$52	$52	$5,000	$42,675
8	7	$125,727	$114,154	$6,401	$5,172	$1,810	$3,362	$3,362	$5,000	$39,313
9	7	$125,727	$114,154	$5,897	$5,676	$1,987	$3,689	$3,689	$5,000	$35,624
10	7	$116,747	$101,744	$5,344	$9,659	$3,381	$6,278	$6,278	$5,000	$29,346
11	6	$107,766	$97,846	$4,402	$5,518	$1,931	$3,587	$3,587	$5,000	$25,759
12	6	$98,786	$85,436	$3,864	$9,485	$3,320	$6,166	$6,166	$5,000	$19,593
13	5	$44,903	$19,487	$2,939	$22,476	$7,867	$14,610	$19,593	$16	$0
14		$0	$0	$0	$0	$0	$0		$16	$0
15		$0	$0	$0	$0	$0	$0		$16	$0
Totals	60	$1,077,660	$995,542	$60,659	$21,459	$21,443	$16	$0	$16	$0

All Dollars Figures in Thousands (000)

Appendix C.1

Matlab Trajectory Analysis Program

APPENDIX C.1 -- **Matlab Trajectory Analysis Program**

```
% This is a ascent trajectory code written for the University of Michigan's Aerospace
% Engineering 483 (Space System Design) Course.  The trajectory code was developed by %
Jeff White, Mary Ann Guariento, Aaron Drielick, and John Ziemer for use with the
% MATLAB program.

clear

%-----     First Sub Stage      -----

%Dry Mass
Struct1     =     715+2385;
Tank1       =     1830;
Engine1     =     2285;
Dmass1      =     Struct1+Tank1+Engine1;

%Engine
Thrust1     =     2437504;
Isp1        =     301;
mdot1       =     Thrust1/(9.8*Isp1);

%Trajectory
Burnt1      =     58;

Obeg1       =     60;
Oend1       =     20;

Odot1       =     (Obeg1-Oend1)/Burnt1;

%Fuel Specs
Fuelm1      =     Burnt1*mdot1;


%-----     Coast Between Stage 1 and 2       -----

%Engine
ThrustC     =     0;
IspC        =     0;
mdotC       =     0;

%Trajectory
BurntC1     =     3;

ObegC1      =     Oend1;
OendC1      =     18;

OdotC1      =     (ObegC1-OendC1)/BurntC1;


%-----       Second Sub Stage        -----

%Dry Mass
Struct2     =     326+835;
Tank2       =     803;
Engine2     =     584;
```

207 - 210

PRECEDING PAGE BLANK NOT FILMED

```
Dmass2      =     Struct2+Tank2+Engine2;

%Engine
Thrust2     =     467040;
Isp2        =     316;
mdot2       =     Thrust2/(9.8*Isp2);

%Trajectory
Burnt2      =     111;

Obeg2       =     OendC1;
Oend2       =     10;

Odot2       =     (Obeg2-Oend2)/Burnt2;

%Fuel Specs
Fuelm2      =     Burnt2*mdot2;


%-----    Coast Between Stage 2 and 3     -----

%Engine
ThrustC     =     0;
IspC        =     0;
mdotC       =     0;

%Trajectory
BurntC2     =     13;

ObegC2      =     Oend2;
OendC2      =     7;

OdotC2      =     (ObegC2-OendC2)/BurntC2;


%-----          Third Sub Stage          -----

%Dry Mass
Struct3     =     230+250+390;
Tank3       =     310;
Engine3     =     2*110;
Dmass3      =     Struct3+Tank3+Engine3;

%Engine
Thrust3     =     2*35584;
Isp3        =     310;
mdot3       =     Thrust3/(9.8*Isp3);

%Trajectory
Burnt3      =     205;

Obeg3       =     OendC2;
Oend3       =     4;
```

```
Odot3       =    (Obeg3-Oend3)/Burnt3;

%Fuel Specs
FuelmEx     =    0*mdot3;
Fuelm3      =    Burnt3*mdot3+FuelmEx;


%-----      Final Coast and Satellite Deployment      -----

BurntC3     =    1000-Burnt1-BurntC1-Burnt2-BurntC2-Burnt3;


%-----  Payload, Shroud, Time Step, and Drag Calculation Setup  -----

Payldm      =    1715;
Shroudm     =    885;

t           =    [0:1:2000];
S           =    5.72;
Cd          =    .2;


%-----     Launching Initial Conditions      -----

%Initial Conditions
Ax(1)       =    0;
Ay(1)       =    -9.8;
A(1)        =    ((Ax(1))^2+(Ay(1))^2)^.5;
Vx(1)       =    460;
Vy(1)       =    -50;
V(1)        =    ((Vx(1))^2+(Vy(1))^2)^.5;
Px(1)       =    0;
Py(1)       =    10000;
O(1)        =    Obeg1;
m(1)        =    Dmass1+Dmass2+Dmass3+Payldm+Shroudm+Fuelm1+Fuelm2
                 +Fuelm3;
F(1)        =    Thrust1;

%-----      First Stage      -----

O(2)        =    O(1);
m(2)        =    m(1);

%Single Second Time Step Loop
for k = 2:Burnt1

          g       =    9.8*(6375400/(6375400+Py(k-1)))^2;
          Dens    =    1.2*exp((-2.9*10^(-5))*(Py(k-1))^1.15);
          Drag    =    .5*Dens*(V(k-1))^2*S*Cd;
          F(k)    =    Thrust1-Drag;
          Ax(k)   =    F(k)/m(k)*cos(O(k)*pi/180);
          Ay(k)   =    F(k)/m(k)*sin(O(k)*pi/180)-g+((Vx(k-1))^2)/
                       (6375400+Py(k-1));
          A(k)    =    ((Ax(k))^2+(Ay(k))^2)^.5;
```

```
        Vx(k)     =     Vx(k-1)+Ax(k);
        Vy(k)     =     Vy(k-1)+Ay(k);
        V(k)      =     ((Vx(k))^2+(Vy(k))^2)^.5;
        Px(k)     =     Px(k-1)+Vx(k);
        Py(k)     =     Py(k-1)+Vy(k);

        m(k+1)    =     m(k)-mdot1;
        O(k+1)    =     O(k)-Odot1;

end


%-----     Coast Stage        -----

O(Burnt1+1)       =  ObegC1;
m(Burnt1+1)       =  Dmass2+Dmass3+Payldm+Shroudm+Fuelm2+Fuelm3;

%Single Second Time Step Loop
for k = (Burnt1+1):(Burnt1+BurntC1)

        g         =     9.8*(6375400/(6375400+Py(k-1)))^2;
        Dens      =     1.2*exp((-2.9*10^(-5))*(Py(k-1))^1.15);
        Drag      =     .5*Dens*(V(k-1))^2*S*Cd;
        F(k)      =     ThrustC-Drag;
        Ax(k)     =     F(k)/m(k)*cos(O(k)*pi/180);
        Ay(k)     =     F(k)/m(k)*sin(O(k)*pi/180)-g+((Vx(k-1))^2)/
                        (6375400+Py(k-1));
        A(k)      =     ((Ax(k))^2+(Ay(k))^2)^.5;
        Vx(k)     =     Vx(k-1)+Ax(k);
        Vy(k)     =     Vy(k-1)+Ay(k);
        V(k)      =     ((Vx(k))^2+(Vy(k))^2)^.5;
        Px(k)     =     Px(k-1)+Vx(k);
        Py(k)     =     Py(k-1)+Vy(k);

        m(k+1)    =     m(k)-mdotC;
        O(k+1)    =     O(k)-OdotC1;

end


%-----     Second Stage       -----

O(Burnt1+BurntC1+1)       =     Obeg2;
m(Burnt1+BurntC1+1)       =     Dmass2+Dmass3+Payldm+Shroudm
                                +Fuelm2+Fuelm3;

%Single Second Time Step Loop
for k = (Burnt1+BurntC1+1):(Burnt1+BurntC1+Burnt2)

        g         =     9.8*(6375400/(6375400+Py(k-1)))^2;
        Dens      =     1.2*exp((-2.9*10^(-5))*(Py(k-1))^1.15);
        Drag      =     .5*Dens*(V(k-1))^2*S*Cd;
        F(k)      =     Thrust2-Drag;
        Ax(k)     =     F(k)/m(k)*cos(O(k)*pi/180);
        Ay(k)    =    F(k)/m(k)*sin(O(k)*pi/180)-g+((Vx(k-1))^2)/
                      (6375400+Py(k-1));
        A(k)     =    ((Ax(k))^2+(Ay(k))^2)^.5;
        Vx(k)    =    Vx(k-1)+Ax(k);
        Vy(k)    =    Vy(k-1)+Ay(k);
        V(k)     =    ((Vx(k))^2+(Vy(k))^2)^.5;
        Px(k)    =    Px(k-1)+Vx(k);
        Py(k)    =    Py(k-1)+Vy(k);

        m(k+1)   =    m(k)-mdot2;
        O(k+1)   =    O(k)-Odot2;

end


%-----    Coast Stage      -----

O(Burnt1+BurntC1+Burnt2+1)       =    ObegC2;
m(Burnt1+BurntC1+Burnt2+1)       =    Dmass3+Payldm+Fuelm3;

%Single Second Time Step Loop
for k = (Burnt1+BurntC1+Burnt2+1):(Burnt1+BurntC1+Burnt2+BurntC2)

        g        =    9.8*(6375400/(6375400+Py(k-1)))^2;
        Dens     =    1.2*exp((-2.9*10^(-5))*(Py(k-1))^1.15);
        Drag     =    .5*Dens*(V(k-1))^2*S*Cd;
        F(k)     =    ThrustC-Drag;
        Ax(k)    =    F(k)/m(k)*cos(O(k)*pi/180);
        Ay(k)    =    F(k)/m(k)*sin(O(k)*pi/180)-g+((Vx(k-1))^2)/
                      (6375400+Py(k-1));
        A(k)     =    ((Ax(k))^2+(Ay(k))^2)^.5;
        Vx(k)    =    Vx(k-1)+Ax(k);
        Vy(k)    =    Vy(k-1)+Ay(k);
        V(k)     =    ((Vx(k))^2+(Vy(k))^2)^.5;
        Px(k)    =    Px(k-1)+Vx(k);
        Py(k)    =    Py(k-1)+Vy(k);

        m(k+1)   =    m(k)-mdotC;
        O(k+1)   =    O(k)-OdotC2;

end


%-----     Third Stage     -----

O(Burnt1+BurntC1+Burnt2+BurntC2+1)    =    Obeg3;
m(Burnt1+BurntC1+Burnt2+BurntC2+1)    =    Dmass3+Payldm+Fuelm3;

%Single Second Time Step Loop
for k = (Burnt1+BurntC1+Burnt2+BurntC2+1):
      (Burnt1+BurntC1+Burnt2+BurntC2+Burnt3)

        g        =    9.8*(6375400/(6375400+Py(k-1)))^2;
        Dens     =    1.2*exp((-2.9*10^(-5))*(Py(k-1))^1.15);
        Drag     =    .5*Dens*(V(k-1))^2*S*Cd;
        F(k)     =    Thrust3-Drag;
        Ax(k)    =    F(k)/m(k)*cos(O(k)*pi/180);
        Ay(k)    =    F(k)/m(k)*sin(O(k)*pi/180)-g+((Vx(k-1))^2)/
                      (6375400+Py(k-1));
        A(k)     =    ((Ax(k))^2+(Ay(k))^2)^.5;
        Vx(k)    =    Vx(k-1)+Ax(k);
        Vy(k)    =    Vy(k-1)+Ay(k);
        V(k)     =    ((Vx(k))^2+(Vy(k))^2)^.5;
        Px(k)    =    Px(k-1)+Vx(k);
        Py(k)    =    Py(k-1)+Vy(k);

        m(k+1)   =    m(k)-mdot3;
        O(k+1)   =    O(k)-Odot3;

end


%-----     Third Coast     -----

O(Burnt1+BurntC1+Burnt2+BurntC2+Burnt3+1)    =    0;
m(Burnt1+BurntC1+Burnt2+BurntC2+Burnt3+1)    =    Payldm;

%Single Second Time Step Loop
for k = (Burnt1+BurntC1+Burnt2+BurntC2+Burnt3+1):2001

        g        =    9.8*(6375400/(6375400+Py(k-1)))^2;
        F(k)     =    0;
        Ax(k)    =    0;
        Ay(k)    =    -g+((Vx(k-1))^2)/(6375400+Py(k-1));
        A(k)     =    ((Ay(k))^2)^.5;
        Vx(k)    =    Vx(k-1)+Ax(k);
        Vy(k)    =    Vy(k-1)+Ay(k);
        V(k)     =    ((Vx(k))^2+(Vy(k))^2)^.5;
        Px(k)    =    Px(k-1)+Vx(k);
        Py(k)    =    Py(k-1)+Vy(k);

        m(k)     =    Payldm;
        O(k)     =    O(k-1);

end


%-----     Plotting     -----

figure(1)
plot(Px,Py)
grid
title('Athena Trajectory')
xlabel('Downrange Distance (m)')
ylabel('Altitude (m)')
print trajectory
```

```
figure(2)
plot(t,Ay)
grid
title('Athena Vertical Acceleration')
xlabel('Time (s)')
ylabel('Acceleration (m/s^2)')
print vaccel

figure(3)
plot(t,Ax)
grid
title('Athena Horizontal Acceleration')
xlabel('Time (s)')
ylabel('Horizontal Acceleration (m/s^2)')
print haccel

figure(4)
plot(Py,V)
grid
title('Athena Velocity with Altitude')
xlabel('Altitude (m    )')
ylabel('Velocity (m/s)')
pause
print velocity

figure(5)
plot(t,m)
grid
title('Athena Mass')
xlabel('Time (s)')
ylabel('Mass (kg)')
pause

figure(6)
plot(t,Vy)
grid
title('Athena Vertical Velocity')
xlabel('Time (s)')
ylabel('Velocity (m/s)')
pause

figure(7)
plot(t,(A/9.8))
grid
title('Athena G-Loading')
xlabel('Time (s)')
ylabel('g-load (m/s^2)')
print gload
```

Appendix C.2

Trajectory Analysis Graphic Results

PRECEDING PAGE BLANK NOT FILMED

APPENDIX C.2 -- **Trajectory Analysis Graphic Results**

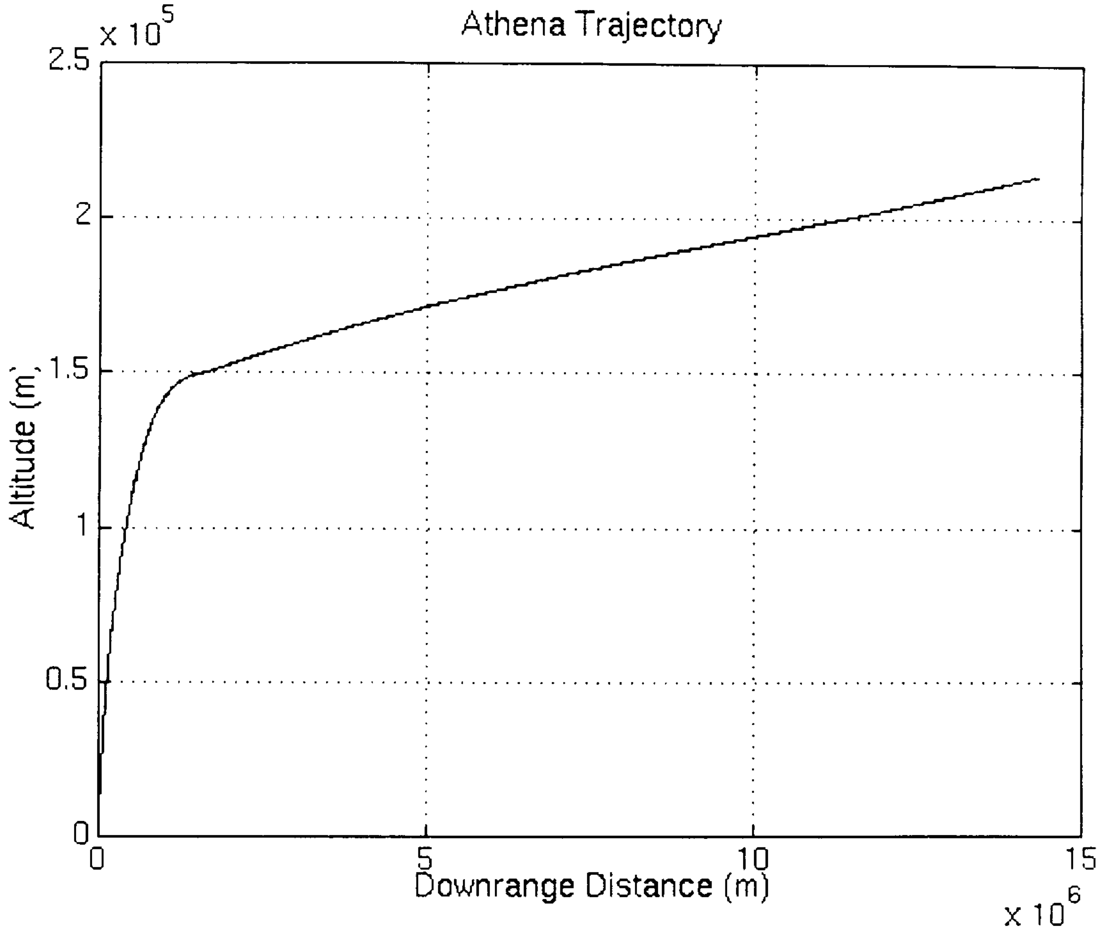

PRECEDING PAGE BLANK NOT FILMED

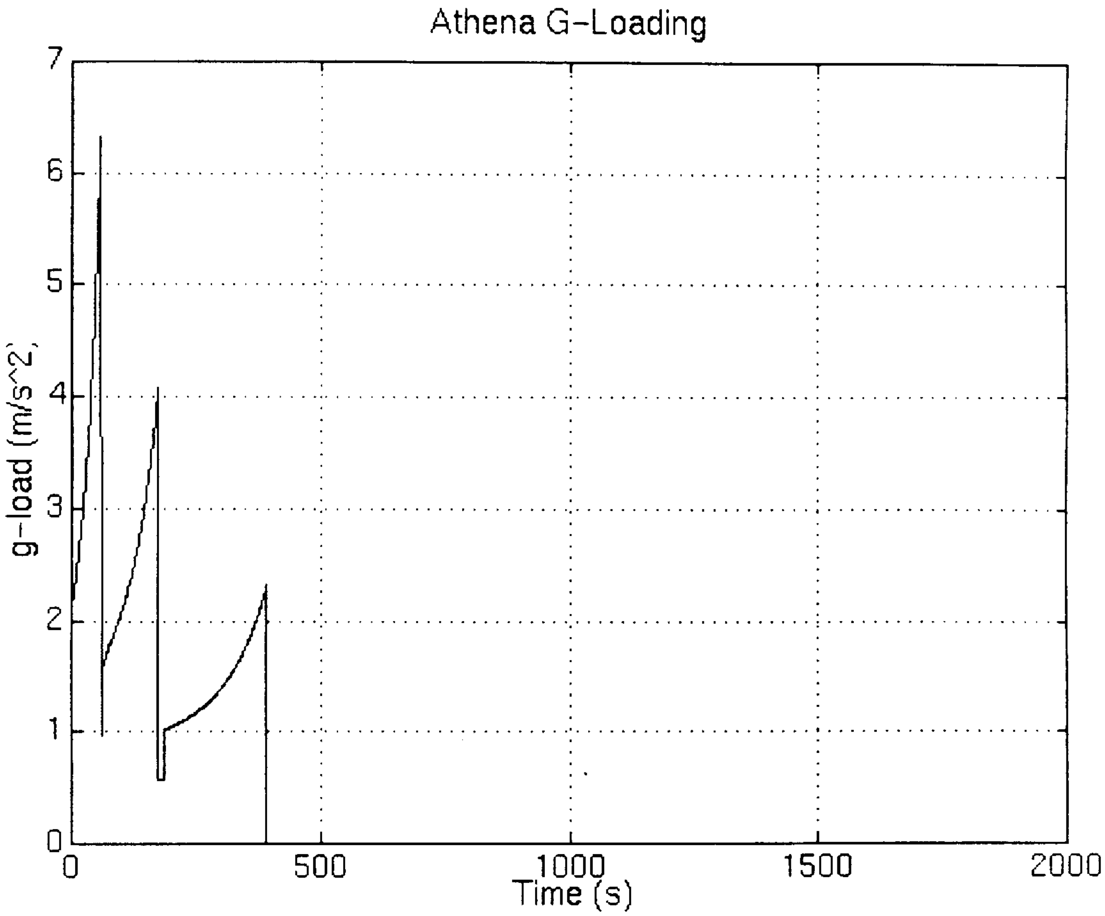
Athena G-Loading
g-load (m/s^2)
Time (s)
0
1
2
3
4
5
6
7
0
500
1000
1500
2000

Appendix D.1

PRELIMINARY PAYLOAD BAY DESIGNS

PRECEDING PAGE BLANK NOT FILMED

APPENDIX D.1 -- Preliminary Payload Bay Designs

Appendix D.1 presents the various payload bay configurations considered for Athena by the Payloads group.

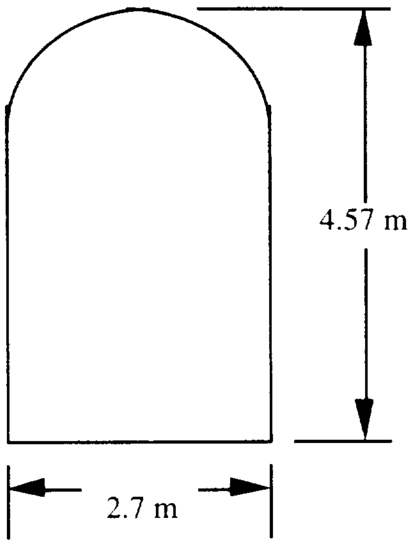

Figure D.1.1: Configuration 1

Figure D.1.1 shows the 4.57 m. long payload bay with the single payload configuration.

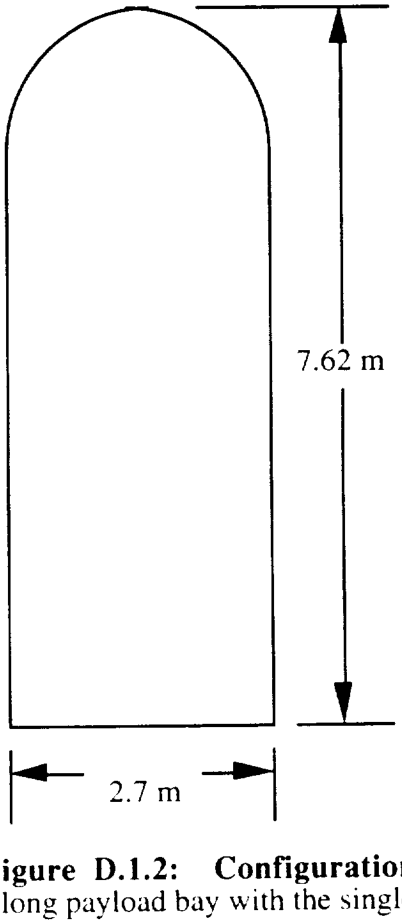

Figure D.1.2: Configuration 2

Figure D.1.2 shows the 7.62 m. long payload bay with the single payload configuration.

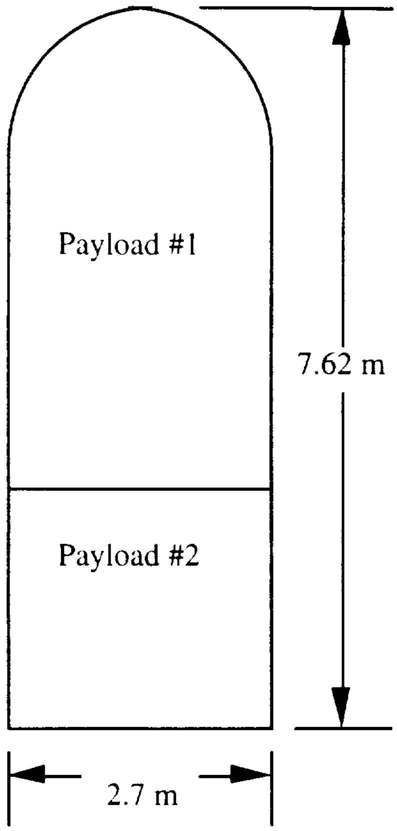
Payload #1
Payload #2
7.62 m
2.7 m

Figure D.1.3: Configuration 3

Figure D.1.3 shows the 7.62 m. long payload bay with the double payload configuration.

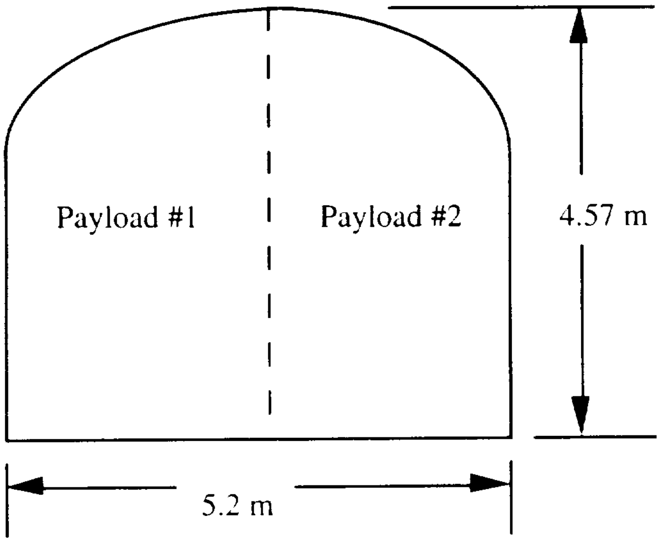
Payload #1
Payload #2
4.57 m
5.2 m

Figure D.1.4: Configuration 4

Figure D.1.4 shows the 4.57 m. long payload bay with the side-by-side double payload configuration.

Appendix D.2

FUTURE SATELLITES

PRECEDING PAGE BLANK NOT FILMED

APPENDIX D.2 -- Future Satellites

Future Satellites:

1) Within Athena's Capability:

Table D.2.1: Satellites within Athena's Capability

Satellite	Origin	Launch Date	Mass (kg)	Size (m) (lxbxh or rxh)	Orbit
Geos 9	USA	1994	443	2.2x1.0	GEO
Geos 10	USA	1996	443	2.2x1.0	GEO
Iridium (66 of them)	Motorola	1996-2002	750	not known	780 km
MedSAT	NASA	not known	340	not known	477 km
STEP	USA	1994-1999	< 454	0.97x0.37	not known
UoSAT	University of Surrey	not known	50	not known	800 km

There is also an Iridium-like network of 77 satellites known as the Leocom system being developed by the an Italian company, ITALSPAZIO. At present, this is still being under planning though some preliminary satellites have been launched.

In addition, there are approximately more than 70 small satellites with masses ranging from 20 to 200 kg with a wide variety of applications. They are invariably placed in low earth orbits (LEO). A sample of these are shown in Table 2:

Table D.2.2: Survey of Small Satellites

Satellite	Origin	Launch Date	Mass (kg)	Size (m) (lxbxh or rxh)	Orbit
Alexis	USA	not known	115	0.6x1.0	LEO
Aries	USA	not known	125	not known	LEO
Ellipso	Ellipsat Corporation	not known	174.6	not known	LEO
Techstar	USA	not known	55 - 91	0.7x0.7x0.5	LEO

II) Beyond Athena's capability:

Table D.2.3: Satellites Beyond Athena's Capability

Satellite	Origin	Launch Date	Mass (kg)	Size (m) (lxbxh or rxh)	Orbit
Astro E	Japan	1999	500	not known	500 km
Dscs III	USA	1992-1996	1125	1.8x1.8x3.0	GEO
MSAt	USA	1994-1995	1545	1.8x2.1x2.1	not known
TDRSS	USA	1995	2273	not known	not known
Telstar 4	USA	1994	1619	2.1x2.4x3.0	not known
UHF Follow on	USA	1992-1995	1293	1.8x2.1x1.8	not known

Appendix D.3

RECENT SATELLITES

PRECEDING PAGE BLANK NOT FILMED

APPENDIX D.3 -- **Recent Satellites**

Initial Survey of Satellites :

Based on the book, 'The Complete Encyclopedia of Satellites" by Giovanni Caprara, there were documented :

a) 6 Remote Sensing Satellites (640 to 1280 km orbits)
b) 4 Weather Satellites (GEO/640 km orbits)
c) 29 Communications Satellites (Mostly GEO)
d) 17 Scientific Satellites (varying orbits)

Based on this data, we can conclude that our initial target should be the communication satellite since this is by far the richest market. They typically weigh less than 1500 kg

NASA missions since 1985:

i)
This analysis is based on our tentative payload configurations:
a) 3.048 m long, 1819 kg to LEO (Configuration 1)
b) 3.048 - 4.572 m long, 2636 kg to LEO (Configuration 2)
c) 7.62 m long, 5454 kg to LEO (Configuration 3)

ii)
Number of NASA missions classified by categories:
a) space systems exploration - 4
b) Astrophysics - 21
c) Earth Sciences - 12
d) Communications - 3
e) Space Transport - 1
f) Utilization of Space Environment - 3
g) Landmark missions - 4

iii)
Breakdown in terms of our original three configurations:

Total number of missions since '85 = 47
Weight:
Configuration 1 = 19 missions
Configuration 2 = 32 missions
Configuration 3 = 39 missions

Length:
Configuration 1 = 1 mission
Configuration 2 = 9 missions
Configuration 3 = 18 missions

It can be deduced that most NASA missions are launched from the Shuttle which has an enormous cargo bay.

Satellite launches from 1990-1992 (April):

a) 1990 - 165 launches

Configuration 1 - 52 launches (32%)

Configuration 2 - 92 launches (56%)
Configuration 3 - 116 launches (70%)

b) 19901- 139 launches

Configuration 1 - 49 launches (35%)
Configuration 2 - 73 launches (53%)
Configuration 3 - 100 launches (68%)

c) 1992 (till April) - 29 launches

Configuration 1 - 1 launches (3%)
Configuration 2 - 13 launches (45%)
Configuration 3 - 16 launches (55%)

Assumptions:
a) That payload to GTO was 40% that to LEO for our three configurations.
b) Sizes are not taken in account.

Appendix E.1

ENGINES

PRECEDING PAGE BLANK NOT FILMED

Engine	Fuel/ Oxidizer	Burn Time (s)	Maximum Thrust (N)	Vacuum Isp(sec)	Length (m)	Width (m)	Dry Mass (kg)	Ox./Fuel Ratio	Ox. Dens. (kg/m^3)	Fuel Dens. (kg/m^3)
Liquids										
LR87-AJ-11	A50/N2O4	200.0	2,437,504	301.0	3.84	2.16	2,285	1.91	1450	906
LR87-AJ-5	A50/N2O4	158.0	1,913,000	259.0	3.13	1.14	739	1.93	1450	906
LR91-AJ-11	A50/N2O4	247.0	467,040	316.0	2.81	1.62	584	1.86	1450	906
LR91-AJ-5	A50/N2O4	175.0	444,800	315.0	2.80	1.68	500	NA	1450	906
AJ10-138	A50/N2O4	500.0	35,584	310.0	2.07	1.20	110	1.9	1450	906
LR86-5	A50/N2O4	200.0	1,912,640	259.0	NA	NA	NA		1450	906
LR-105	A50/N2O4	NA	372,298	304.0	NA	NA	NA		1450	906
Transtar	MMH/N2O4	NA	16,680	328.0	1.27	NA	67	1.800	1450	
Cryos										
H-1	RP-1/LOX	155.0	974,112	287.0	2.59	1.68	918			
J-2S	LH2/LOX	NA	1,178,720	436.0	NA	NA	1,727			
J-2	LH2/LOX	500.0	889,600	426.0	3.38	2.05	1,582			
MA-5 (bstr)	RP-1/LOX	167.0	1,679,120	259.1	2.46	1.19(x2)	1,427	2.25		
MA-5 (sustr)		368.0	269,104	220.4	2.46	1.22	470	2.27		
MA-5A (bstr)	RP-1/LOX	170.0	1,883,728	263.9	2.57	1.22(x2)	1,516	2.25		
MA-5A (sustr)		368.0	269,104	220.0	2.46	1.22	470	2.27		
RSX	RP-1/LOX	NA	2,135,040	299.0	3.40	1.85	2,045	NA		
RS-53	LH2/LOX	NA	2,090,560	453.5	NA	NA	3,273			
RS-27	RP-1/LOX	265.0	1,030,602	295.0	3.61	1.93	1,041	2.245		
RS-27A	RP-1/LOX	265.0	1,054,176	302.0	3.79	1.93	1,111	2.245		
RL10A-3-3A	LH2/LOX	4000.0	73,390	444.4	1.78	1.02	138	5		
RL10A-4	LH2/LOX	3000.0	92,518	449.0	2.44	1.22	168	NA		
SSME	LH2/LOX	NA	2,090,560	455.0	4.27	2.44	2,864	6		
STBE	CH4/LOX	NA	3,336,000	348.0	NA	NA	3,947			
Aerospike	LH2/LOX	NA	22,240	450.0	NA	NA	NA			
Linear Aerospike	LH2/LOX	NA	1,156,480	455.0	NA	NA	NA			

Engine	Propellant	Burn Time (s)	Maximum Thrust (N)	Vacuum Isp(sec)	Length (m)	Max Dia (m)	Total Mass (kg)	Mass Ratio	Empty Mass (kg)	Delta V* (m/s)
Solids										
Algol III	PBAN	90	385,642	NA	9.04	1.14	14,200	0.105		NA
Minuteman St 3	CTPB	60.0	153,456	NA	2.26	1.32	3,773			NA
Trident Stage 2	Class 1.1	NA	NA	NA	3.28	0.81	2,213			NA
Orbus 21	HTPB	140.0	198,381	295.5	3.15	2.34	10,420	0.065	639	4066
Orbus 21S†	HTPB	138.4	196,602	293.8	3.15	2.34	10,320			3715
Orbus 6	HTPB	105.0	80,153	NA	1.98	1.61	14,716			NA
Orbus 6E†	HTPB	101.0	111,067	303.8	1.98	1.61	3,023	0.098		2028
Orbus 6S†	HTPB	100.0	77,173	289.5	1.89	1.61	2,969			1904
Orbus 7	CTPB	60.0	153,456	NA	2.26	1.32	3,591			NA
Orbus 7S†	CTPB	60.0	153,456	284.9	2.27	1.32	3,555	0.065		2225
Orbus 3	Class 1.1	NA	NA	NA	2.03	1.17	1,485			NA
Orbus 1	HTPB	38.7	30,602	293.3	1.25	0.73	470			442
Orbus .5	HTPB	14.0	51,597	NA	1.84	0.42	278			NA
Orbus .1	HTPB	13.0	11,298	NA	0.82	0.36	54			NA
ASRM	HTPB	140.0	15,850,000	269.2	38.43	3.81	610,233	0.104		5886
SRM	HB poly.	123.6	14,770,000	268.6	38.47	3.71	569,893	0.117		5568
TSB (7 seg.)	PBAN	119.5	7,117,000	272.0	34.43	3.11	316,600	0.154		4879
TSB (5.5 seg)	PBAN	113.7	6,227,000	265.2	27.57	3.11	238,000	0.115		5427
Castor 120GT	NA	86.0	1,546,510	249.3	8.89	2.36	54,430	NA		4817
Castor 120	HTPB	78.0	1,795,920	292.0	9.15	3.05	53,494			5628
Castor 25GT	NA	54.0	527,000	253.5	7.57	1.17	11,360	NA		3328
Castor XX	NA	NA	479,850	395.0	NA	NA	15,864			5823
Castor 4A	HTPB	53.1	476,660	237.6	9.20	1.02	11,578	0.126		2957
Castor 4B	HTPB	60.9	429,000	267.6	8.98	1.02	11,482	0.132		3275
Castor 4	PBAA	53.9	428,000	228.4	9.07	1.02	10,534	0.220		2230
Castor 2(v.5)	CTPB	37.0	259,000	262.2	6.04	0.79	4,424	0.259		1650
Castor 1	PBAA	27.4	286,000	241.0	5.92	0.79	3,852	0.139		1746

† E - Extended Exit Nozzle, S - Spin Stablized (fixed nozzle)

* Payload Mass (kg) equals 2500

Appendix E.2

TANK DESIGN

PRECEDING PAGE BLANK NOT FILMED

Stage	Mox/Mf	Total Stage Mass (kg)	+ 5% Safety Fuel (kg)	Propellant Vol (m^3)	+ 5% Ullage Vol (m^3)	Propellant Costs ($M)	Engine Costs ($M)	Tank Costs ($)	Total Costs ($M)
First (Ox)			27335		19.79	.190		5805	
First (Fuel)			14312		16.59	.410		1735	
Sub-Total	*1.91*	*39664*	*41647*	*34.65*	*36.38*	*.600*	*3.00*	*7539*	*3.61*
Second (Ox)			14006		10.14	.097		1928	
Second (Fuel)			7530		8.73	.216		1384	
Sub-Total	*1.86*	*20511*	*21537*	*17.97*	*18.87*	*.313*	*2.50*	*3312*	*2.82*
Third (Ox)			4546		3.77	.036		734	
Third (Fuel)			2392		3.17	.078		549	
Sub-Total	*1.90*	*6560*	*6938*	*6.61*	*6.94*	*.115*	*5.00*	*1282*	*5.12*
Totals		**66735**	**70122**	**59.23**	**62.19**	**1.027**	**10.50**	**12134**	**11.54**

		Stage 1	Stage 2	Stage 3
Spheres	Oxid. Dia.	-	-	1.93
	Fuel Dia.	-	-	1.82
	Total	-	-	**3.75**
Cyl. w/ Sph.	Oxid. Len.	4.87	2.90	-
	Fuel Len.	4.21	2.61	-
	Total	**9.08**	**5.51**	-
Cly. w/ Elip.	Oxid. Len.	4.53	2.57	-
	Fuel Len.	3.88	2.28	-
	Total	**8.41**	**4.84**	-
	Shortest Lengths	8.41	4.84	3.75
Total Tank Length (m)		**17.01**		

	Stage 1	Stage 2	Stage 3
Oxid. Rad.	1.25	1.25	-
Fuel Rad.	1.25	1.25	-
Oxid. Rad.	1.25	1.25	-
Fuel Rad.	1.25	1.25	-

Stage	Tank Rad (m)	ph End & C Length (m	Tank Rad (m)	Eliptical Width (m)	Two Elip Length (m)	Tank Rad (m)	Eliptical Width (m)	lip End & Cyl Length (m)
First (Ox)	1.25	4.87	0.00	0.75	0.00	1.25	0.75	4.53
First (Fuel)	1.25	4.21	0.00	0.75	0.00	1.25	0.75	3.88
Sub-Total		*9.08*			*0.00*			*8.41*
Second (Ox)	1.25	2.90	0.00	0.75	0.00	1.25	0.75	2.57
Second (Fuel)	1.25	2.61	0.00	0.75	0.00	1.25	0.75	2.28
Sub-Total		*5.51*			*0.00*			*4.84*
Third (Ox)	1.25	0.00	0.97	0.75	1.50	1.25	0.75	0.00
Third (Fuel)	1.25	0.00	0.91	0.75	1.50	1.25	0.75	0.00
Sub-Total		*0.00*			*3.00*			*0.00*
Totals								

Stage	Tank Rad (m)	Two Shp Length (m)	Tank Rad (m)	Eliptical Width (m)	S/S Elip Length (m)	S/S Elip Width (m)
First (Ox)	0.00	0.00	1.25	0.75	4.53	5.00
First (Fuel	0.00	0.00	1.25	0.75	3.88	5.00
Sub-Total		*0.00*			*4.53*	*5.00*
Second (O	0.00	0.00	1.25	0.75	2.57	5.00
Second (F	0.00	0.00	1.25	0.75	2.28	5.00
Sub-Total		*0.00*			*2.57*	*5.00*
Third (Ox)	0.97	1.93	0.50	0.75	5.30	2.00
Third (Fue	0.91	1.82	0.50	0.75	4.54	2.00
Sub-Total		*3.75*			*5.30*	*2.00*
Totals						

Stage	Tank ress (psi	Metal ASAI #	Max Work Stress (psi)	Weld Efficiency	Density (lb/in^3)	Cyl. Wall Thick. (in)	Cyl. Wall Thick. (cm)	End Wall Thick (in)	End Wall Thick (cm)	Baffle Mass (kg)	Total Tank Mass (kg)
First (Ox)	87.9	304	25926	0.75	0.29	.2224	.5649	.1260	.3201	135.35	1407.3
First (Fuel)	24.1	304	25926	0.75	0.29	.0611	.1551	.0346	.0879	135.35	420.5
Sub-Total										*270.69*	*1827.7*
Second (Ox)	61.6	304	25926	0.75	0.29	.1560	.3962	.0884	.2245	67.67	467.5
Second (Fuel)	50.4	304	25926	0.75	0.29	.1275	.3238	.0722	.1835	67.67	335.5
Sub-Total										*135.35*	*803.0*
Third (Ox)	61.6	304	25926	0.75	0.29	.0602	.1529			33.84	177.9
Third (Fuel)	50.4	304	25926	0.75	0.29	.0465	.1181			33.84	133.0
Sub-Total										*67.67*	*310.9*
Totals											**2941.6**

Appendix E.3

CONFIGURATIONS

PRECEDING PAGE BLANK NOT FILMED

Explanation of Configuration

Conf	Description	Side View	Top View
A	1 X liquid 1 X liquid 1/2 X liquid/ solid	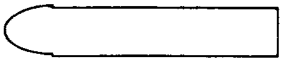	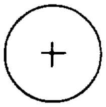
B	2 X solid + 1 X liquid 1 X liquid 1/2 X liquid/ solid	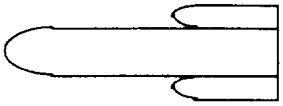	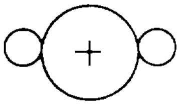
C	4 X solid + 1 X liquid 1 X liquid 1/2 X liquid/ solid	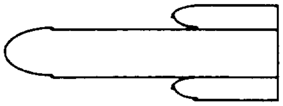	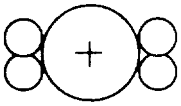
D	2 X liquid 2 X liquid 1/2 X liquid/ solid	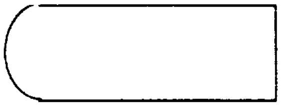	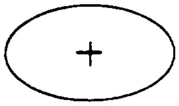
E	2 X solid + 1 X liquid 2 X liquid 1/2 X liquid/ solid	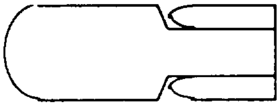	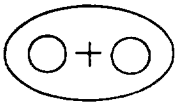
F	4 X solid + 1 X liquid 2 X liquid 1/2 X liquid/ solid	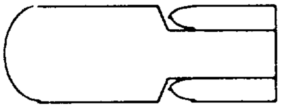	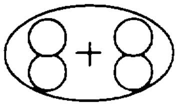
G	2/4 X solid 2 X liquid 1/2 X liquid/ solid	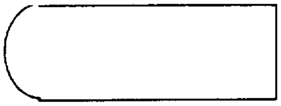	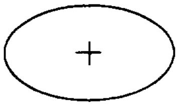

FINCON.FIG

Engine/ motor properties

Qty	Stage	Engine name	Fuel/oxidizer	max Tb (s)	Max F (N)	Isp (s)	L (m)	Dia. (m)	Dry M (kg)	O/F	Oxid d	Fuel d
1	First 1	LR-87-AJ-11	A50/N2O4	200.00	2437504.00	301.00	3.840	2.160	2285.00	1.910	1450.00	906.00
	First 2											
1	Second 1	LR-91-AJ-11	A50/N2O4	247.00	467000.00	316.00	2.810	1.630	589.00	1.860	1450.00	906.00
	Second 2											
2	Third 1	AJ10-138	A50/N2O4	500.00	35584.00	310.00	2.070	1.200	110.00	1.900	1450.00	906.00
	Third 2											

Physical properties of each stage ALONE

	Stage	Mf (kg)	Flw rt(kg/s)	Mp (kg)	Mo (kg)	Oxid M (kg)	Fuel M (kg)	Tk A (m^2)	Oxid L (m)	Fuel L (m)	Tk L (m)	Stage L (m)
	First 1	2285.00	825.49	39623.34	41908.34	26007.07	13616.27	5.309	3.378	2.831	6.209	10.049
	First 2											
Sub-total		*2285.00*	*825.49*	*39623.34*	*41908.34*							*10.049*
	Second 1	589.00	150.65	20488.01	21077.01	13324.37	7163.64	5.309	1.731	1.489	3.220	6.030
	Second 2											
Sub-total		*589.00*	*150.65*	*20488.01*	*21077.01*							*6.030*
	Third 1	220.00	23.40	6552.58	6772.58	4293.07	2259.51	5.309	0.558	0.470	1.027	3.097
	Third 2											
Sub-total		*220.00*	*23.40*	*6552.58*	*6772.58*							*3.097*
	Payload				2500.00			5.309			8.000	8.000
Total					*72257.9*							*27.176*
With +5% allowance					***75870.8***							***28.535***

Mass properties of stages

Stage	Moi (kg)	Mfi (kg)	Mo/Mf	Payld ratio
First 1	72257.92	32634.58	2.214	1.724
First 2				
Second 1	30349.58	9861.58	3.078	1.440
Second 2				
Third 1	9272.58	2720.00	3.409	1.369
Third 2				
Payload	2500.00	2500.00	1.000	

Propellant info.

Stage	Vol (mc)	Price (m$)
First 1	32.965	0.570
First 2		
Second 1	17.096	0.297
Second 2		
Third 1	5.455	0.094
Third 2		
Payload		
	55.516	**0.961**

FINCON.FIG

Performance of each stage

Stage	**F (N)**	**Tb (s)**	**C (m/s)**	**dV (m/s)**	**H (m)**	**Gmax**
First 1	2437504.00	48.00	2952.81	1876.22	37644.11	7.614
First 2						
				1876.22	*37644.11*	
Second 1	467000.00	136.00	3099.96	2150.62	102753.04	4.827
Second 2						
				2150.62	*102753.04*	
Third 1	71168.00	280.00	3041.10	982.89	33457.01	2.667
Third 2						
				982.89	*33457.01*	
Payload	0.00					
				5009.73	***173854***	

Appendix G.1

Extraction Spreadsheet

PRECEDING PAGE BLANK NOT FILMED

Spreadsheet used to track booster during egress

Wp	Wb	Cmp	Cmb	dp	dcb	dcb 2 b
550000	183680	80	36.24	173	39	4.76
den air	g	Drop v	Cdp	Lp	Lb	Max g
0.000708	32.2	230	0.75	248	99.4	3.987318
Time	x'force b	x vel b	x boost	Cgt	mom	
0	732390.6	0	0	80	0	
0.1	679373.6	12.83916	0.641958	80.16072	117914.9	
0.2	632033.4	24.74891	2.521362	80.63123	463123.8	
0.3	589581.3	35.82877	5.550246	81.38953	1019469	
0.4	551361.5	46.16442	9.649906	82.4159	1772495	
0.5	516825.5	55.83005	14.74963	83.69263	2709212	
0.6	485511.3	64.89026	20.78564	85.20378	3817907	
0.7	457027.6	73.40151	27.70023	86.93487	5087979	
0.8	431040.8	81.41342	35.44098	88.8728	6509799	
0.9	407265.6	88.96978	43.96014	91.00561	8074598	
1	385456.4	96.10934	53.2141	93.32238	9774365	
1.1	365401	102.8666	63.16289	95.81311	11601760	
1.2	346915.2	109.2722	73.76983	98.4686	13550043	
1.3	329838.3	115.3538	85.00114	101.2804	15613009	
1.4	314030.1	121.1361	96.82563	104.2407	17784932	
1.5	299367.2	126.6412	109.2145	107.3423	20060518	
1.6	285741	131.8892	122.141	110.5785	22434861	
1.71	249419.4	137.3993	136.9519	114.2865	25155321	

Wp	Wb	Cmp	Cmb	dp	dcb	dc
550000	183680	80	36.24	173	39	4
den air	g	Drop v	Cdp	Lp	Lb	M
0.000708	32.2	230	0.75	248	99.4	3.9
Time	x'force b	x vel b	x boost	Cgt	mom	
0	732390.6	0	0	80	0	

The terms used in the spreadsheet have the following meaning. Wp = Weight of C-5 in pounds. Wb = weight of booster and sled in pounds. Cmp = location of the C-5's center of mass from its nose. Cmb = location of the center of mass of the booster from its tail. dp = equivalent diameter of parachutes in feet. dcb = distance from nose of C-5 to cargo bay in feet. dcb 2 b = distance from cargo bay to end of booster in feet. den air = density of air at 35,000 ft in slugs/ft^2. g = acceleration of gravity in ft/s^2. Drop v = deployment speed of C-5 in mph. Cdp = drag coefficient of parachutes. Lp = length of C-5. Max g = maximum G forces on booster caused by parachute steady force. Time = time from chutes opening in seconds. x'force b = force on booster in pounds. x vel b = Velocity of booster in ft/s relative to cargo bay. x boost = distance booster has moved from initial point in relation to C-5 cargo bay in feet. Cgt = center of gravity of total system from nose of C-5. mom = Moment induced by booster on C-5 due to cg shift that needs to be overcome by the tail lift force in ft/lbs.

Appendix G.2

Post-extraction Spreadsheet

PRECEDING PAGE BLANK NOT FILMED

Spreadsheet used to track Athena Booster After Extraction

Vi Horz	Mass	Para Diam	Cd Para	Air Den	g
60.58	80191	52 .8	0.75	0.3648	9.81

Time	X force	Y force	X vel	Y vel	X pos	Y pos	Dist to C-5	G Load	Theata	pitch rate	total v	mission time
0	-1099264	786673.7	60.58	0	0	0	0	1.397357	0	0	60.58	4.2
0.5	-868189	707411	53.72596	4.905	28.57649	1.22625	62.78548	1.10362	5.216451	10.4329	53.9494	4.7
1	-712022	649379.7	48.31271	9.315788	54.08616	4.781447	128.7027	0.905105	10.91398	11.39506	49.20266	5.2
1.5	-602713	603073.8	43.87317	13.36474	77.13263	10.45158	197.1945	0.766154	16.9419	12.05584	45.86362	5.7
2	-524099	562938.2	40.11518	17.12498	98.12972	18.07401	267.8807	0.666222	23.1174	12.351	43.61757	6.2
2.5	-466112	525645.6	36.84736	20.63496	117.3704	27.514	340.4931	0.59251	29.24934	12.26389	42.23186	6.7
3	-422098	489294.4	33.9411	23.91242	135.0675	38.65084	414.837	0.53656	35.16573	11.83276	41.5187	7.2
3.5	-387498	452964.3	31.30928	26.96323	151.3801	51.36975	490.7658	0.492578	40.73469	11.13794	41.31932	7.7
4	-359145	416412.4	28.89318	29.78751	166.4307	65.55744	568.1642	0.456536	45.87316	10.27692	41.49833	8.2
4.5	-334853	379834	26.65387	32.38389	180.3174	81.10029	646.9361	0.425657	50.54358	9.340853	41.94217	8.7
5	-313157	343667.8	24.56602	34.7522	193.1224	97.88431	726.9974	0.398077	54.74385	8.400524	42.55825	9.2
5.5	-293112	308446.1	22.61345	36.89501	204.9173	115.7961	808.2704	0.372597	58.4953	7.502905	43.27366	9.7
6	0	786673.7	20.78587	38.8182	215.7671	134.7244	890.6811	0	61.83242	6.674246	44.033	10.2
6.5	0	786673.7	20.78587	43.7232	226.16	155.3598	973.8621	0	64.57374	5.482639	48.4125	10.7
7	0	786673.7	20.78587	48.6282	236.553	178.4476	1057.512	0	66.85597	4.564465	52.88435	11.2

The terms used in the spreadsheet have the following meaning. Vi Horz = Initial Horizontal Velocity. Mass = Mass of Athena in kg. Para Diam = Equivalent Parachute Diameter in m. Cd Para = Coefficient of drag of Parachute. Air Den = density of air at 11,00 m in kg/m^3. g = acceleration due to gravity in m/s^2. Time = time from extraction in seconds. x force = force on booster due to parachutes in horizontal direction in newtons. Y force = force on booster due to parachutes and gravity in vertical direction. X vel = velocity of booster in horizontal direction, m/s. Y vel = Velocity of booster in vertical direction, m/s. X pos = displacement of booster from initial point in the horizontal direction, meters. Dist to C-5 = Total distance from booster to C-5 in meters. G Load = G forces on booster. Theata = angle of boosters axis form horizontal in deg. pitch rate = angular velocity of booste in deg/s. total v = boosters resultant velocity in m/s. mission time = time from deployment of Chutes in seconds.

Appendix G.3

CONTROL AND STABILITY

PRECEDING PAGE BLANK NOT FILMED

APPENDIX G.3 -- **Control and Stability**

This section includes all technical details in developing the state-space dynamics from the differential equations of the system so as to explain how the design concept is elaborated. Analysis such as time response of and pitch rate as well as phase plots are investigated. Also, the pitch error correction for RCS thruster control is explained. Moreover, time response of gimbal angle as well as the ON/OFF of thrusters is included. All results are obtained by using MATLAB/SIMULINK and are explained in the following sections.

Longitudinal Dynamics and Stability of Stage 1

The controller for Stage I is of error-rejection type by using the gimbaled engines as control actuators.

State-Space Dynamics:

Since the thrust of the main engines is assumed to be zero before time starts, the effect of the initial conditions for the bending modes are negligible. By modeling the system as a spring-mass system with a negative damping ratio, we can obtain the differential equations in state-space form,

$$\begin{bmatrix} \dot{\theta} \\ \ddot{\theta} \end{bmatrix} = \begin{bmatrix} 0 & 1 \\ -q_\infty d_P / I_{yy} & 0 \end{bmatrix} \begin{bmatrix} \theta \\ \dot{\theta} \end{bmatrix} + \begin{bmatrix} 0 \\ T d_T / I_{yy} \end{bmatrix} \delta$$

$$\begin{bmatrix} \dot{\theta} \\ \ddot{\theta} \end{bmatrix} = \begin{bmatrix} 0 & 1 \\ -3.5E-8 & 0 \end{bmatrix} \begin{bmatrix} \theta \\ \dot{\theta} \end{bmatrix} + \begin{bmatrix} 0 \\ 6.906859725 \end{bmatrix} \delta$$

From the mode shapes and frequencies, the bending mode transfer function can be approximated. For the first bending mode,

$$\left(\frac{\gamma\beta}{s^2 + 2\zeta\omega s + \omega^2} \right)_{i=1} \cong \frac{100}{s^2 + 4s + 100}$$

By including the modes of the booster in the system, the controller greatly decreases the amplitude of pitch and pitch rate when the booster comes to vibrate at the natural mode frequencies. It works as a bank filter which avoids resonance of the booster. The transfer functions of higher bending modes are obtained similarly from the mode shapes and frequencies of the booster.

The initial conditions are basically the pitch and pitch rate at the instant when the main engines fire. From egress dynamics, the initial conditions are [66.47501° 4.58904°/s]. Then we can input the state-space matrices into MATLAB/SIMULINK.

Gimbal Saturation Limit:

Due to spacious constraints for the nozzles, the maximum allowable gimbal angle is set to be 6°. This makes the system non-linear. The relationship between the input and output of the saturation function is displayed in the following.

PRECEDING PAGE BLANK NOT FILMED

Performance of Stage I:

The time response plots show that both pitch and pitch rate die down to zero in five seconds given the initial conditions of Stage I. As compared to the burn time of Stage I, the controller allows the booster to ascend at a high pitch angle and make a sharp turn so as to attain the horizontal velocity before getting to Stage II. Also, the phase plot shows that the final conditions converge to zero. In other words, the steady state errors for both pitch and pitch rate will die down to zero in finite time interval. This can be verified by previous section which talks about the BIBO stability of the system using a PID controller.

Figure 8.11: Stage 1 simulation plots

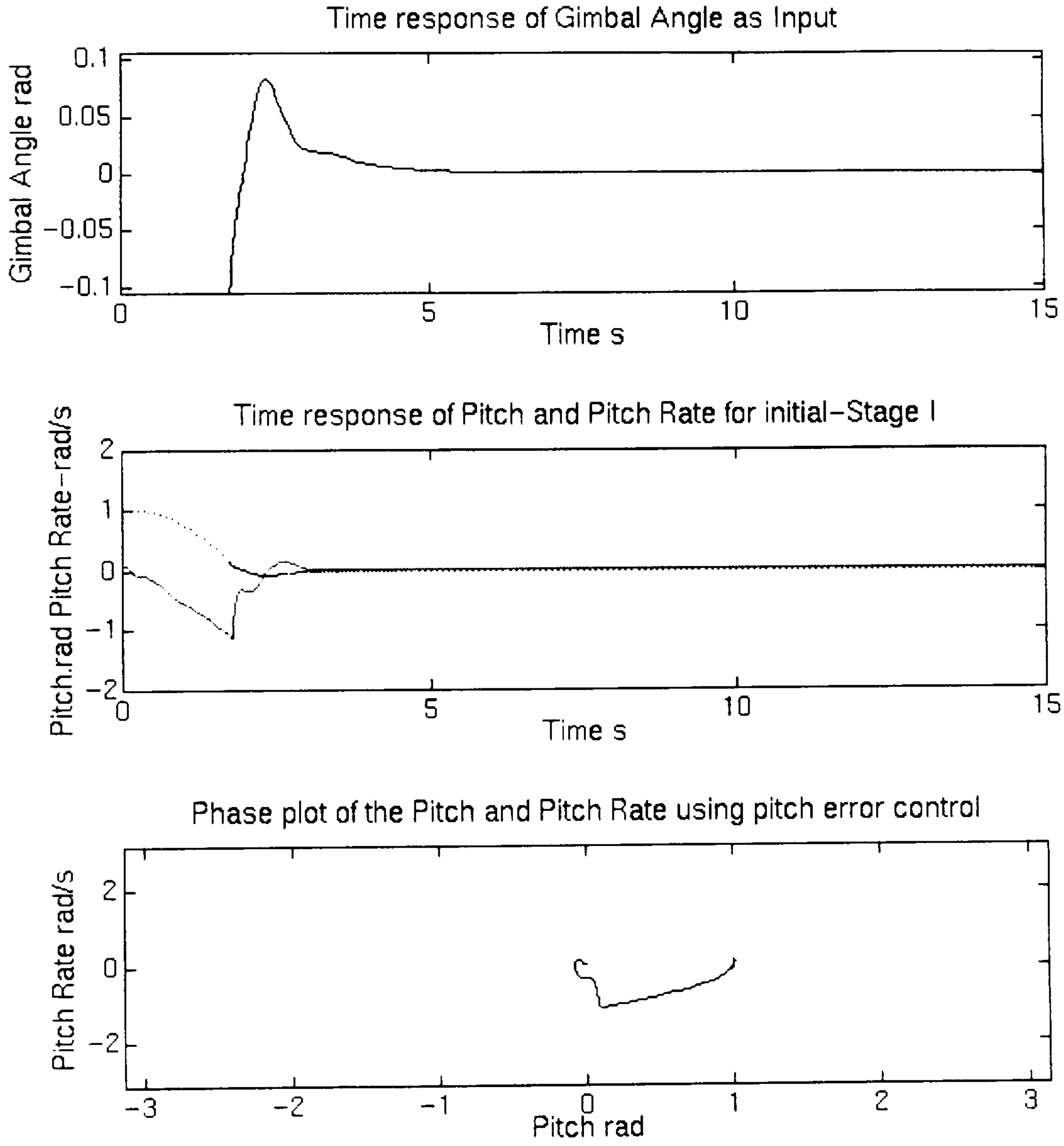

LONGITUDINAL DYNAMICS AND STABILITY OF STAGE III

The controller for Stage III is a of disturbance-rejection type. It has to work with the RCS. Due to the 'ping ping' maneuver of the system, it is a non-linear feedback control system.

State-Space Dynamics:

Unlike Stage I, unstable aerodynamic effect is neglected in Stage III. Hence, the system can simplified be modeled as a second order spring-mass system. The most interesting thing is that the mass is connected to two springs with positive damping ratio. The differential equations in state-space form are,

$$\begin{bmatrix}\dot{\theta}\\ \ddot{\theta}\end{bmatrix}=\begin{bmatrix}0 & 1\\ 0 & 0\end{bmatrix}\begin{bmatrix}\theta\\ \dot{\theta}\end{bmatrix}+\begin{bmatrix}0\\ T_t d_t / I_{yy}\end{bmatrix}u$$

$$\begin{bmatrix}\dot{\theta}\\ \ddot{\theta}\end{bmatrix}=\begin{bmatrix}0 & 1\\ 0 & 0\end{bmatrix}\begin{bmatrix}\theta\\ \dot{\theta}\end{bmatrix}+\begin{bmatrix}0\\ 0.2832686728\end{bmatrix}u$$

Similar to Stage I, the bending mode transfer functions can be obtained from the mode shapes and frequencies. However, the analysis for Stage III is based on rigid body mode assumption due to lacking of data on mode shapes and frequencies for Stage III which are highly dependent on the type and mass distribution of payload.

Pitch Error Control Logic:

Any disturbance acting on the system will lead to oscillation of the mass about the equilibrium position. To make sure that the oscillation is convergent, we need to set an error bound for the system. The pitch error control logic is designed for this purpose. The 'ping ping' maneuver is explained in previous section while the relationship between the input and output of the control logic is plotted as follows. The time response of two opposite thruster pairs working for pitch control is plotted which gives an ideal on how the thrusters work.

Performance of Stage III:

The time response plots show that both pitch and pitch rate die down within the error bound of the controller in about eighty seconds assuming a very large disturbance [Pitch=20° Pitch Rate=5°/s]. As compared to the burn time of Stage III, the controller allows the booster to stabilize and make a gradual turn so as to attain pitch angle for ascend trajectory of orbital transfer. Also, the phase plot shows that the final conditions converge to confined region. It is because the oscillation caused by the 'ping ping' maneuver will never attain a zero steady state error. However, the error is greatly reduced by a PID controller which also speeds up the decay time.

Figure 8.12: Stager 3 simulation plots

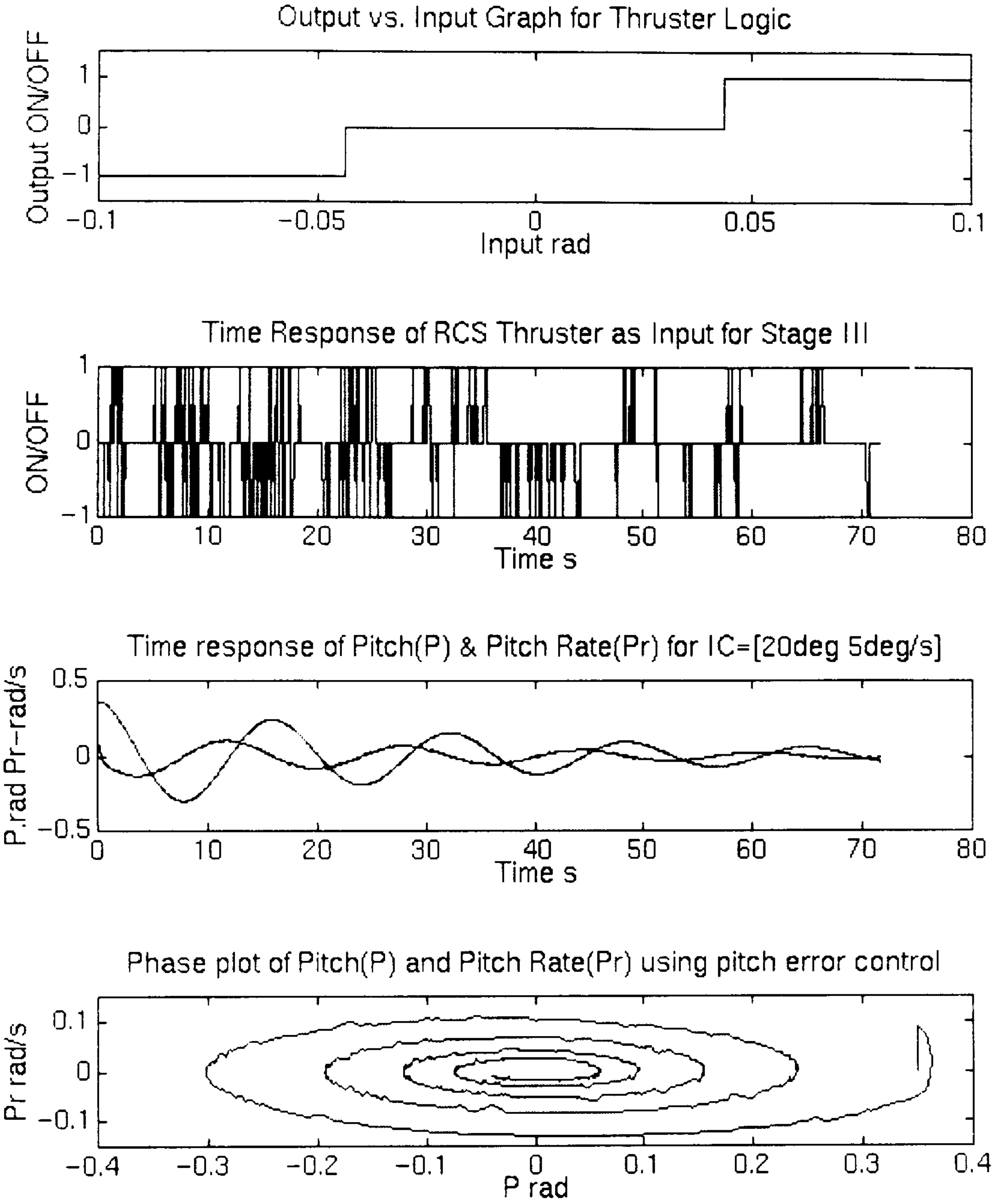
Output vs. Input Graph for Thruster Logic
Output ON/OFF
1
0
−1
−0.1
−0.05
0
0.05
0.1
Input rad
Time Response of RCS Thruster as Input for Stage III
ON/OFF
1
0
−1
0
10
20
30
40
50
60
70
80
Time s
Time response of Pitch(P) & Pitch Rate(Pr) for IC=[20deg 5deg/s]
P.rad Pr−rad/s
0.5
0
−0.5
0
10
20
30
40
50
60
70
80
Time s
Phase plot of Pitch(P) and Pitch Rate(Pr) using pitch error control
Pr rad/s
0.1
0
−0.1
−0.4
−0.3
−0.2
−0.1
0
0.1
0.2
0.3
0.4
P rad